Synthesis of New Pullulan Derivatives for Drug Delivery

Junia Motta Pereira

Dissertation submitted to the faculty of the Virginia Polytechnic Institute and State University in partial fulfillment of the requirements for the degree of

Doctor of Philosophy

In

Macromolecular Science and Engineering

Kevin J. Edgar, Chair
Maren Roman
Judy S. Riffle
Nammalwar Sriranganathan
Lynne S. Taylor

August 9, 2013
Blacksburg, VA

Keywords: polysaccharides, regioselective, oxidation, amphiphilic, Staudinger reaction, amorphous solid dispersion, clarithromycin, HIV drugs, bioavailability

Synthesis of New Pullulan Derivatives for Drug Delivery

Junia Motta Pereira

Abstract

Pullulan is a non-ionic water-soluble polysaccharide which is produced from starch by the yeast-like fungus *Aureobasidium pullulans*. Pullulan is known for its non-toxicity and biocompatibility. Most pullulan modifications are intended to reduce its water solubility or to introduce charged or reactive groups for functionality. Polysaccharides that have been hydrophobically modified and contain carboxyl groups are commonly used in drug delivery systems because of their ability to provide pH-controlled drug release. We demonstrated in this dissertation the regioselective synthesis of a range of 6-carboxypullulan ethers that are promising anionic derivatives for drug delivery applications. These compounds have also shown impressive surfactant properties. Another class of pullulan derivatives was synthesized by regioselective introduction of amine and amide groups to the pullulan backbone. These chemical groups are known to play a fundamental role in the biological activity of important polysaccharides, such as chitin and chitosan, therefore, the pullulan derivatives synthesized herein, which are structural isomers of those polymers, possess great potential for biomedical applications.

Clarithromycin (CLA) is an aminomacrolide antibiotic whose physical properties are fascinating and challenging. It has very poor solubility at neutral intestinal pH, but much higher solubility under acidic conditions. Therefore, CLA dissolves better in the stomach than in the small intestine; but CLA is also quite labile towards acid-catalyzed degradation. We report herein a study on amorphous solid dispersion (ASD) of CLA with promising carboxyl-containing cellulose derivatives, both as macro and nanoparticles. This approach was intended to improve CLA solubility in neutral media, to protect it from acid degradation, and thereby increase its uptake from the small intestine and ultimately its bioavailability.

We have also prepared ASDs of selected anti-HIV drugs, ritonavir (RTV), efavirenz (EFV) and etravirine (ETR) with the cellulosic derivative carboxymethyl cellulose acetate butyrate (CMCAB). This polymer was efficient in stabilizing RTV and EFV in their amorphous form in the solid phase and all ASDs provided significant enhancement of drug solution concentration.

Dedication

To my family, the best part of my life.

Not even the first page of this dissertation would have been possible without your love beyond limits.

Acknowledgements

I wish to thank my advisor Dr. Kevin Edgar for giving me the opportunity to pursue my PhD under his mentorship. He believed in me since the beginning, even when I performed terribly in the GRE, and I will be forever thankful for this. Dr. Edgar is the true meaning of a great mentor. His expertise in polysaccharides and his knowledge of a variety of subjects have always been a big support during my studies. I admire his patience and his unique way of bringing out the best of me. He would make me want to conquer the world every time I left his office after bi-weekly meetings. I am grateful from the bottom of my heart to have known him and to have learned so much from him.

I would like to thank Dr. Judy Riffle for having supported my admission to the MACR program and for being part of my graduate committee. I also wish to express deep gratitude to my other committee members, Dr. Lynne Taylor, Dr. Nammalwar Sriranganathan and Dr. Maren Roman. Their guidance and suggestions have proven most valuable through my research.

I wish to give a big thanks to all my past and present colleagues in the cellulose research group. Their friendship and knowledge have turned my days in the lab into a joy.

I would like to thank the Macromolecules and Interfaces Institute (MII) for academic support and the Institute for Critical Technology and Applied Science (ICTAS) for financial and facilities support.

Lastly, thank you to my husband, Diego, for his patience and love throughout our journey together, specially this big USA/PhD journey.

Table of Contents

Abstract ... **ii**

List of Figures ... **ix**

List of Tables ... **xiii**

List of Abbreviations ... **xiv**

Chapter 1 Dissertation Overview ... **1**

Chapter 2 Literature Review ... **3**

2.1 Pullulan ... *3*
2.1.1 Pullulan properties ... 4
2.1.2 Pullulan from *A. pullulans* ... 5
2.1.3 Commercial production of pullulan ... 6
2.1.4 Pullulan biosynthesis ... 7
2.1.5 Food industry and pharmaceutical applications ... 8
2.1.6 Chemical modifications and biomedical applications ... 9

2.2 Drug Delivery ... *20*

2.3 References ... *24*

Chapter 3 Synthesis of Amphiphilic 6-Carboxypullulan Ethers ... **30**

3.1 Abstract ... *30*

3.2 Introduction ... *30*

3.3 Experimental ... *33*
3.3.1 Materials and methods ... 33
3.3.2 Oxidation of pullulan with TEMPO and NaOCl/NaBr ... 35
3.3.3 Etherification of 6-carboxypullulan TBA salt ... 36
3.3.4 General procedure for the etherification of 6-carboxypullulan TBA salt ... 37
3.3.5 Synthesis of 6-carboxypullulan ethers by reaction with iodomethane and iodoethane ... 37

3.4 Results and Discussion ... *38*
3.4.1 Pullulan oxidation ... 38
3.4.2 Synthesis and characterization of 6-carboxypullulan ethers ... 39
3.4.3 Determination of critical micelle concentration of 6-carboxypullulan ethers ... 48

3.5 Conclusions ... *50*

3.6 References *51*

3.7 Copyright Authorization *54*

Chapter 4 Regioselectively Modified Pullulan Derivatives Containing Amine and Amide Groups: Potential for Biomedical Applications **55**

4.1 Abstract *55*

4.2 Introduction *55*

4.3 Experimental *61*

4.3.1 Materials and methods 61

4.3.2 Calculation of degree of substitution of ester and amide groups 62

4.3.3 Synthesis of 6-bromo-6-deoxy-pullulan 63

4.3.4 Esterification of 6-bromo-6-deoxy-pullulan 64

4.3.5 Displacement of bromide in the 6-bromo-6-deoxy-pullulan esters to obtain 6-azido-6-deoxy-pullulan esters 65

4.3.6 Conversion of 6-azido-6-deoxy-2,3,4-O-acetyl-pullulan to 6-amino-6-deoxy-2,3,4-O-acetyl-pullulan 65

4.3.7 Conversion of 6-azido-6-deoxy-pullulan esters to 6-amido-6-deoxy-pullulan esters 65

4.4 Results and Discussion *66*

4.4.1 Pullulan bromination 66

4.4.2 Esterification of 6-bromo-6-deoxy-pullulan 69

4.4.3 Conversion of 6-bromo-6-deoxy-pullulan esters to 6-azido-6-deoxy-pullulan esters 69

4.4.4 Selective azide reduction to produce 6-amino-6-deoxy-2,3,4-O-acetyl-pullulan 71

4.4.5 Selective synthesis of 6-amido-6-deoxy-pullulan esters 73

4.5 Conclusions *80*

4.6 References *82*

Chapter 5 Interplay of Degradation, Dissolution and Stabilization of Clarithromycin and its Amorphous Solid Dispersions **87**

5.1 Abstract *87*

5.2 Introduction *88*

5.3 Experimental *93*

5.3.1 Materials 93

5.3.2 Preparation of ASDs by spray-drying 95

5.3.3 Preparation of nanoparticle ASDs using a multi-inlet vortex mixer 95

5.3.4 CLA quantification by high-performance liquid chromatography with diode-array detection (HPLC-DAD) ... 96
5.3.5 Powder X-ray diffraction (XRD) ... 97
5.3.6 Differential scanning calorimetry (DSC) ... 97
5.3.7 Dynamic light scattering (DLS) ... 97
5.3.8 Scanning electron microscopy (SEM) ... 98
5.3.9 Long-term physical stability of ASDs ... 98
5.3.10 Calculation of drug loaded in the ASD particles ... 98
5.3.11 Determination of polymer matrix solubility ... 99
5.3.12 Maximum CLA solution concentration from the ASDs ... 99
5.3.13 *In vitro* drug release of CLA from ASDs ... 99
5.3.13.1 Experiment A: Dissolution experiment to evaluate CLA release profile from ASDs at pH 6.8 ... 100
5.3.13.2 Experiment B: Dissolution experiment to evaluate CLA release profile from ASDs at pH 1.2 followed by pH 6.8 ... 100
5.3.14 Release profile of CLA in pH 1.2 HCl solution: Degradation versus crystallization and release rate ... 101
5.3.14.1 Quantification of CLA remaining dissolved and intact ... 101
5.3.14.2 Quantification of CLA degradation ... 102

5.4 Results and Discussion ... 102
5.4.1 Characterization of solid dispersions ... 102
5.4.2 Solution concentration enhancement by ASDs ... 107
5.4.3 Release profile of CLA from ASDs at pH 6.8 ... 108
5.4.4 CLA degradation versus crystallization ... 110
5.4.5 Release profile of CLA from ASDs with pH Change ... 112

5.5 Conclusions ... 121

5.6 References ... 124

Chapter 6 Preliminary Studies on Amorphous Solid Dispersions of Anti-HIV Drugs: Ritonavir, Efavirenz and Etravirine ... 130

6.1 Abstract ... 130

6.2 Introduction ... 130

6.3 Experimental ... 133
6.3.1 Materials ... 133
6.3.2 Preparation of ASDs by co-precipitation ... 134
6.3.3 Preparation of nanoparticles ASDs using a multi-inlet vortex mixer ... 134
6.3.4 Powder X-ray diffraction (XRD) ... 135
6.3.5 Differential scanning calorimetry (DSC) ... 136

6.3.6 Quantification of HIV drugs by high-performance liquid chromatography with diode-array detection (HPLC-DAD) 136
6.3.7 Calculation of drug loaded in the ASDs particles 136
6.3.8 *In-vitro* drug release of anti-HIV drugs from ASDs 137
6.3.9 Preparation of ETR/CMCAB films from different solvents 137
6.3.10 Preparation of CAAdP/drug films 137

6.4 Results and Discussion 138
6.4.1 Characterization of amorphous solid dispersions 138
6.4.2 Release profile of anti-HIV drugs from CMCAB ASDs 144
6.4.3 Evaluation of ETR/CMCAB film from different solvents 145
6.4.4 Evaluation of CAAdP/drug films 146

6.5 Conclusions 146

6.6 References 148

Chapter 7 Summary and Future Work 152

7.1 Synthesis of Amphiphilic 6-Carboxypullulan Ethers 152

7.2 Regioselectively Modified Pullulan Derivatives Containing Amine and Amide Groups: Potential for Biomedical Applications 155

7.3 Interplay of Degradation, Dissolution and Stabilization of Clarithromycin and its Amorphous Solid Dispersions 160

7.4 Preliminary Studies on Amorphous Solid Dispersions of Anti-HIV Drugs: Ritonavir, Efavirenz and Etravirine 164

7.5 References 168

Appendix 172

List of Figures

Figure 2.1 Chemical structure of pullulan 3

Figure 2.2 Proposed scheme for the synthesis of phospholipid-oligosaccharide intermediates that may participate in pullulan biosynthesis 8

Figure 2.3 Chemical structure of carboxymethylpullulan showing substitution at C-2 13

Figure 2.4 Chemical structure of cholesterol-pullulan and formation of self-aggregate complex 15

Figure 2.5 Synthesis of DEAE-pullulan and its amphiphilic derivatives 17

Figure 2.6 Oxidation of pullulan with TEMPO 19

Figure 2.7 Mechanism for the oxidation of pullulan with TEMPO 20

Figure 3.1 Pullulan oxidation and synthesis of 6-carboxypullulan ethers 31

Figure 3.2 (a) ^{1}H and (b) ^{13}C NMR spectra of 6-CO_2TBAPullulan in d_6-DMSO 42

Figure 3.3 (a) ^{1}H and (b) ^{13}C NMR spectra of butylpullulan-6-carboxylate in d_6-DMSO 46

Figure 3.4 IR spectrum of butyl pullulan-6-carboxylate 48

Figure 3.5 Determination of CMC for (a) propyl-6-CO_2HPull and (b) butyl-6-CO_2HPull 49

Figure 4.1 Synthesis of 6-amino and 6-amido-6-deoxy-pullulan esters 57

Figure 4.2. Chemical structures of chitin and chitosan 58

Figure 4.3. Mechanism for the C-6 bromination of pullulan with NBS and PPh_3 67

Figure 4.4 ^{13}C NMR spectrum of 6-bromo-6-deoxy-pullulan 68

Figure 4.5 ^{13}C NMR spectrum of 6-azido-6-deoxy-2,3,4-O-acetyl-pullulan 70

Figure 4.6 Mechanism for the Staudinger reduction 72

Figure 4.7 Solid state ^{13}C NMR spectrum of 6-amino-6-deoxy-2,3,4-O-acetyl-pullulan 73

Figure 4.8 Proposed mechanism for the N-acylation of 6-deoxy-6-iminophophoranepullulan ... 75

Figure 4.9 ^{13}C NMR spectrum of 6-acetamido-6-deoxy-2,3,4-O-acetyl-pullulan in $CDCl_3$..... 76

Figure 4.10 ^{13}C NMR spectrum of 6-acetamido-6-deoxy-2,3,4-O-butyryl-pullulan in $CDCl_3$.... 77

Figure 4.11 DSC thermograms of 6-acetamido-6-deoxy-pullulan esters 79

Figure 5.1 Chemical structure of clarithromycin 90

Figure 5.2 Chemical structures of a) CMCAB, b) HPMCAS and c) CAAdP 92

Figure 5.3 SEM images of a) CLA/CMCAB 25% at 1K magnification, b) CLA/CMCAB 25%, c) CLA/HPMCAS 25%, d) CLA/CAAdP 25%. b, c, and d at 10K magnification..... 104

Figure 5.4 X-ray diffraction spectra of: (a) CLA/CMCAB ASDs, spray-dried and nanoparticles, (b) CLA/HPMCAS ASDs, (c) CLA/CAAdP ASDs, all in comparison with crystalline CLA. . 105

Figure 5.5 DSC thermograms of CLA/CAAdP ASDs, in comparison with crystalline CLA 106

Figure 5.6 Max CLA solution concentration from ASDs in pH 6.8 phosphate buffer, 37 ºC 107

Figure 5.7 Dissolution profiles of CLA and ASDs at pH 6.8 buffer.. 108

Figure 5.8 Loss of dissolved CLA at pH 1.2. Comparison between amount of dissolved CLA, and amount of dissolved plus recrystallized CLA 112

Figure 5.9 Dissolution profiles of CLA and ASDs; pH 1.2 buffer for 2h, then pH 6.8 buffer for 6h (Exp B)..... 114

Figure 5.10 Percentage of CLA that remains intact either in solution or inside the ASD particles vs. time at pH 1.2. 118

Figure 5.11 Schematic illustration of the different processes occurring during the dissolution of CLA/polymer ASDs under GI-tract mimicking pH conditions. 119

Figure 6.1 Chemical structures of ritonavir, efavirenz and etravirine 132

Figure 6.2 Chemical structures of CMCAB and CAAdP 133

Figure 6.3 X-ray diffraction spectra of spray-dried ASDs: (a) RTV/CMCAB, (b) EFV/CMCAB and (c) ETR/CMCAB, in comparison with crystalline RTV, EFV and ETR respectively 140

Figure 6.4 DSC thermograms of (a) RTV/CMCAB, (b) EFV/CMCAB and (c) ETR/CMCAB ASDs, in comparison with crystalline RTV, EFV and ETR respectively. 143

Figure 6.5 Dissolution profiles of anti-HIV drugs ASDs at pH 6.8 buffer..... 144

Figure 7.1 Pullulan oxidation and synthesis of 6-carboxypullulan ethers 152

Figure 7.2 Mechanism for crosslinking during esterification of 6-carboxypullulan 154

Figure 7.3 Synthesis of 6-amino and 6-amido-6-deoxy-pullulan esters 156

Figure 7.4 Reaction mechanism for the traceless Staudinger ligation mediated by (diphenylphosphino)methanethioester 158

Figure 7.5 Illustration of a bottlebrush structure formed after grafting of a polysaccharide macroinitiator 159

Figure 7.6 Reaction of pullulan iminophosphorane intermediate with 2-bromoisobutyryl bromide to form a pullulan macroinitiator 160

Figure 7.7 Dissolution profile of CLA/CAAdP ASDs (10 and 25 wt% drug loading); pH 1.2 buffer for 2h, then pH 6.8 buffer for 6h 162

Figure 7.8 Chemical structure of cellulose ω-carboxyalkanoates 163

Figure 7.9 Dissolution profiles of anti-HIV drugs ASDs in pH 6.8 buffer 164

Figure A3.1 ^{13}C NMR spectra of pullulan (above) and 6-carboxypullulan (below) in D_2O 172

Figure A3.2 ^{1}H (a) and ^{13}C (b) NMR spectra of ethyl pullulan-6-carboxylate in d_6-DMSO 173

Figure A3.3 ^{1}H NMR spectra of propyl pullulan-6-carboxylate in D_2O 174

Figure A3.4 IR spectra of (a) 6-carboxypullulan and (b) butyl pullulan-6-carboxylate..... 175

Figure A4.1 (a) ^{1}H and (b) ^{13}C NMR of 6-bromo-6-deoxy-2,3,4-O-acetyl-pullulan..... 177

Figure A4.2 ^{1}H NMR of 6-azido-6-deoxy-2,3,4-O-acetyl-pullulan 178

Figure A4.3 (a) ^{1}H and (b) ^{13}C NMR of 6-azido-6-deoxy-2,3,4-O-butyryl-pullulan 179

Figure A4.4 (a) ^{1}H and (b) ^{13}C NMR of 6-azido-6-deoxy-2,3,4-O-hexanoyl-pullulan 180

Figure A4.5 ^{1}H NMR of (a) 6-acetamido-6-deoxy-2,3,4-O-acetyl-pullulan and (b) 6-acetamido-6-deoxy-2,3,4-O-butyryl-pullulan..... 181

Figure A4.6 ^{13}C NMR of (a) 6-acetamido-6-deoxy-2,3,4-O-propionyl and (b) 6-acetamido-6-deoxy-2,3,4-O-hexanoyl-pullulan..... 182

Figure A5.1 DSC thermograms of a) CLA/CMCAB ASDs (results from nanoparticles ASDs are shown in Table 1, Chapter 5), and b) CLA/HPMCAS ASDs, all in comparison with crystalline CLA..... 185

List of Tables

Table 2.1 Solubility of PA in several solvents 11

Table 3.1 Optimization of reaction conditions for etherification of 6-carboxypullulan with bromobutane 39

Table 3.2 Solubility of 6-carboxypullulan – protonated form and as Na and TBA salts 40

Table 3.3 Properties of 6-carboxypullulan ethers 44

Table 4.1 Ester DS (DS_E) for 6-bromo- and 6-azido-6-deoxypullulan esters 71

Table 4.2 Amide and ester DS of 6-acetamido-6-deoxy-pullulan esters 78

Table 4.3 MW of 6-acetamido-6-deoxy-pullulan esters 80

Table 5.1 Polymer physical properties 110

Table 5.2 Quantification of polymer influence on CLA stability and solubility at pH 1.2 and 6.8 121

Table 6.1 T_g of ASDs - experimental vs. predicted by Fox equation 143

Table 6.2 Evaluation of ETR/CMCAB films cast from different solvents 146

Table 6.3 Evaluation of drug/CAAdP films 146

Table A3.1 DS of ester groups in the 6-carboxypullulan ethers 176

Table A5.1 T_g of ASDs - experimental vs. predicted by Fox equation 184

List of Abbreviations

AGU: Anhydroglucose unit

AIDS: Acquired Immune Deficiency Syndrome

ASD: Amorphous Solid Dispersion

ATRP: Atom Transfer Radical Polymerization

CAAdP: Cellulose Acetate Adipate Propionate

CAB: Cellulose Acetate Butyrate

$CDCl_3$: Chloroform

CHP: Cholesterol-Pullulan

CLA: Clarithromycin

CMC: Critical Micelle Concentration

CMP: Carboxymethylpullulan

DAD: Diode Array Detector

DEAE: Diethylaminoethyl

DLS: Dynamic Light Scattering

DMAc: Dimethylacetamide

DMF: Dimethylformamide

DMSO: Dimethylsulfoxide

DNA: Deoxyribonucleic Acid

DOX: Doxorubicin

DS: Degree of Substitution

DSC: Differential Scanning Calorimetry

EDC: 1-Ethyl-3[3-(dimethylamino)propyl]carbodiimide

EFV: Efavirenz

ETR: Etravirine

FDA: Food and Drug Administration

FTIR: Fourier Transform Infrared Spectroscopy

GI: Gastrointestinal

HAART: Highly Active Antiretroviral Therapy

HIV: Human Immunodeficiency Virus

HPLC: High Performance Liquid Chromatography

HPMCAS: Hydroxypropylmethylcellulose Acetate Succinate

IFN: Interferon

IR: Infrared

MIVM: Multi-Inlet Vortex Mixer

MW: Molecular Weight

MWCO: Molecular Weight Cut-off

NBS: *N*-Bromosuccinimide

NMP: *N*-Methylpyrrolidone

NMR: Nuclear Magnetic Resonance

PA: Pullulan Acetate

PEO: Polyethylene Oxide

PPO: Polypropylene Oxide

PTFE: Polytetrafluoroethylene

PVA: Polyvinylacetate

RTV: Ritonavir

SEM: Scanning Electrical Microscopy

S_N2: Bimolecular Nucleophilic Substitution

SP: Solubility Parameter

TBA: Tetrabutylammonium

T_d: Decomposition Temperature

TEMPO: 2,2,6,6-tetramethyl-1-piperidinyloxy free radical

T_g: Glass Transition Temperature

THF: Tetrahydrofuran

UDPG: Uridine 5'-(D-gluco-pyranosyl pyrophosphate)

UNAIDS: Joint United Nations Program on HIV/AIDS

WHO: World Health Organization

XRD: X-Ray Diffraction

Chapter 1 **Dissertation Overview**

Pullulan is a natural water-soluble polysaccharide, produced from starch by the fungus *Aureobasidium pullulans*. It has several commercial applications, primarily in the food and pharmaceutical industries. Pullulan biodegrades in the body and does not evoke an immune response. Therefore, recently, pullulan is also being investigated for its biomedical applications in several areas; for example targeted drug and gene delivery, tissue engineering, and wound healing. Most of the current research is focused on obtaining hydrophobized pullulan derivatives to be used as drug delivery carriers.

In view of the attractive characteristics of pullulan and the possibility of chemically modifying it according to the desired application, the goal in this dissertation was to synthesize a range of pullulan derivatives with appealing properties for use in drug delivery systems. These derivatives may be used in oral and intravenous drug formulations, and their physical properties are expected to help improve drug performance, such as provide sustained release of the drug and improve the drug's solubility and stability.

The incorporation of carboxylic acid groups in the pullulan backbone will provide anionic compounds that will interact more effectively with drugs containing cationic groups. Similarly, cationic pullulan derivatives containing amine/amide groups can be better candidates in the delivery of anionic drugs. Furthermore, the ionic characteristics of these polymers will allow for pH controlled release of the drug within the GI tract. Since these ionic compounds will be very hydrophilic, some hydrophobicity may be desirable to attain intermediate properties. Hydrophobic interactions with the drugs also play an important role in the drug-polymer system. Hydrophobicity will enhance miscibility and slow the release rate of drugs. It is also important to tailor the polymer solubility to facilitate the processing into drug delivery formulations. The hydrophobicity of the prepared anionic compounds will be achieved by the esterification or etherification of the remaining hydroxyl groups. The type of ester/ether and degree of substitution will allow for tailoring the hydrophobicity to attain the desired properties.

One of the possible applications for the pullulan derivatives synthesized herein is for amorphous solid dispersions (ASDs). The preparation of ASDs is a technique currently used in our research group and was also a research focus in this dissertation. Low drug solubility and inadequate oral bioavailability have been addressed using a number of strategies; complexation with cyclodextrins, formulation with lipid excipients, conversion into a higher energy polymorph, particle size reduction, or by formulation as an amorphous solid. Incorporation into a solid polymer matrix can enhance solubility by trapping the drug in a metastable amorphous state, eliminating the need to disrupt the crystal lattice in order for the drug to dissolve. Generation of supersaturated drug solutions from ASDs in polymer matrices represents an increasingly important approach for enhancing drug solubility and bioavailability.

An outline for this dissertation is as follows: **Chapter 2** will start with introduction of structure of pullulan, its properties and applications. A review of the most important chemical modifications of pullulan and its biomedical applications will follow. Then, this chapter will close with a brief introduction to drug delivery. **Chapter 3** will present the synthesis and characterization of amphiphilic 6-carboxypullulan ethers. These compounds have shown outstanding surfactant properties. **Chapter 4** will cover the synthesis of pullulan containing amine and amide groups regioselectively introduced at carbon 6 via the dynamic Staudiger reaction. **Chapter 5** will discuss the complex processes involved in the dissolution of ASDs of the antibiotic clarithromycin with several carboxyl-containing cellulose derivatives. **Chapter 6** will present preliminary studies on ASDs of selected anti-HIV drugs with carboxymethylcellulose acetate butyrate. **Chapter 7** will provide a summary of the research results in this dissertation and suggest future explorations to be pursued.

Chapter 2 **Literature Review**

2.1 Pullulan

Pullulan is a linear polysaccharide, and its structural formula may be represented as a regular sequence of panoses or isopanoses bonded by α-(1→4)-linkages (**Fig 2.1**). Panose: [α-D-Glc*p*-(1→6)-α-D-Glc*p*-(1→4)-α-D-Glc*p*] and isopanose: [α-D-Glc*p*-(1→4)-α-D-Glc*p*-(1→6)-α-D-Glc*p*]. Alternatively, it can be described as having maltotriosyl [α-(1→4)Glc*p*-α-(1→4)Glc*p*] repeating units joined by α-(1→6)-linkages.

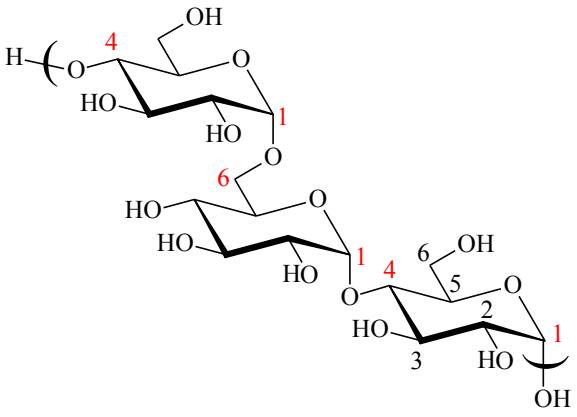

Figure 2.1 Chemical structure of pullulan

The history of the discovery of pullulan was reviewed by Leathers (2003).[1] The production of an extracellular polymer by the fungus *Aureobasidium pullulans* (*A. pullulans)* was first observed by Bauer (1938),[2] but this exopolysaccharide was not isolated in pure form until 20 years later by Bernier (1958)[3] from cultures of *A. pullulans* and characterization of the monosaccharides after acid hydrolysis revealed D-glucose as the main product. Bender, Lehmann and Wallenfels (1959)[4] showed the polymer to be an α-D-glucan with predominantly α-(1→4)-linkages based on its positive optical rotation and infrared spectrum. Elemental analysis of pullulan suggested the compound to have the chemical formula $(C_6H_{10}O_5)_n$. In the early 1960s, the basic structure of pullulan was resolved. Bender and Wallenfels (1961)[5] and other

researchers[6] concluded that pullulan is a linear α-D-glucan possessing (1→4) and (1→6) linkages in a ratio of 2:1. This conclusion was supported by infrared spectroscopic, periodate oxidation and methylation data. Discovery of an extracellular enzyme from *Aerobacter aerogenes,* pullulanase, was a breakthrough in the analysis of pullulan structure.[5] This enzyme exclusively hydrolyzes the α-(1→6)-linkages in pullulan and converts the polysaccharide almost quantitatively to maltotriose. Consequently, pullulan is commonly described as an α-(1→6) linked polymer of maltotriose subunits. Partial acid hydrolysis of pullulan yields isomaltose, maltose, panose and isopanose. Thus, pullulan can also be considered to be composed of panose or isopanose subunits. The later representation is the more appropriate from the viewpoint of the mechanism of pullulan biosynthesis.[7] Catley and coworkers (1966),[8] after hydrolysis of pullulan by exo- and endoenzymes, found the occurrence of a minor percentage of randomly distributed maltotetraose subunits [α-(1→4)Glc*p*-α-(1→4)Glc*p*-α-(1→4)Glc*p*-α-(1→6)Glc*p*]. The maximum extent to which maltotetraose subunits have been detected is 7% and this minor structural irregularity should not affect the overall physico-chemical properties of the polymer.[9] This is the main reason why currently in the literature the term pullulan is used for both the polymaltotriose produced by *A. pullulans* and the polysaccharide varieties, similar to pullulan, produced by other microbes. Moreover, α-(1→3) and even β-(1→3) as well as β-(1→6) linkages were found in the main backbone of pullulan produced by some strains, in addition to the α-(1→4) linkages (reviewed by Singh, Saini & Kennedy, 2008).[10] Pullulan structure has also been clearly determined by employing proton and carbon-13 NMR and Raman spectroscopy. The number of α-(1→4) and α-(1→6) linkages could be quantified by these techniques.[10]

2.1.1 Pullulan properties

Due to the co-existence of both α-(1→4)- and α-(1→6)-linkages, pullulan structure is often seen as an intermediate between amylose [α-(1→4)-glucan] and dextran [α-(1→6)-glucan] structures. The segmental mobility of pullulan is not uniform, with the regions of increased mobility centered on the α-(1→6) linkages.[10] The distinctive properties of pullulan are attributed to its unique linkage sequence. Pullulan is water soluble, partially soluble in dimethylformamide (DMF) and dimethylsulfoxide (DMSO) and insoluble in other organic solvents. Its aqueous

solutions are stable and show relatively low viscosity as compared to other water soluble polysaccharides. Viscosities of solutions are proportional to pullulan molecular weight. Detailed studies have been carried out for hydrodynamic and molecular properties of pullulan in solution and it was concluded that pullulan molecules in solution behave as an expanded flexible coil.[11] Pullulan decomposes at 250-280 ^{o}C. It is moldable and spinable, being a good adhesive and binder. It is also non-toxic, non-mutagenic, odorless, tasteless, edible, and biodegradable.[10]

The average molecular weight of pullulan varies in very broad ranges, from hundreds to thousands of kilodaltons, depending on the culture strain, pH, cultivation techniques, and substrates used. In the initial stages of its biosynthesis, pullulan produced from glucose, maltose, or sucrose is characterized by a high molecular weight,[10] although the molecular weight distribution is broad and will become narrow late in the stationary growth phase because of an increase of the relative amounts of the high- and medium-molecular weight fractions. The polydispersity values reported for pullulan lie between 2.1 and 4.1 and are significantly lower when compared to other industrially important polysaccharides such as amylose and dextran. A possible explanation for this may be the mechanism of pullulan biosynthesis, which it thought to be regulated by a specific cell morphology of the fungus *A. pullulans.*[12]

2.1.2 Pullulan from *A. pullulans*

The producer of pullulan, *A. pullulans*, is a ubiquitous yeast-like fungus isolated commonly from the environment. It is found in forests, soil, water, litter, wood and plant and animal tissues. *A. pullulans* is a polymorphic fungus and its three distinctive forms are: elongated branched septate filaments, large chlamydospores, and smaller elliptical yeast-like cells.[10] The extent of a given polymorphic form is strongly affected by growth conditions. Often it has been reported that there is a correlation between pullulan formation and a particular morphology of *A. pullulans*, although there is a lot of controversy with respect to which morphology is responsible for pullulan production (reviewed by Singh et al., 2008).[10]

An undesirable characteristic feature of *A. pullulans* is the production of a dark pigment (characteristic to chlamydospores form), which is a melanin-like compound and is dark green to

black in color. Another undesirable characteristic of this fungus occurs during its growth; as the fermentation progresses, the culture viscosity increases due to an increase in the average molecular weight of the accumulated extracellular pullulan. Many, but not all, strains of *A. pullulans* are able to produce this polysaccharide, and a number of publications have reported the production of pullulan by other microorganisms (reviewed by Singh et al., 2008).[10]

2.1.3 Commercial production of pullulan

The commercial production of pullulan began in 1976 by the Hayashibara Company (Okayama, Japan). Pullulan films were commercialized in 1982 by the same company and they remain the principal commercial source of pullulan today. In 2003, the production was approximately 300 metric tons per year.[1] Food grade pullulan was approximately US $20/kg, and pharmaceutical grade (deionized) pullulan was approximately US $25/Kg.[1] In commercial production, *A. pullulans* is cultivated batch-wise on medium containing starch hydrolysates of dextrose, at 10-15% concentration.[10] The medium includes peptone, phosphate, and basal salts. Culture pH is initially adjusted to 6.5, and falls, especially during the first 24 h, to a final pH of approximately 3.5. Maximal culture growth occurs within 75 h, and optimal pullulan yields are obtained within about 100 h. Cultures are stirred and aerated, and the temperature is held at 30 ^{o}C. Yields greater than 70% of initial substrate are claimed. Culture conditions and strain selection are important in obtaining high molecular weight pullulan that is relatively free of melanin. *A. pullulans* cells are removed by filtration of diluted culture broth. Melanin is removed by treatment with activated charcoal, and pullulan is recovered and purified by precipitation with organic solvents, particularly alcohols. Pullulan may be further purified through the use of ultrafiltration and ion exchange resins. *A. pullulans* is considered to be one of the "black yeasts" and melanin removal is a unique problem that may add to the cost of pullulan production. Another peculiar quality control issue is the tendency for enzymes from *A. pullulans* to reduce the molecular weight of pullulan in late cultures. Comparative studies reveal that *A. pullulans* strains differ considerably with respect to growth, pullulan yield and cell morphology. Sugars such as sucrose, glucose, fructose, maltose, starch, or maltooligosaccharides can be sources for pullulan production by *A. pullulans*. Other sugars are used less frequently and give reduced

yields. Several methods and conditions for pullulan production have been reported (reviewed by Singh at al., 2008).[10] Wastes from the agricultural and food industries, such as deproteinized whey, beet molasses, sugar cane juice, and peat hydrolysate are also considered as economical and efficient substrates for pullulan production. Much of the published research in recent years has been concerned with improving the economics of production, mainly by identifying even less expensive feedstocks, isolating improved production strains, and developing alternative fermentation processes.

2.1.4 Pullulan biosynthesis

Despite intense investigations on cytological and physiological characteristics of *A. pullulans*, the mechanism of pullulan biosynthesis is still not fully understood. A rather accepted mechanism was proposed by Catley and McDowell (1982) after combining experimental results from previous researchers with their own results.[7] These results indicated that glucose, isomaltose, panose, and isopanose linked to lipid by pyrophosphate bonds are synthesized during pullulan biosynthesis. The concurrent production of both pullulan and the characterized glycolipids strongly suggested that the latter are intermediates in the assembly of this extracellular polysaccharide. Unlike bacterial dextrans, which are synthesized extracellularly by secreted glucansucrases, pullulan is synthesized intracellularly. It is proposed that the lipid acts as a carrier in the transport of pullulan to the outside of the plasma membrane.

Lipid linked glucosyl is formed by transfer of D-glucopyranosyl phosphate from UDPG to phospholipid (**Fig 2.2**). A further glucosyl residue is transferred with the formation of a (1→6)-α-D-glucosyl bond to produce lipid-linked isomaltosyl. Lipid-linked trisaccharides panose or isopanose would then be formed by transfer reactions between lipid-linked D-glucose and lipid-linked isomaltose by way of insertion mechanisms. Thus (1→6) bonds are formed by glucosyl transfer from the nucleotide donor (UDPG), whereas (1→4) bonds arise through transfer from lipid-linked precursors. Maltotriosyl repeating-unit could be incorporated into the macromolecule by the polymerization of either panosyl or isopanosyl moieties. Maltotetraosyl units could arise through the combination of panosyl and isopanosyl.

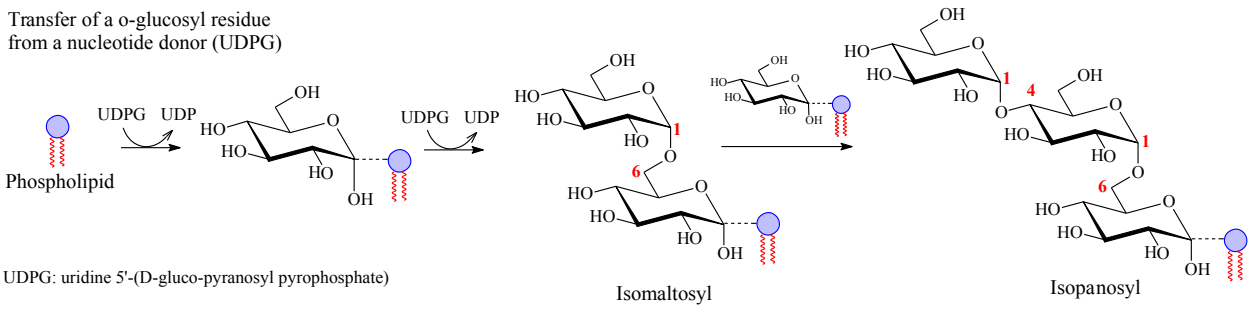

Figure 2.2 Proposed scheme for the synthesis of phospholipid-oligosaccharide intermediates that may participate in pullulan biosynthesis

Besides direct conversion of glucose residues into pullulan, another pathway was proposed, which involves polymerization of the carbohydrate precursors stored inside the cells. The evidence for this hypothesis was the inverse correlation between the concentrations of pullulan and content of intracellular glycogen. However the mechanism by which glycogen is transformed into pullulan is not well understood.[13]

2.1.5 Food industry and pharmaceutical applications

The applications of pullulan, mostly in the food and pharmaceutical industries, have been comprehensively reviewed.[1, 10] Its biomedical applications have also been recently reviewed.[14] There is a twenty year history of safe use of pullulan in Japan as a food ingredient and as a pharmaceutical bulking agent. Pullulan films have been used for various food applications in Japan, including food decorations for candies and bakery goods, in beverages, as a binder for seasoning, sheet for wrapping various food items, and as edible packaging material for instant noodles or packages of table top sweeteners. Pullulan film is commercially used in the US in Listerine PocketPacks® oral care strips.

Pullulan has several potential commercial applications, primarily in the food and pharmaceutical industries. It's edible, odorless, and flavorless, thus it can be used as food additive to improve appearance, reduce blemishes, and increase shelf life. It has excellent

adhesive properties and extremely low viscosity, being suitable for use in pan coating of chewing gums, chocolate, and candies, and also as low-viscosity filler in beverages and sauces. The viscosity of pullulan is not affected by heating, changes in pH and most metal ions. Pullulan may be incorporated in solid as well as liquid food in order to convey consistency and dispersibility. The excellent oxygen barrier properties, in addition to the fact that pullulan is not a readily digested carbon source for bacteria, molds, and fungi, guarantee the use of pullulan films in packaging and preservation. The oxygen resistance of pullulan films makes them suitable for protection of readily oxidized fats and vitamins in food. Also, the films are clear with excellent mechanical properties. The shapes of the films are retained during printing. They can be used for printing decoration in bakery products or thin films can serve as food coatings. Pullulan films are prepared by drying a pullulan solution (usually 5-10%) on a smooth surface and they can be as thin as 5-60 μm. Pullulan film formation can be used to entrap flavors, colors, and other active ingredients. Due to its excellent oxygen barrier properties these ingredients are effectively stabilized in the film. It was reported to be a slowly digested carbohydrate, being appropriate for incorporation into beverages and meal replacement products and also into dietetic foods designed for diabetics.

2.1.6 Chemical modifications and biomedical applications

In the past two decades there have been significant developments in the study of pullulan derivatives for diversified applications in the biomedical field including targeted drug and gene delivery, tissue engineering, wound healing, and diagnostic imaging. This is mainly due to its non-toxic, non-immunogenic, and biodegradable properties. The degradation rate of pullulan in serum is faster than that of dextran, a similar but more popular polysaccharide.[14] The degradation rate can be reduced or regulated by varying degrees of chemical modification.

In the pullulan structure, nine OH groups per repeating unit are available for substitution (**Fig 2.1**). The relative reactivity of these groups may vary greatly, depending on the solvents, reagents, and reaction conditions. Most pullulan derivatizations are intended to reduce its water solubility or to introduce charged or reactive groups for functionality. For the preparation of

polymer-drug conjugates, conversion of the polysaccharide into a reactive derivative is usually required. Various methods have been elaborated to convert pullulan to a reactive derivative in order to make possible the attachment of bioactive compounds. These derivatives involve mainly hydrophobically-modified pullulan with lipophilic-hydrophilic groups, cationic, amphoteric derivatives with both acidic and basic groups of different strengths, as well as sulfur-containing compounds.[14]

Pullulan substituted with cholesterol or fatty acids can be used to entrap and stabilize small molecules.[15] Pullulan has been sulfated,[16] chlorinated,[17] perfluoroalkylated,[18] and chloroalkylated.[17] Succinoylation[19] and chloroformate activation[20] of pullulan were performed. Other derivatives were prepared from the reaction of pullulan with isocyanate.[21] Selective oxidation at C-6 was readily achieved.[22] Carboxylation enhances its solubility in cold water. Cationic and anionic derivatives have been prepared and evaluated for gene delivery.[23] [24] Pullulan derivatives are promising as conjugates with drugs.[25] [26] In this review, the most significant chemical modifications performed on pullulan will be discussed and also the properties of products with respect to their biomedical applications.

Jung, Jeong and Kim (2003) prepared pullulan acetate (PA) derivatives with different degrees of acetylation and self-assembling nanospheres of these hydrophobized pullulans in water were studied as a carrier for clonazepam.[27] Acetylation of pullulan was conducted in formamide, with pyridine as catalyst and acetic anhydride as the acetylating agent. PA was readily soluble in DMSO, DMF, tetrahydrofuran (THF), dichloromethane, chloroform, acetone, and 1,4-dioxane. Nanoparticles were prepared by dialysis with different solvents, which had great influence on particle size and drug loading, giving remarkably different drug release profiles. Higher drug loadings and bigger particle sizes resulted in lower drug release rates. These behaviors were associated with crystallization of the drug at higher loadings and the different diffusion rates of drug molecules from the particles. Increased degree of acetylation afforded nanospheres with slower drug release rate.

As discussed above, Jung et al. (2003) has investigated the morphology and self-association behavior of pullulan acetate nanoparticles for the application to controlled drug release. The highest acetylation degree of the PA that they prepared was 87%, which corresponds to a degree of substitution (DS) 2.6. On the other hand, Teramoto and Shibata (2006) has

reported details on solubility, biodegradability, thermal, and mechanical properties of PA.[28] Teramoto and Shibata (2006) prepared PA with various degrees of substitution by the reaction of pullulan with acetyl chloride in dimethylacetamide (DMAc) in the presence of pyridine. The solubilities of these derivatives are showed in the **Table 2.1**. It is considered that the solubility of PA is influenced by molecular weight as well as DS. While Jung et al. (2003) did not give any information about molecular weight, Teramoto and Shibata (2006) reported some reduction in molecular weight of the products. They stated that the use of acetyl chloride afforded the product with a higher molecular weight, compared to the acetic anhydride method in their prior study, but these data are not published. All the PAs exhibited a clear T_g, while pullulan showed no clear T_g. Decomposition temperature (T_d) and glass transition temperature (T_g) increased with increasing DS. The PA with DS 3.0 had the highest T_d (363 ^oC). T_d of pullulan is 295 ^oC. Furthermore, biodegradability of PA, just as in cellulose acetates, decreased with higher degrees of acetylation. PA with DS 1.0 and 1.7 have biodegradability comparable to pullulan, while PA with DS 3.0 did not show any biodegradation until 30 days later.

Table 2.1 Solubility of PA in several solvents

Solvent	Sample				
	Pullulan	**PA**			
		DS 1.0	DS 1.7	DS 2.4	DS 3.0
Water	O	Δ	X	X	X
DMSO	O	O	O	O	Δ
DMF	Δ	O	O	O	Δ
Pyridine	Δ	O	O	O	Δ
Acetone	X	X	X	Δ	Δ
Ethyl acetate	X	X	X	Δ	Δ
THF	X	X	X	Δ	Δ
Chloroform	X	X	X	Δ	Δ
Toluene	X	X	X	X	Δ

O Soluble Δ Partially soluble X Insoluble

Long chain esters of pullulan were prepared by reaction of pullulan with stearic anhydride in DMAc and iodine as catalyst.[29] The product was soluble in DMSO, DMAc, and acetone. More complex esters such as pullulan abietate[30] with different degrees of substitution were synthesized homogeneously in DMAc via *in situ* activation of abietic acid with *p*-toluenesulfonyl chloride, *N,N'*-carbonyldiimidazole or iminium chloride formed from oxalyl chloride/DMF. Samples with a DS $\leq$ 0.14 were soluble in water and the higher DS products were mostly soluble in DMSO and DMAc. Acylation of pullulan by ring-opening of lactones was also reported.[31] Reaction was performed with ε-caprolactone and [L]-lactide using a tin octanoate [$Sn(Oct)_2$] catalyst system in DMSO. The products from ring opening of caprolactone had solubility similar to pullulan, while the pullulan derivatives produced by [L]-lactide ring opening were no longer soluble in water, but showed solubility in both acetone and methanol.

The most common anionic pullulan derivative is carboxymethylpullulan (CMP) (**Fig 2.3**). CMP is a promising polymeric carrier for many drugs since introduction of negative charges into the macromolecules of CMP results in prolonged retention of the polymer within the organism.[32] This pullulan ether was synthesized by reaction of pullulan in aqueous isopropyl alcohol with sodium chloroacetate.[33] The distribution of carboxymethyl substituents in the pullulan was investigated by high resolution NMR spectroscopy on very short oligomers obtained by acid hydrolysis.[34] The reactivity order was found to be OH-2 > OH-4 > OH-6 > OH-3 (**Fig 2.3**). CMP was hydrophobically modified by esterification of the carboxyl groups with long alkyl chains.[35] These derivatives self-assemble in aqueous media and efficiently solubilize hydrophobic drugs. Amidation with perfluoroalkylamines ($C_7F_{15}CH_2NH_2$) also furnished hydrophobic derivatives of CMP.[18] As opposed to introducing the hydrophobic groups through ester or amidic linkages on carboxylic groups, Mocanu et al. (2004) have prepared hydrophobic anionic derivatives by introducing palmitoyl groups to crosslinked CMP through ester linkages on the hydroxyl groups. This approach gave derivatives containing the same anionic charge as the anionic precursor.[36] Ampholytic compounds were synthesized by coupling of CMP with dimethylaminopropylamine activated by 1-ethyl-3-[3-(dimethylamino)propyl]carbodiimide (EDC).[37] Additionally, cross-linking of such modified polysaccharides has been performed. CMP hydrogels were prepared under aqueous conditions with adipic acid dihydrazide as cross-linker in the presence of EDC. The entrapment capacity of these hydrogels was evaluated with cationic and amphiphilic

molecules.[24] Other anionic derivatives such as sulfoethyl and sulfopropyl pullulan were also prepared by Picton et al.[33]

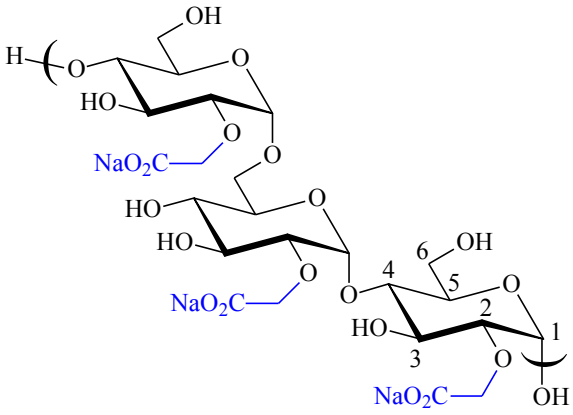

Carboxymethylpullulan
(CMP)

Figure 2.3 Chemical structure of carboxymethylpullulan showing substitution at C-2

Pullulan-drug conjugates have been investigated for application in chemotherapy. Low pH is a unique characteristic of the tumor microenvironment, therefore a number of pH-responsive pullulan-drug conjugates have been prepared. Different approaches were used to synthesize pullulan-doxorubicin conjugates. Doxorubicin (DOX) is a drug currently used in cancer therapy and the high dose necessary for treatment causes several side effects. Interesting results were obtained when CMP was conjugated to DOX through different types of peptide linkers.[38] Plasma and tissue distribution of CMP-DOX conjugates in rats with carcinosarcoma were compared with that of free DOX. CMP-DOX conjugates were found to have a longer circulation time in plasma and higher accumulation in the tumor. Conjugates were also distributed in the reticuloendothelial organs, such as liver, spleen, and bone marrow; however, the tissue concentrations of the conjugates in the heart, lung, and muscle were lower than those of DOX. The authors showed that *in vivo* drug release results were in agreement with *in vitro* release studies from Pull-DOX conjugates. Drug loads varied from 7-17%, depending on the peptide linker. Recently, Lu et al. (2009)[25] prepared pH-sensitive CMP-DOX conjugate nanoparticles. The carboxyl group in CMP was converted to hydrazide by condensation with hydrazine hydrate in water with EDC as condensing agent. The DOX was then attached to

pullulan through a pH-sensitive hydrazone bond. The nanoparticles were spontaneously formed because of hydrophobic interactions of DOX. The drug content in the conjugate was only 3.18% because precipitation occurred at higher concentrations. *In vitro* studies showed higher and faster release at pH 5.0 than at pH 7.4 buffer; but compared to free DOX, CMP-DOX conjugate nanoparticles were less potent against 4T1 mouse breast cancer cells.

Incorporation of carboxylic groups into pullulan was also achieved by reaction with succinic anhydride, 4-nitrophenylchloroformate or isocyanates. A series of succinoylated pullulan derivatives were prepared with a degree of substitution ranging from 0 to 100%.[19] The authors used NMR as a tool to investigate the selectivity of the reaction, which occurs mostly at C-6. The resulting derivatives could be coupled to amines through activation with *N,N'*-carbonyldiimidazol. The succinoylated pullulan was interestingly used in a multicompartimental system for oral delivery of diclofenac. Cellulose acetate butyrate (CAB) microcapsules containing aminated polyvinylacetate (PVA) microspheres loaded with diclofenac were also loaded with succinoylated pullulan, and the role of this derivative was essential in this multicompartimental system. CAB is not an enterosoluble polymer and loaded PVA microspheres do not swell enough to produce the rupture of CAB shell either in gastric or in intestinal fluids. Succinoylated pullulan microspheres do not swell in acidic pH, but swell up to 20-times in intestinal fluids causing the rupture of CAB shell and facilitating the escape of loaded PVA microspheres.[39]

Isocyanate-modified pullulans were synthesized by the reaction of pullulan with phenyl and hexyl isocyanates in DMSO/toluene. It was suggested that reactivity of pullulan to phenyl isocyanate is also highest for the C-6 hydroxyl group, but such assumption was based only on qualitative observation of the ^{1}H NMR spectra of the product.[21] Chloroformate activation of pullulan and further reaction with an amine also leads to carbamate ester derivatives.[20]

Another hydrophobic derivative that has been extensively investigated for its biomedical applications is cholesterol-pullulan (CHP). It forms stable self-aggregates that can form complexes with various hydrophobic drugs and also with macromolecules such as proteins (insulin) (**Fig 2.4**).[15, 40] Hydrophobic interactions are thought to be the main driving force to form such complexes.[15] These CHP complexes are understood to have a hydrophobic domain formed by the cholesterol groups and a hydrophilic domain formed by the polysaccharide. CHP was

synthesized by reaction of pullulan with a cholesterol derivative, cholesteryl *N*-(6-isocyanatohexyl)carbamate in toluene and with pyridine. The nanoparticles of hydrophobized pullulan can have application as drug-delivery systems and in the stabilization of proteins.

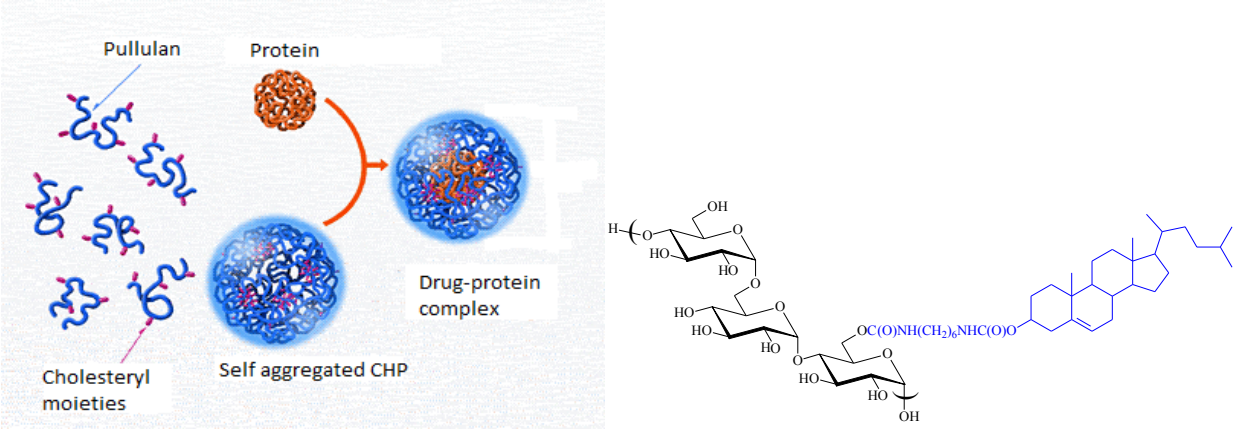

Figure 2.4 Chemical structure of cholesterol-pullulan and formation of self-aggregate complex

Another interesting application of these hydrophobized pullulan nanoparticles is that they can function as artificial chaperones. Chaperones are proteins that assist the non-covalent folding or unfolding and the assembly or disassembly of other macromolecular structures. CHP can trap denatured proteins and prevent their aggregation. The structure of the CHP nanogel is then disrupted by the addition of cyclodextrins and the protein complexed with the nanogel is released and folds into its native form, with almost 100% of the enzyme activity recovered. This is similar to the two-step mechanism of a molecular chaperone, that is, capture of a denatured protein and release of the refolded protein.[41, 42] Similar molecular chaperone-like activity in protein refolding was investigated for spiropyrane-bearing pullulan nanogel.[43] In this case, the nanogel controls the refolding of protein by photostimulation. Pullulan derivatives are also promising as antigen delivery systems for vaccines. Complexes of CHP nanoparticles that contain tumor antigens were administered as vaccines in clinical studies, which have shown that this vaccine could be administered repeatedly without serious adverse effects and induced antigen cell and humoral immunity.[44]Even tumor regressions were observed in cancer patients.

The reaction of pullulan with mesyl chloride can either furnish the chlorodeoxy or O-mesyl pullulan, depending on the reaction conditions. These derivatives can be useful intermediates in nucleophilic substitutions, leading to other interesting products. Mocanu, Constantin and Carpov (1996) studied the influence of temperature, solvent, and reagent ratios on the degree of substitution with chlorodeoxy and/or mesyl ester groups.[45] It was reported that the main product in DMF was chlorodeoxypullulan, while in pyridine, at low temperatures, it was the mesyl ester pullulan. In DMAc, the two products are formed in about 2:1 ratio. Both pullulan derivatives were found to become hydrophobic, their water regain decreased with DS increase.

Mocanu et al. (1999) has also studied the chloroalkylation reaction of crosslinked pullulan with chloroalkyl chlorides (C2-C5).[17] The effect of temperature, solvent, and reagent ratios on the degree of substitution was evaluated. The maximum DS value obtained was 2.44 in DMAc and the lowest DS obtained was in DMSO, due to the side reaction between DMSO and the acid chlorides forming paraformaldehyde. Temperature was found to have little influence on the chloroacetylation of pullulan, unlike the chloroacetylation of dextran, which starts just at 40 ^{o}C and rapidly increases from 40 to 60 ^{o}C. This higher reactivity for pullulan is thought to be due to the higher content of primary hydroxyl groups of pullulan in comparison with dextran. These new derivatives obtained can be used as intermediates for chemical modifications with substances containing amine, carboxyl, hydroxyl, thiol or other groups.

Recently, cationized pullulans have been investigated as a non-viral gene delivery carrier. It was demonstrated that some spermine-pullulan samples enabled plasmid DNA to efficiently deliver to the liver.[46, 47] Spermine pullulan derivatives were prepared by reaction of pullulan with spermine. Spermine is ubiquitously found at high concentrations in human cells, where it is thought to naturally interact with nucleic acids.[48] Derivatives with different spermine percentages were evaluated for gene expression, which was dependent on the percentage of spermine in the pullulan and also the pullulan molecular weight.[49, 50] However, the liver targetability of pullulan was not investigated in relation to the spermine-content extent.

Another cationic pullulan derivative was prepared and evaluated as a gene transfer agent. Aminated pullulan microspheres were prepared by chemically crosslinking pullulan with 1-chloro-2,3-epoxypropane, followed by amination with N,N-diethyl-2-chloroethyl amine

hydrochloride. All the produced diethylaminoethyl-pullulan (DEAE-Pullulan) microspheres were able to quantitatively load DNA with no degradation observed after 14 days.[23] DEAE-pullulan (not crosslinked) was also employed as an intermediate for the synthesis of amphiphilic compounds (**Fig 2.5**).[51] The cationic derivative was alkylated with different alkyl chains (C_{10}, C_{12}, and C_{16}). Furthermore, during reaction of pullulan with DEAE, a secondary addition of DEAE occurred (DEAE-DEAE-Pullulan) and thus the final product had quaternary ammonium functions. These quaternary functions constituted a permanent cationic charge and imparted partial water solubility to the final product. These derivatives also had higher solubility in organic solvents and showed a high aggregation behavior due to intermolecular hydrophobic associations between the alkyl chains.[51, 52]

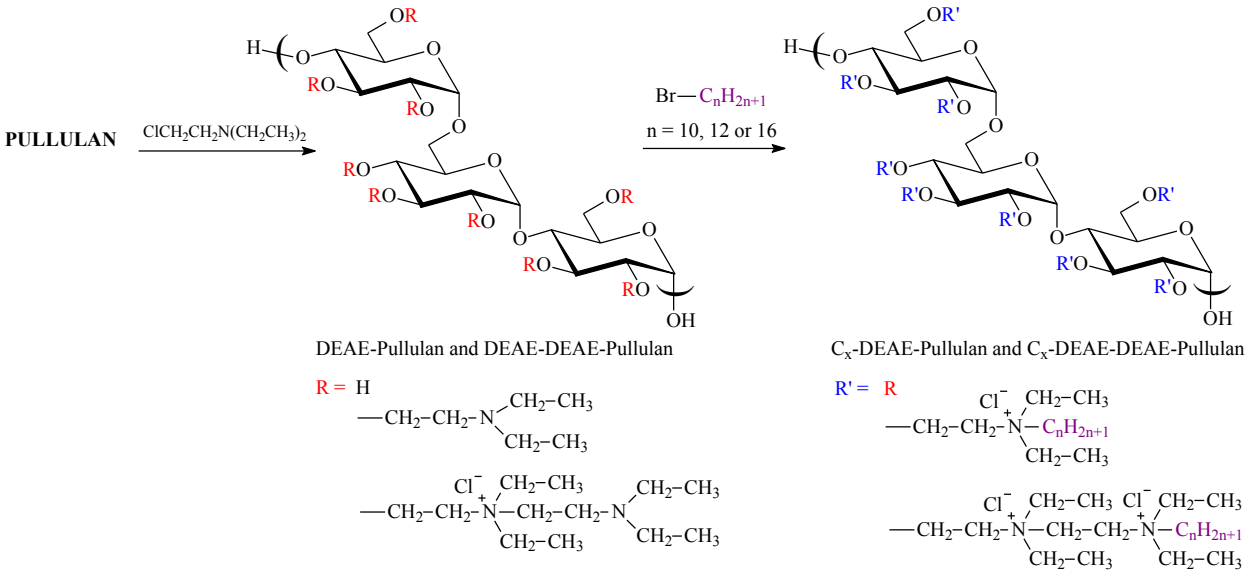

Figure 2.5 Synthesis of DEAE-pullulan and its amphiphilic derivatives

More recently, it has been shown that pullulan exhibits a greater affinity towards the liver compared to other water-soluble polymers, such as poly(ethylene glycol)[32] and dextran.[53] Hepatic uptake of intravenously administered pullulan is markedly reduced by the co-administration of asialofetuin and arabinogalactan having a high affinity to the corresponding cell receptors.[54] This indicates that pullulan, in contrast with dextran, binds asialoglycoprotein

receptors and penetrates the hepatocyte membrane via receptor-mediated endocytosis. Furthermore, the liver vasculature is comprised of discontinuous blood vessels and negatively charged cell surfaces, which allows most positively charged water-soluble substances to penetrate through the vascular walls, resulting in their high accumulation in the extravascular tissue of the liver.[55] The characteristics of liver morphology may be one factor in determining the high affinity of pullulan towards the liver in the case of cationic pullulan derivatives, while biospecific interactions of pullulan with liver receptors are thought to be the main reason for the great affinity of pullulan toward the liver.

Reaction of pullulan with cyanuric chloride gave cyanurated pullulan, which was conjugated with interferon (IFN; effective against viral hepatitis, but frequent and high dose injections cause several side effects).[26] When injected intravenously to mice, this IFN-pullulan conjugate was effective in targeting IFN to the liver. Consequently, antiviral response was induced at much lower dose and for longer time than those of free IFN injection. Similar *in vivo* results were achieved by IFN-pullulan conjugate through metal coordination. Pullulan was first esterified with a coordinating ligand (diethylenetriaminepentaacetic acid), zinc ion was added along with IFN-β, and a coordination complex was formed.[56, 57]

In view of the importance of polysaccharide sulfates in several biomedical applications, for example, heparin sulfate as anticoagulant[58] and dextran sulfate in the treatment of peptic ulcer,[59] sulfation of pullulan was studied in two different solvent complexes, SO_3·Py and SO_3·DMF.[16] A wide range of DS (0.08-1.45) was obtained and was influenced by reaction time and temperature. Samples with the same DS, obtained in SO_3·DMF, had lower viscosity, possibly because in DMF the reaction is homogeneous, while pullulan only swells in Py. Therefore, products will have different substitution patterns and thus distinct properties. When compared to dextran, higher substitution was attained for pullulan in SO_3·DMF, whereas in SO_3·Py, substitution was higher for dextran. This trend was attributed to the better solubility of pullulan and dextran in DMF and Py respectively. The authors didn't make any correlation, but this could also explain the higher reaction rate for pullulan in DMF complex. Mähner, Lechner and Nordmeier (2001) determined for the first time, by ^{13}C NMR spectroscopy, that the reactivity of OH groups towards sulfation in SO_3·Py occurred in the order C-6 > C-3 > C-2 > C-4, which is the same as that for dextran (no C-6 sulfation being possible for this

polysaccharide).[60] Alban, Schauerte and Franz (2002) and has found similar activity results, with opposite trend for C-2 and C-3.[61] In this case the substitution and DS were calculated from pullulan sulfate hydrolysis followed by methylation of the components and high performance liquid chromatography (HPLC) analysis. Alban et al. (2002) has also evaluated the anticoagulant activity of the sulfated pullulans, and they proved to be potent anticoagulants reaching the activity of heparin. Their activity improves with increasing DS and molecular weight (MW). Based on results from coagulation assays, that record interactions at different stages of the coagulation, it was possible to have information about the mode of action of the anticoagulants. They specifically interfere with several stages of the coagulation cascade, and these interactions have different requirements on the chemical structure. The distribution of the sulfate groups on the various positions of the glucose markedly influences the activity and the action profile, for example, activity is improved with increasing substitution of sulfate groups in positions 2, 3 and 4.

Pullulan can be readily oxidized at C-6 to the carboxylic acid by using the free radical nitroxyl TEMPO (2,2,6,6-tetramethyl-1-piperidinyloxy) and a primary oxidant such as sodium hypochlorite (NaOCl) (**Fig 2.6**). De Nooy, Basemer and Van Bekkum (1995)[62] showed that selectivity for this reaction is higher than 95%, and no side products were detected. The 6-carboxy-pullulan obtained was comprehensively characterized by ^{13}C NMR.

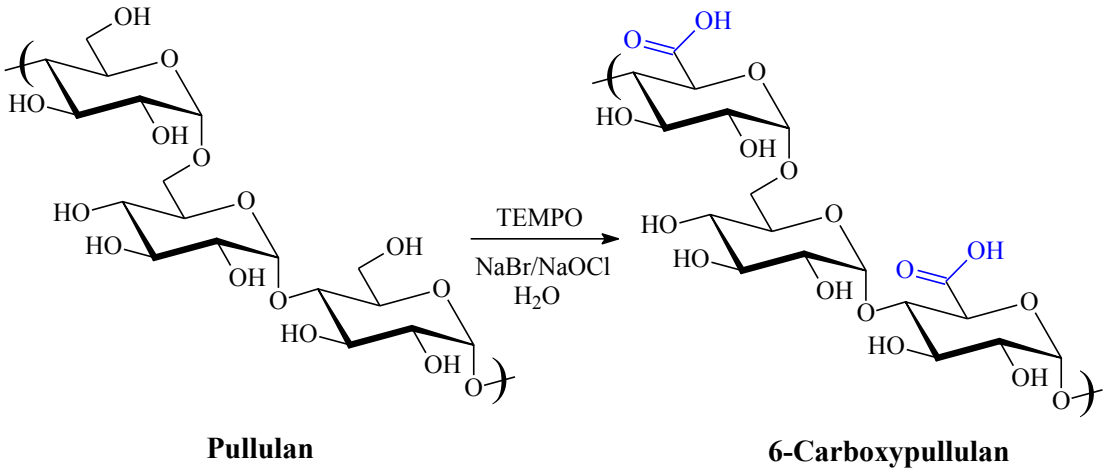

Figure 2.6 Oxidation of pullulan with TEMPO

The degree of oxidation can be easily controlled by adjusting the sodium hypochlorite stoichiometry and the reaction is highly selective for C-6 because of the formation of a sterically cyclic intermediate (**Fig 2.7**). The actual oxidant is the nitrosonium salt. First, in the reaction conditions, the nitroxyl radical is converted into the more powerful nitrosonium salt. The salt will then react with C-6 hydroxy of pullulan and form a sterically cyclic intermediate. The aldehyde is first formed, which is then further oxidized to the carboxylic acid. The reduced form of TEMPO is oxidized to the radical and the nitrosonium ion is continuously regenerated during the reaction.

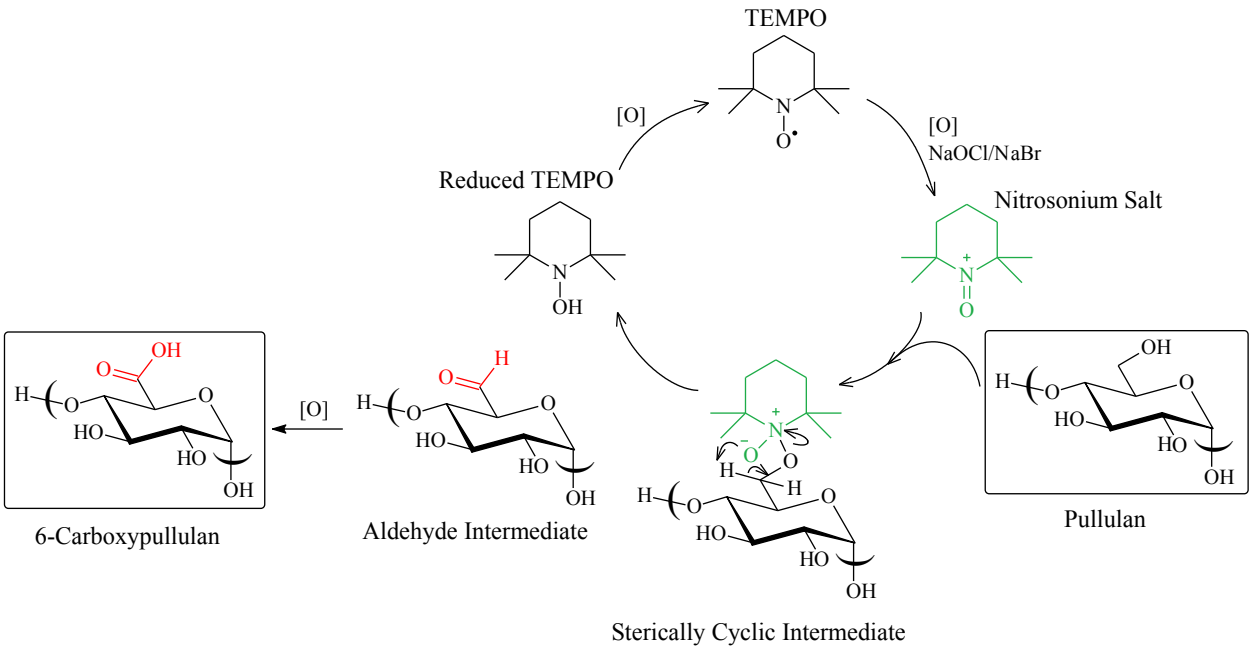

Figure 2.7 Mechanism for the oxidation of pullulan with TEMPO

2.2 Drug Delivery

Drug delivery is the method or process of administering a pharmaceutical compound to achieve a therapeutic effect in humans or animals. Drug delivery technologies are responsible for modifying drug release profile, absorption, distribution and elimination for the benefit of improving product efficacy and safety, as well as patient convenience and compliance. Most common drug delivery routes include the preferred oral delivery, transdermal, inhalation and intravenous routes.[63] Transdermal administration is a comfortable method for the patients, there

is however only a few drug preparations that are suitable for this mode of delivery. Inhalation is a fast delivery method and allows for the user to control the amount of drug they are receiving. Disadvantages of inhalation are: Difficulties in regulating the exact amount of dosage and in the clearance of the drug from the lungs, and some patients may have difficulties administering a drug via inhaler. Intravenous delivery is also a fast delivery method. It is a vital mode for patients in acute care situations and precise doses can be administered. Intravenous is though the most dangerous route of administration because it bypasses most of the body's natural defenses, exposing the user to health problems such as hepatitis, abscesses, infections, and undissolved particles or additives/contaminants. Furthermore, patients are not typically able to self-administer, and the need for qualified professionals leads to high expense and/or poor patient compliance. Oral drug delivery is the most preferred method of patients because it is easy to take pills/capsules; compliance is higher than for any other form of administration. Administered dose can be very precise. Drawbacks include barriers in the gastrointestinal (GI) tract that lead to low bioavailability for many drugs, resulting in imprecision and variability in delivered dose.[63] Furthermore, compliance can be compromised by having to take multiple pills, of large size, and very frequently. A modest sized pill, once a day is ideal.

The term bioavailability is used to describe the fraction of an administered dose of drug that reaches the systemic circulation intact, one of the principal pharmacokinetic properties of drugs. By definition, when a medication is administered intravenously, its bioavailability is 100%. However, when administered via other routes (such as orally), its bioavailability decreases (due to incomplete absorption and first-pass metabolism) or may vary from patient to patient (due to inter-individual variation). Bioavailability is one of the essential criterias in pharmacokinetics, as bioavailability must be considered when calculating dosages for non-intravenous routes of administration. Various physiological factors reduce the availability of drugs prior to their entry into the systemic circulation.[64]

For a drug to be effective, it has to reach the systemic circulation and ultimately its site of action. From the moment we take a pill to the moment the drug reaches the systemic circulation, the drugs have to overcome various biological barriers which are imposed by the body. When a drug is administered orally, it will be directed through the digestive system until it reaches the systemic circulation. Thus, one important requirement is that the drug has to be soluble in the

aqueous environment of the GI tract. After a drug is swallowed, it reaches the stomach, where it has to survive the acidic pH and the digestive enzymes present in the stomach. Some drug absorption occurs in the stomach (desired specially for stomach treatment). From the stomach, the drug will move to the small intestine, from which it may be absorbed into the bloodstream. As the pH level changes in the small intestine and gradually becomes basic, more enzymes are activated that can degrade the drug. Small, finger-like structures called villi, each of which is covered with even smaller hair-like structures called microvilli, improve the absorption of molecules by providing a large surface area of the small intestine. During absorption, the drug is faced with the challenge of traversing a highly hydrophobic barrier, the epithelium layer of the gastrointestinal tract. Blood containing the absorbed drug is carried away from the small intestine via the hepatic portal vein and goes to the liver for filtering, removal of toxins, and processing to be further excluded by the kidneys. Many drugs that are absorbed through the GI tract are substantially metabolized by the liver before reaching the circulatory system. This is known as the first pass effect. The four primary systems that affect the first pass effect of a drug are the enzymes of the GI lumen, gut wall enzymes, bacterial enzymes, and hepatic enzymes. Finally, after the drug has survived all these barriers it has to reach its site of action. It should act only on the target organ, as it may elicit unwanted side effects if it acts on receptors elsewhere. Whether a drug is taken with or without food will also affect absorption (fatty foods enhance solubility/absorption of nonpolar drugs). Other drugs taken concurrently may alter absorption and first-pass metabolism. Disease states affecting liver metabolism or gastrointestinal function will also have an effect.

As it was just discussed, the efficacy of a drug depends on its solubility and absorption into the systemic circulation and its availability at the site of action. Poor water solubility of a drug is associated with variability in its absorption. Such variability can lead to reduced efficacy of the drug. Variability in the bioavailability of a drug impacts on patient compliance, disease management, and quality of life. It is estimated that approximately 50% of existing therapeutic agents have poor solubility and that many emerging leads from pharma drug discovery programs have solubility limitations which hinder their development. Improving the solubility of a drug may therefore lead to improvement in the variability of drug levels in systemic circulation, resulting in an enhancement of new therapeutics and a reduction in the required therapeutic dose.

Poor solubility and poor oral bioavailability have been addressed by the pharmaceutical industry using a number of strategies; changing the physiochemical properties of the drug, complexing the drug with cyclodextrins, formulating the drug in lipid excipients or by conversion of the drug into an amorphous form. Development of amorphous drugs has been an inspiring topic in pharmaceutical research for both industrial and academic scientists.[65, 66] Amorphous drugs are advantageous over their crystalline counterparts with higher solubility, faster dissolution rate, and enhanced oral bioavailability. On the other hand, amorphous solids are physically unstable relative to the crystalline state and the stability of amorphous drugs against crystallization is critical for pharmaceutical development. The incorporation of pharmaceutical actives into polymer matrices is a well-recognized strategy for conversion of a drug into an amorphous form and stabilization of the drug against crystallization.[67] Furthermore, such formulations can also provide sustained release of the drug in the GI tract. Such amorphous drug–polymer complex, called an amorphous dispersion, is generated by methods such as spray drying and hot-melt extrusion. The mechanisms as to why solid dispersions can stabilize amorphous drugs are not yet fully understood but have several commonly accepted viewpoints.[68] For example, the addition of a high-T_g (glass transition temperature) polymer elevates the T_g of the amorphous system and therefore may reduce its molecular mobility required for crystallization at higher storage temperatures and humidities. Thermodynamically the drug has a lower chemical potential when mixed with a polymer, resulting in a change of crystallization driving force. It is also generally accepted that drug–polymer intermolecular interactions are important for the stabilization of the solid dispersion. Underpinning these considerations is an important assumption that the two components (drug and polymer) are mixed homogeneously at the molecular level. This assumption is directly related to the solubility (for the crystalline drug) and/or miscibility (for the amorphous drug) in the polymer matrix. Amorphous formulations in polymer matrices are becoming a rather well-known technique for enhancing drug solubility and bioavailability.[69]

2.3 References

1. Leathers, T. D., Biotechnological production and applications of pullulan. *Applied Microbiology and Biotechnology* **2003,** *62* (5-6), 468-473.

2. Bauer, R., Physiology of *Dematium pullulans* de Bary. *Zentralbl Bacteriol Parasitenkd Infektionskr Hyg Abt* **1938,** *2* (98), 133-167.

3. Bernier, B., The production of polysaccharides by fungi active in the decomposition of wood and forest litter. *Can. J. Microbiol.* **1958,** *4*, 195-204.

4. Bender, H.; Lehmann, J.; Wallenfels, K., Pullulan, an extracellular glucan from *Pullularia pullulans*. *Biochim Biophys Acta* **1959,** *36*, 309-316.

5. Bender, H.; Wallenfels, K., Investigations on pullulan: II. Specific degradation by means of a bacterial enzyme. *Biochemische Zeitschrift* **1961,** *334*, 79-95.

6. Bouveng, H. O.; Kiessling, H.; Lindberg, B.; McKay, J., Polysaccharides elaborated by *Pullularia pullulans*. I. The neutral glucan synthesized from sucrose solutions. *Acta Chemica Scandinavica* **1963,** *16*, 615-622.

7. Catley, B. J.; Mcdowell, W., Lipid-linked saccharides formed during pullulan biosynthesis in *Aureobasidium-pullulans*. *Carbohydrate Research* **1982,** *103* (1), 65-75.

8. Catley, B. J.; Robyt, J. F.; Whelan, W. J., A minor structural feature of pullulan. *Biochemical Journal* **1966**, 5P-8P.

9. Catley, B. J.; Ramsay, A.; Servis, C., Observations on the structure of the fungal extracellular polysaccharide, pullulan. *Carbohydrate Research* **1986,** *153* (1), 79-86.

10. Singh, R. S.; Saini, G. K.; Kennedy, J. F., Pullulan: Microbial sources, production and applications. *Carbohydrate Polymers* **2008,** *73* (4), 515-531.

11. Fishman, M. L.; Damert, W. C.; Phillips, J. G.; Barford, R. A., Evaluation of root-mean-square radius of gyration as a parameter for universal calibration of polysaccharides. *Carbohydrate Research* **1987,** *160*, 215-225.

12. Shingel, K. I., Current knowledge on biosynthesis, biological activity, and chemical modification of the exopolysaccharide, pullulan. *Carbohydrate Research* **2004,** *339* (3), 447-460.

13. Simon, L.; Bouchet, B.; Bremond, K.; Gallant, D. J.; Bouchonneau, M., Studies on pullulan extracellular production and glycogen intracellular content in Aureobasidium pullulans. *Canadian Journal of Microbiology* **1998,** *44* (12), 1193-1199.

14. Rekha, M. R.; Sharma, C. P., Pullulan as a promissing biomaterial for biomedical applications: a perspective. *Trends. Biomater. Artif. Organs* **2007,** (20), 116-121.

15. Akiyoshi, K.; Kobayashi, S.; Shichibe, S.; Mix, D.; Baudys, M.; Kim, S. W.; Sunamoto, J., Self-assembled hydrogel nanoparticle of cholesterol-bearing pullulan as a carrier of protein drugs: Complexation and stabilization of insulin. *Journal of Controlled Release* **1998,** *54* (3), 313-320.

16. Mihai, D.; Mocanu, G.; Carpov, A., Chemical reactions on polysaccharides: I. Pullulan sulfation. *European Polymer Journal* **2001,** *37* (3), 541-546.

17. Mocanu, G.; Vizitiu, D.; Mihai, D.; Carpov, A., Chemical reaction on polysaccharides: V. Pullulan chloroalkylation. *Carbohydrate Polymers* **1999,** *39* (3), 283-288.

18. Glinel, K.; Huguet, J.; Muller, G., Comparison of the associating behaviour between neutral and anionic alkylperfluorinated pullulan derivatives. *Polymer* **1999,** *40* (25), 7071-7081.

19. Bruneel, D.; Schacht, E., Chemical modification of pullulan .3. Succinoylation. *Polymer* **1994,** *35* (12), 2656-2658.

20. Bruneel, D.; Schacht, E., Chemical modification of pullulan .2. Chloroformate activation. *Polymer* **1993,** *34* (12), 2633-2637.

21. Shibata, M.; Asahina, M.; Teramoto, N.; Yosomiya, R., Chemical modification of pullulan by isocyanate compounds. *Polymer* **2001,** *42* (1), 59-64.

22. Bragd, F. L.; Besemer, A. C.; Van Bekkum, H., TEMPO-derivatives as catalysts in the oxidation of primary alcohol groups in carbohydrates. *Journal of Molecular Catalysis a-Chemical* **2001,** *170* (1-2), 35-42.

23. Constantin, M.; Fundueanu, G.; Cortesi, R.; Esposito, E.; Nastruzzi, C., Aminated polysaccharide microspheres as DNA delivery systems. *Drug Delivery* **2003,** *10* (3), 139-149.

24. Dulong, V.; Le Cerf, D.; Picton, L.; Muller, G., Carboxymethylpullulan hydrogels with a ionic and/or amphiphilic behavior: Swelling properties and entrapment of cationic and/or hydrophobic molecules. *Colloids and Surfaces a-Physicochemical and Engineering Aspects* **2006,** *274* (1-3), 163-169.

25. Lu, D. X.; Wen, X. T.; Liang, J.; Gu, Z. W.; Zhang, X. D.; Fan, Y. J., A pH-sensitive nano drug delivery system derived from pullulan/doxorubicin conjugate. *J Biomed Mater Res B* **2009,** *89B* (1), 177-183.

26. Xi, K. L.; Tabata, Y.; Uno, K.; Yoshimoto, M.; Kishida, T.; Sokawa, Y.; Ikada, Y., Liver targeting of interferon through pullulan conjugation. *Pharmaceutical Research* **1996,** *13* (12), 1846-1850.

27. Jung, S. W.; Jeong, Y. I.; Kim, S. H., Characterization of hydrophobized pullulan with various hydrophobicities. *International Journal of Pharmaceutics* **2003,** *254* (2), 109-121.

28. Teramoto, N.; Shibata, M., Synthesis and properties of pullulan acetate. Thermal properties, biodegradability, and a semi-clear gel formation in organic solvents. *Carbohydrate Polymers* **2006,** *63* (4), 476-481.

29. Hussain, M. A.; Shahwar, D.; Hassan, M. N.; Tahir, M. N.; Iqbal, M. S.; Sher, M., An efficient esterification of pullulan using carboxylic acid anhydrides activated with iodine. *Collection of Czechoslovak Chemical Communications* **2010,** *75* (1), 133-143.

30. Hussain, M. A.; Heinze, T., Unconventional synthesis of pullulan abietates. *Polymer Bulletin* **2008,** *60* (6), 775-783.

31. Donabedian, D. H.; McCarthy, S. P., Acylation of pullulan by ring-opening of lactones. *Macromolecules* **1998,** *31* (4), 1032-1039.

32. Yamaoka, T.; Tabata, Y.; Yoshito, I., Body distribution profile of polysaccharides after intravenous administration. *Drug Delivery* **1993,** *1* (1), 75-82.

33. Picton, L.; Mocanu, G.; Mihai, D.; Carpov, A.; Muller, G., Chemically modified exopolysaccharide pullulans: Physico-chemical characteristics of ionic derivatives. *Carbohydrate Polymers* **1995,** *28* (2), 131-136.

34. Glinel, K.; Sauvage, J. P.; Oulyadi, H.; Huguet, J., Determination of substituents distribution in carboxymethylpullulans by NMR spectroscopy. *Carbohydrate Research* **2000,** *328* (3), 343-354.

35. Henni-Silhadi, W.; Deyme, M.; Boissonnade, M. M.; Appel, M.; Le Cerf, D.; Picton, L.; Rosilio, V., Enhancement of the solubility and efficacy of poorly water-soluble drugs by hydrophobically-modified polysaccharide derivatives. *Pharmaceutical Research* **2007,** *24* (12), 2317-2326.

36. Mocanu, G.; Mihai, D.; LeCerf, D.; Picton, L.; Muller, G., Synthesis of new associative gel microspheres from carboxymethyl pullulan and their interactions with lysozyme. *European Polymer Journal* **2004,** *40* (2), 283-289.

37. Souguir, Z.; Roudesli, S.; About-Jaudet, E.; Le Cerf, D.; Picton, L., Synthesis and physicochemical characterization of a novel ampholytic pullulan derivative with amphiphilic behavior in alkaline media. *Journal of Colloid and Interface Science* **2007,** *313* (1), 108-116.

38. Nogusa, H.; Yamamoto, K.; Yano, T.; Kajiki, M.; Hamana, H.; Okuno, S., Distribution characteristics of carboxymethylpullulan-peptide-doxorubicin conjugates in tumor-bearing rats: Different sequence of peptide spacers and doxorubicin contents. *Biological & Pharmaceutical Bulletin* **2000,** *23* (5), 621-626.

39. Constantin, M.; Fundueanu, G.; Bortolotti, F.; Cortesi, R.; Ascenzi, P.; Menegatti, E., A novel multicompartimental system based on aminated poly(vinyl alcohol) microspheres/succinoylated pullulan microspheres for oral delivery of anionic drugs. *International Journal of Pharmaceutics* **2007,** *330* (1-2), 129-137.

40. Nishikawa, T.; Akiyoshi, K.; Sunamoto, J., Supramolecular assembly between nanoparticles of hydrophobized polysaccharide and soluble-protein complexation between the self-aggregate of cholesterol-bearing pullulan and alpha-chymotrypsin. *Macromolecules* **1994,** *27* (26), 7654-7659.

41. Akiyoshi, K.; Sasaki, Y.; Sunamoto, J., Molecular chaperone-like activity of hydrogel nanoparticles of hydrophobized pullulan: Thermal stabilization with refolding of carbonic anhydrase B. *Bioconjugate Chemistry* **1999,** *10* (3), 321-324.

42. Sasaki, Y.; Nomura, Y.; Sawada, S.; Akiyoshi, K., Polysaccharide nanogel-cyclodextrin system as an artificial chaperone for in vitro protein synthesis of green fluorescent protein. *Polymer Journal* **2010,** *42* (10), 823-828.

43. Hirakura, T.; Nomura, Y.; Aoyama, Y.; Akiyoshi, K., Photoresponsive nanogels formed by the self-assembly of spiropyrane-bearing pullulan that act as artificial molecular chaperones. *Biomacromolecules* **2004,** *5* (5), 1804-1809.

44. Kitano, S.; Kageyama, S.; Nagata, Y.; Miyahara, Y.; Hiasa, A.; Naota, H.; Okumura, S.; Imai, H.; Shiraishi, T.; Masuya, M.; Nishikawa, M.; Sunamoto, J.; Akiyoshi, K.; Kanematsu, T.; Scott, A. M.; Murphy, R.; Hoffman, E. W.; Old, L. J.; Shiku, H., HER2-specific T-cell immune responses in patients vaccinated with truncated HER2 protein complexed with nanogels of cholesteryl pullulan. *Clinical Cancer Research* **2006,** *12* (24), 7397-7405.

45. Mocanu, G.; Constantin, M.; Carpov, A., Chemical reactions on polysaccharides: 5. Reaction of mesyl chloride with pullulan. *Angewandte Makromolekulare Chemie* **1996,** *241*, 1-10.

46. Hosseinkhani, H.; Aoyama, T.; Ogawa, O.; Tabata, Y., Liver targeting of plasmid DNA by pullulan conjugation based on metal coordination. *Journal of Controlled Release* **2002,** *83* (2), 287-302.

47. Jo, J.; Yamamoto, M.; Matsumoto, K.; Nakamura, T.; Tabata, Y., Liver targeting of plasmid DNA with a cationized pullulan for tumor suppression. *Journal of Nanoscience and Nanotechnology* **2006,** *6* (9-10), 2853-2859.

48. Tabor CW; H, T., Polyamines. *Annu Rev Biochem.* **1984,** *53*, 749-90.

49. Jo, J. I.; Ikai, T.; Okazaki, A.; Nagane, K.; Yamamoto, M.; Hirano, Y.; Tabata, Y., Expression profile of plasmid DNA obtained using spermine derivatives of pullulan with different molecular weights. *Journal of Biomaterials Science-Polymer Edition* **2007,** *18* (7), 883-899.

50. Thakor, D. K.; Teng, Y. D.; Tabata, Y., Neuronal gene delivery by negatively charged pullulan-spermine/DNA anioplexes. *Biomaterials* **2009,** *30* (9), 1815-1826.

51. Souguir, Z.; Roudesli, S.; Picton, L.; Le Cerf, D.; About-Jaudet, E., Novel cationic and amphiphilic pullulan derivatives I: Synthesis and characterization. *European Polymer Journal* **2007,** *43* (12), 4940-4950.

52. Souguir, Z.; Roudesli, S.; About-Jaudet, E.; Picton, L.; Le Cerf, D., Novel cationic and amphiphilic pullulan derivatives II: pH dependant physicochemical properties. *Carbohydrate Polymers* **2010,** *80* (1), 123-129.

53. Yamaoka, T.; Tabata, Y.; Ikada, Y., Comparison of body distribution of poly(vinyl alcohol) with other water-soluble polymers after intravenous administration. *Journal of Pharmacy and Pharmacology* **1995,** *47* (6), 479-486.

54. Ashwell, G.; Harford, J., Carbohydrate-specific receptors of the liver. *Annual Review of Biochemistry* **1982,** *51*, 531-554.

55. Taylor, A. E.; Granger, D. N., Equivalent pore modeling - Vesicles and channels. *Federation Proceedings* **1983,** *42* (8), 2440-2445.

56. Suginoshita, Y.; Tabata, Y.; Moriyasu, F.; Ikada, Y.; Chiba, T., Liver targeting of interferon-beta with a liver-affinity polysaccharide based on metal coordination in mice. *Journal of Pharmacology and Experimental Therapeutics* **2001,** *298* (2), 805-811.

57. Suginoshita, Y.; Tabata, Y.; Matsumura, T.; Toda, Y.; Nabeshima, M.; Moriyasu, F.; Kada, Y.; Chiba, T., Liver targeting of human interferon-beta with pullulan based on metal coordination. *Journal of Controlled Release* **2002,** *83* (1), 75-88.

58. Hirsh, J.; Anand, S. S.; Halperin, J. L.; Fuster, V., Guide to anticoagulant therapy: Heparin a statement for healthcare professionals from the American Heart Association. *Circulation* **2001,** *103* (24), 2994-3018.

59. Barnes, W. A.; Redo, S. F.; Ecker, R. R.; Wenig, J., Dextran sulfate. A new and potent antiulcer agent. *Am J Surg.* **1967,** *113* (1), 27-31.

60. Mahner, C.; Lechner, M. D.; Nordmeier, E., Synthesis and characterization of dextran and pullulan sulphate. *Carbohydrate Research* **2001,** *331* (2), 203-208.

61. Alban, S.; Schauerte, A.; Franz, G., Anticoagulant sulfated polysaccharides: Part I. Synthesis and structure-activity relationships of new pullulan sulfates. *Carbohydrate Polymers* **2002,** *47* (3), 267-276.

62. Denooy, A. E. J.; Besemer, A. C.; Vanbekkum, H., Highly Selective Nitroxyl Radical-Mediated Oxidation of Primary Alcohol Groups in Water-Soluble Glucans. *Carbohyd Res* **1995,** *269* (1), 89-98.

63. Binghe Wang, T. S., and Richard A. Soltero, *Drug delivery. Principles and applications*. John Wiley & Sons, Inc: Hoboken, New Jersey, 2005; p 448.

64. Wang, B.; Siahaan, T.; Soltero, R. A., *Drug delivery. Principles and applications*. John Wiley & Sons, Inc: Hoboken, New Jersey, 2005; p 448.

65. Edgar, K. J., Cellulose esters in drug delivery. *Cellulose* **2007,** *14* (1), 49-64.

66. Posey-Dowty, J. D.; Watterson, T. L.; Wilson, A. K.; Edgar, K. J.; Shelton, M. C.; Lingerfelt, L. R., Zero-order release formulations using a novel cellulose ester. *Cellulose* **2007,** *14* (1), 73-83.

67. Singhal, D.; Curatolo, W., Drug polymorphism and dosage form design: a practical perspective. *Advanced Drug Delivery Reviews* **2004,** *56* (3), 335-347.

68. Qian, F.; Huang, J.; Hussain, M. A., Drug-polymer solubility and miscibility: Stability consideration and practical challenges in amorphous solid dispersion development. *Journal of Pharmaceutical Sciences* **2010,** *99* (7), 2941-2947.

69. Leuner, C.; Dressman, J., Improving drug solubility for oral delivery using solid dispersions. *European Journal of Pharmaceutics and Biopharmaceutics* **2000,** *50* (1), 47-60.

Chapter 3 **Synthesis of Amphiphilic 6-Carboxypullulan Ethers**

(Used with permission of Elsevier: Pereira, J. M.; Mahoney, M.; Edgar K. J. Carbohydrate Polymers 2013, in press)

3.1 Abstract

Hydrophobically modified polysaccharides that contain carboxyl groups possess exceptional features for drug delivery and other applications. Carboxyl groups were introduced at C-6 in the pullulan backbone by applying the well-established oxidation with TEMPO and NaOCl/NaBr. The oxidized product, 6-carboxypullulan, is even more water-soluble than pullulan. Consequently, further chemical modifications have been mainly restricted to reactions that can be performed in water or under heterogeneous conditions. We find that the tetrabutylammonium (TBA) salt of 6-carboxypullulan is soluble in a range of organic solvents and can be reacted homogeneously with various alkyl halides in dimethylsulfoxide and sodium hydroxide at 40 ºC to yield 6-carboxypullulan ethers. A full degree of substitution (DS) of 7 (per trisaccharide repeat unit) was achieved upon reaction with iodoethane, while the products from the reaction with longer chain alkyl halides (propyl and butyl derivatives) had a DS of up to about 3. The amphiphilic products have impressive surfactant properties.

3.2 Introduction

Pullulan is a non-ionic water-soluble polysaccharide which is produced from starch by the yeast-like fungus *Aureobasidium pullulan.*[1 2] It consists predominantly of maltotriose units, i.e. units of three 1,4-linked α-D-glucose molecules, which are polymerized in a linear fashion via 1,6-linkages, as shown in **Fig 3.1**.[3] Pullulan has low toxicity and has been used for more than 20 years as an additive in the food industry.[4] It biodegrades in the body and does not evoke an immune response. It has been shown to be non-toxic also when administered intravenously.[5] In view of the attractive characteristics of pullulan and the possibility of chemical modification to

suit the desired application, there have been many reports of the synthesis of new pullulan derivatives with application in drug delivery.[6 7] Pullulan is concentrated disproportionately in the liver after intravenous administration, and so has been studied as a promising polymeric carrier for liver related diseases.[8 9]

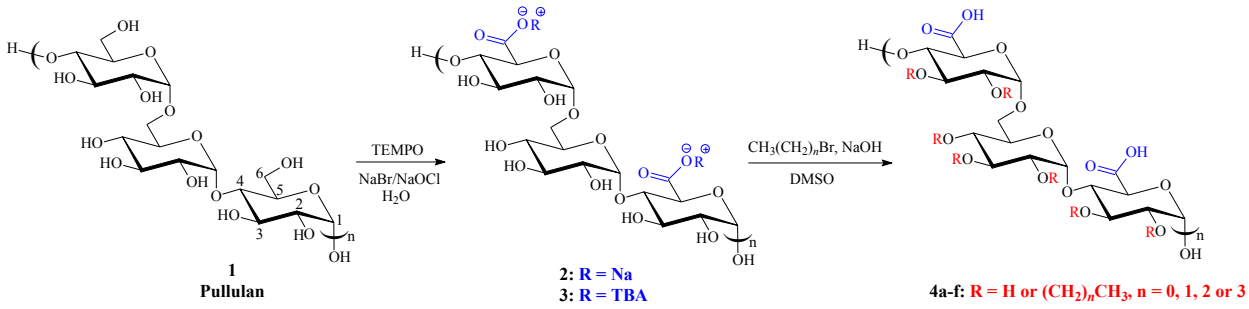

Figure 3.1 Pullulan oxidation and synthesis of 6-carboxypullulan ethers

Most pullulan modifications are intended to reduce its water solubility or to introduce charged or reactive groups for functionality.[10 11 12] For drug delivery applications, the ability of the drug carrier to swell or disperse in water is often more desirable than water solubility.[13] Highly water soluble polymer carriers tend to release drugs quickly; while polymers that only swell or disperse in water have the ability to provide slow drug release.[14]

Polysaccharides that have been hydrophobically modified and contain carboxyl groups are commonly used in drug delivery systems because of their ability to provide pH-controlled drug release.[15 16 17 18] For example, hydrophobic drugs often are released from carboxyl-containing polysaccharide matrices only at the neutral pH of the small intestine and colon, when the carboxyl group becomes ionized and the polymer swells, thus limiting exposure of the stomach to the drug. Moreover, polymer-drug interactions also play an important role in drug delivery systems. An important example is the strong interaction of carboxyl groups with amines (many drugs contain amine functional groups) by hydrogen bonding. The presence of hydrophobic groups is also important; hydrophobicity will enhance miscibility with hydrophobic drugs, and slow their release. Due in part to these valuable features, polysaccharide derivatives, especially cellulose derivatives containing pendant carboxyl groups, have been recently explored

with success for amorphous solid dispersion (ASD) of drugs. These drug-polysaccharide matrix dispersions have shown the ability to significantly enhance solution concentrations and stability of many otherwise poorly soluble drugs by forming a matrix of drug, in a metastable amorphous form, entrapped within the polymer.[19] Hydroxypropylmethylcellulose acetate succinate (HPMCAS)[20] and cellulose acetate adipate propionate (CAAdP)[21] [22] are examples of carboxylated cellulose derivatives that combine several of those attractive drug delivery functions and are promising polymers for drug delivery formulations.

Introduction of carboxyl groups to the non-ionic pullulan backbone should give an anionic derivative with interesting properties for drug delivery applications. The most widely investigated pullulan derivative containing a carboxylic acid group is carboxymethylpullulan (CMP).[15] CMP is a promising polymeric carrier for many drugs since its high proportion of negative charges results in prolonged retention of the polymer within the organism.[5] CMP has been hydrophobically modified by esterification of the carboxyl groups with long alkyl chains.[23] These derivatives self-assemble in aqueous media and efficiently solubilize hydrophobic drugs.

In the early 1990, DeNooy[24] described the TEMPO (2,2,6,6-tetramethyl-1-piperidinyloxy free radical)-mediated selective oxidation of various water-soluble polysaccharides with hypochlorite/bromide as the regenerating oxidant. The reaction is performed under homogeneous conditions in water and primary alcohol groups are selectively oxidized to yield carboxylates. The regioselectivity of the reaction is essentially complete, and chemoselective, favoring oxidation of the primary OH to a carboxylic acid; partial oxidation to aldehyde, or oxidation at the secondary OH groups to ketones, is minimal. Such high chemo- and regioselectivity is useful for potential use of oxidized pullulan derivatives in formulations that might reach the circulation, since full characterization and structural control on such polymers is important for regulatory approval. Oxidation of pullulan by this methodology has been reported, but modified 6-carboxypullulan compounds have not been studied much for their biomedical applications, although they may have great potential for use in drug delivery systems.[25] [26] One possible reason for this is the fact that 6-carboxypullulan is even more water soluble than pullulan, therefore further chemical modification is mainly restricted to reactions which can be performed in water or under heterogeneous conditions. Additionally, highly water-soluble polysaccharide derivatives may not be highly miscible with hydrophobic drugs, and may give faster than desired release profiles (and/or with inadequate pH responsiveness) for particular drugs.

In this work we introduced carboxyl groups to the pullulan backbone by applying the selective TEMPO oxidation. We then explored methods for conversion of the oxidized pullulan product, 6-carboxypullulan, to its TBA (tetrabutylammonium) salt, seeking enhanced organic solubility that would permit more facile reactions of the remaining pullulan OH groups with electrophiles. We pursued this strategy by attempting homogeneous reaction of 6-carboxypullulan salts with various alkyl halides in DMSO, employing sodium hydroxide as base, as a route to the potentially useful 6-carboxypullulan ethers.

3.3 Experimental

3.3.1 Materials and methods

Pullulan (Mw = 450 KDa, Mn = 200 > KDa) was from the Hayashibara Company (Okayama, Japan) and was dried under vacuum at 120 °C overnight prior to use. Water was deionized. TEMPO (99%, Aldrich), sodium hypochlorite (NaOCl, 14.5% chlorine, Alfa Aesar), NaBr (99%, Alfa Aesar), ethyl acetate (HPLC grade, Fisher), tetrabutylammonium fluoride trihydrate (99%, TBAF), pyridine (Py), tetrabutylammonium hydroxide (TBAOH, 1.0 M in water, Fluka Analytical), ethylene glycol (laboratory grade, Fisher), lithium chloride (99%, LiCl) were used as supplied. Dimethylsulfoxide (DMSO, HPLC grade, Acros) was dried using 4 Å molecular sieves. Dimethylacetamide (DMAc, HPLC grade, Fisher) and dimethylformamide (DMF, Fisher) were used as supplied. Bromoethane (98%, Alfa Aesar), bromopropane (98%, Aldrich), bromobutane (99%, Aldrich), iodomethane (99%, Aldrich), iodoethane (98%, stabilized with silver, Acros Organics) and iodobutane (98%, stabilized, Acros Organics) were used as supplied. Proton exchange resin was DOWEX 50WX8 100-200 (H) from Alfa Aesar. Deuterium oxide (99.9 atom % D; D_2O) containing 0.75% 3-(trimethylsilyl)propionic-2,2,3,3-d_4 acid, sodium salt and d_6-DMSO for NMR were acquired from Sigma-Aldrich. Trifluoroacetic acid (99%) used for ^{1}H NMR was from Acros and potassium bromide (KBr) used for Fourier transform infrared (FTIR) analysis was obtained from International Crystal Laboratories.

For NMR analysis, samples were prepared by dissolving 8−10 mg (for ^{1}H) or 50-80 mg (for ^{13}C) of polymer in 0.7 mL of D_2O or d_6-DMSO. The solution was filtered through a pipette containing glass wool into a standard 5 mm NMR tube. ^{1}H and ^{13}C NMR spectra were acquired on Varian INOVA or Varian UNITY 400 MHz spectrometers with 32-128 scans for ^{1}H and minimum of 10,000 scans for ^{13}C. Chemical shifts are reported relative to the solvents, except for ^{13}C spectra acquired in D_2O, when TMS is used as the reference.

The degree of substitution (DS) of the 6-carboxypullulan ethers is described as per trisaccharide repeat unit with a maximum DS of 7 with respect to etherification. The DS was calculated by ^{1}H NMR using the following formula:

$$DS = \frac{17A}{3B - 2A}$$

This formula was derived from the following relation:

$$\frac{3DS}{17} = \frac{A}{B - \frac{2}{3}A}$$

Each OH substitution in the pullulan backbone with either an ethyl, propyl or butyl group brings to the pullulan backbone 3 methyl protons (3DS) and there are 17 protons (C-H) resulting from each pullulan trisaccharide repeat unit, regardless of its DS. A is the integration of the methyl peak of the alkyl group, and was observed at 0.87 ppm for butyl, 0.93 ppm for propyl and 1.11 ppm for ethyl in the ^{1}H NMR spectra of the respective 6-carboxypullulan ether. The 6-carboxypullulan ethers backbone protons in the NMR spectrum were calculated by the integration of the peak observed in the 2.6 - 6.1 ppm region (B) minus the integration of the protons from the O-CH_2- of the respective alkyl group that overlaps with the backbone protons (2/3 A). For each ether substituent, there will be one methyl (3H) per overlapping methylene group (2H).

The DS for all the products was calculated by ^{1}H NMR, with exception for methyl pullulan-6-carboxylate, in which case the DS was calculated by quantitative ^{13}C NMR (data not

shown) because the only peak from the ether substituent (CH_3) in the ^1H NMR spectrum overlapped with the protons from the backbone.

FTIR spectra were acquired using a Thermo Electron Nicolet 8700 instrument in transmission mode. Samples were prepared using the KBr pellet method. 6-Carboxypullulan ether samples (1 mg) were mixed with 99 mg of KBr using a mortar and pestle. The mixture was compressed in the sample holder between two screws to form a KBr disk. 64 scans were obtained for each spectrum.

Dynamic light scattering (DLS) data were obtained using a Malvern Instruments Zetasizer Nano-ZS. The polymer solutions with different concentrations were prepared by dissolving the polymer in water.

Dialysis was performed against water in a 4 L beaker using dialysis tubing (MWCO 3,500 Da) for 3 days, by replacing the water twice each 24 h.

Freeze-drying of pullulan derivatives was performed using Labconco Freezone 4.5 lyophilizer.

Solubility testing on 6-carboxypullulan ethers samples was performed by adding 5 mg of sample to a glass vial, then adding 1 mL of solvent. The mixture was subjected to vortex mixing for 5-10 min at room temperature, and then solubility was judged by visual examination.

Hydrolysis of 6-carboxypullulan ethers to calculate the DS with respect to any small carboxylate esterification (ester DS): The 6-carboxypullulan ether sample (30 mg) was stirred in NaOH (0.1 M, 5 mL) at room temperature for 20 h. After the hydrolysis reaction, the resulting solution was dialyzed against water for 24 h and freeze-dried.

3.3.2 Oxidation of pullulan with TEMPO and NaOCl/NaBr

Pullulan (2.0 g, 7% water, 11.5 mmol anhydroglucose units) was dissolved in 250 mL of demineralized water in a 3 neck round bottom flask equipped with 2 addition funnels. TEMPO (0.040 g, 0.26 mmol) and NaBr (0.20 g, 1.9 mmol) were added, and the solution was cooled in an ice bath to approximately 2 ºC. A 15% NaOCl solution (12 mL, 25 mmol) was brought to pH

9.4 by adding 4 M aqueous HCl and also cooled in an ice bath. This solution was added to one of the addition funnels. A 0.5 M aqueous NaOH solution was added to the other addition funnel. The solution of NaOCl was slowly added to the reaction mixture and the pH was maintained at 9.4 during the oxidation by concomitantly adding the aqueous NaOH. After approximately 1h, 15.0 mL of 0.5 M NaOH had been added and the reaction was quenched by adding methanol (5 mL) and neutralized by adding 4 M HCl. Then, $NaBH_4$ (0.5 g, 13 mmol) was added and the solution was stirred overnight at room temperature. The reaction mixture was brought to pH 6 by adding 4 M HCl, and the oxidized polymer was desalted by dialysis, after which the solution was freeze-dried and the polyelectrolyte isolated in a yield of 95% (based on the ideal molar mass of completely oxidized pullulan).

Pullulan. ^{1}H NMR (400 MHz, D_2O): δ 5.61-5.47 (m, 2 H-1), 4.98-4.9 (m, H-1), 4.11-3.4 (m, H2-H6). ^{13}CNMR (400 MHz, D_2O): δ 100.12 (C-1), 99.66 (C-1), 97.83 (C-1), 77.65, 77.27, 77.35, 73.26, 72.96, 71.62, 71.53, 71.42, 71.24, 71.01, 70.24, 69.38, 66.38, 60.62 (C-6), 60.31 (C-6).

6-CO_2NaPull. ^{1}H NMR (400 MHz, D_2O): δ 5.67-5.42 (m, 2 H-1), 5.05-4.9 (m, `H-1), 4.18-3.2 (m, H2-H6). ^{13}C NMR (400 MHz, D_2O): δ 176 (C=O), 175.83 (C=O), 99.35 (C-1), 98.14 (C-1), 97.82 (C-1), 76.58 (C-4), 76.39 (C-4), 73.78 (C-3), 73.32 (C-3), 73.18 (C-3), 72.72 (C-5), 72.16 (C-5), 71.77 (C-2), 71.73 (C-2), 71.64 (C-2), 70.73 (C-4), 69.29 (C-5), 65.62 (C-6). Carbon peaks were assigned based on literature values.[24]

3.3.3 Etherification of 6-carboxypullulan TBA salt

6-Carboxypullulan Na salt (CO_2NaPull) was dissolved in water and passed through an ion exchange column. A solution with pH = 3-4 containing the protonated form of 6-carboxypullulan (CO_2HPull) was obtained. To convert CO_2HPull to CO_2TBAPull, aqueous TBAOH was added dropwise with continuous stirring to this solution until the pH was approximately 8. The resulting mixture was dialyzed against water for 48 h and freeze-dried. The final product, CO_2TBAPull, was a white solid.

CO_2TBAPull. ^{1}H NMR (400 MHz, d_6-DMSO): δ 5.18−2.98 (m, CO_2TBAPull backbone), 3.18−3.14 (m, N($\underline{CH_2}CH_2CH_2CH_3)_4$ of TBA), 1.6−1.52 (m, N($CH_2\underline{CH_2}CH_2CH_3)_4$ of TBA), 1.3

(tq, $N(CH_2CH_2\underline{CH_2}CH_3)_4$ of TBA), 0.92 (t, $N(CH_2CH_2CH_2\underline{CH_3})_4$ of TBA). ^{13}C NMR (400 MHz, d_6-DMSO): 171.98 (C=O), 171.49 (C=O), 98-97.51 (m, 3 C-1), 78.98 (C-4), 78.18 (C-4), 73.85-69.3 (m, C2-C5), 65.97 (C-6).

3.3.4 General procedure for the etherification of 6-carboxypullulan TBA salt

Synthesis of 6-carboxypullulan ethers by reaction with alkyl bromides and iodobutane. 6-Carboxypullulan TBA salt (0.250 g, 0.25 mmol) and DMSO (40 mL) were added to a 100 mL 3-neck round bottom flask under nitrogen containing a magnetic stirrer. The reactions performed with a low boiling point alkylating reagent were equipped with a reflux condenser. Pulverized NaOH (0.370 g, 9.25 mmol) was added to this clear solution and the suspension was stirred for 1h at 40 ^oC. The reaction solution became more viscous, with a jelly-like appearance. The alkylating reagent (9.25 mmol) was added dropwise within 10 min; the mixture became fluid and was stirred for 2.5 h at 40 ^oC. The reaction mixture was poured into 120 mL of ethyl acetate and the resulting precipitate was filtered and washed with extra ethyl acetate. The product was then dissolved in water, passed through a column containing a proton exchange resin and the resulting solution was dialyzed against water for 3 days and freeze-dried to yield the 6-carboxypullulan ethers in protonated form.

3.3.5 Synthesis of 6-carboxypullulan ethers by reaction with iodomethane and iodoethane

The etherification of 6-carboxypullulan TBA salt with iodomethane and iodoethane furnished products with a higher DS that could not be precipitated in any organic solvent upon the reaction work up. Thus, the experimental procedure for the isolation of these products was slightly different from the one described above. Upon reaction completion, instead of pouring the reaction mixture into ethyl acetate, the reaction mixture was dialyzed against water for 3 days and the resulting solution was passed through a column containing a proton exchange resin and freeze-dried to yield 6-carboxypyllulan ethers in protonated form.

Methyl-6-CO_2HPull: ^{1}H NMR (400 MHz, d_6-DMSO): δ 5.96-5.95, 5.84-5.83, 5.57-5.55, 5.05-5.03, 4.8-4.78, 4.19-4.15, 3.94-3.01, 2.83-2.78 (m, backbone and CH_3 of methyl). Quantitative ^{13}C NMR (400 MHz, d_6-DMSO): 169.16, 162.16 (C=O), 108.26 (C-1), 102.81 (C-1), 97.07-95.1 (m, C-1), 85.25-65.85 (m, C2-C6 backbone), 59.76-54.37 (CH_3 of methyl).

Ethyl-6-CO_2HPull: ^{1}H NMR (400 MHz, d_6-DMSO): δ 6.1-2.6 (m, backbone and CH_2 of ethyl), 1.08 (s, CH_3 of ethyl). ^{13}C NMR (400 MHz, d_6-DMSO): 170.3 (C=O), 99.0 (C-1), 96.93 (C-1), 96.54 (C-1), 81.77-65.07 (m, C2-C6 backbone and CH_2 of ethyl), 15.4 (CH_3 of ethyl).

Propyl-6-CO_2HPull: ^{1}H NMR (400 MHz, D_2O): δ 6.1-4.9 (m, backbone) 4.67-2.82 (m, backbone and $CH_2CH_2CH_3$ of propyl), 1.62 (s, $CH_2\underline{CH_2}CH_3$ of propyl), 0.93(s, CH_3 of propyl).

Butyl-6-CO_2HPull: ^{1}H NMR (400 MHz, d_6-DMSO): δ 6.1-4.9 (m, backbone) 4.67-2.82 (m, backbone and $\underline{CH_2}CH_2CH_2CH_3$ of butyl), 1.59 (s, $CH_2\underline{CH_2}CH_2CH_3$ of butyl), 1.37 (s, $CH_2CH_2\underline{CH_2}CH_3$ of butyl), 0.92 (s, CH_3 of butyl). ^{13}C NMR (400 MHz, d_6-DMSO): 170.38 (C=O), 99.2-96.69 (3C-1), 80.89-65.08 (C2-C6 backbone and $\underline{CH_2}CH_2CH_2CH_3$ of butyl), 32.10 ($CH_2\underline{CH_2}CH_2CH_3$ of butyl), 18.97 ($CH_2CH_2\underline{CH_2}CH_3$ of butyl), 13.93 (CH_3 of butyl).

3.4 Results and Discussion

3.4.1 Pullulan oxidation

Our approach to hydrophobically-modified anionic pullulan derivatives began with oxidation with TEMPO and NaOCl/NaBr to obtain 6-carboxypullulan (2) (**Fig 3.1**).[24] The potential for complete oxidation of pullulan to its carboxylate, and the high regioselectivity of this reaction for C-6 were the motivation to employ this methodology to obtain pullulan derivatives containing carboxyl groups.

Pullulan was completely oxidized at C-6 as indicated by the ^{13}C NMR spectrum (**Fig A3.1** in Appendix). Peaks at 60.6 and 60.3 ppm arising from the primary hydroxyl carbons (C-6, **Fig A3.1**) in pullulan were no longer present in the product spectrum, while two carbonyl peaks

from the new, chemically distinct carboxylic acids appeared at 175.8 and 176 ppm in the oxidized pullulan.

3.4.2 Synthesis and characterization of 6-carboxypullulan ethers

The oxidized pullulan product was recovered from the reaction mixture mainly as the sodium salt of the carboxylic acid, which was not soluble in DMSO. The etherification of 6-CO_2NaPull was first attempted by reacting it as a suspension in DMSO with NaOH (added in a small amount of water) and 1-bromobutane for 20h at room temperature (**Table 3.1**). No reaction occurred under heterogeneous conditions, and only starting material was recovered. When the reaction began homogeneously with the CO_2NaPull dissolved in water (40 mL) and the bromobutane was added in DMSO (40 mL), CO_2NaPull immediately precipitated from the reaction mixture and the reaction could not be continued (results not shown).

Table 3.1 Optimization of reaction conditions for etherification of 6-carboxypullulan with bromobutane

6- Carboxypullulan	Temp (°C)	Time (h)	DS
6-CO_2Na Pull	rt	20	No reaction
6-CO_2TBA Pull	rt	20	0.41
6-CO_2TBAPull	40*	20	3.4
6-CO_2TBAPull	40	3.5	3.6
6-CO_2TBAPull	60*	20	2.91

* Only 1h at this temperature

6-CO_2NaPull was then treated with a proton exchange resin, converting it to its protonated form (6-CO_2HPull). Neutralization of the CO_2HPull with TBAOH yielded 6-carboxypullulan-TBA salt (6-CO_2TBAPull). The solubility of 6-carboxy pullulan vs. counterion (H, Na, or TBA) was then investigated (**Table 3.2**). In previous studies from our laboratory, Pawar [27] found that alginic acid, another poly(uronic acid), could be converted to its TBA salt to enhance its organic solubility. Natural alginic acid, a copolymer of β-D-mannuronic acid and its

C-5 epimer, α-L-guluronic acid, is insoluble in all common organic solvents, but could be dissolved as its TBA salt in a variety of polar aprotic solvents containing TBAF. The results from our solubility tests indicated that conversion of 6-carboxypullulan to its TBA salt provides similar solubility benefits (**Table 3.2**). Indeed, 6-CO_2TBAPull is soluble in DMSO without the need to add TBAF. This difference in solubility is believed to be because of the disruption of H-bonding interactions between the carboxylic acid and the hydroxyl groups. Furthermore, the remarkable solubility of 6-CO_2TBA-pullulan in organic media is believed to be due to the increased hydrophobicity conveyed by the n-butyl chains of the TBA anion and to the disruption of H-bonding by this bulky group.

Table 3.2 Solubility of 6-carboxypullulan – protonated form and as Na and TBA salts

	6-CO_2NaPull	**6-CO_2HPull**	**6-CO_2TBAPull**
Water	O	O	O
DMSO	X	Ø	O
DMF	X	Ø	O
DMSO/TBAF	X	X	O
DMF/TBAF	X	X	O
MeOH	X	X	O
EtOH	X	X	Ø
Ethylene Glycol	X	O	Ø
DMAc	X	X	Ø
ACN	X	X	Ø
Pyridine	X	X	X
THF	X	X	X

O = Soluble, Ø = Partially soluble, X = Insoluble. DMSO: dimethylsulfoxide, DMF: dimethylformamide, TBAF: tetrabutylammonium fluoride, MeOH: methanol, EtOH: ethanol, DMAc: dimethylacetamide, ACN: acetonitrile, THF: tetrahydrofuran.

The ^{1}H NMR spectrum of 6-CO_2TBA-pullulan in d_6-DMSO is shown in **Fig 3.2**. The polymer backbone peaks appear in the region 2.8-5.5 ppm and overlap with 2 hydrogens from

the butyl chain of the TBA [$N(\underline{CH_2}CH_2CH_2CH_3)_4$]. The other protons from the butyl chains of TBA appear at 0.9, 1.3, and 1.6 ppm. Integration of the TBA peaks against the polymer backbone demonstrates that all carboxyl groups are present as TBA salts.

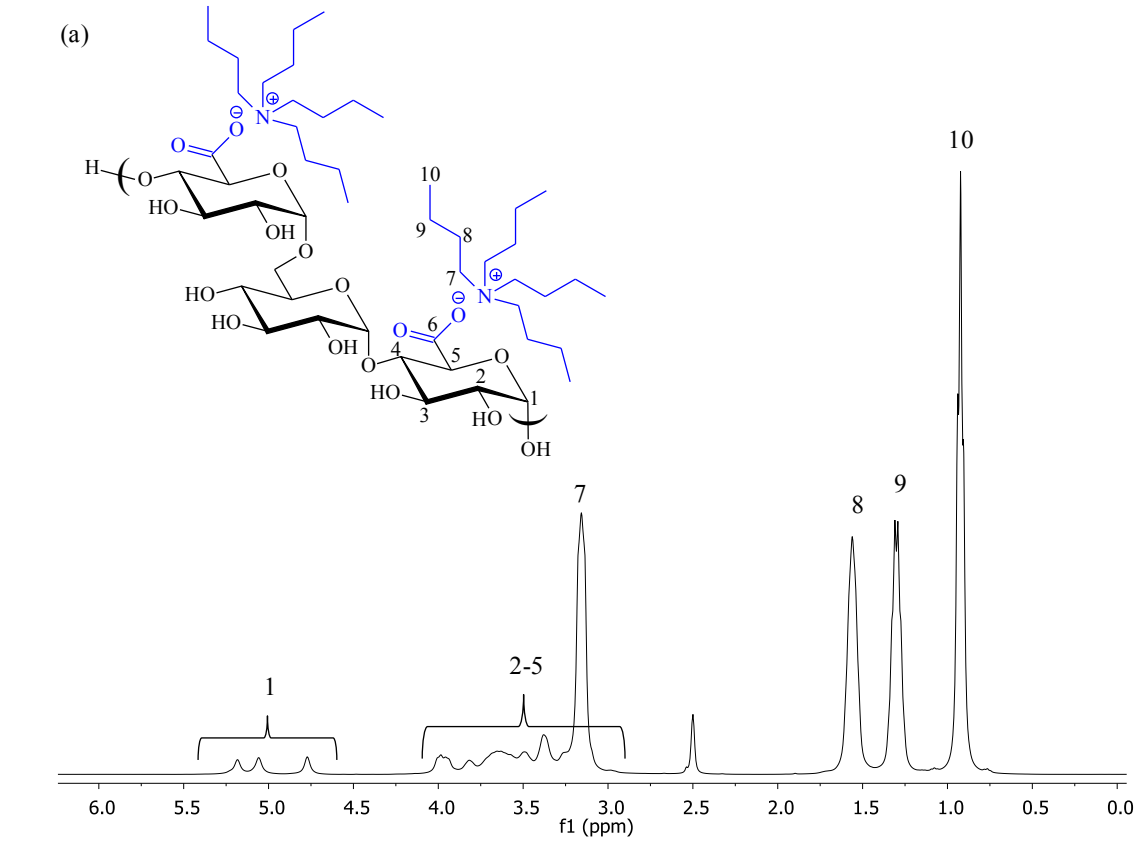

(b)

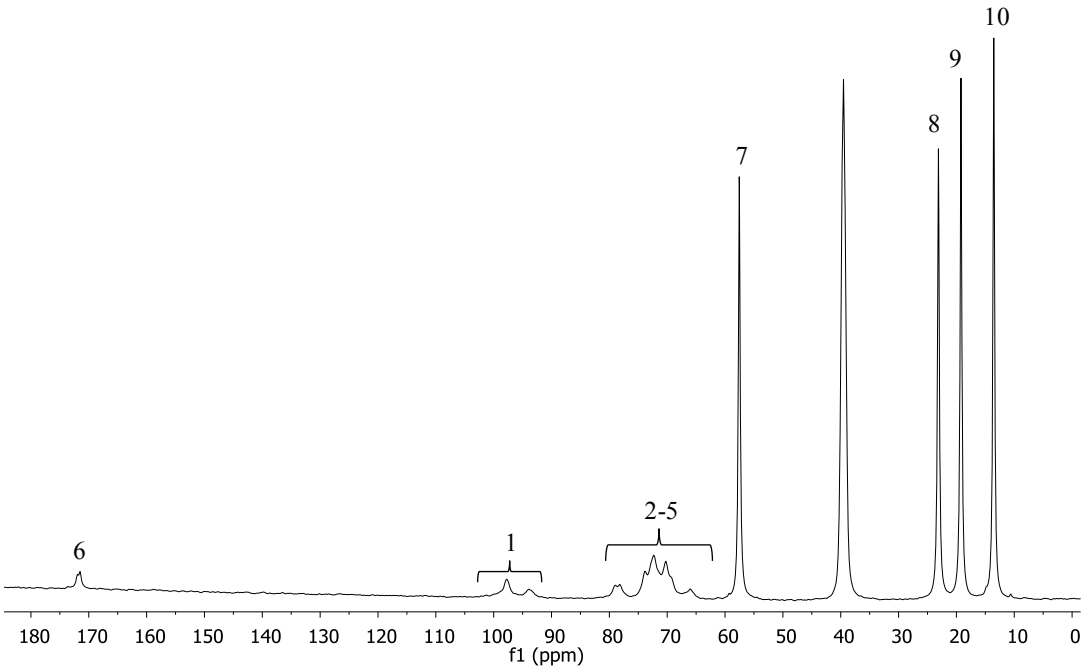

Figure 3.2 (a) ^{1}H and **(b)** ^{13}C NMR spectra of 6-CO_2TBAPullulan in d_6-DMSO

It's well known that etherification is most facile in homogeneous solution.[28] Therefore, we performed etherification with the 6-CO_2TBAPull, which was initially dissolved in DMSO. After addition of NaOH, equilibrium is established between the TBA and Na forms of oxidized pullulan and the solution becomes viscous (due to partial formation of insoluble 6-CO_2NaPull), but no precipitate forms in the reaction mixture; the presence of the TBA ion keeps the carboxypullulan in solution. Upon addition of the alkyl halide, the reaction mixture turns fluid (the etherified product is soluble in DMSO). This procedure allows for the reaction to take place homogeneously and etherification proceeds successfully.

Process experiments were performed in order to optimize the reaction conditions (**Table 3.1**). When the etherification was conducted with 6-CO_2TBAPULL in DMSO at room temperature for 20h, a DS of 0.41 was obtained. When the reaction was allowed to proceed at 40 ºC for 1 hour after the addition of NaOH, followed by reaction with bromobutane for 20 h at room temperature, the DS increased to 3.4. To optimize the reaction time, another experiment was conducted where, after reaction with NaOH for 1h at 40 ºC, bromobutane was added and the etherification was continued for 2.5 h, still at 40 ºC. The DS obtained under these conditions (DS = 3.6) was similar to when the etherification was carried out for a much longer time at room temperature, indicating that high DS products can be obtained at shorter reaction times. In another experiment, the temperature was also increased to 60 ºC during the reaction with NaOH, but no increase in DS resulted (DS = 2.91). If water was present during the etherification of 6-CO_2TBAPull, a sticky precipitate was formed that prevented further reaction. This is probably due to ion exchange forming 6-CO_2NaPull, which is insoluble in DMSO but soluble in water. Therefore, all experiments were carried out in dry DMSO and 6-CO_2TBA-pullulan and NaOH were dried before use.

We explored the scope of the reaction by homogeneous etherification of 6-carboxypullulan TBA salt with different alkyl halides in DMSO with NaOH at 40 ºC for 3.5 h to furnish a variety of 6-carboxypullulan ethers. Measured DS and solubility properties of the products are summarized in **Table 3.3**.

For the reactions performed with longer chain alkyl halides, the products, propyl pullulan-6-carboxylate (propyl-6-CO_2HPull, **4b**) and butyl pullulan-6-carboxylate (butyl-6-CO_2HPull, **4c, 4f**), had a similar DS of around 3, and were partially soluble in water, which is a result of the partial substitution of the hydroxyl groups. The solubility in DMSO and DMF

seemed to depend on the chain length and also the DS of the ether substituent. Butyl-6-CO_2HPull, which was the product substituted with the longer chain alkyl group (butyl, more hydrophobic) was soluble in DMSO and DMF, but not the propyl substituted one, which had a similar DS, but because the propyl group has a shorter chain length, the hydrophobicity of Propyl-6-CO_2HPull was lower and hindered its organic solubility. Reaction with shorter chain alkyl halides (methyl and ethyl), afforded products with higher DS, indicating that the smaller reagent more readily accesses the pullulan carboxyl groups. The DS was around 5 for the reaction with bromoethane and full substitution (DS = 7) was achieved upon reaction with alkyl idodide. These products (Methyl-6-CO_2HPull, **4d** and Ethyl-6-CO_2HPull, **4e**) still have partial water solubility and in this case, the much higher DS achieved lead to products with good organic solubility, despite the lower hydrophobicity of the ethyl group.

Table 3.3 Properties of 6-carboxypullulan ethers

Product	Alkylating reagent	DS[a]	Solubility		Yield[c] (%)
			Water	DMSO DMF	
4a Ethyl-6-CO_2HPull	Bromoethane	5.12	Ø	O	53
4b Propyl-6-CO_2HPull	Bromopropane	3.37	Ø	X	48
4c Butyl-6-CO_2HPull	Bromobutane	3.6	Ø	O	46
4d Methyl-6-CO_2HPull	Iodomethane	7[b]	Ø	O	45
4e Ethyl-6-CO_2HPull	Iodoethane	7.36	Ø	O	45
4f Butyl-6-CO2HPull	Iodobutane	3.22	Ø	O	49

[a] Calculated from ^{1}H NMR spectra (see experimental section), with exception for product 4d. [b] Based on quantitative ^{13}C NMR. [c] Based on the molar mass of product with DS shown in this table.

The chemical structure of all the products was confirmed by ^{1}H and ^{13}C NMR. Due to the poor solubility of propyl-6-CO_2HPull, it was not possible to acquire a ^{13}C NMR spectrum, which requires a higher sample concentration, thus, its chemical structure characterization was restricted to ^{1}H NMR. **Fig. 3.3a** shows the ^{1}H NMR spectrum of butyl-6-CO_2HPull. The region between 2.8 and 6.1 ppm corresponds to the backbone protons in the butyl-6-CO_2HPull which overlap with 2 protons of one CH_2 from the butyl group ($\underline{CH_2}CH_2CH_2CH_3$). The other butyl

group peaks are at 0.8, 1.3 and 1.4 ppm. The ^{13}C NMR spectrum of butyl-6-CO_2HPull **(Fig. 3.3b**) shows anomeric carbon peaks between 94 and 104 ppm. The other backbone carbon peaks are between 60 and 85 ppm and overlap with the CH_2 carbon of the butyl group ($\underline{CH_2}CH_2CH_2CH_3$). The other peaks from the butyl group are at 13.89, 18.87 and 33.72 ppm. The carboxylic acid carbonyls appear as a slightly broadened single peak at 170.9 ppm.

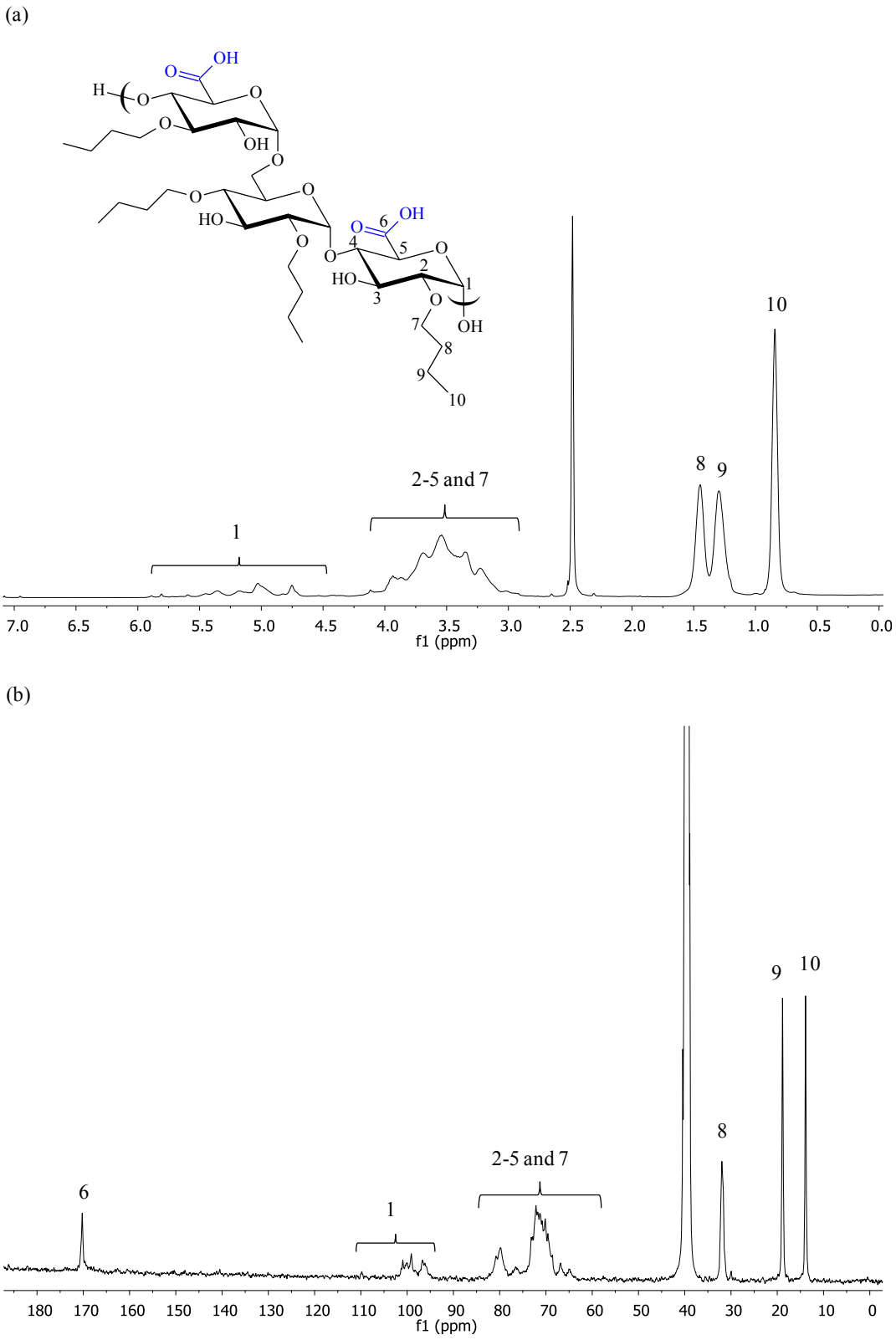

Figure 3.3 (a) ^{1}H and **(b)** ^{13}C NMR spectra of butylpullulan-6-carboxylate in d_6-DMSO

We must consider the possibility that, under these reaction conditions, there is also formation of ester groups by the reaction of the alkyl halide with the carboxyl group in the 6-carboxypullulan. Etherification should be the major reaction occurring since, in the presence of NaOH, deprotonation of the hydroxyl groups should occur and once the alkoxide is formed, this is a stronger and more reactive nucleophile than the carboxylate towards the alkylating reagent. The ^{1}H and ^{13}C NMR spectra showed single peaks for the carbons of the alkyl and the carbonyl groups, which is a strong indication that mainly the etherification is taking place. Furthermore, the chemical shifts for those groups, although they should occur within a similar range, also indicate that the proton and carbon peaks observed in the ^{1}H and ^{13}C NMR spectra correspond to the carboxylic acid carbonyl and alkyl groups from the ethers. The carbonyl peaks for the 6-carboxypullulan ether products appear consistently at 171 ppm. The ^{13}C NMR chemical shifts for acid and ester carbonyls are expected at 170-180 ppm and 165-170 ppm respectively.[29]

The infrared (IR) spectrum also showed strong evidence that the carboxyl groups are mostly not esterified (**Fig 3.4**). The carbonyl stretching absorption is one of the strongest IR absorptions, and is very useful in determining functional group identity. The carbonyl peak for esters should appear between 1750-1735 cm^{-1} and for acids 1700-1750 cm^{-1}.[29] There is a small overlap in the frequency range for the carboxylic acid and ester carbonyls, thus, in order to be more precise in the carbonyl identification, IR was performed with the sodium salt of the 6-carboxypullulan ethers. The carbonyl absorbance so observed (around 1600 cm^{-1}) is readily identified as carboxylate rather than ester (**Fig. 3.4**). The carbonyl peak for the protonated carboxylic acid appears at 1727 cm^{-1} for CO_2HPull and at 1728 cm^{-1} for the alkylated CO_2H pullulan (**Fig A3.4a-b** in Appendix). Furthermore, there is no absorbance at around 1200 cm^{-1}, which is characteristic for C-O stretch in esters.

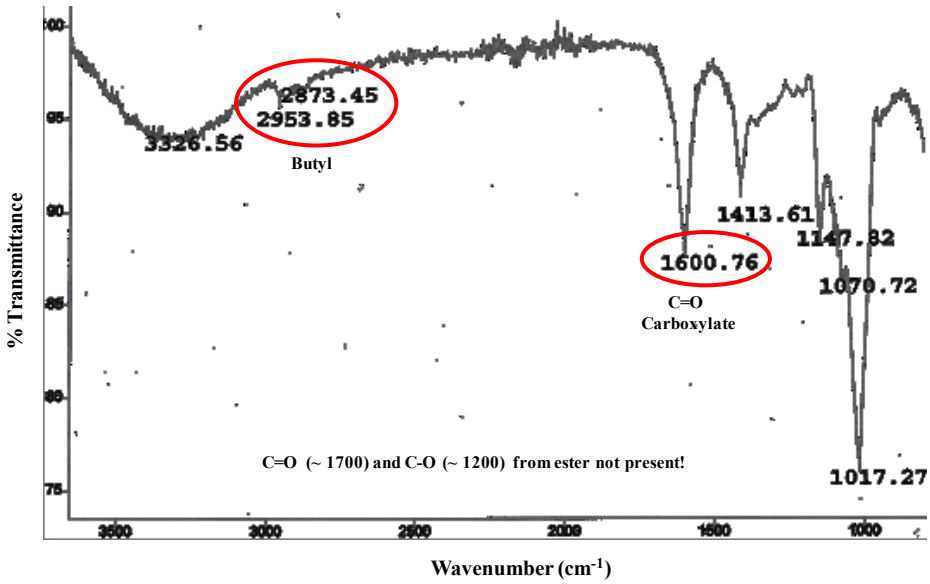

Figure 3.4 IR spectrum of butyl pullulan-6-carboxylate

In order to quantify any possible carboxylate esterification reaction, alkaline hydrolysis of selected 6-carboxypullulan ethers was performed. The 6-carboxypullulan ether was stirred for 20 h in NaOH (0.1 M) in order to hydrolyze any esters that might be present. After hydrolysis, the resulting solution was dialyzed against water for 24 h and freeze-dried. The product was analyzed by ^{1}H NMR, and the DS was calculated and compared to the DS observed prior to hydrolysis. This experiment was performed with butyl-CO_2HPull (**4c**), ethyl-6-CO_2HPull (**4a**) and ethyl-6-CO_2HPull (**4e**), which were representative samples of a DS around 3, 5 and 7 respectively. The results showed that the DS of the samples before and after the hydrolysis changed by only a small amount (up to approximately 0.3) for the 3 samples (**Table 3.S1** in Appendix). This indicates that carboxyl esterification is at most a minor side reaction, in agreement with the observations from the NMR and IR characterization. If desired, any ester groups can be saponified by a short alkaline post-treatment as described above.

3.4.3 Determination of critical micelle concentration of 6-carboxypullulan ethers

Amphiphilic polymers have the ability to form micellar aggregates in aqueous environments.[30 31] Hydrophobized polysaccharides[32 33] have received considerable attention due

to their self-assembling characteristics with potential in drug delivery. We therefore investigated the self-assembly behavior of two 6-carboxypullulan ethers in water by dynamic light scattering (DLS).

A plot of the intensity of scattered light as a function of polymer concentration is shown in **Fig 3.5a** for propyl-6-CO_2HPull and **3.5b** for butyl-6-CO_2HPull. These results indicate that 6-carboxypullulan ethers are forming micelles at very low concentrations and the slope change in the crossover region could be related to the critical micelle concentration (CMC) value. For propyl-6-CO_2Pull, the CMC obtained was 7.8 µg/mL and for butyl-6-CO_2Pull, 25 µg/mL. The mean hydrodynamic diameter obtained using DLS for both samples in water was between 170 nm and 300 nm. The CMC values encountered for our 6-carboxypullulan ethers were within the same range obtained for other hydrophobically modified pullulans that showed interesting physicochemical properties. For example, amphiphilic cholesterol-modified pullulan had a CMC of 10 µg/mL.[32] Poly(DL-lactide-co-glycolide)-grafted pullulan derivatives had CMC values ranging from 5.4 to 17 µg/mL and were successfully used in the incorporation and release of adriamycin.[34]

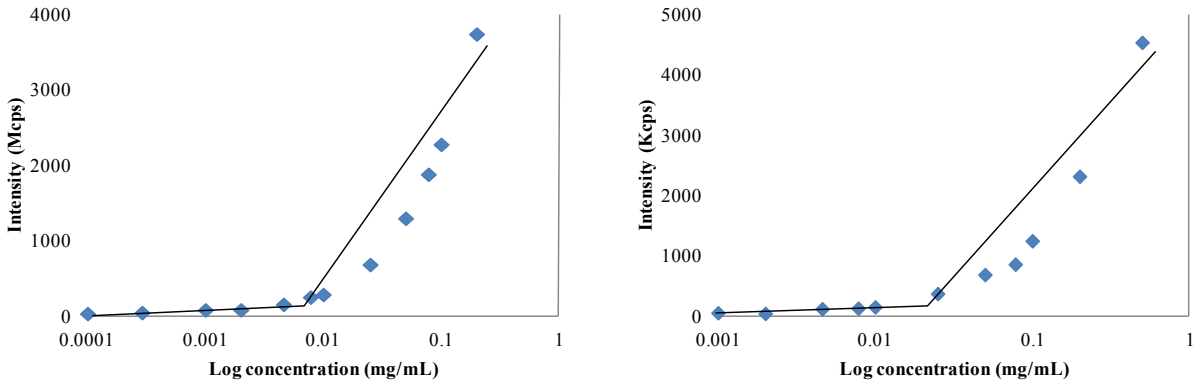

Figure 3.5 Determination of CMC for **(a)** propyl-6-CO_2HPull and **(b)** butyl-6-CO_2HPull

3.5 Conclusions

Carboxyl groups were introduced to the pullulan backbone by oxidation with TEMPO and NaOCl/NaBr. Oxidation was complete and selective for C-6, as expected. The oxidized product, 6-carboxypullulan, is even more water-soluble than pullulan, but we found that the TBA salt of 6-carboxypullulan is soluble in many organic solvents. Therefore, a range of 6-carboxypullulan ethers was synthesized by reaction of 6-carboxypullulan TBA salt homogeneously with various bromo- and iodoalkane reagents in DMSO and sodium hydroxide at 40 °C. Complete substitution (7 per trisaccharide repeat unit) was achieved upon reaction with iodoethane, vs. DS 5 upon reaction with bromoethane. Reaction with longer chain alkyl halides led to products with maximum DS ca. 3. Polymer structures were confirmed by ^{1}H and ^{13}C NMR and IR spectroscopy. Solubility properties strongly depend on the size of the alkyl group and also on the DS. We investigated the possibility of ester formation by reaction of the alkyl halide with the carboxyl group in the 6-carboxypullulan by analysis of the NMR and IR spectra, and by alkaline hydrolysis, which showed that at most only a small amount of carboxylate esterification occurs under these conditions. The amphiphilic character of these polymers led to formation of micellar aggregates, and very low critical micelle concentrations were found for selected 6-carboxypullulan ethers. We have not yet successfully measured the molecular weight of the 6-carboxypullulan ethers because of their strong tendency to self-aggregate in all solvents tested. 6-Carboxypullulan ethers with interesting properties can be obtained by a simple methodology, so the next step will be evaluation of these polymers for drug delivery and other applications.

3.6 References

1. Bauer, R., Physiology of *Dematium pullulans* de Bary. *Zentralbl Bacteriol Parasitenkd Infektionskr Hyg Abt* **1938,** *2* (98), 133-167.

2. Bernier, B., The production of polysaccharides by fungi active in the decomposition of wood and forest litter. *Can. J. Microbiol.* **1958,** *4*, 195-204.

3. Bender, H.; Lehmann, J.; Wallenfels, K., Pullulan, an extracellular glucan from *Pullularia pullulans*. *Biochim Biophys Acta* **1959,** *36*, 309-316.

4. Leathers, T. D., Biotechnological production and applications of pullulan. *Applied Microbiology and Biotechnology* **2003,** *62* (5-6), 468-473.

5. Yamaoka, T.; Tabata, Y.; Yoshito, I., Body distribution profile of polysaccharides after intravenous administration. *Drug Delivery* **1993,** *1* (1), 75-82.

6. Rekha, M. R.; Sharma, C. P., Pullulan as a promissing biomaterial for biomedical applications: a perspective. *Trends. Biomater. Artif. Organs* **2007,** (20), 116-121.

7. Shingel, K. I., Current knowledge on biosynthesis, biological activity, and chemical modification of the exopolysaccharide, pullulan. *Carbohydrate Research* **2004,** *339* (3), 447-460.

8. Xi, K. L.; Tabata, Y.; Uno, K.; Yoshimoto, M.; Kishida, T.; Sokawa, Y.; Ikada, Y., Liver targeting of interferon through pullulan conjugation. *Pharmaceutical Research* **1996,** *13* (12), 1846-1850.

9. Hosseinkhani, H.; Aoyama, T.; Ogawa, O.; Tabata, Y., Liver targeting of plasmid DNA by pullulan conjugation based on metal coordination. *Journal of Controlled Release* **2002,** *83* (2), 287-302.

10. Akiyoshi, K.; Yamaguchi, S.; Sunamoto, J., Self-Aggregates of hydrophobic polysaccharide derivatives. *Chemistry Letters* **1991,** (7), 1263-1266.

11. Hirakura, T.; Nomura, Y.; Aoyama, Y.; Akiyoshi, K., Photoresponsive nanogels formed by the self-assembly of spiropyrane-bearing pullulan that act as artificial molecular chaperones. *Biomacromolecules* **2004,** *5* (5), 1804-1809.

12. Jung, S. W.; Jeong, Y. I.; Kim, S. H., Characterization of hydrophobized pullulan with various hydrophobicities. *International Journal of Pharmaceutics* **2003,** *254* (2), 109-121.

13. Kost, J.; Langer, R., Responsive polymeric delivery systems. *Advanced Drug Delivery Reviews* **2001,** *46* (1-3), 125-148.

14. Edgar, K. J., Cellulose esters in drug delivery. *Cellulose* **2007,** *14* (1), 49-64.

15. Dulong, V.; Le Cerf, D.; Picton, L.; Muller, G., Carboxymethylpullulan hydrogels with a ionic and/or amphiphilic behavior: Swelling properties and entrapment of cationic and/or hydrophobic molecules. *Colloids and Surfaces a-Physicochemical and Engineering Aspects* **2006,** *274* (1-3), 163-169.

16. Lu, D. X.; Wen, X. T.; Liang, J.; Gu, Z. W.; Zhang, X. D.; Fan, Y. J., A pH-sensitive nano drug delivery system derived from pullulan/doxorubicin conjugate. *J Biomed Mater Res B* **2009,** *89B* (1), 177-183.

17. Posey-Dowty, J. D.; Watterson, T. L.; Wilson, A. K.; Edgar, K. J.; Shelton, M. C.; Lingerfelt, L. R., Zero-order release formulations using a novel cellulose ester. *Cellulose* **2007,** *14* (1), 73-83.

18. George, M.; Abraham, T. E., Polyionic hydrocolloids for the intestinal delivery of protein drugs: Alginate and chitosan - a review. *Journal of Controlled Release* **2006,** *114* (1), 1-14.

19. Konno, H.; Handa, T.; Alonzo, D. E.; Taylor, L. S., Effect of polymer type on the dissolution profile of amorphous solid dispersions containing felodipine. *European Journal of Pharmaceutics and Biopharmaceutics* **2008,** *70* (2), 493-499.

20. Friesen, D. T.; Shanker, R.; Crew, M.; Smithey, D. T.; Curatolo, W. J.; Nightingale, J. A. S., Hydroxypropyl methylcellulose acetate succinate-based spray-dried dispersions: An overview. *Molecular Pharmaceutics* **2008,** *5* (6), 1003-1019.

21. Ilevbare, G. A.; Liu, H.; Edgar, K. J.; Taylor, L. S., Understanding polymer properties important for crystal growth inhibition-impact of chemically diverse polymers on solution crystal growth of ritonavir. *Crystal Growth & Design* **2012,** *12* (6), 3133-3143.

22. Kar, N.; Liu, H.; Edgar, K. J., Synthesis of cellulose adipate derivatives. *Biomacromolecules* **2011,** *12* (4), 1106-1115.

23. Henni-Silhadi, W.; Deyme, M.; Boissonnade, M. M.; Appel, M.; Le Cerf, D.; Picton, L.; Rosilio, V., Enhancement of the solubility and efficacy of poorly water-soluble drugs by hydrophobically-modified polysaccharide derivatives. *Pharmaceutical Research* **2007,** *24* (12), 2317-2326.

24. Denooy, A. E. J.; Besemer, A. C.; van Bekkum, H., Highly Selective Nitroxyl Radical-Mediated Oxidation of Primary Alcohol Groups in Water-Soluble Glucans. *Carbohydrate Research* **1995,** *269* (1), 89-98.

25. Paris, E.; Stuart, M. A. C., Adsorption of hydrophobically modified 6-carboxypullulan on a hydrophobic surface. *Macromolecules* **1999,** *32* (2), 462-470.

26. Yang, J. H. D., Y. M.; Huang, R. H.; Wan, Y. Y.; Wen, Y., The structure-anticoagulant activity relationships of sulfated lacquer polysaccharide - Effect of carboxyl group and position of sulfation. *International Journal of Biological Macromolecules* **2005,** *36* (1-2), 9-15.

27. Pawar, S. N.; Edgar, K. J., Chemical Modification of Alginates in Organic Solvent Systems. *Biomacromolecules* **2011,** *12* (11), 4095-4103.

28. Durand, A.; Dellacherie, E., Neutral amphiphilic polysaccharides: chemical structure and emulsifying properties. *Colloid and Polymer Science* **2006,** *284* (5), 536-545.

29. Robert Milton Silverstein, G. C. B., Terence C. Morrill, *Spectrometric identification of organic compounds*. 5th ed.; John Wiley & Sons: 1991; p 502.

30. Gref, R.; Minamitake, Y.; Peracchia, M. T.; Trubetskoy, V.; Torchilin, V.; Langer, R., Biodegradable long-circulating polymeric nanospheres. *Science* **1994,** *263* (5153), 1600-1603.

31. Jung, S. W.; Jeong, Y. I.; Kim, Y. H.; Kim, S. H., Self-assembled polymeric nanoparticles of poly(ethylene glycol) grafted pullulan acetate as a novel drug carrier. *Archives of Pharmacal Research* **2004,** *27* (5), 562-569.

32. Akiyoshi, K.; Deguchi, S.; Moriguchi, N.; Yamaguchi, S.; Sunamoto, J., Self-aggregates of hydrophobized polysaccharides in water - Formation and characteristics of nanoparticles. *Macromolecules* **1993,** *26* (12), 3062-3068.

33. Nishikawa, T.; Akiyoshi, K.; Sunamoto, J., Supramolecular assembly between nanoparticles of hydrophobized polysaccharide and soluble-protein complexation between the self-aggregate of cholesterol-bearing pullulan and alpha-chymotrypsin. *Macromolecules* **1994,** *27* (26), 7654-7659.

34. Jeong, Y.-I.; Na, H.-S.; Oh, J.-S.; Choi, K.-C.; Song, C.-E.; Lee, H.-C., Adriamycin release from self-assembling nanospheres of poly(dl-lactide-co-glycolide)-grafted pullulan. *Journal of Pharmaceutical Sciences* **2006,** *322*, 154-160.

3.7 Copyright Authorization

Copyright Clearance Center RightsLink®

Account Info | Help

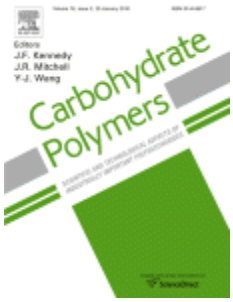

Title: Synthesis of amphiphilic 6-carboxypullulan ethers
Author: Junia M. Pereira,Michelle Mahoney,Kevin J. Edgar
Publication: Carbohydrate Polymers
Publisher: Elsevier
Date: Dec 25, 2012
Copyright © 2012, Elsevier

Logged in as:
Junia Pereira
Account #:
3000669578
LOGOUT

Order Completed
Thank you very much for your order.

This is a License Agreement between Junia Pereira ("You") and Elsevier ("Elsevier") The license consists of your order details, the terms and conditions provided by Elsevier, and the payment terms and conditions.

License number	Reference confirmation email for license number
License date	Jun 22, 2013
Licensed content publisher	Elsevier
Licensed content publication	Carbohydrate Polymers
Licensed content title	Synthesis of amphiphilic 6-carboxypullulan ethers
Licensed content author	Junia M. Pereira, Michelle Mahoney, Kevin J. Edgar
Licensed content date	25 December 2012
Number of pages	1
Type of Use	reuse in a thesis/dissertation
Portion	full article
Format	both print and electronic
Are you the author of this Elsevier article?	Yes
Will you be translating?	No
Order reference number	
Title of your thesis/dissertation	Synthesis of pullulan derivatives for drug delivery
Expected completion date	Aug 2013
Elsevier VAT number	GB 494 6272 12

Chapter 4 **Regioselectively Modified Pullulan Derivatives Containing Amine and Amide Groups: Potential for Biomedical Applications**

(Adapted from Pereira, J. M. and Edgar, K. J. Manuscript submitted to publication in Cellulose)

4.1 Abstract

Hydrophobically modified polysaccharides that contain amine and amide groups possess exceptional features for drug delivery and other applications. These chemical groups are known to play a fundamental role in the biological activity of important polysaccharides. Pullulan is known for its non-toxicity and biocompatibility, therefore, we have applied the versatile Staudinger reaction for the synthesis of regioselective pullulan derivatives containing amino or amido groups with promising biological properties. The synthesis began with the regioselective bromination of pullulan at C-6 with NBS and Ph_3P. We have demonstrated the facile synthesis of 6-bromo-6-deoxy-pullulan, which is soluble in a range of organic solvents and therefore is a dynamic intermediate for the synthesis of other pullulan derivatives. Azide displacement of bromide from 6-bromo-6-deoxy-pullulan esters yielded corresponding 6-azido-6-deoxy-pullulan esters, which were finally converted to amino or amidopullulan compounds.

4.2 Introduction

Pullulan is a non-ionic water-soluble polysaccharide which is produced from starch by the yeast-like fungus *Aureobasidium pullulans*.[1 2] Its structural formula may be represented as a regular sequence of panoses or isopanoses bonded by α-(1→4)-linkages (**Fig 4.1**).[3] Panose: [α-D-Glc*p*-(1→6)-α-D-Glc*p*-(1→4)-α-D-Glc*p*] and isopanose: [α-D-Glc*p*-(1→4)-α-D-Glc*p*-(1→6)-α-D-Glc*p*]. Alternatively, it can be described as consisting predominantly of maltotriose units, i.e. units of three 1,4-linked α-D-glucose molecules, which are polymerized in a linear fashion via 1,6- linkages. Pullulan has low toxicity and has been used for more than 20 years as an additive in the food industry.[4] It biodegrades in the body and does not evoke an immune response. It has

also been shown to be non-toxic when administered intravenously.[5] In view of the attractive characteristics of pullulan and the possibility of chemical modification to suit the desired application, there have been many reports of the synthesis of new pullulan derivatives with application in drug delivery.[6] [7] Pullulan is concentrated disproportionately in the liver after intravenous administration, and as a result it has been studied as a promising polymeric carrier for treatment of liver-related diseases.[8] This accumulation of pullulan in the liver appears to be a short-term effect and thus it does not represent a health concern.

In the pullulan structure, nine OH groups per trisaccharide repeating unit are available for substitution. When the hydroxyl groups in a polysaccharide are reacted, substitution can occur randomly or in a regular fashion. It's well established that the properties of a polysaccharide can be greatly affected by the substitution pattern.[9] Regioselectivity is important in achieving compounds with well-controlled properties.[10] Regioselectively substituted products, due to their well-defined structures and the resulting simpler spectra, can be characterized much more precisely than randomly substituted products, permitting deeper insight into polymer structure-property relationships. Furthermore, regioselectivity is potentially important to facilitate FDA (Food and Drug Administration) approval of formulations where the polymer might reach circulation (i.e., intravenous formulations or oral nanoparticles), since FDA requires full characterization and structural control on such polymers.

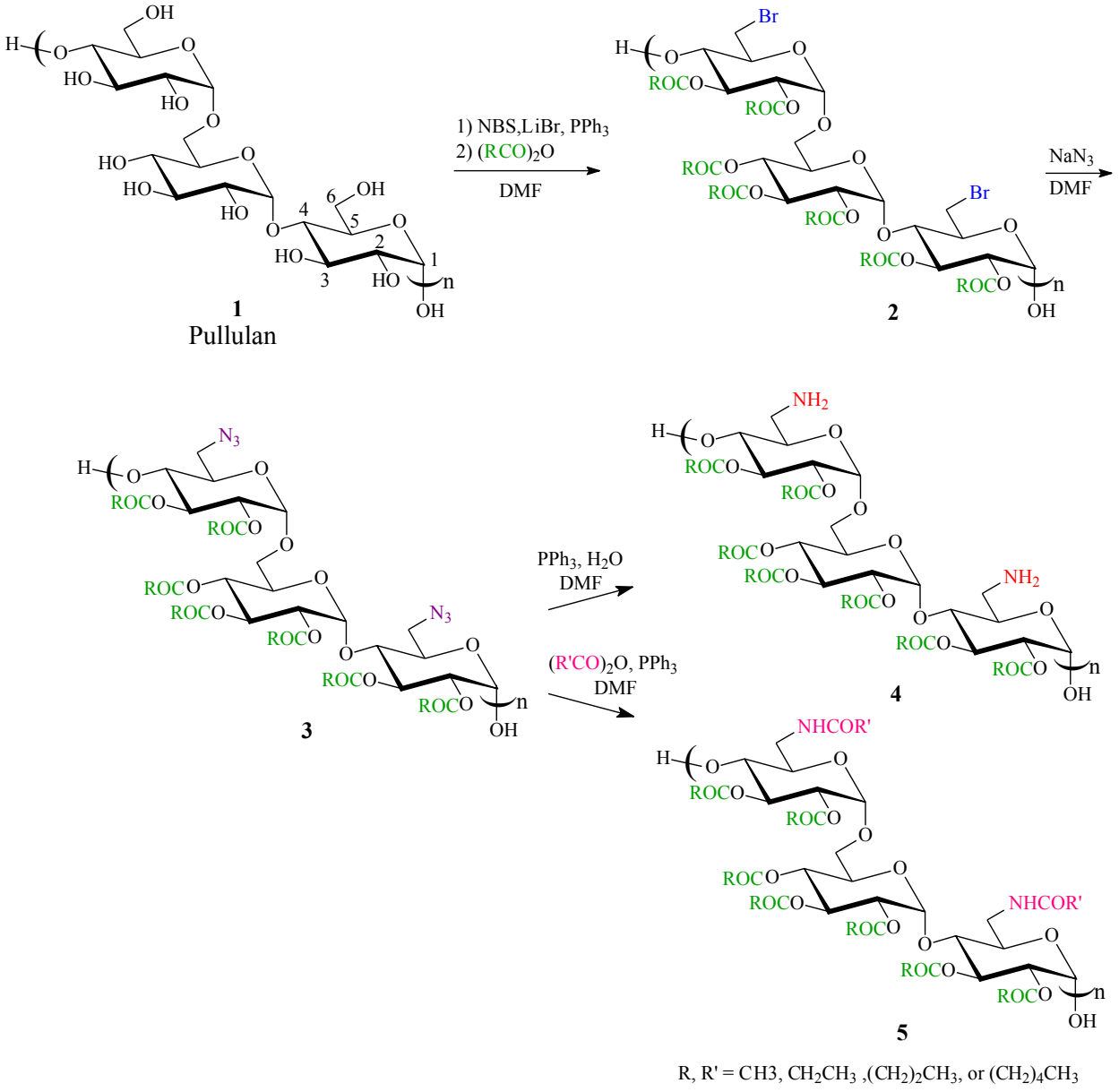

Figure 4.1 Synthesis of 6-amino and 6-amido-6-deoxy-pullulan esters

Most pullulan modifications are intended to reduce its water solubility or to introduce charged or reactive groups for functionality.[11 12 13 14]

We designed the synthesis of a range of regioselectively modified pullulan derivatives, containing amide and amine groups (**Fig 4.1**). These chemical groups are known to play a fundamental role in the biological activity of important polysaccharides, such as chitin and

chitosan. Chitin is a β-(1,4)-linked polymer of N-acetyl-D-glucosamine and chitosan is the semi-synthetic deacetylated derivative of chitosan, a β-(1,4)-linked copolymer of N-acetyl-D-glucosamine and D-glucosamine[15] (**Fig 4.2**). Chitin is an important component in crustacean shells and insect exoskeletons, and components of the cell wall of infectious pathogens such as bacteria and yeast. These polysaccharides are widely used in a variety of pharmaceutical and commercial applications.[16] [17] [18] Importantly, many of the biological properties of aminopolysaccharides like chitosan and glycosaminoglycans (e.g. heparin, chondroitin sulfate) are exerted through interactions with proteins. For example chitosan opens up the tight junctions between enterocytes in the small intestine, permitting absorption of molecules that would otherwise permeate poorly from the intestines to the bloodstream. This property has been shown to result from specific interactions between chitosan and proteins such as integrin, that help to create the tight junctions.[19] Therefore the regiospecific synthesis of novel aminopolysaccharide derivatives is of intense interest as a tool for elucidating structural requirements for interactions with proteins, and potentially to create derivatives with interesting ability for valuable and specific biological effects mediated by such protein interactions. To date, there have been no reports of the investigation of aminopullulan derivatives with structures isomeric to chitin or chitosan for protein interaction or drug delivery applications.

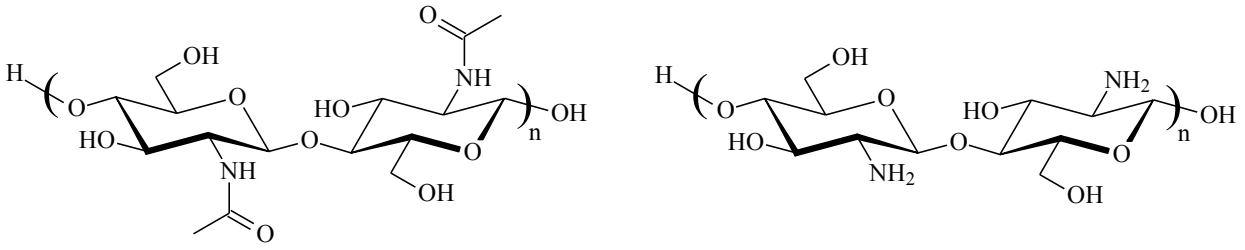

Figure 4.2. Chemical structures of chitin and chitosan

Pullulan derivatives synthesized herein are in fact structural isomers of chitin and chitosan. Amino or amido groups were regioselectively introduced at carbon 6 in the pullulan backbone, while they naturally occur at carbon 2 in chitin and chitosan.

Physico-chemical and biological properties are distinct for chitin and chitosan mainly due to the presence of acetylated or free amino groups in the glucosamine residue, respectively; the free amine groups also strongly influence the polarity of the polysaccharide, since they are partly or entirely protonated within physiological pH ranges. The degree of *N*-acetylation is therefore an important characteristic that influences the performance of chitin/chitosan in many of its applications. Kofuji et al. (2005)[20] stated that the proper selection of physicochemical properties of chitosan is important for the choice of the appropriate chitosan as a drug delivery vehicle. Among several physicochemical properties, degree of acetylation seems to be one of the most important. Many properties have been studied for these polymers as a function of degree of acetylation, such as solubility, conformation and dimensions of chains,[21 22 23] biodegradability,[24 25] biocompatibility,[26] mucoadhesion,[27] ability to form microspheres,[20] drug loading capacity[28] and rate of drug release.[29] Degree of acetylation is a key parameter in the biomedical activity of chitin/chitosan, such as the preparation of chitosan/DNA complexes,[30] gene delivery,[31] tissue engineering,[32] wound healing,[33] and antioxidant activity.[34]

In an attempt to synthesize pullulan derivatives with potential biological properties and considering the impact of degree of acetylation in chitin/chitosan, we introduced amino and amide groups to pullulan backbone. These substitutions may affect the biomedical properties of pullulan derivatives as a result of changes in the solubility, inter-chain interactions due to H-bonds and the hydrophobic nature of the acyl group. Other groups such as esters are known to greatly affect the properties of polysaccharides.[9, 35] Esterification of hydroxyl groups in polysaccharides is the most conventional way of modifying their properties such as solubility, affinity for active compounds, and drug release rate. Therefore, herein, ester groups were also introduced to the regioselectively synthesized amino and amidopullulan derivatives.

The most common method used to synthesize pullulan containing amino groups has been by the attachment of amine containing side chains to its backbone. Pullulans modified in this manner have been investigated as non-viral gene delivery carriers. It was demonstrated that some spermine-pullulan samples enabled efficient delivery of plasmid DNA to the liver.[8 36] Aminated pullulan microspheres were prepared by chemically crosslinking pullulan with 1-chloro-2,3-epoxypropane, followed by amination with N,N-diethyl-2-chloroethyl amine hydrochloride.[37] All the produced diethylaminoethyl-pullulan microspheres were able to quantitatively load DNA with no DNA degradation observed after 14 days.

Our approach in this work is the introduction of amine/amide groups to pullulan by substitution of the polysaccharide hydroxyl groups by amine or amides. An important tool for regioselective derivatization of polysaccharides like pullulan and cellulose lies in the higher reactivity of the C-6 primary hydroxyl group. Steric accessibility of this site either lends itself to direct derivatization or facilitates its protection and deprotection, thus enabling further chemistry at the secondary positions. Among these, regiospecific halogenation is one of the most effective routes for activation of the primary site, facilitating further transformations at this position.[38] These C-6 halogeno intermediates can then be employed to prepare, after a few steps, other derivatives such as 6-deoxy-6-amino polysaccharides.

We demonstrate in this paper regioselective synthesis of pullulan derivatives starting from 6-bromo-6-deoxy-pullulan. We have not found any publication where 6-deoxy-6-bromo-pullulan was isolated. Only 6-chloro-6-deoxy-pullulan was prepared by reaction with another reagent, methanesulfonyl chloride, in which the prominent mesylation of the hydroxyl groups occurs as a side reaction.[39] Brominated polysaccharides can then be converted to their corresponding azides by S_N2 displacement of the bromide. Cimecioglu et al. (1997)[40] reported azidation of pullulan and amylase using PPh_3/CBr_4 in DMF/LiN_3 that presumably involved 6-bromopullulan as an intermediate, and Shey has extended this reaction to starches.[41] Cimecioglu et al. (1997) found that the azidation reactions of pullulan and amylase did not go to completion, and they also mentioned that reduction of the azide occurred in some products, as it is expected in reactions employing CBr_4 with excess PPh_3. Indeed, our attempts to use this procedure have led to pullulan products containing azide and amino groups as well (results not shown). Furthermore, it has been reported that formation of the primary azidodeoxy compounds under these reaction conditions is accompanied by simultaneous formation of the corresponding primary bromodeoxy compounds.[42] We then explored the use of sodium azide to convert 6-bromo-6-deoxy-pullulan esters to 6-azido-6-deoxy-pullulan esters. 6-Azido-6-deoxy-pullulan esters were then used as intermediate in the dynamic Staudinger reaction. Cimecioglu et al. (1994)[38] have demonstrated the utility of the Staudinger reaction for amylose, but they did not demonstrate it in the presence of other substituents.

Fox and Edgar (2012)[43] have established this reaction for cellulose in the presence of short chain esters, thus we explored its scope for pullulan, which is a polysaccharide that, owing

to its safety, could be used not only for oral drug delivery but many other biomedical applications that might reach circulation.

4.3 Experimental

4.3.1 Materials and methods

Pullulan was from the Hayashibara Company. Pullulan, lithium bromide (LiBr, Fisher) and sodium azide (NaN_3, Acros) were dried under vacuum at 120 °C. N-Bromosuccinimide (NBS, Sigma), triphenylphosphine (Ph_3P, Strem), sodium carbonate (Na_2CO_3, Sigma), anhydrous pyridine and carboxylic acid anhydrides (acetic, propionic, butyric and hexanoic anhydrides (Acros) were used as received. Dimethylformamide (DMF) was kept over 4 Å molecular sieves. Ethanol and acetone (reagent grade, Fisher) were used as received.

For NMR analysis, samples were prepared by dissolving 10−15 mg (for ^1H) or 80-100 mg (for ^{13}C) of polymer in 0.7 mL of d_6-DMSO or $CDCl_3$. The solution was filtered through a pipette containing glass wool into a standard 5 mm NMR tube. ^1H and ^{13}C NMR spectra were acquired on Varian INOVA 400 MHz or Bruker AVANCE 500 MHz spectrometers with 32–64 scans for ^1H and 20,000-25,000 scans for ^{13}C. Chemical shifts are reported relative to the solvents.

Differential scanning calorimetry (DSC) analysis was performed using a TA Instruments Q2000 (TA Instruments, New Castle, DE) attached to a refrigerated cooling accessory. Powders (3-8 mg) were loaded in aluminum T-zero pans. Dry N_2 was used as the purge gas at 50 mL/min. All analyses were performed using a heat/cool/heat procedure. Samples were heated to 150 °C at 20 °C/min, cooled to -20 °C at 100°C/min and heated again to 220 °C at 20 °C/min. Glass transition temperatures (T_g) were determined from second heat scans. The data was analyzed using the Universal Analysis 2000 software for Windows 2000/XP provided with the instrument.

Molecular weight determination was achieved by gel permeation chromatography in N-methylpyrrolidone containing 0.05% lithium bromide using a Waters 1515 isocratic HPLC

pump, Viscotek 270 dual detector, and Waters 2414 refractive index detector. Mobile phase flow rate was 0.5 mL/min. Universal calibration curves were prepared using polystyrene standards.

4.3.2 Calculation of degree of substitution of ester and amide groups

Degree of substitution of ester groups (DS_E) in the 6-bromo or 6-azido-6-deoxy-pullulan esters is described as per trisaccharide repeat unit, with a maximum DS of 7. DS_E values were calculated by ^{1}H NMR using the following formula:

$$DS_E = 7\frac{A}{B}$$

A is the integration of the methyl peak of the acyl group, which was observed at approximately 2.0 ppm for acetyl, 1.0 ppm for propionyl, 0.9 ppm for butyryl and 0.8 ppm for hexanoyl in the ^{1}H NMR spectra of the respective 6-bromo or 6-azido-6-deoxy-pullulan ester. B is the integration of the backbone protons observed in the 3.2-5.9 ppm region.

This formula was derived from the following relation:

$$\frac{3DS_E}{21} = \frac{A}{B}$$

Each OH substitution in the pullulan backbone with an acetyl, propionyl, butyryl or hexanoyl brings to the pullulan backbone 3 methyl protons ($3DS_E$) and there are 21 backbone protons (C–H) resulting from each pullulan trisaccharide repeat unit.

Degree of substitution of amide groups (DS_A) in the 6-acetamido-6-deoxy-pullulan esters is described as per trisaccharide repeat unit, with a maximum DS of 2.

DS_A values were calculated by ^{1}H NMR using the following formula:

$$DS_A = \frac{7 \times (C - \frac{2}{3}A)}{B}$$

A is the integration of the methyl peak of the ester group and was observed at approximately 2.0 ppm for acetyl, 1.0 ppm for propionyl, 0.8 ppm for butyryl and 0.9 ppm for hexanoyl in the ^{1}H NMR spectra of the respective 6-acetamido-6-deoxy-pullulan ester. C is the integration of the peaks observed in the 1.7-2.6 ppm region (CH_3 amide + CH_2 ester). B is the integration of the backbone protons (2.6-5.8 ppm).

This formula was derived from the following relation:

$$\frac{3DS_A}{21} = \frac{C - \frac{2}{3}A}{B}$$

Each acetamide group brings to the pullulan backbone 3 methyl protons ($3DS_A$) and there are 21 backbone protons (C–H) resulting from each pullulan trisaccharide repeat unit. The CH_3 of the acetamide group was quantified by the integration of the peaks observed in the 1.7-2.6 ppm region (C) minus the integration of the protons from the CH_2 of the respective alkyl ester group (2/3 A) that overlap with the CH_3 acetamide protons. For each ester substituent, there will be one methyl (3H) per overlapping methylene group (2H).

Note that for 6-acetamido-6-deoxy-2,3,4-O-acetyl-pullulan, the above relation is simplified to:

$$DS_A = 7\frac{C}{B}$$

as there are no CH_2 protons from ester groups that overlap with the CH_3 acetamide protons, C is simply the integration of the CH_3 of the acetamide group.

4.3.3 Synthesis of 6-bromo-6-deoxy-pullulan

Pullulan (2 g, 12.3 mmol anhydroglucose units, AGU) and LiBr (2.34 g, 27.06 mmol) were dissolved in DMF (80 mL) at 70 °C with stirring under a nitrogen atmosphere until homogeneous (≈ 1.5 h). The solution was cooled to room temperature, and treated by dropwise addition over a 10 min period of a solution of PPh_3 (6.44 g, 24,06 mmol, 2 fold excess/AGU) in

DMF (12 mL). Then, a 2-fold excess/AGU of NBS (4.38 g, 24.06 mmol) was added at once. The solution turned yellow, a fine precipitate formed, and the mixture progressively darkened in color. After stirring at room temperature for 30 min, the temperature was raised to 70 °C (oil bath temperature), and mechanical stirring was continued for 3 h. The brown and homogeneous mixture was then cooled to room temperature and slowly poured into 1 L of ice-water containing 20 g of Na_2CO_3. After stirring overnight, the light brown precipitate was collected by filtration and rinsed extensively with water. The solids were stirred for 12h in ethanol, then 12h in acetone to remove triphenylphosphine oxide or PPh_3 impurities. Finally the product was isolated by filtration, then dried under vacuum at 50 °C.

4.3.4 Esterification of 6-bromo-6-deoxy-pullulan

6-Bromo-6-deoxy-pullulan (Br-Pull, 2 g, 8.9 mmol) was dissolved in DMF at 70 ºC. Pyridine (1.43 mL, 18 mmol), then 20 eq per Br-Pull AGU of a carboxylic anhydride (acetic, propionic, butyric or hexanoic) was slowly added to the reaction and the solution was stirred at 70 ºC for 16h. The product from the reaction with acetic anhydride was isolated by adding the reaction mixture slowly to 300 mL of water, followed by vacuum filtration. The products from the reactions with propionic, butyric and hexanoic anhydride could not be precipitated in water (probably due to plasticization by the respective co-product carboxylic acid). The propionic and butyric reaction solutions were then dialyzed against ethanol for 5h. The products were isolated by adding the ethanol solution to 300 mL of water, followed by vacuum filtration. The solution from the reaction with hexanoic anhydride was extensively dialyzed against acetone and the product was isolated by adding the acetone solution to 300 mL of water, followed by vacuum filtration. All products were washed with water and dried overnight in a vacuum oven at 50 ºC.

4.3.5 Displacement of bromide in the 6-bromo-6-deoxy-pullulan esters to obtain 6-azido-6-deoxy-pullulan esters

6-Bromo-6-deoxy-pullulan ester (1g) was dissolved in 60 mL of anhydrous DMF at 60 ºC under nitrogen and 5 equiv per reagent-AGU of NaN_3 was added to the flask. The suspension was stirred for 8 h. The reaction suspension was then filtered under vacuum to remove the unreacted NaN_3. The product was isolated by pouring the filtrate into 150 mL of water followed by vacuum filtration. The solids were washed extensively with water and dried overnight in a vacuum oven at 50 ºC.

4.3.6 Conversion of 6-azido-6-deoxy-2,3,4-O-acetyl-pullulan to 6-amino-6-deoxy-2,3,4-O-acetyl-pullulan

6-Azido-6-deoxy-2,3,4-O-acetyl-pullulan (0.300 g, 1.1 mmol) was dissolved in 10 mL DMF followed by addition of 0.250 mL of deionized water and 2 equiv per reagent-AGU of Ph_3P. The reaction solution was stirred for 16 h at room temperature in a stoppered flask. Afterward, the solution was transferred to 3,500 MWCO dialysis tubing (prewet with water) that was then placed in a large beaker containing acetone. Dialysis was continued for 2 days, and the acetone from the beaker was replaced twice every day. Then, dialysis was performed against ethanol for 2 days, and the ethanol from the beaker was replaced twice every day. As the dialysis of the reaction solution progressed, a precipitate slowly formed within the tubing. The contents of the dialysis tubing were removed, and the precipitate was isolated by vacuum filtration. The solids were washed extensively with water and dried overnight in a vacuum oven at 50 ºC.

4.3.7 Conversion of 6-azido-6-deoxy-pullulan esters to 6-amido-6-deoxy-pullulan esters

6-Azido-6-deoxy-pullulan ester (0.300 g) was dissolved in 10 mL of anhydrous DMF under nitrogen, and 20 equiv per reagent-AGU of a carboxylic acid anhydride was added to the flask. In a separate flask, Ph_3P (2 equiv per reagent-AGU) was dissolved in 10 mL anhydrous

DMF and added to the first flask. The reaction solution was stirred for 16 h at room temperature under nitrogen. Afterward, the solution was transferred to 3,500 MWCO dialysis tubing (prewet with water) that was then placed in a large beaker containing acetone. Dialysis was continued for 2 days, and the acetone from the beaker was replaced twice every day. Then, dialysis was performed against ethanol for 2 days, and the ethanol from the beaker was replaced twice every day. The contents of the dialysis tubing were finally transferred to a round-bottom flask and dried on a rotary evaporator. The product was then dissolved in a minimal amount of acetone and then precipitated in water. The precipitate was isolated by filtration, washed with additional water, and dried in a vacuum oven at 50 °C.

4.4 Results and Discussion

4.4.1 Pullulan bromination

Synthesis of new pullulan derivatives began with the bromination of pullulan at C-6 with NBS and Ph_3P (**Fig 4.1**) to obtain 6-bromo-6-deoxy-pullulan (**7**). Bromination of polysaccharides with NBS/Ph_3P was pioneered by the Furuhata group (1992)[44], and is recognized for its high C-6 regioselectivity. The strong preference for bromination at C-6 is due in part to the low steric hindrance and resulting stronger reactivity of the primary (vs. secondary) hydroxyl groups. Furthermore, the mechanism of the reaction involves an S_N2 substitution by halide, which powerfully favors the observed regioselectivity (**Fig 4.3**). The S_N2 reaction involves backside attack by the bromide nucleophile (**6**); such attack on the secondary alcohol positions is disfavored due to restricted approach angles across the pyranoside ring. Moreover, this mechanism would lead to stereochemical inversion at the secondary positions, energetically disfavored due to the motion of the entire polymer chain that would result.

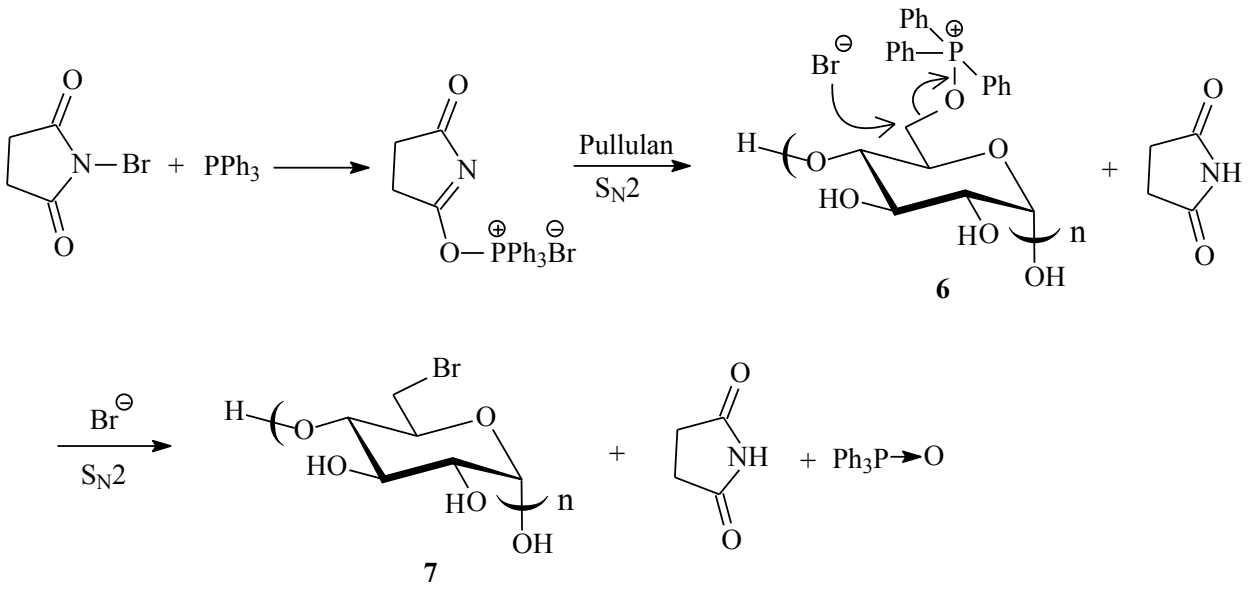

Figure 4.3. Mechanism for the C-6 bromination of pullulan with NBS and PPh_3

Brominated polysaccharides have proved to be versatile intermediates for the regioselective synthesis of several new polysaccharide derivatives by S_N2 displacement of the bromide. For cellulose, further reaction with 6-bromo-6-deoxy-cellulose has been limited due to its poor organic solubility. Work from our lab has shown that the brominated cellulose can be esterified *in situ* to produce cellulose derivatives that are readily soluble in a range of organic solvents, extending the utility of the bromination reaction. [45]

However, there is a side reaction that occurs during the bromination step between the reaction solvent and the polysaccharide alkoxyphosphonium salt intermediate. In the case of cellulose bromination in dimethylacetamide (DMAc), this side reaction leads to acetate ester groups attached to C-6 of cellulose.[46] The acetates present at C-6 can be easily hydrolyzed off by treatment of the brominated product with aqueous Na_2CO_3 solution, but when *in situ* esterification is performed, this hydrolysis step cannot be conducted since it will affect the other esterified hydroxyl groups. Therefore, products from *in situ* esterification will contain a small proportion of acetate groups at C-6, which will be carried through subsequent chemical modifications. When we performed *in situ* esterification of 6-bromo-6-deoxy-pullulan in DMF, the side reaction between pullulan alkoxyphosphonium salt and DMF led to a formate group

attached to C-6 of pullulan. This is the first time that the synthesis of 6-bromo-6-deoxy-pullulan has been described, and we found that, in contrast to 6-bromo-6-deoxy-cellulose, brominated pullulan has very good organic solubility. Thus, the possibility of carrying-out the esterification of 6-bromo-6-deoxy-pullulan hydroxyl groups homogeneously in DMF allowed us to treat 6-bromo-6-deoxy-pullulan with a simple hydrolysis step so as not to contain any undesired formate groups at C-6.

Pullulan was completely brominated at C-6 as indicated by ^{13}C NMR spectroscopy (**Fig 4.4**). Peaks at 60.6 and 60.3 ppm arising from the primary hydroxyl carbons (spectrum not shown) in pullulan were no longer present in the product spectrum, while the carbon peak from the new, chemically distinct CH_2-Br appeared at 35.3 ppm in the brominated pullulan. The anomeric carbons and backbone peaks appear in the region 95 – 105 and 65 – 85 ppm respectively.

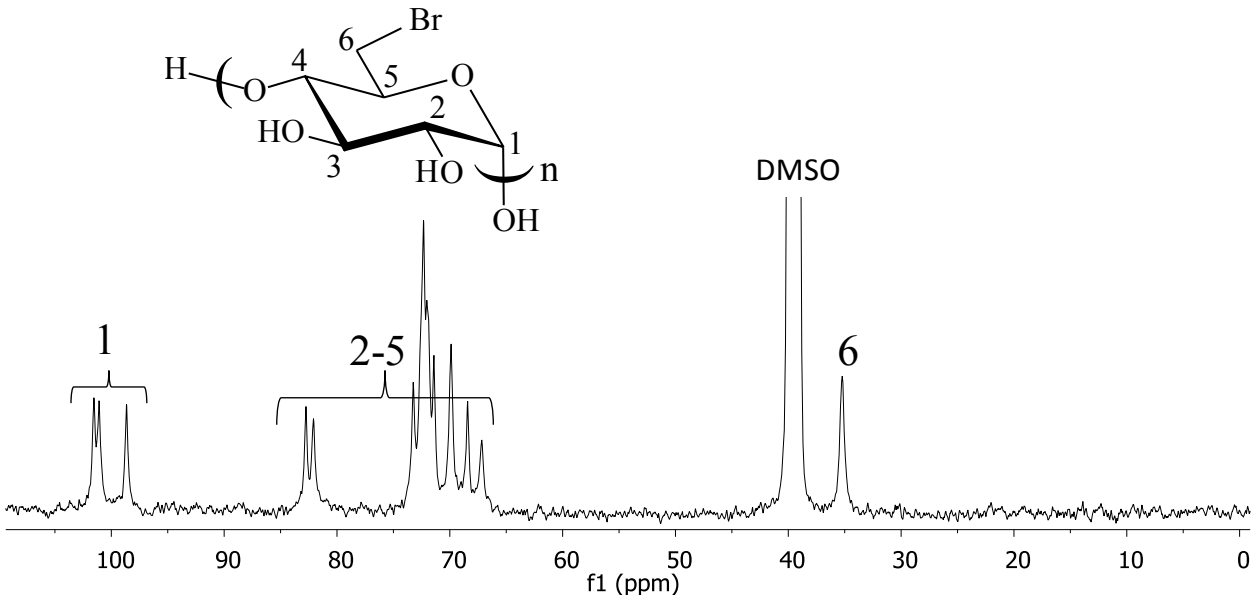

Figure 4.4 ^{13}C NMR spectrum of 6-bromo-6-deoxy-pullulan

4.4.2 Esterification of 6-bromo-6-deoxy-pullulan

Esterification of the remaining hydroxyl groups in 6-bromo-6-deoxy-pullulan with a variety of carboxylic acid anhydrides (acetic, propionic, butyric and hexanoic), homogeneously in DMF, furnished 6-bromopullulan esters (see **Fig A4.1** in appendix for ^{1}H and ^{13}C NMR spectra of 6-bromo-6-deoxy-2,3,4-O-acetyl-pullulan). The esterified 6-bromopullulan products were soluble in a range of organic solvents such as dimethylsulfoxide (DMSO), DMF, N-methyl-2-pyrrolidone (NMP), tetrahydrofuran (THF), chloroform, ethanol and acetone. These derivatives are very promising precursors to other regioselectively substituted pullulan derivatives due to their good solubility, nearly perfect regioselectivity of substitution, and the lability of the 6-bromo group towards further substitution reactions.

4.4.3 Conversion of 6-bromo-6-deoxy-pullulan esters to 6-azido-6-deoxy-pullulan esters

6-Bromo-6-deoxy-pullulan esters were then reacted with NaN_3 to yield the corresponding 6-azido-6-deoxy-pullulan esters (see **Figs S4.2, S4.3** in appendix for ^{1}H and ^{13}C NMR spectra of 6-azido-6-deoxy-2,3,4-O-butyryl and -O-hexanoyl-pullulan). Fox and Edgar (2012)[43] have monitored the azide substitution progress during the conversion of 6-bromo- to 6-azido-6-deoxy-cellulose esters and found that azidation is nearly complete after 8h. The ^{13}C NMR spectrum of 6-azido-6-deoxy-2,3,4-O-acetyl-pullulan (**Fig 4.5**), obtained from reaction at 60 °C for 8h, shows the chemical shift for CH_2-N_3 at 50.8 ppm. The peak for CH_2-Br from the brominated starting material is no longer present at 35 ppm, indicating that the azidation reaction was complete and also that the bromination/azidation sequence was regioselective, since different substituents at carbon 2 (C-2) are known to cause multiplicity of signals for the anomeric carbons (C-1). No such multiplicity is evident here. The anomeric carbon peaks appear as a slightly broad peak at 96 ppm and the other backbone carbon peaks are between 62 and 82 ppm. The chemical shift for the carbonyl peak from the acetate groups is 169.6 ppm. The ^{1}H NMR spectrum of 6-azido-6-deoxy-2,3,4-O-acetyl-pullulan is shown in **Fig A4.2** in the appendix).

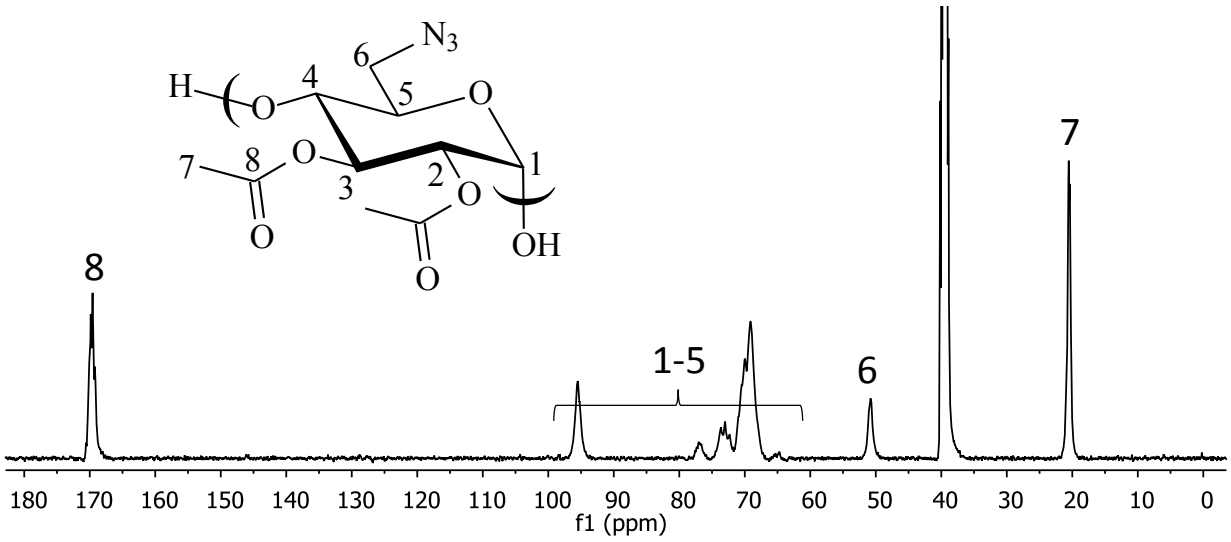

Figure 4.5 ^{13}C NMR spectrum of 6-azido-6-deoxy-2,3,4-O-acetyl-pullulan

Ester degrees of substitution (DS_E) for 6-bromo and 6-azido-6-deoxy-pullulan esters were calculated as described in the experimental section 2.2 and are shown in **Table 4.1**. Despite the high excess (20 eq) of carboxylic acid anhydride used during the esterification of 6-bromo-6-deoxy-pullulan, complete esterification (DS_E = 7) was only attained for 6-bromo-6-deoxy-2,3,4-O-acetyl-pullulan. The other 6-bromo-6-deoxy-pullulan esters, although not fully esterified, had high DS values of around 6. Very little change in DS_E was observed after 6-bromo-6-deoxy-pullulan esters were converted to 6-azido-6-deoxy-pullulan esters, indicating that bromide displacement employing NaN_3 is a mild reaction that largely preserves the ester groups.

Table 4.1 Ester DS (DS_E) for 6-bromo- and 6-azido-6-deoxypullulan esters

6-Bromo-6-deoxy-pullulan esters	DS_E	6-Azido-6-deoxy-pullulan esters	DS_E
6-bromo-6-deoxy-2,3,4-O-acetyl-pullulan	7.0	6-azido-6-deoxy-2,3,4-O-acetyl-pullulan	6.1
6-bromo-6-deoxy-2,3,4-O-propionyl-pullulan	6.2	6-azido-6-deoxy-2,3,4-O-propionyl-pullulan	6.2
6-bromo-6-deoxy-2,3,4-O-butyryl-pullulan	6.2	6-azido-6-deoxy-2,3,4-O-butyryl-pullulan	5.9
6-bromo-6-deoxy-2,3,4-O-hexanoyl-pullulan	5.8	6-azido-6-deoxy-2,3,4-O-hexanoyl-pullulan	5.4

4.4.4 Selective azide reduction to produce 6-amino-6-deoxy-2,3,4-O-acetyl-pullulan

Herein, we employed the Staudinger reduction, which is a mild and selective way to reduce azides to amines, to convert 6-azido-6-deoxy-2,3,4-O-acetyl-pullulan (**8**) to 6-amino-6-deoxy-2,3,4-O-acetyl-pullulan (**11**). The general mechanism for the Staudinger reaction leading to an amine is illustrated in **Fig 4.6**. When the azide group reacts with PPh_3, it forms a phosphazide (**9**), which loses nitrogen gas to form an iminophosphorane intermediate (**10**). Upon hydrolysis, the iminophosphorane leads to the amine substituted derivative (**11**).

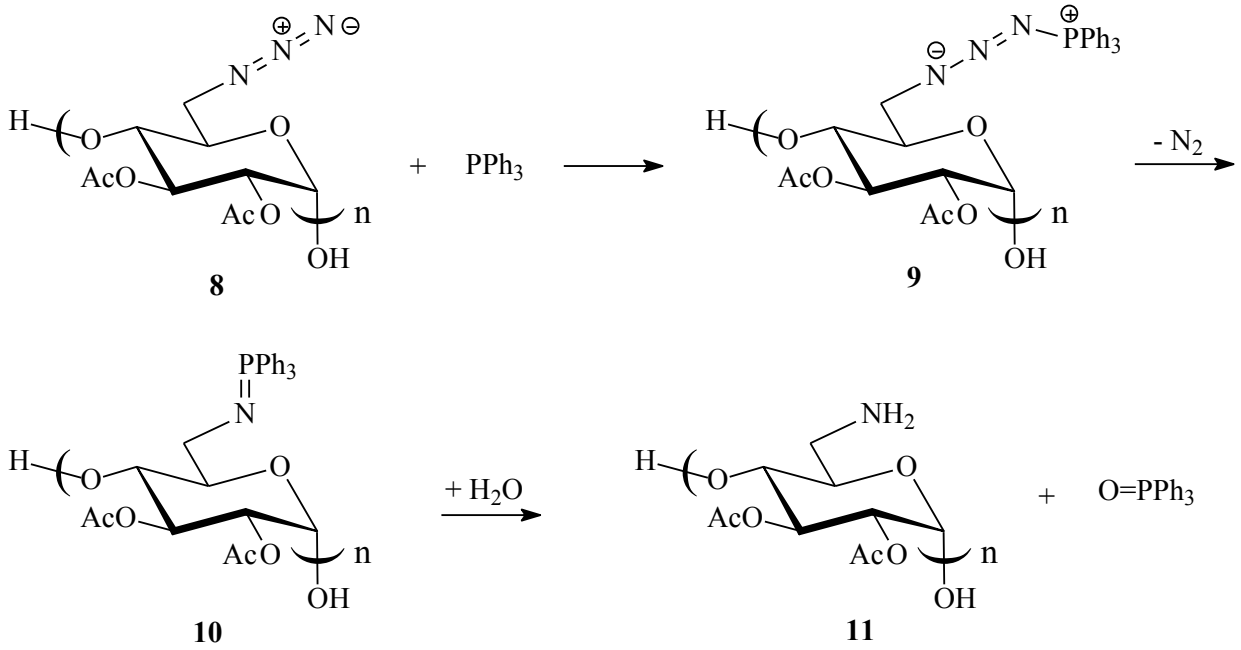

Figure 4.6 Mechanism for the Staudinger reduction

Surprisingly, once 6-amino-6-deoxy-2,3,4-O-acetyl-pullulan was isolated from the reaction solution, it was found to be insoluble in common organic solvents, water, and 1% aqueous HCl. Therefore, characterization of 6-amino-6-deoxy-2,3,4-O-acetyl pullulan was performed by solid state ^{13}C NMR (**Fig 4.7**). **Fig 4.7** shows the chemical shift for CH_2-NH_2 at approximately 40 ppm. The backbone carbon peaks are between 55 and 107 ppm. The chemical shifts for the CH_3 and carbonyl peaks from the acetate groups are approximately 21 and 170 ppm respectively.

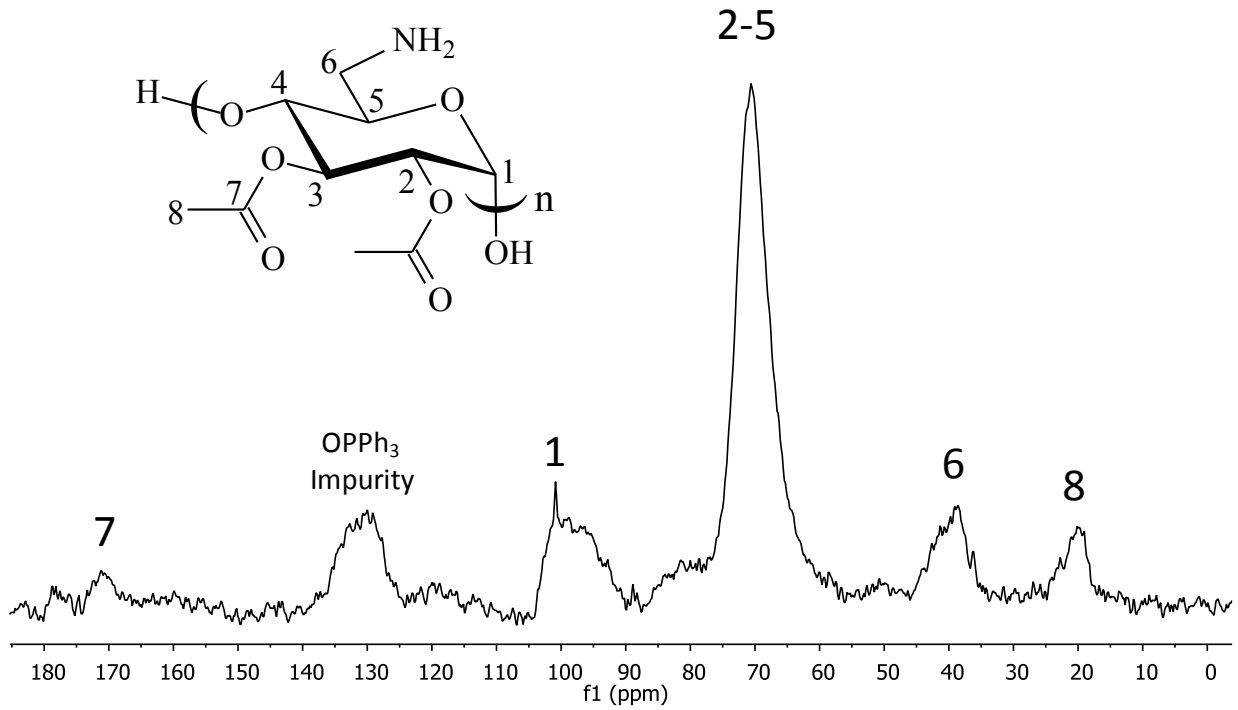

Figure 4.7 Solid state ^{13}C NMR spectrum of 6-amino-6-deoxy-2,3,4-O-acetyl-pullulan

4.4.5 Selective synthesis of 6-amido-6-deoxy-pullulan esters

As illustrated in **Fig 4.6**, reaction of an azide with PPh_3 affords an iminophosphorane, which is a versatile intermediate. Depending on the reaction conditions, the iminophosphorane can be converted to an amine, as described above, or an amide. Therefore, the Staudinger reaction is a useful way to obtain new regioselectively modified derivatives, containing either amine or amide groups, from a common intermediate. When water is present in the reaction, the iminophosphorane intermediate is rapidly hydrolyzed to the amine (**Fig 4.6**). Under anhydrous conditions, the iminophosphorane persists and is the reactive species that leads to the formation of amides. The proposed mechanism by Fox and Edgar (2012) is depicted in **Fig 4.8**. Beginning with the iminophosphorane (**11**) formed as in **Fig 4.6**, the nitrogen atom attacks an electrophilic carbonyl carbon in the carboxylic anhydride. The positively charged phosphonium species then migrates to the carbonyl oxygen of the newly formed amide, now creating a new imine (**13**). Triphenylphosphine oxide is then eliminated as the acyl anion attacks the imino carbon. The resulting species (**15**) is then readily hydrolyzed to an amide (**17**) upon exposure to moisture.

This mechanism was proposed based on the fact that the nitrogen in the iminophosphorane is a more reactive nucleophile than the free amine (suggesting significant contribution from the ylide structure in which a positive charge resides on phosphorus and a negative charge on nitrogen). The reactivity of iminophosphoranes with carbonyl carbons has been well documented in the literature and, in fact, is the basis of the Staudinger ligation, a variation on the Staudinger reduction used to connect two different molecules through an amide bond [47].

6-Azido-6-deoxy-pullulan esters were then reduced with Ph_3P under anhydrous conditions in the presence of excess carboxylic anhydride. The result was selective N-acylation to form an amide; the 2,3,4-O-ester groups remained intact. This procedure allows for the synthesis of derivatives in which the N- and O-acyl groups are separately specified, and they may be selected independently in order to target desired properties. Similar conversions of azides to amides have been previously reported for low molecular weight compounds;[48] in polysaccharides, such conversion has only been demonstrated for cellulose [43]. This methodology was employed to synthesize a variety of 6-acetamido-6-deoxypullulan esters: 6-acetamido-6-deoxy-2,3,4 -O-acetyl, -O-propionyl, -O-butyryl, and -O-hexanoyl-pullulan.

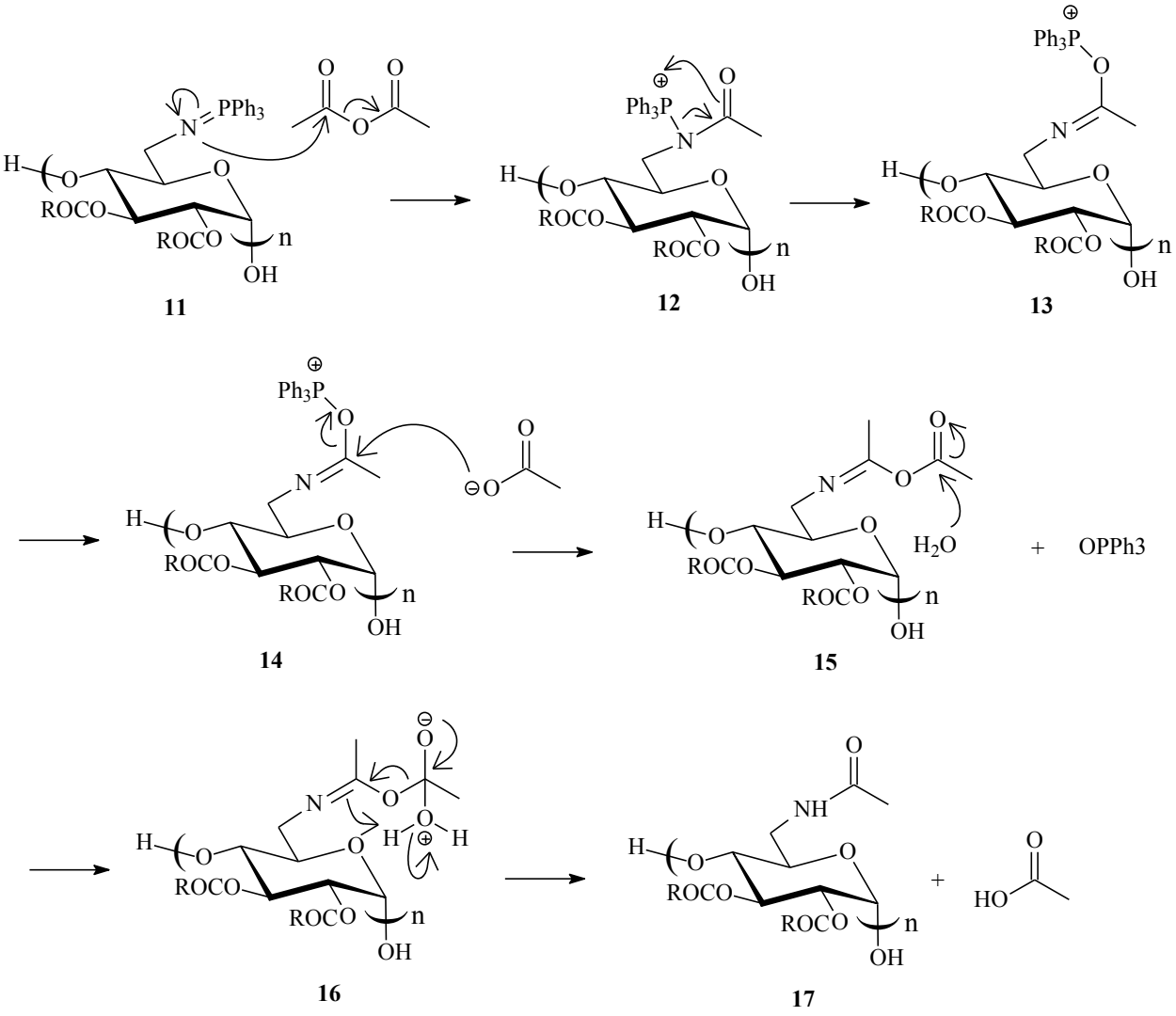

Figure 4.8 Proposed mechanism for the N-acylation of 6-deoxy-6-iminophophoranepullulan. Adapted from Fox and Edgar (2012)[33]

^{13}C NMR spectra of 6-acetamido-6-deoxy-2,3,4-O-acetyl-pullulan and 6-acetamido-6-deoxy-2,3,4-O-butyryl-pullulan are shown in **Figs 4.9 and 4.10**. In each case, the chemical shift for C-6 with a pendant amide group is found at approximately 46 ppm, whereas the aminated C-6 in **Fig 4.7** occurs at approximately 40 ppm. Both figures also show the CH_3 and carbonyl peaks for the acetamide groups at approximately 26 and 174 ppm respectively. In **Fig 4.9**, for the 6-acetamido-6-deoxy-2,3,4-O-acetyl-pullulan, the chemical shift for the CH_3 from the acetyl ester groups is 21.7 ppm, while the carbonyl from the same groups appears at 170 ppm. In **Fig 4.10**,

for 6-acetamido-6-deoxy-2,3,4-O-butyryl-pullulan, the carbon peaks for the butyryl ester groups appear at 13.6, 18.2 and 35.9 ppm, while its carbonyl peak chemical shift is 172.09 ppm.

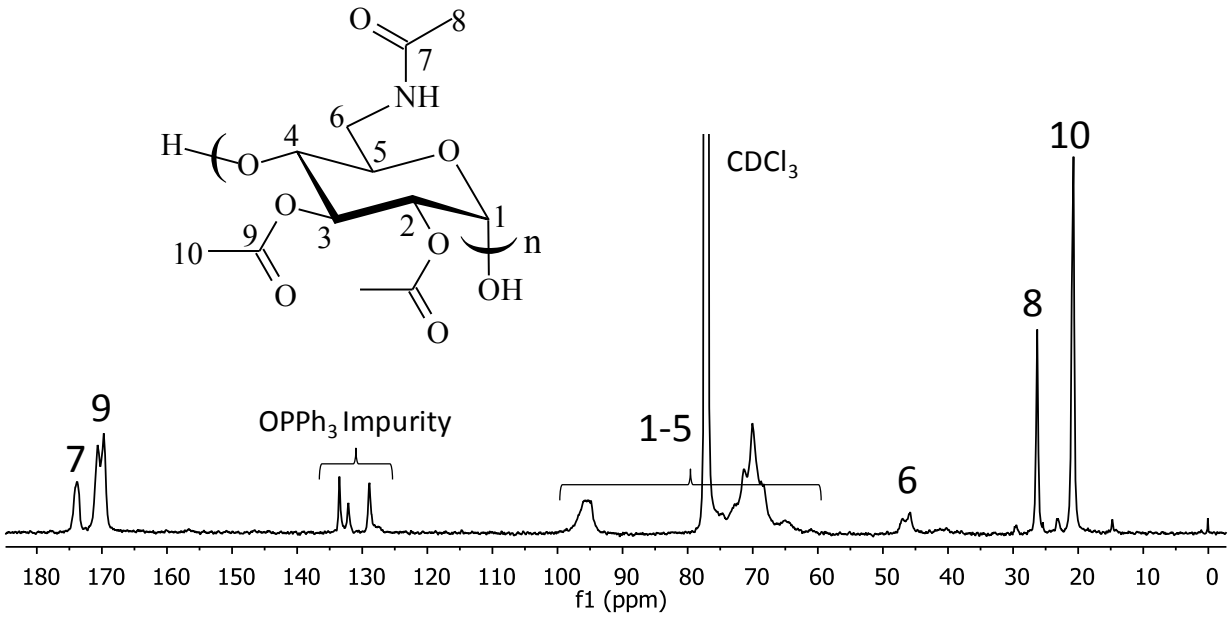

Figure 4.9 ^{13}C NMR spectrum of 6-acetamido-6-deoxy-2,3,4-O-acetyl-pullulan in $CDCl_3$

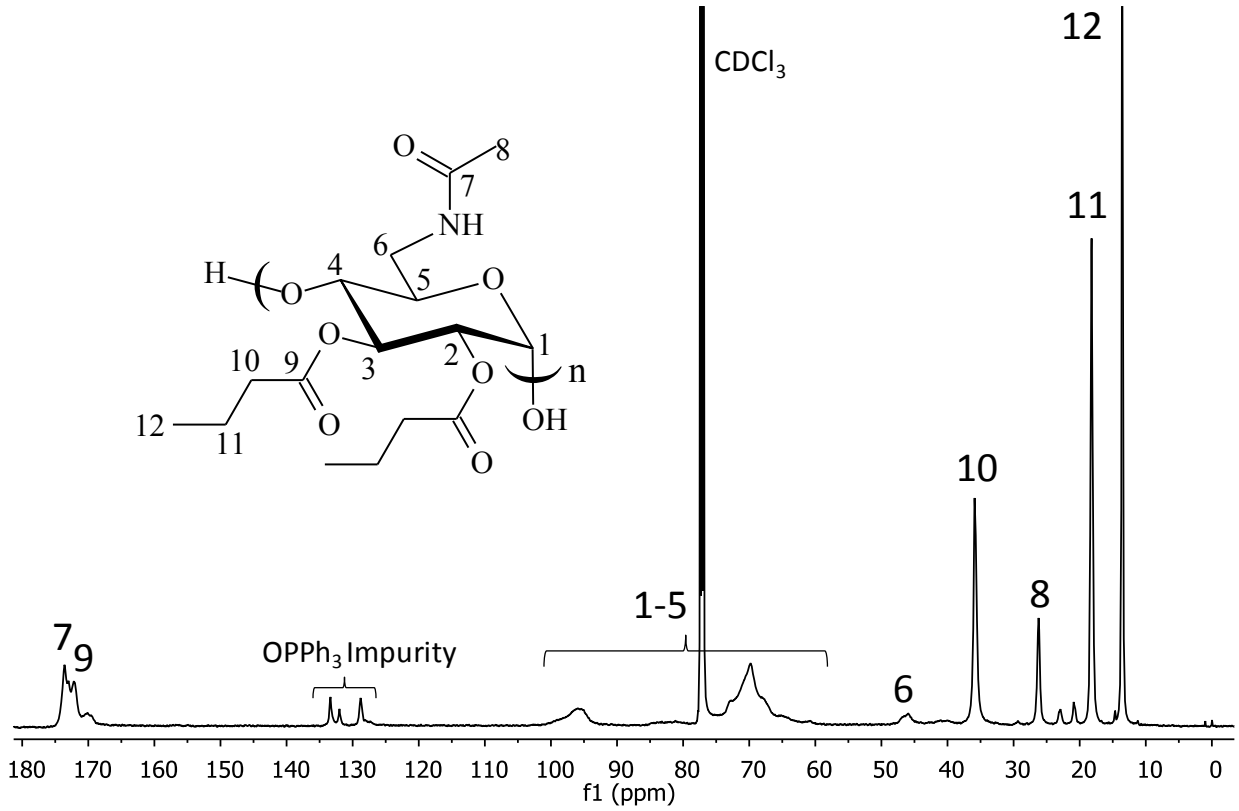

Figure 4.10 ^{13}C NMR spectrum of 6-acetamido-6-deoxy-2,3,4-O-butyryl-pullulan in $CDCl_3$

^{13}C NMR characterization of the other 6-amido-6-deoxy-pullulan esters synthesized (6-acetamido-6-deoxy-2,3,4 -O-propionyl and -O-hexanoyl-pullulan) is presented in the appendix of this thesis (**Fig A4.6**) along with the ^{1}H NMR spectra of 6-acetamido-6-deoxy-2,3,4-O-acetyl and -O-butyryl-pullulan (**Fig A4.5)**.

The DS of ester and amide was calculated as described in the experimental section 2.2 and is shown in **Table 4.2**.

Table 4.2 Amide and ester DS of 6-acetamido-6-deoxy-pullulan esters

Amidopullulan esters	Ester DS (DS_E)[1]	Amide DS (DS_A)[2]
6-acetamido-6-deoxy-2,3,4-O-acetyl-pullulan	6.2	2.0
6-acetamido-6-deoxy-2,3,4-O-propionyl-pullulan	5.4	2.5
6-acetamido-6-deoxy-2,3,4-O-butyryl-pullulan	5.8	2.1
6-acetamido-6-deoxy-2,3,4-O-hexanoyl-pullulan	5.2	2.3

DS per trisaccharide repeat unit: [1]Max DS_E possible is 7, [2]Max DS_A possible is 2

Note that very little change in DS_E was observed after 6-azido-6-deoxy-pullulan esters (**Table 4.1**) were converted to 6-acetamido-6-deoxy-pullulan esters, indicating that the mild reaction conditions of Staudinger reduction allow the esters to remain intact. DS_A calculated is slightly higher than the max DS_A possible (2) for the last 3 samples in **Table 4.2**, which is due to a minor amount of hydroxyl acetylation during the Staudinger reaction. The CH_3 hydrogens of the ester group acetyls overlap with the CH_3 hydrogens of the acetamide groups and thus DS_A values will be overexpressed depending upon the extent of hydroxyl acetylation. The simplicity (non-overlapped peaks) afforded by the ^1H NMR spectrum of 6-acetamido-6-deoxy-2,3,4-O-acetyl-pullulan permitted straightforward calculation of DS_A = 2.0 (experimental section 2.2), which means that full azide reduction to the acetamide was achieved. Therefore, if we assume that the same is true for the other 6-acetamido-6-deoxy-pullulan esters (DS_A = 2); we can estimate the extent of hydroxyl acetylation by simply subtracting DS_A = 2 from the calculated DS_A values for each sample in Table 4.2; we estimate thereby that it ranges from 0.1 to 0.4. So at the most, 4% of the hydroxyl groups have been acetylated during the Staudinger reduction.

Each ^{13}C NMR spectrum of the 6-acetamido-6-deoxy-pullulan esters also has peaks between 128 and 135 ppm that are likely due to residual aryl phosphines in the samples. The samples were submitted to extensive purification; they were washed and dialyzed against ethanol and acetone for several days. Soxhlet extraction of the solids using ethanol or toluene was also attempted, but since the products were soluble in these solvents when heated, this procedure was not efficient. The persistence of these peaks suggests either that some triphenylphosphine and triphenylphosphine oxide persist despite the purification attempts (they are challenging to remove even from small molecules[49]), or that some of the iminophosphorane reaction

intermediates may still persist on the pullulan backbone. Further investigation will be required to confirm the source of these peaks.

The products were soluble in DMSO, DMF, NMP, acetone and chloroform.

The thermal properties of the 6-acetamido-6-deoxy- pullulan esters were evaluated using TGA and DSC. TGA analysis showed that the samples were thermally stable up to 225 °C (results not shown). DSC analysis was performed to determine transition temperatures of the products. None of the samples displayed any crystalline melting endotherms or crystallization exotherms upon heating. Glass transition temperatures (T_g, second heating scan) were detected for each of the 6-acetamido-6-deoxy-pullulan esters (**Fig 4.11**). Unmodified pullulan showed no cleat T_g upon the DSC experimental conditions used. T_g of pullulan has been reported to be difficult to observe.[35] The T_g values for all samples synthesized increased with decreasing acyl chain length, as intermolecular interactions are more favorable in polymers substituted with shorter chain length acyl groups.

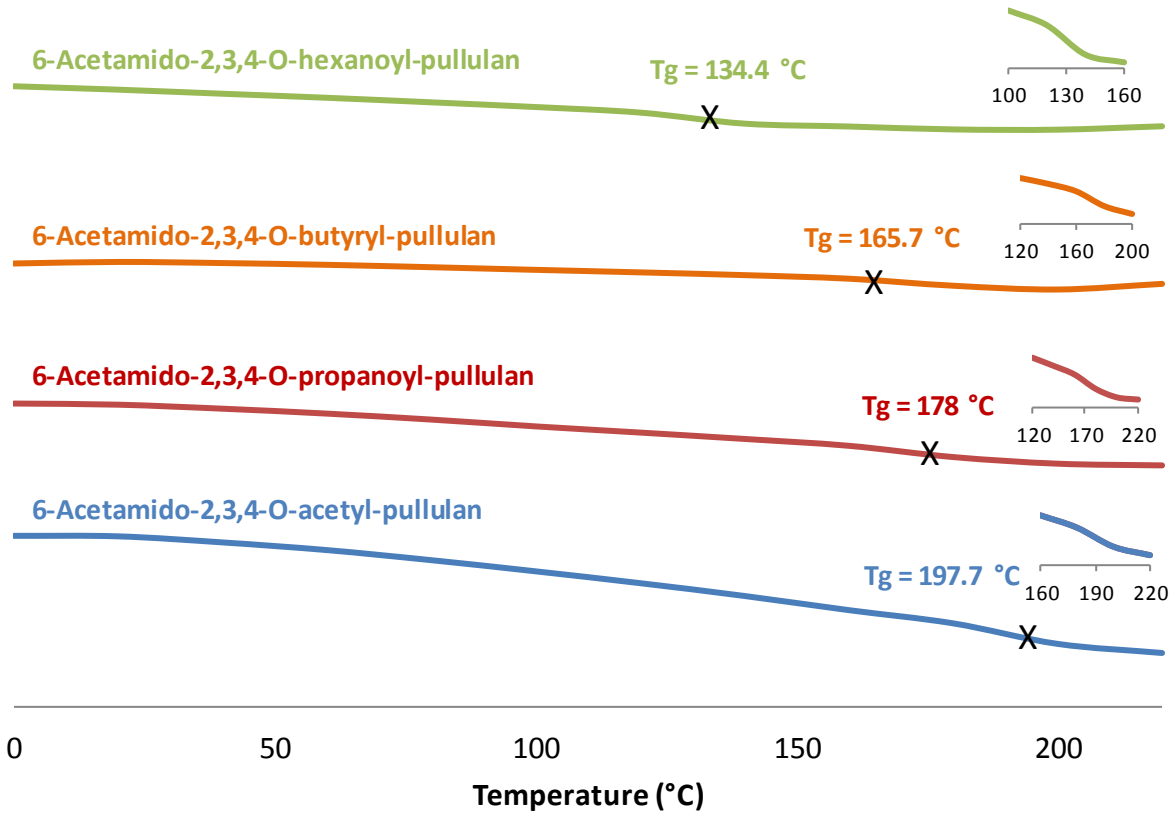

Figure 4.11 DSC thermograms of 6-acetamido-6-deoxy-pullulan esters

Molecular weight analysis of 6-acetamido-6-deoxy-pullulan esters showed that polymer degradation occurred during the 4-step synthesis of these compounds (**Table 4.3**), about 17-fold decrease in product molecular weight when compared to pullulan. Further MW analysis of the intermediate products will be performed in order to identify which reaction steps are causing the MW loss.

Table 4.3 MW of 6-acetamido-6-deoxy-pullulan esters

	Dp
Pullulan	1234
6-Acetamido-6-deoxy-2,3,4-O-hexanoyl-pullulan	71
6-Acetamido-6-deoxy-2,3,4-O-butyryl-pullulan	UA
6-Acetamido-6-deoxy-2,3,4-O-propionyl-pullulan	UA
6-Acetamido-6-deoxy-2,3,4-O-acetyl-pullulan	UA

UA: Under analysis

4.5 Conclusions

New regioselectively modified pullulan derivatives containing amine or amide groups were synthesized. The synthesis began with the regioselective bromination of pullulan at C-6 with NBS and Ph_3P to obtain 6-bromo-6-deoxy-pullulan. The azidation of the later yielded the corresponding 6-azido-6-deoxy-pullulan intermediates that could be converted, depending on the reaction conditions (Staudinger reaction) to the amino or amidopullulan compounds. To date, the only polysaccharide that has been modified using this methodology was cellulose. Pullulan is known for its non-toxicity and biocompatibility, therefore, the pullulan derivatives synthesized herein, which are structural isomers of important polysaccharides such as chitin and chitosan, possess strong potential for biomedical applications.

The successful application of the Staudinger reaction to prepare amino and amidopullulan compounds creates new possibilities for the synthesis of other interesting pullulan derivatives which will be further explored. The iminophosphorane intermediate formed during this reaction is a versatile intermediate and can be reacted with a range of other reagents to furnish distinct regioselectively modified pullulan compounds.

Furthermore, this is the first time that isolation of 6-bromo-6-deoxypullulan has been described. In contrast to 6-bromo-6-deoxy-cellulose, brominated pullulan was found to have good organic solubility. This is a powerful intermediate for the synthesis of other pullulan derivatives by S_N2 displacement of the bromide and thus, the bromination of pullulan described herein illuminates a pathway for the synthesis of new pullulan compounds.

4.6 References

1. Bauer, R., Physiology of *Dematium pullulans* de Bary. *Zentralbl Bacteriol Parasitenkd Infektionskr Hyg Abt* **1938,** *2* (98), 133-167.

2. Bernier, B., The production of polysaccharides by fungi active in the decomposition of wood and forest litter. *Can. J. Microbiol.* **1958,** *4*, 195-204.

3. Bender, H.; Lehmann, J.; Wallenfels, K., Pullulan, an extracellular glucan from *Pullularia pullulans*. *Biochim Biophys Acta* **1959,** *36*, 309-316.

4. Leathers, T. D., Biotechnological production and applications of pullulan. *Applied Microbiology and Biotechnology* **2003,** *62* (5-6), 468-473.

5. Yamaoka, T.; Tabata, Y.; Yoshito, I., Body distribution profile of polysaccharides after intravenous administration. *Drug Delivery* **1993,** *1* (1), 75-82.

6. Rekha, M. R.; Sharma, C. P., Pullulan as a promissing biomaterial for biomedical applications: a perspective. *Trends. Biomater. Artif. Organs* **2007,** (20), 116-121.

7. Shingel, K. I., Current knowledge on biosynthesis, biological activity, and chemical modification of the exopolysaccharide, pullulan. *Carbohydrate Research* **2004,** *339* (3), 447-460.

8. Hosseinkhani, H.; Aoyama, T.; Ogawa, O.; Tabata, Y., Liver targeting of plasmid DNA by pullulan conjugation based on metal coordination. *Journal of Controlled Release* **2002,** *83* (2), 287-302.

9. Dicke, R. E., A straight way to regioselectively functionalized polysaccharide esters. *Cellulose* **2004,** *11* (2), 255-263.

10. Fox, S. C.; Li, B.; Xu, D.; Edgar, K. J., Regioselective Esterification and Etherification of Cellulose - A Review. *Biomacromolecules* **2011,** *12*, 1956-1972.

11. Akiyoshi, K.; Yamaguchi, S.; Sunamoto, J., Self-Aggregates of hydrophobic polysaccharide derivatives. *Chemistry Letters* **1991,** (7), 1263-1266.

12. Hirakura, T.; Nomura, Y.; Aoyama, Y.; Akiyoshi, K., Photoresponsive nanogels formed by the self-assembly of spiropyrane-bearing pullulan that act as artificial molecular chaperones. *Biomacromolecules* **2004,** *5* (5), 1804-1809.

13. Jung, S. W.; Jeong, Y. I.; Kim, Y. H.; Kim, S. H., Self-assembled polymeric nanoparticles of poly(ethylene glycol) grafted pullulan acetate as a novel drug carrier. *Archives of Pharmacal Research* **2004,** *27* (5), 562-569.

14. Jung, S. W.; Jeong, Y. I.; Kim, S. H., Characterization of hydrophobized pullulan with various hydrophobicities. *International Journal of Pharmaceutics* **2003,** *254* (2), 109-121.

15. Neville, A. C.; Parry, D. A. D.; Woodhead-Galloway, J., *Journal of Cell Science* **1976,** *21* (1), 73-82.

16. Morganti, P.; Morganti, G., Chitin nanofibrils for advanced cosmeceuticals. *Clinics in Dermatology* **2008,** *26* (4), 334-340.

17. Jayakumar, R.; Prabaharan, M.; Nair, S. V.; Tamura, H., Novel chitin and chitosan nanofibers in biomedical applications. *Biotechnology Advances* **2010,** *28* (1), 142-150.

18. Nakagawa, Y.; Murai, T.; Hasegawa, C.; Hirata, M.; Tsuchiya, T.; Yagami, T.; Haishima, Y., Endotoxin contamination in wound dressings made of natural biomaterials. *Journal of Biomedical Materials Research Part B-Applied Biomaterials* **2003,** *66B* (1), 347-355.

19. Rosenthal, R.; Günzel, D.; Finger, C.; Krug, S. M.; Richter, J. F.; Schulzke, J.-D.; Fromm, M.; Amasheh, S., The effect of chitosan on transcellular and paracellular mechanisms in the intestinal epithelial barrier. *Biomaterials* **2012,** *33* (9), 2791-2800.

20. Kofuji, K.; Qian, C. J.; Nishimura, M.; Sugiyama, I.; Murata, Y.; Kawashima, S., Relationship between physicochemical characteristics and functional properties of chitosan. *European Polymer Journal* **2005,** *41* (11), 2784-2791.

21. Berth, G.; Dautzenberg, H.; Peter, M. G., Physico-chemical characterization of chitosans varying in degree of acetylation. *Carbohydrate Polymers* **1998,** *36* (2-3), 205-216.

22. Berth, G.; Dautzenberg, H., The degree of acetylation of chitosans and its effect on the chain conformation in aqueous solution. *Carbohydrate Polymers* **2002,** *47* (1), 39-51.

23. Schatz, C.; Viton, C.; Delair, T.; Pichot, C.; Domard, A., Typical physicochemical behaviors of chitosan in aqueous solution. *Biomacromolecules* **2003,** *4* (3), 641-648.

24. Aiba, S., Studies on chitosan: 4. Lysozymic hydrolysis of partially N-acetylated chitosans. *International Journal of Biological Macromolecules* **1992,** *14* (4), 225-228.

25. Kurita, K.; Kaji, Y.; Mori, T.; Nishiyama, Y., Enzymatic degradation of beta-chitin: Susceptibility and the influence of deacetylation. *Carbohydrate Polymers* **2000,** *42* (1), 19-21.

26. Schipper, N. G. M.; Varum, K. M.; Artursson, P., Chitosans as absorption enhancers for poorly absorbable drugs: 1. Influence of molecular weight and degree of acetylation on drug transport across human intestinal epithelial (Caco-2) cells. *Pharmaceutical Research* **1996,** *13* (11), 1686-1692.

27. Mao, J. S.; Cui, Y. L.; Wang, X. H.; Sun, Y.; Yin, Y. J.; Zhao, H. M.; De Yao, K., A preliminary study on chitosan and gelatin polyelectrolyte complex cytocompatibility by cell cycle and apoptosis analysis. *Biomaterials* **2004,** *25* (18), 3973-3981.

28. Gupta, K. C.; Jabrail, F. H., Effects of degree of deacetylation and cross-linking on physical characteristics, swelling and release behavior of chitosan microspheres. *Carbohydrate Polymers* **2006,** *66* (1), 43-54.

29. Chiou, S. H.; Wu, W. T.; Huang, Y. Y.; Chung, T. W., Effects of the characteristics of chitosan on controlling drug release of chitosan coated PLLA microspheres. *Journal of Microencapsulation* **2001,** *18* (5), 613-625.

30. Lavertu, M.; Methot, S.; Tran-Khanh, N.; Buschmann, M. D., High efficiency gene transfer using chitosan/DNA nanoparticles with specific combinations of molecular weight and degree of deacetylation. *Biomaterials* **2006,** *27* (27), 4815-4824.

31. Kiang, T.; Wen, H.; Lim, H. W.; Leong, K. W., The effect of the degree of chitosan deacetylation on the efficiency of gene transfection. *Biomaterials* **2004,** *25* (22), 5293-5301.

32. Tigli, R. S.; Karakecili, A.; Gumusderelioglu, M., In vitro characterization of chitosan scaffolds: Influence of composition and deacetylation degree. *Journal of Materials Science-Materials in Medicine* **2007,** *18* (9), 1665-1674.

33. Minagawa, T.; Okamura, Y.; Shigemasa, Y.; Minami, S.; Okamoto, Y., Effects of molecular weight and deacetylation degree of chitin/chitosan on wound healing. *Carbohydrate Polymers* **2007,** *67* (4), 640-644.

34. Koryagin, A. S.; Erofeeva, E. A.; Yakimovich, N. O.; Aleksandrova, E. A.; Smirnova, L. A.; Mal'kov, A. V., Analysis of antioxidant properties of chitosan and its oligomers. *Bulletin of Experimental Biology and Medicine* **2006,** *142* (4), 461-463.

35. Teramoto, N.; Shibata, M., Synthesis and properties of pullulan acetate. Thermal properties, biodegradability, and a semi-clear gel formation in organic solvents. *Carbohydrate Polymers* **2006,** *63* (4), 476-481.

36. Jo, J.; Yamamoto, M.; Matsumoto, K.; Nakamura, T.; Tabata, Y., Liver targeting of plasmid DNA with a cationized pullulan for tumor suppression. *Journal of Nanoscience and Nanotechnology* **2006,** *6* (9-10), 2853-2859.

37. Constantin, M.; Fundueanu, G.; Cortesi, R.; Esposito, E.; Nastruzzi, C., Aminated polysaccharide microspheres as DNA delivery systems. *Drug Delivery* **2003,** *10* (3), 139-149.

38. Cimecioglu, A. L.; Ball, D. H.; Kaplan, D. L.; Huang, S. H., Preparation of amylose derivatives selectively modified at C-6. -6amino-6-deoxyamylose. *Macromolecules* **1994,** *27* (11), 2917-2922.

39. Mocanu, G.; Constantin, M.; Carpov, A., Chemical reactions on polysaccharides: 5. Reaction of mesyl chloride with pullulan. *Angewandte Makromolekulare Chemie* **1996,** *241*, 1-10.

40. Cimecioglu, A. L.; Ball, D. H.; Huang, S. H.; Kaplan, D. L., A direct regioselective route to 6-azido-6-deoxy polysaccharides under mild and homogeneous conditions. *Macromolecules* **1997,** *30* (1), 155-156.

41. Shey, J.; Holtman, K. M.; Wong, R. Y.; Gregorski, K. S.; Klamczynski, A. P.; Orts, W. J.; Glenn, G. M.; Imam, S. H., The azidation of starch. *Carbohyd Polym* **2006,** *65* (4), 529-534.

42. Blanco, J. L. J.; Fernandez, J. M. G.; Gadelle, A.; Defaye, J., A mild one-step selective conversion of primary hydroxyl groups into azides in mono- and oligo-saccharides. *Carbohydrate Research* **1997,** *303* (3), 367-372.

43. Fox, S. C.; Edgar, K. J., Staudinger reduction chemistry of cellulose: Synthesis of selectively O-acylated 6-amino-6-deoxy-cellulose. *Biomacromolecules* **2012,** *13* (4), 992-1001.

44. Furuhata, K.; Koganei, K.; Chang, H.-S.; Aoki, N.; Sakamoto, M., Dissolution of cellulose in lithium bromide-organic solvent systems and homogeneous bromination of cellulose with N-bromosuccinimide triphenylphosphine in lithium bromide - N,N-dimethylacetamide. *Carbohydr. Res.* **1992,** *230*, 165-177.

45. Fox, S. C.; Edgar, K. J., Synthesis of regioselectively brominated cellulose esters and 6-cyano-6-deoxycellulose esters. *Cellulose* **2011,** *18* (5), 1305-1314.

46. Furuhata, K. I.; Koganei, K.; Chang, H. S.; Aoki, N.; Sakamoto, M., Dissolution of cellulose in lithium bromide organic-solvent systems and homogeneous bromination of cellulose with N-bromosuccinimide triphenylphosphine in lithium bromide N,N-dimethylacetamide. *Carbohydrate Research* **1992,** *230* (1), 165-177.

47. Saxon, E.; Armstrong, J. I.; Bertozzi, C. R., A "traceless" Staudinger ligation for the chemoselective synthesis of amide bonds. *Organic Letters* **2000,** *2* (14), 2141-2143.

48. Garcia, J.; Urpi, F.; Vilarrasa, J., New synthetic tricks - Triphenylphosphine-mediated amide formation from carboxylic acids and azides. *Tetrahedron Letters* **1984,** *25* (42), 4841-4844.

49. O'Neil, I. A.; Thompson, S.; Murray, C. L.; Kalindjian, S. B., DPPE: A convenient replacement for triphynylphosphine in the staudinger and Mitsunobu reactions. *Tetrahedron Lett.* **1998,** *39* (42), 7787-7790.

Chapter 5 **Interplay of Degradation, Dissolution and Stabilization of Clarithromycin and its Amorphous Solid Dispersions**

(Adapted from Pereira, J.M.; Mejia-Ariza, R.; Edgar, K.J.; Davis, R.M.; Sriranganathan, N.; Taylor, L.T.; Ilevbare, G.A.; McGettigan H. Manuscript submitted to publication in Molecular Pharmaceutics)

5.1 Abstract

Clarithromycin (CLA) is an aminomacrolide antibiotic whose physical properties are fascinating and challenging. It has very poor solubility at neutral intestinal pH, but much better solubility under acidic conditions due to amine protonation. The improved solubility in an acid environment is confounded by the poor chemical stability of clarithromycin that is quite labile towards acid-catalyzed degradation. This creates a complex system under gastrointestinal (GI) conditions; dissolution in the stomach, degradation, potential for precipitation in the small intestine, and interplay with the formulation components. We report herein a study of amorphous solid dispersion (ASD) of CLA with carboxyl-containing cellulose derivatives; these polymers have recently been shown to be excellent ASD matrices for maximizing oral bioavailability. This approach was intended to improve CLA solubility in neutral media while minimizing release in an acid environment, and thereby increase its uptake from the small intestine. Amorphous polymer/CLA nanoparticles were also prepared by high-shear mixing in a multi-inlet vortex mixer (MIVM). Different extents of release were observed at low pH from the various formulations. Thus the solubility increase from nanosizing was deleterious to the concentration of intact CLA obtained upon reaching small intestine conditions, since the high extent of release at gastric pH led to the subsequent degradation of CLA. Using pH-switch experiments, it was possible to separate the effects of loss of CLA from solution by crystallization vs. that from chemical degradation. It was found that the hydrophobic cellulose derivative cellulose acetate adipate propionate (CAAdP) was exceptionally effective at protecting CLA from dissolution in the stomach, and preventing decomposition of released CLA at low-pH, thereby minimizing permanent CLA loss due to chemical degradation. We conclude that protection against

degradation is central to enhancing overall release of *intact* CLA from ASD formulations; the formulations studied herein have great promise for simultaneous CLA solubility enhancement and protection from loss to chemical degradation, thereby reducing dose requirements and potentially decreasing colonic exposure to CLA (reduced colonic exposure is expected to minimize killing of beneficial colonic bacteria by CLA).

5.2 Introduction

Drug efficacy depends upon its solubility and absorption into the systemic circulation, which influence its availability at the site of action. According to one estimate, more than one-third of the drugs listed in the United States Pharmacopeia are either poorly soluble or insoluble in water.[1] It is estimated that approximately 40% of active substances currently in development fail because of low efficacy, often as a result of poor bioavailability, which can arise from ineffective intestinal absorption and/or undesirable metabolic activity.[2] [3] [4] Improving the solubility of a drug may therefore lead to improvement in its bioavailability. Drug delivery systems that enhance solubility can enable testing and development of poorly soluble drug candidates, and can enhance performance of existing drugs by reducing dosage, cost, side-effects, and/or variability. Efficacy of a drug is also vitally dependent on its stability; cases are known in which drugs undergo retro-aldol decomposition at neutral pH,[5] are photochemically labile,[6] and importantly a number of drugs are unstable under the acidic conditions of the stomach.[7] For these drugs that are sensitive to low pH, the extent to which the drug is released and dissolved in the stomach, and stabilized by polymers after release, is entwined in complex fashion with its apparent solubility and its bioavailability.

Clarithromycin (CLA) is a semi-synthetic 14-member macrolide antibiotic used to treat many different types of bacterial infection affecting the skin and respiratory system (**Fig 5.1**). It is also used together with other medicines to treat stomach ulcers caused by *Helicobacter pylori.*[8] CLA is a high-melting crystalline solid (m.p. 220 ºC) with low aqueous solubility (0.342 µg/mL H_2O at 25 ºC).[9] Furthermore, its solubility is pH dependent; CLA is reasonably soluble in the stomach (pH 1.2) and fairly soluble in the upper region of the small intestine (pH 5.0) where

absorption is most likely to occur. Salem reported CLA solubility as 9.22 mg/mL at pH 2.4, vs. < 1 mg/mL at pH 6.8.[10] This drastic decrease in CLA solubility upon reaching small intestine pH may contribute to its limited oral bioavailability, reported as no more than 50%.[11] Moreover, while highly soluble at low pH, CLA degrades quickly under acidic conditions; the decomposition obeying pseudo first-order kinetics with degradation half-lives of 10.2 min[12] at pH 1.2 and 17 min at pH 1.39.[13] Erah et al.[14] have observed that CLA is stable over the pH range 5.0 – 8.0. At pH values below 5.0, the degradation rate increased markedly, with 90.2% and 41.1% of CLA lost from aqueous samples at pH 1.0 and pH 2.0, respectively, within the first hour of the experiment.

We studied the antibiotic CLA because of its importance in treating mycobacterial infections, its relatively poor solubility, acid instability, and moderate bioavailability. CLA bioavailability enhancement could improve patient treatment by enabling dose reduction, reducing the cost of treating globally important mycobacterial infections. The ability to use lower doses and to enhance bioavailability from the small intestine may also decrease colonic exposure to the antibiotic, thereby decreasing potentially serious gastrointestinal side effects caused by undesired killing of beneficial colonic bacteria.[15]

It's well known that CLA has higher bioavailability than erythromycin, another potent agent against gram-positive bacteria that has a number of disadvantages including very poor gastric stability.[13] This increased bioavailability is primarily afforded by superior CLA acid stability, which suggests that further improvement in acid stability may enhance its bioavailability. Although CLA acid stability is better than for erythromycin, CLA still degrades rather quickly under acidic conditions. Enhanced protection against acid degradation could enhance bioavailability of these sensitive aminomacrolide antibiotics.

CLA bioavailability is also affected by food. Chu et al[11, 16] reported that the bioavailability of CLA 500 mg tablets was increased by approximately 18% and maximum CLA serum concentration was increased by 52% when the tablets were administered with food, which may increase gastric pH. These results support the hypothesis that stomach acidity is an impediment to CLA bioavailability. Other researchers showed that the co-administration of CLA with the proton pump inhibitor omeprazole increases its effectiveness against *H. pylori,*[14] possibly due to the increased gastric pH caused by omeprazole. Therefore, formulations that can

improve CLA acid stability may not only enhance bioavailability but also patient-to-patient and dosing time variability.

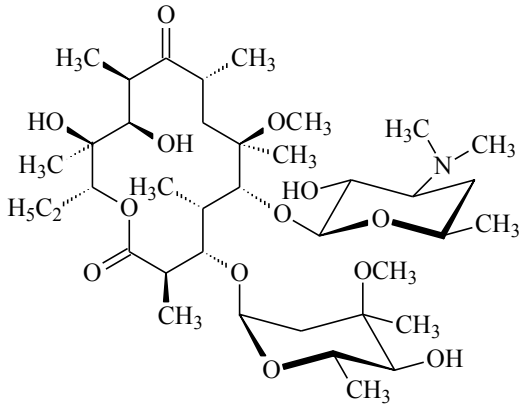

Figure 5.1 Chemical structure of clarithromycin

Low drug solubility and inadequate oral bioavailability have been addressed using a number of strategies; complexation with cyclodextrins,[17 18] formulation with lipid excipients,[19] conversion into a higher energy polymorph[20], particle size reduction,[21] or by formulation as an amorphous solid.[22] Incorporation into a solid polymer matrix can enhance solubility by trapping the drug in a metastable amorphous state, eliminating the need to disrupt the crystal lattice in order for the drug to dissolve.[23] Amorphous solid dispersions (ASDs) in polymer matrices represent an increasingly important approach for enhancing drug solubility,[24 25 26] and have been an inspiring topic in pharmaceutical research for both industrial and academic scientists, receiving much attention in recent years.[27,28] They are able to generate supersaturated solutions, dissolve faster, and provide enhanced oral bioavailability.[29 23] On the other hand, the amorphous forms of normally crystalline drugs are inherently unstable with regard to crystallization. It is essential to create a molecular dispersion of the drug within a polymeric matrix so that the polymer can stabilize the drug against crystallization, by means of strong polymer-drug interactions; the high glass transition (T_g) temperatures of properly designed matrix polymers also serve to limit drug mobility and thereby retard crystallization. High polymer T_g means that even in the presence of 10% or more of added drug (which may be a plasticizer for the matrix polymer), and even in the presence of high ambient humidity (water is a plasticizer for most cellulose derivatives) and temperature, the T_g of the dispersion remains higher than the ambient

temperature. In addition to the need for stabilization of the drug against crystallization in the solid dosage form, the polymer must also provide stabilization against crystallization of the drug after it is released, and before it permeates through the enterocytes into the bloodstream. This need for solution stabilization means that a useful ASD polymer must have at least minimal aqueous solubility (at least in the μg/mL range in our experience). The third critical requirement for an ASD polymer is adequate release rate; stabilization against crystallization is not useful for bioavailability enhancement if the drug is not released.

Cellulose esters have useful properties for drug delivery systems, including very low toxicity, endogenous and/or dietary decomposition products, stability, compatibility with a wide range of actives, and ability to form micro- and nanoparticles.[27] These properties have enabled the creation of a wide range of drug delivery systems employing cellulose esters as key ingredients. Due in part to these valuable features, cellulose derivatives containing pendent carboxyl groups have been recently explored with success for ASD of drugs.[30] Polymer requirements for effective generation of drug supersaturation from ASDs are multifaceted; the ability to provide specific interactions with diverse drug molecules in the solid state to prevent drug crystallization, high T_g to prevent drug molecular mobility in the solid state, and of course a mechanism for drug release (carboxyl groups) at a therapeutically adequate rate. Another ASD polymer requirement is for at least slight aqueous solubility to enable solution stabilization of the released drug against crystallization, prior to its permeation through the enterocytes into circulation. This is of particular importance in the current context, since such solution association has been implicated not only in stabilization against crystallization,[31] but also in enhancing chemical stability of drugs like ellagic acid[32] and curcumin.[33] Given the previously observed chemical stabilization of labile compounds by polymers, it is of interest to explore whether clarithromycin release can be improved by identifying a polymer that enables a combined strategy of solubility enhancement by amorphous dispersion, with improvement of chemical stability. Since the ability of cellulose derivatives to deliver these properties is highly dependent on their structure,[34 35] we selected several structurally diverse cellulosic polymers for these experiments.

Carboxymethylcellulose acetate butyrate (CMCAB) (**Fig 5.2a**) is a cellulose ether ester that has shown interesting properties for solid pharmaceutical formulation.[36 28] ASDs of certain

drugs that have some water solubility with CMCAB (e.g., ibuprofen) afford more rapid and complete dissolution, while ASDs of certain poorly water-soluble drugs with CMCAB (e.g., glyburide) afford greatly enhanced solubility and slow release. ASD of quercetin in CMCAB was effective in inhibiting its crystallization from solution, but did not prevent its chemical degradation.[37]

Hydroxypropylmethylcellulose acetate succinate (HPMCAS) (**Fig 5.2b**), also known as hypromellose acetate succinate, is a cellulose ether ester that is currently used in pharmaceutical applications. HPMCAS has significant hydrophilicity even when un-ionized, due to its hydroxypropyl groups; they impact its solubility and release characteristics including at low pH. HPMCAS is one of the most promising ASD matrix polymers.[38] [39] [40] [41] We have recently demonstrated that HPMCAS ASDs not only inhibit ellagic acid crystallization, but also its solution degradation.[32]

Cellulose acetate adipate propionate (CAAdP) (**Fig 5.2c**) is a newly synthesized carboxylated cellulose derivative, designed specifically for effectiveness in ASDs. The tetramethylene chain of the adipate group and the alkyl portions of other ester substituents impart hydrophobic character, enhancing affinity for hydrophobic drugs.[42] [43] CAAdP is an effective nucleation inhibitor for the anti-HIV drugs efavirenz and ritonavir,[35] and inhibits ritonavir crystal growth.[44] CAAdP forms ASDs with curcumin, and strongly inhibits both curcumin crystallization and chemical degradation from solution (as do CMCAB and HPMCAS).[45]

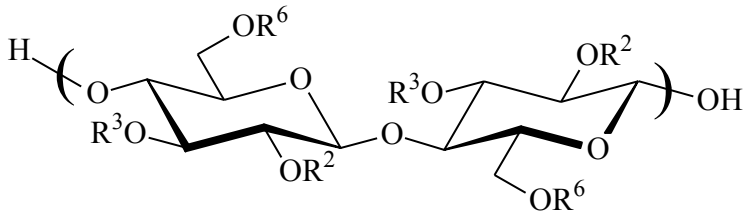

a) CMCAB: R^2, R^3, R^6 = H, CH_2CO_2H, $COCH_3$ or $COCH_2CH_2CH_3$

b) HPMCAS: R^2, R^3, R^6 = H, $CH_2CH_2OHCH_3$, CH_3, $COCH_3$, $COCH_2CH_2CO_2H$

c) CAAdP: R^2, R^3, R^6 = H, $COCH_3$, $CO(CH_2)_4CO_2H$, $COCH_2CH_3$

Figure 5.2 Chemical structures of **a)** CMCAB, **b)** HPMCAS and **c)** CAAdP

We hypothesized that CLA/cellulosic polymer ASDs could strongly enhance CLA oral bioavailability by enhancing its solution concentration, both by preventing acid-catalyzed degradation and by creating stable supersaturated solutions. Success would depend on polymer ability to form amorphous dispersions with CLA, the degree of (in)solubility of these carboxylated polymers at low pH (directly impacting their ability to inhibit low pH CLA release), and their ability to release at intestinal pH and stabilize released CLA against degradation and recrystallization (requiring at least slight polymer solubility at neutral pH).

We further hypothesized that it might be possible to combine thermodynamic and kinetic approaches to drug solubility enhancement in a novel way to achieve synergistic results, since in principle these two approaches are orthogonal to one another. That is, if we molecularly dispersed the drug in a polymer matrix so as to eliminate crystallinity and gain the thermodynamic advantage of favorable polymer-CLA interactions, and at the same time isolated these matrix particles in such a way that they had diameters in the size range of a few hundred nanometers, we might also realize the separate, kinetic advantages of nanosizing.[46] Herein we test this hypothesis, using a multi-inlet vortex mixer (MIVM) to co-precipitate CMCAB/CLA amorphous nanoparticles. We compare their ability to solubilize CLA with that of macroparticulate CLA/CMCAB ASDs, and crystalline CLA as a negative control.

5.3 Experimental

5.3.1 Materials

CLA (CLA) was purchased from Attix Pharmaceuticals, Toronto, Ontario, Canada. Carboxylmethyl cellulose acetate butyrate (CMCAB CAS 641-0.2, approximate MW 22,000, degree of substitution (DS) (butyrate) = 1.64, DS (acetate) = 0.44, and DS (carboxymethyl) = 0.33) was obtained from Eastman Chemical Company (Kingsport, Tennessee). Hydroxypropylmethylcellulose acetate succinate (HPMCAS AS-LG grade, approximate MW 18,000, substituents wt%: methoxyl = 20-24%, hydroxypropyl = 5-9%, acetyl = 5-9%, succinoyl = 14-18%) was supplied by Shin-Etsu Chemical Co., Ltd. (Tokyo, Japan). Cellulose acetate

propionate adipate 0.85 (CAAdP, approximate MW 12,000) was synthesized from cellulose acetate propionate (CAP-504-0.2, Eastman Chemical) as previously reported;[43] and had DS (acetate) = 0.04, DS (propionate) = 2.09, and DS (adipate) = 0.33. Acetone and acetonitrile were HPLC-grade. Tetrahydrofuran (THF) and reagent ethanol were reagent-grade. All solvents, potassium phosphate monobasic, and sodium hydroxide (NaOH) were purchased from Fisher Scientific and used as received. Potassium phosphate buffer 0.05M pH 6.8 and HCl 1N pH 1.2 solutions were prepared according to United States Pharmacopeia and National Formulary 2005: USP 28/NF 23 2005b. Water was purified by reverse osmosis and ion exchange using the Barnstead RO pure ST (Barnstead/Thermolyne, Dubuque, IA, U.S.A.) purification system.

ASDs of CLA with 3 different cellulosic polymers (CMCAB, CAAdP and HPMCAS), at two drug weight percentages (10 and 25%) were prepared by spray-drying. Furthermore, 2 samples of CLA in CMCAB at 10 and 25 wt% were made as nanoparticles using the MIVM. Samples prepared in this study are referred to in this study using the following abbreviations:

1. Free CLA (as received, crystalline form): CLA
2. CLA/CMCAB, 10 wt% of drug, prepared by spray-drying: CLA/CMCAB 10%
3. CLA/CMCAB, 25 wt% of drug, prepared by spray-drying: CLA/CMCAB 25%
4. CLA/CMCAB, 10 wt% of drug, nanoparticles, prepared with the MIVM: CLA/CMCAB 10% nano
5. CLA/CMCAB, 25 wt% of drug, nanoparticles, prepared with the MIVM: CLA/CMCAB 25% nano
6. CLA/CAAdP, 10 wt% of drug, prepared by spray-drying: CLA/CAAdP 10%
7. CLA/CAAdP, 25 wt% of drug, prepared by spray-drying: CLA/CAAdP 25%
8. CLA/HPMCAS, 10 wt% of drug, prepared by spray-drying: CLA/HPMCAS 10%
9. CLA/HPMCAS, 25 wt% of drug, prepared by spray-drying: CLA/HPMCAS 25%

5.3.2 Preparation of ASDs by spray-drying

ASDs of CLA/polymer were prepared (10 and 25% CLA). For the dispersions of CLA/CMCAB and CLA/HPMCAS (4.0 g total weight), polymer (CMCAB or HPMCAS, 3.0 g for 25 wt% dispersion) in 100 mL THF was stirred at room temperature until completely dissolved (approximately 1h). CLA (1.0 g for 25 wt% dispersion) was added to this solution and stirred for 10 min. For the dispersions of CLA in CAAdP (2.0 g total weight), CAAdP in 50 mL of acetone was stirred at room temperature until the polymer was completely dissolved (approximately 1 h). Ethanol (50 mL) was added and stirred for 20 min. CLA was added to this solution and stirred for 10 min. Solid dispersions were prepared by spray-drying the resulting CLA/polymer solutions. A nitrogen-blanketed spray dryer (B-290 from Buchi) was used to produce the spray-dried particles. The parameters for the preparation of CLA/CMCAB and CLA/HPMCAS solid dispersions were: inlet temp 76 ^{o}C, outlet temp 53 ^{o}C, aspirator rate 100% (38 m^3/h), compressed nitrogen height 30 mm, nozzle cleaner 5, and the solution was pumped continuously at a rate of 6 mL/min. The parameters for the preparation of CLA/CAAdP solid dispersions were: inlet temp 90 ^{o}C, outlet temp 55 ^{o}C, aspirator rate 100% (38 m^3/h), compressed nitrogen height 30 mm, nozzle cleaner 5, and the solution was pumped continuously at a rate of 9 mL/min.

5.3.3 Preparation of nanoparticle ASDs using a multi-inlet vortex mixer

Flash nanoprecipitation[47 48 49 50] is a recently developed process for producing well-defined nanoparticles that involves rapid mixing of two or more streams to create high supersaturation of the precipitating species in the presence of an amphiphilic polymer. The high supersaturation leads to rapid nucleation and growth that is ultimately limited by a repulsive barrier that forms on the particle surfaces. This barrier can be steric, electrostatic, or a combination of both. This process is scalable and has been used to produce stable nanoparticles that incorporated a variety of species including drugs, imaging agents, peptides, and pesticides with controlled particle size distributions.[51 52 53] Importantly for our purposes, drug particles in

the range of tens to the low hundreds of nanometers in diameter have been shown to be advantageous for enhancing dissolution by kinetic means,[54] providing greater relative surface area than larger particles, and larger curvature.

In this work, nanoparticles were formed using a four-jet multi-inlet vortex mixer (MIVM) that was constructed based on a previously reported design[55] in which the diameter and height of the circular mixing chamber were 6.1 mm and 1.1 mm, respectively. CMCAB (100 mg) in 20 mL THF was stirred at room temperature until the polymer was completely dissolved (approximately 30 min). CLA (33 mg) was added to this mixture and stirred for 10 min. This solution comprised the organic stream that was injected into the MIVM along with the three water streams at 25 ^{o}C. The flow rates were controlled with syringe pumps so that the total volumetric ratio of the four injected streams was 90/10 (V/V) water/THF and the Reynolds number in the mixer was > 3900.[41] The solution containing the nanoparticles was collected and THF was removed by using a rotary evaporator with water bath at 60 ºC for approximately 30 min. The nanoparticles were then isolated by freeze-drying the resulting aqueous mixture.

5.3.4 CLA quantification by high-performance liquid chromatography with diode-array detection (HPLC-DAD)

The HPLC system was an Agilent 1200 Series consisting of a quaternary pump, online degasser, autosampler, and Agilent Chemstation LC 3D software. Chromatography was conducted in reversed phase mode using an Eclipse XDB-C18 column (4.6 x 150 mm ID, particle size 5 μm). The mobile phase was prepared according to a previously developed method for CLA.[56] Potassium phosphate monobasic (9.11 g) was dissolved in 1 L of water, 2 mL of triethylamine was added and the pH was adjusted to 5.5 with phosphoric acid. Flow rate was 0.5 mL/min and column temperature was 45 ºC. Detection was by a DAD detector at 210 nm. The retention time for CLA was 4.9 min.

5.3.5 Powder X-ray diffraction (XRD)

Powder X-ray diffraction patterns were obtained using a Shimadzu XRD 6000 diffractometer (Shimadzu Scientific Instruments. Columbia, Maryland). The geometry of the X-ray diffractometer was the Bragg Brentano parafocusing. The instrument was calibrated using a silicon standard which has a characteristic peak at 28.44^{o} 2θ. The X-ray tube consisted of a target material made of copper (Cu), which emits K_{α} radiation with a power rating of 2,200 Watts and accelerating potential of 60 kV. Experiments were performed using a 40 kV accelerating potential and current of 30 mA. Divergence and scattering slits were set at 1.0 mm and the receiving slit at 10 iris. The experiments were conducted with a scan range from 5 to 35^{o} 2θ. Scanning speed was 5º/min.

5.3.6 Differential scanning calorimetry (DSC)

Differential scanning calorimetry was performed using a TA Instruments Q2000 (TA Instruments, New Castle, DE) attached to a refrigerated cooling accessory. Powders (3-8 mg) were loaded in aluminum T-zero pans. Dry N_2 was used as the purge gas at 50 mL/min. All analyses were performed using a heat/cool/heat procedure. Samples were heated to 180 °C at 20 °C/min, cooled to -20 °C at 100°C/min and heated again to 240 °C at 20 °C/min. Glass transition temperatures were determined from second heating scans. The data was analyzed using the Universal Analysis 2000 software for Windows 2000/XP provided with the instrument.

5.3.7 Dynamic light scattering (DLS)

Nanoparticle hydrodynamic size was characterized by dynamic light scattering at 25 ± 0.1 °C using a Zetasizer Nano ZS (Malvern Instruments Ltd., Malvern, U.K.) equipped with a 4 mW He-Ne laser source operating at 633 nm and a scattering angle of 173°. The autocorrelation functions of the scattered intensity were fitted using cumulants analysis to extract the average

translational diffusion coefficient and the hydrodynamic diameters were determined through the Stokes-Einstein relation.[57] Typically, samples were diluted in de-ionized water to approximately 0.1-1 mg/mL.

5.3.8 Scanning electron microscopy (SEM)

Particle size and morphology of spray-dried and nanoparticles were analyzed by scanning electron microscopy on a LEO 1550 Field Emission Scanning Electron Microscope (FESEM). Powdered samples were mounted on a double-faced adhesive tape and sputtered with thin gold-palladium layer (~ 10 nm) using sputter coater Cressington 208HR. Micrographs were taken at an excitation voltage of 5 kV. Electron detector was in lens secondary electron detector.

5.3.9 Long-term physical stability of ASDs

The long-term stability of 3 selected samples that were stored at ambient temperature for 3 years, CLA/CMCAB 25%, spray-dried and nanoparticles, and HPMCAS 25% spray-dried particles, was determined by XRD and DSC as previously described for the newly prepared samples in sections 5.3.5 and 5.3.6 respectively.

5.3.10 Calculation of drug loaded in the ASD particles

Drug loading is expressed as weight percent CLA in the polymer matrix. To calculate drug loading, a 10 mg particle sample was dissolved in 10 mL acetonitrile and the concentration of drug was measured by HPLC as described in section 5.3.4.

5.3.11 Determination of polymer matrix solubility

Each polymer (0.5 g; CMCAB, HPMCAS, CAAdP) was dispersed in 10 mL pH 6.8 buffer at 37 °C, and magnetically stirred (200 rpm, 24h). The suspension was then centrifuged at 14,000 × g, 1 mL of the supernatant was collected, and the solvent was evaporated in an oven (100 °C, 10 h). The dissolved polymer weight was calculated by subtracting the weight of salt in the buffer solution (8.8 mg/mL). The dissolved polymer concentration (w/v) was then calculated by dividing the dissolved polymer weight by the volume of solution withdrawn.

5.3.12 Maximum CLA solution concentration from the ASDs

Each ASD (CLA content of approximately 10 mg) was dispersed in 10 mL pH 6.8 phosphate buffer at 37 ºC with magnetic stirring (200 rpm). CLA concentration in solution was measured by collecting a 0.3 mL aliquot from the sample every 8h until CLA concentration became constant (after 24-30 h). Each 0.3 mL aliquot was centrifuged at 14,000 × g for 10 min and CLA concentration in the supernatant was determined by HPLC (section 5.3.4).

5.3.13 *In vitro* drug release of CLA from ASDs

Dissolution profiles of CLA from ASD particles were compared with that of free CLA under two different dissolution conditions (Experiments A and B). The apparatus used in both dissolution experiments consisted of 250-mL jacketed flasks with circulating ethylene glycol/water (1:1) to control the temperature at 37 °C. Dissolution experiments with the ASDs were performed with initial amount of CLA of approximately 10 mg. ASD dissolution experiments were not run under sink conditions since the goal of those experiments was to evaluate the effectiveness of each polymer in creating and maintaining supersaturated solutions.

5.3.13.1 **Experiment A: Dissolution experiment to evaluate CLA release profile from ASDs at pH 6.8**

Dissolution medium (100 mL 0.05 M potassium phosphate buffer, pH 6.8) was continuously magnetically stirred (37 °C, 200 rpm). Aliquots (0.5 mL) were withdrawn from the suspension every 0.5 h (during the first 2 h), then every hour for 8 h. Phosphate buffer (0.5 mL) was added to maintain constant volume after each aliquot was withdrawn. Each sample from spray-dried CLA/CMCAB and CLA/CAAdP, and CLA/CMCAB nano ASDs was filtered through a 0.45 μm pore size hydrophilic PTFE filter, and samples from CLA/HPMCAS ASDs were centrifuged because the filter would easily get clogged. No significant difference in CLA concentration was found between centrifuged and filtered samples, for both micro and nanoparticles. Finally, samples were assayed for CLA concentration using HPLC as previously described (section 5.3.4). ASD dissolution profiles were presented as concentration of CLA in solution vs. time.

5.3.13.2 **Experiment B: Dissolution experiment to evaluate CLA release profile from ASDs at pH 1.2 followed by pH 6.8**

This experiment was performed to evaluate the effect of low pH during the first 2 h on the dissolution of CLA from the ASDs. In this experiment, ASDs were first dispersed in 75 mL 1N HCl (pH 1.2) for 2 h. This suspension was magnetically stirred at 37 °C and 200 rpm. Aliquots (0.5 mL) were withdrawn every 0.5 h and neutralized with NaOH 5N (approximately 6.5 μL). Each sample from spray-dried CLA/CMCAB ASDs was filtered through 0.45 μm pore size hydrophilic Polytetrafluoroethylene (PTFE) filter, and samples from CLA/HPMCAS, CLA/CAAdP and CLA/CMCAB nano ASDs were centrifuged because the filter would easily get clogged. HCl 1N solution (0.5 mL) was added to the dissolution flask to maintain constant volume after each aliquot was withdrawn. After 2 h, 25 mL of 0.05M potassium phosphate buffer pH 6.8 was added to the flask and the pH of the dissolution medium was adjusted to 6.8 with 5N NaOH (approximately 0.85 mL). The dissolution experiment was continued for 6 h at

pH 6.8 with aliquots (0.5 mL) withdrawn every 0.5 h (for the first hour), then every hour. Phosphate buffer pH 6.8 (0.5 mL) was added to maintain constant volume after each aliquot was withdrawn. Each sample was filtered or centrifuged as described above. CLA concentration was determined by HPLC as previously described (section 5.3.4). ASD dissolution profiles were presented as concentration of CLA in solution (C_n) vs. time.

For comparison of results from **Fig 5.9a-c** and **Fig 5.10**, CLA solution concentration was converted to percentage (CLA%) as follows:

$$CLA\% = \frac{C_n}{C_o \times drug\ loading} \times 100\%$$

where C_n = concentration of CLA measured by HPLC at each time interval and C_o = initial CLA concentration in the ASD particles.

5.3.14 Release profile of CLA in pH 1.2 HCl solution: Degradation versus crystallization and release rate

5.3.14.1 **Quantification of CLA remaining dissolved and intact**

CLA (10 mg) was dissolved in acetonitrile (10 mL) and added to 90 mL pH 1.2 HCl solution, then stirred at 37 °C (200 rpm) for 2h. Aliquots (0.5 mL) were withdrawn from the suspension every 0.5 h, filtered through a 0.45 μm membrane hydrophilic PTFE filter and neutralized with 5N NaOH (approximately 6.5 μL). CLA concentration in solution was measured by HPLC (section 5.3.4) and represented the amount of CLA remaining in solution (not degraded, not recrystallized).

5.3.14.2 **Quantification of CLA degradation**

Multiple samples of CLA (10 mg) or ASD (approximately 10 mg CLA) were each dispersed in 5 mL 1N HCl at pH 1.2, then each suspension was magnetically stirred (200 rpm) for 2 h at 37 °C. At the specified time interval, one entire sample was neutralized with 5N NaOH (approximately 0.65 mL), then 5 mL organic solvent (acetonitrile for CLA and CLA/CMCAB ASDs, THF for HPMCAS ASDs, and acetone for CAAdP ASDs) was added to dissolve all of the insoluble organic material. Each sample was filtered through a 0.45 μm membrane PTFE filter, then CLA concentration was measured by HPLC (section 5.3.4).

5.4 Results and Discussion

First we needed to establish whether it was possible to make amorphous solid dispersions of clarithromycin in these cellulose ester matrices; clarithromycin is of course structurally quite dissimilar from drugs that have previously been shown to be miscible with these cellulose derivatives.[34 35 32 58]

5.4.1 Characterization of solid dispersions

Solid dispersions of CLA with three structurally distinct cellulosic polymers (CMCAB, CAAdP and HPMCAS), at two drug loadings (10 and 25%) were prepared by spray-drying. Furthermore, we chose to test our hypothesis about the potentially synergistic effects of creating ASDs of drug in polymer to reduce crystallinity, and creating those dispersion particles at nanometer-scale diameters, by comparing spray-dried macroparticles of CLA in CMCAB (10 and 25 wt% CLA), with nanoparticles of similar CLA content prepared using the MIVM. We then evaluated the ability of those polymers to stabilize CLA against crystallization in the solid phase by looking at the solid state properties of CLA in the ASD particles by X-ray diffraction, DSC and SEM. Sizes of nanoparticles and spray-dried particles were measured by DLS and

SEM respectively. We found that the intensity-average hydrodynamic diameters of CLA/CMCAB 25% nanoparticles as measured by DLS were in the range of 100 nm, which is in agreement with sizes measured by SEM (results not shown) that ranged from 20 to 100 nm. It should be noted that nanoparticles have a strong tendency to aggregate, as shown by the appearance of oversized particles by DLS. **Fig 5.3a-d** show SEM micrographs of spray-dried 25% drug loaded ASDs. **Fig 5.3a** depicts a low magnification image of CLA/CMCAB 25% sample, which illustrates the particle size distribution. Similar low magnification images were obtained for the other spray-dried ASDs (results not shown). Particles are in the size range 1-25 μm and showed corrugated morphology with dented surfaces for all ASDs. There was no notable difference in the morphology between the 10 and 25% drug loaded particles (results not shown). CAAdP ASDs (**Fig 5.3d**) had more irregularly shaped particles with prominent dented surfaces, while CMCAB (**Fig 5.5.3b**) and HPMCAS (**Fig 5.3c**) ASDs showed a lens-like shape with smoother surface and lighter indentation. Spray-dried particles will have different morphologies, depending on their size and the properties of their shells in the final stages of the drying process. Hollow spheres with smooth surfaces are formed, if the shell becomes rigid rapidly and does not buckle or fold.[59] The hollow particle may finally collapse or wrinkle (corrugate structure), depending on the thickness and mechanical properties of the shell. Previous investigators demonstrated that spray-dried particles with wall materials consisting of polysaccharides exhibit distinguished surface indentation.[60] [61] Furthermore, no drug crystals were observed within the samples; virtually all solid dispersions appeared as amorphous particles with the previously described morphology.

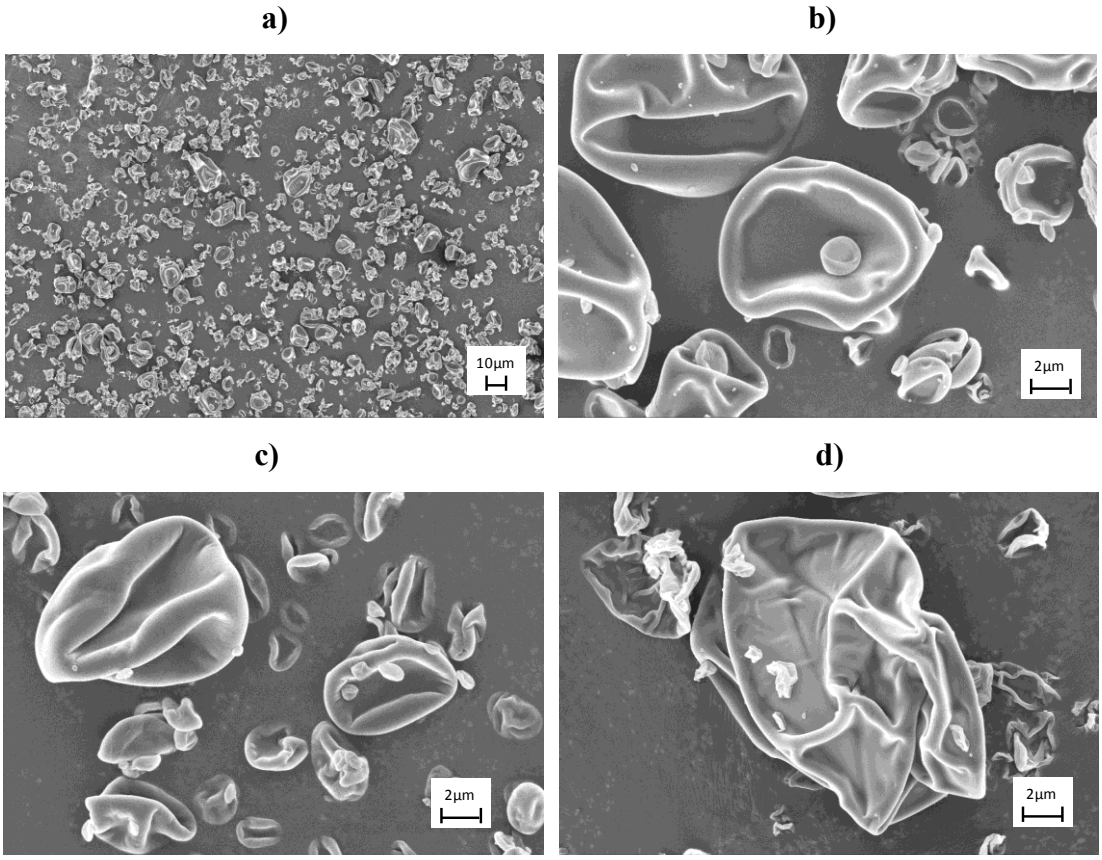

Figure 5.3 SEM images of a) CLA/CMCAB 25% at 1K magnification, b) CLA/CMCAB 25%, c) CLA/HPMCAS 25%, d) CLA/CAAdP 25%. b, c, and d at 10K magnification. Particle size and morphology of spray-dried and nanoparticles were analyzed by SEM. Powdered samples were mounted on a double-faced adhesive tape and sputtered with thin gold-palladium layer.

The extent of CLA crystallinity in the solid dispersions was investigated by XRD. An overlay of the XRD diffraction patterns of crystalline CLA and the ASDs is shown in **Fig 5.4a-c**. Crystalline CLA shows characteristic diffraction peaks (8.0, 9.8, 11.0 and 12.0 2θ), while the ASDs, both macro- and nanoparticle samples, showed no diffraction peaks, instead displaying an amorphous halo, confirming that CLA can be made amorphous by dispersion in CMCAB (**Fig 5.4a**), CAAdP (**Fig 5.4b**) and HPMCAS (**Fig 5.4c**) at 10 and 25% drug loading. Furthermore, nanoparticulate CLA/CMCAB ASDs, prepared using the MIVM, are also amorphous (**Fig 5.4a**). Overall, these data clearly show that it is possible to make both micron and nanometer-sized particles of amorphous CLA dispersions with these polymers, confirming strong polymer-CLA interaction in the solid phase.

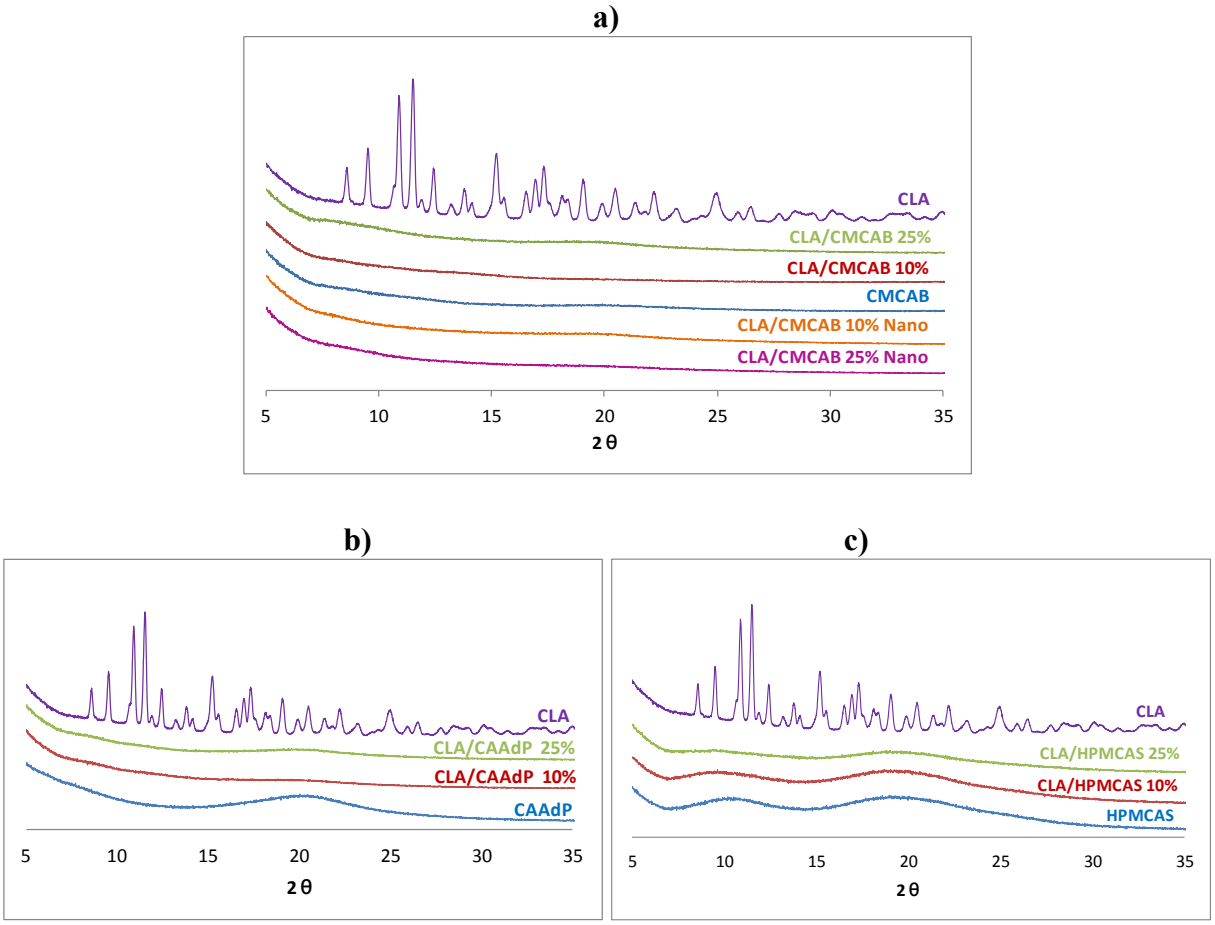

Figure 5.4 X-ray diffraction spectra of: **(a)** CLA/CMCAB ASDs, spray-dried and nanoparticles, **(b)** CLA/HPMCAS ASDs, **(c)** CLA/CAAdP ASDs, all in comparison with crystalline CLA.

To confirm the XRD results, we carried out thermal analysis of all ASDs by DSC. The data fully confirm CLA miscibility with the three cellulosic polymers at both loadings and in both macro- and nanoparticles. We include the DSC thermograms for the CAAdP samples for illustration (**Fig 5.5**); a table of T_g values vs. those predicted by the Fox-Flory equation, the other DSC thermograms (**Fig A5.1 a, b**), and full data interpretation are included in the Appendix.

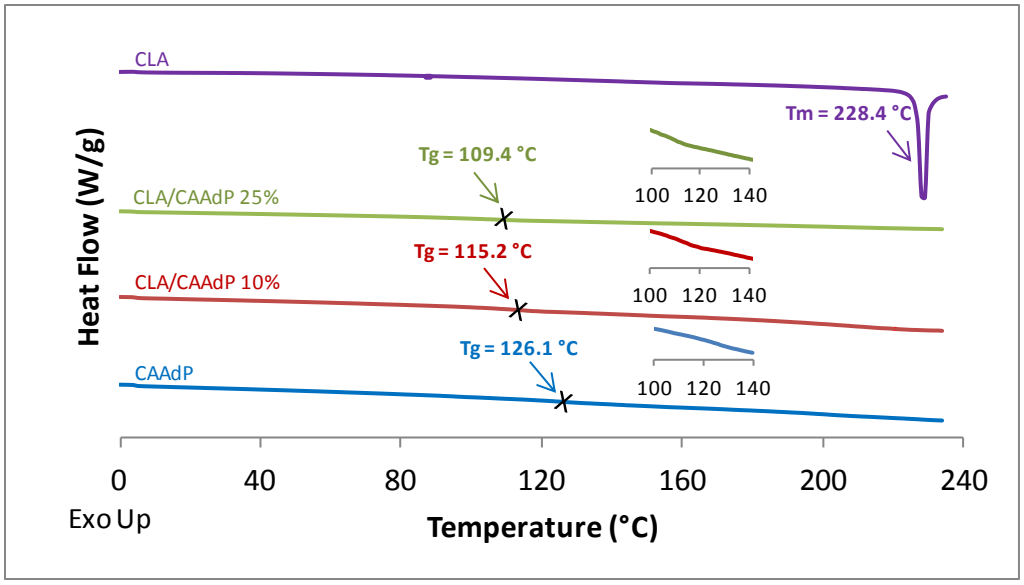

Figure 5.5 DSC thermograms of CLA/CAAdP ASDs, in comparison with crystalline CLA

Formal accelerated aging studies were not performed since they are outside the scope of this fundamental work. However, we did use XRD and DSC to investigate the solid state properties of 3 samples, CLA/CMCAB 25%, spray-dried and nanoparticles, and HPMCAS 25% spray-dried particles, that had been stored for 3 years at ambient laboratory temperature (25-30 ºC) and humidity. The XRD spectra and DSC thermograms showed patterns similar to those of freshly prepared samples (results not shown), demonstrating that all three samples were physically stable, remaining amorphous for at least 3 years from the preparation date.

Drug loading of ASD particles was measured by HPLC. The properties of drug, polymer, and solvent, along with the drying process conditions will influence the efficiency and degree of drug retention.[62] While detailed investigation of different spray-drying or flash nanoprecipitation parameters was outside the scope of this work, high drug incorporation into the polymer matrices was achieved, with loading efficiency ranging from 75 to 90%. For 10% targeted drug loading CLA/CMCAB nanoparticles, and spray-dried CLA/CMCAB and CLA/HPMCAS ASDs, actual drug loading was 7.5% for the three samples, resulting in a loading efficiency of 75%. For the 25% targeted drug loading CLA/CMCAB nanoparticles, and spray-dried CLA/CMCAB and CLA/HPMCAS, the actual value was 19% for the three samples, also resulting in a loading efficiency of 75%. For CLA/CAAdP ASDs, 10 and 25% targeted drug loading, the actual values were 9 and 22.5% respectively, for an efficiency of 90% for both samples.

5.4.2 Solution concentration enhancement by ASDs

Maximum CLA solution concentration from the ASDs at pH 6.8 was found to depend strongly on polymer structure in the following sequence HPMCAS > CMCAB > CAAdP (**Fig 5.6**), which corresponds with the relative aqueous solubility (**Table 5.1**) and hydrophobicity of the three polymers (discussed in section 5.4.3). More hydrophilic polymer matrices swell or dissolve more rapidly in aqueous buffer, affording faster release kinetics. Increased CLA solution concentration could also result from the higher polymer solution concentrations observed with HPMCAS. In contrast, less water soluble and more hydrophobic polymers like CAAdP afford slower release and low drug solution concentration. Moreover, ASDs with higher CLA content led to higher CLA solution concentrations, which is not the expected behavior for ASDs.[63] Since CLA is hydrophilic when compared to these polymers, for these ASDs CLA release is primarily drug controlled. ASDs with higher content of the relatively hydrophilic CLA (25%) will furnish higher solution concentration than those with less CLA.

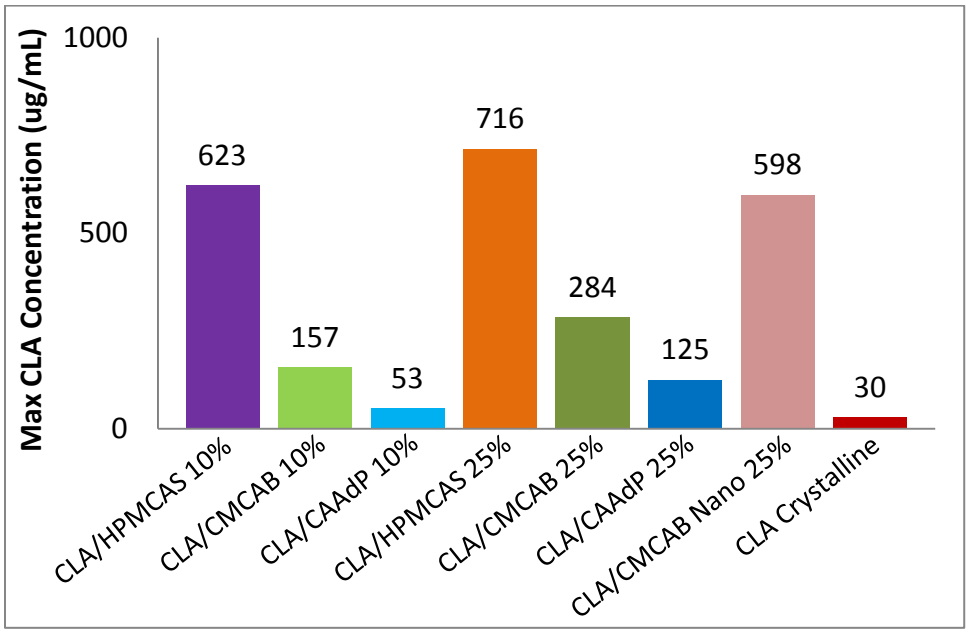

Figure 5.6 Max CLA solution concentration from ASDs in pH 6.8 phosphate buffer, 37 ºC

5.4.3 Release profile of CLA from ASDs at pH 6.8

Two different dissolution experiments (A and B) were performed to evaluate the solubility and release rate profile of CLA from the polymer matrices. ASDs are designed to generate supersaturated solutions and maintain supersaturation for a practical period of time (the residence time in the absorptive zone of the GI tract). In order to evaluate the ability of each ASD system to generate and maintain a supersaturated drug solution, as commonly occurs under finite volume conditions in the GI tract,[64] non-sink conditions were used and all experiments were performed with fixed maximum CLA concentration (approximately 100 µg/mL).

We first studied dissolution under conditions mimicking the small intestine (pH 6.8 phosphate buffer, 37 °C, Exp A). The dissolution profile is presented as the concentration of CLA in solution vs. time (**Fig 5.7**).

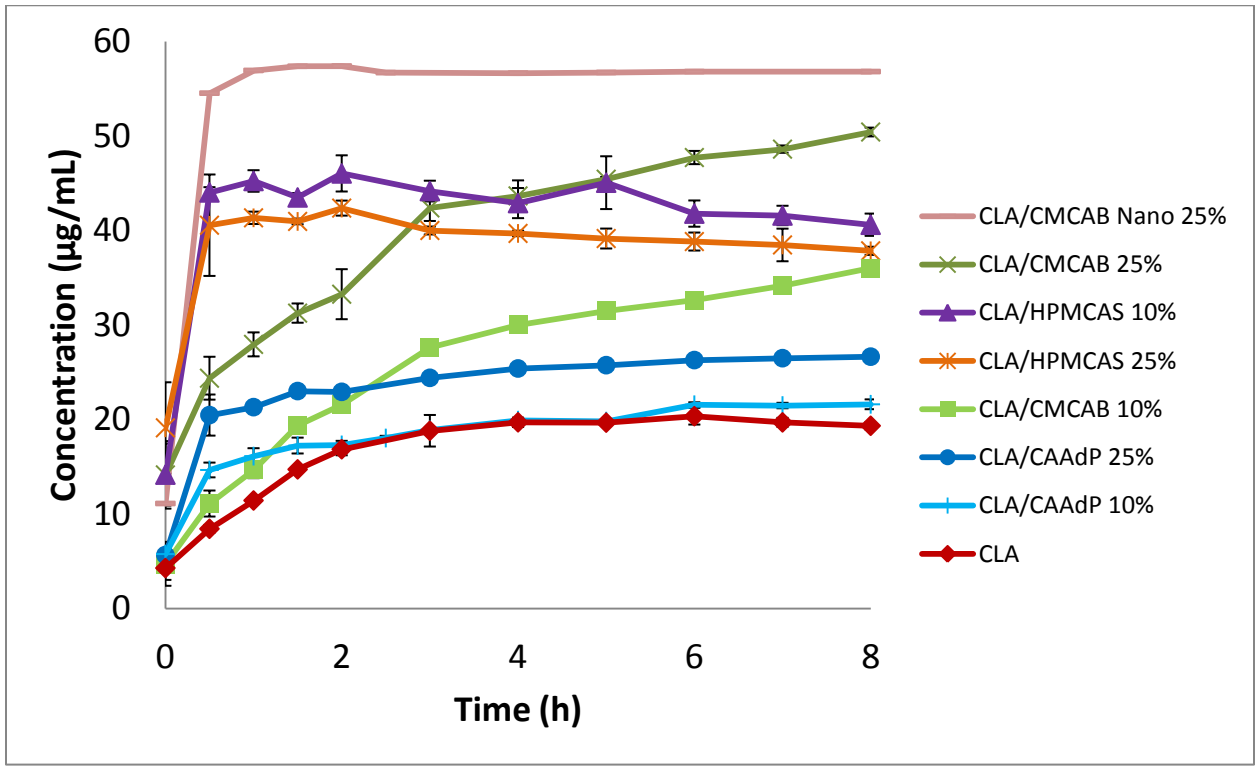

Figure 5.7 Dissolution profiles of CLA and ASDs at pH 6.8 buffer. Each point is an average of 3 experiments, and error bars indicate one standard deviation, with the exception of CLA/CMCAB 25% nano, for which only one experiment was performed due to limited sample availability.

The results from these dissolution experiments showed polymer-dependent enhancement of CLA solution concentration from spray-dried macroparticle ASDs **(Fig 5.7)**, generating high and stable levels of supersaturation. Moreover, nanoparticles of the CLA/CMCAB 25% formulation generated even higher (and very rapid) supersaturation than macroparticles of the same composition. Among the spray-dried ASDs, CLA/CMCAB 25% affords the highest supersaturation, furnishing more than 2-fold increase in solution concentration as well as slow and almost constant drug release rate. Ten and 25% CLA in HPMCAS gave release profiles similar to each other, affording the second highest CLA concentration amongst the spray-dried particles (about 2-fold increase in solution concentration). They both release CLA rapidly (due to higher solubility of HPMCAS) in the first 30 min, reaching high supersaturation that remains constant over the remainder of the 8h experiment. CLA/CMCAB 10% gave a final drug concentration similar to the one achieved by the HPMCAS ASDs, in addition to providing a slow and almost constant release over 8h. For CLA/CAAdP ASDs, the 25% formulation provides some supersaturation vs. crystalline CLA, but CLA release was slower from this polymer (the most hydrophobic of the three tested) than from CMCAB and HPMCAS ASDs.

Recently calculated solubility parameters (SP) for these polymers allow us to compare their relative hydrophobicities.[35] The SP provides a numerical estimate of the intermolecular forces within a material and can be a good indication of solubility, particularly for nonpolar materials such as polymers. The calculated SPs of the polymers were 20.56, 22.44 and 23.18 $MPa^{1/2}$ for CAAdP, HPMCAS, and CMCAB respectively (**Table 5.1**; SP of water is 49.01 $MPa^{1/2}$). The CLA supersaturation generated depends also on polymer ability to inhibit CLA nucleation and crystal growth in the solid phase and in solution. Previous collaborative studies from the Taylor and Edgar groups found that polymers with SP ranging from 20.56 to 23.28 $MPa^{1/2}$ (intermediate hydrophobicity) were good crystal growth inhibitors of ritonavir, while more hydrophobic polymers (SP < 20.56 $MPa^{1/2}$) were ineffective. CAAdP has a lower SP and is thus more hydrophobic than CMCAB, helping to explain the much higher solution concentration obtained for CMCAB vs. CAAdP ASDs. HPMCAS has an intermediate hydrophobicity but much higher neutral water solubility, which usually leads to fast dissolution rate of drugs from HPMCAS matrices, as seen for CLA/HPMCAS ASDs. Cellulose derivative solubility impacts CLA solution concentration because its release is a result of pH-triggered swelling and/or

dissolution of the polymer. CMCAB and CAAdP have lower water solubility, swelling when partially ionized, providing slower drug release.

Table 5.1 Polymer physical properties

Polymer	Solubility pH 1.2[1] (mg/mL)	Solubility pH 6.8[2] (mg/mL)	Solubility Parameter
HPMCAS	0.4	17.7	22.44
CMCAB	0.5	0.8	23.18
CAAdP	0.3	0.3	20.56

[1]pH 1.2 HCl solution, 37 ºC
[2]pH 6.8 Potassium phosphate buffer 0.05M, 37 ºC

5.4.4 CLA degradation versus crystallization

It's interesting and can be informative to test drug solubility, from ASD or otherwise, *in vitro* at small intestine pH. However, we must remember that *in vivo* the oral dosage form will always experience the low pH of the stomach first, then the near-neutral pH of the small intestine. Therefore, especially with drugs like CLA that are both more soluble and more unstable at low pH, *in vitro* studies at pH 6.8 may not accurately predict what will happen *in vivo*.

Therefore, improvement of CLA bioavailability through solubility enhancement is a multifaceted problem. The ideal drug delivery system for CLA would be one that would not release CLA in the stomach, or upon release, would be able to protect the drug from acid decomposition. Subsequently, the delivery system would efficiently enhance CLA solution concentration upon reaching the neutral pH of the small intestine. Such a system could be a breakthrough in CLA bioavailability enhancement. Polymers used in this study were chosen primarily for their promise for forming ASDs, thereby enhancing CLA solution concentration. However we also believed that the pH-dependent solubility of these carboxyl-containing cellulosic polymers could protect CLA from degradation at low pH.

In order to understand these competing processes, we designed experiments that separately examined the impact of degradation and recrystallization upon CLA solution concentration. First we carried out an experiment (experimental section 5.13.14.1), in which CLA was dissolved in minimal acetonitrile, and then added to aqueous pH 1.2 buffer. Supernatants from aliquots removed over 2h were analyzed for CLA content by HPLC, revealing the amount of CLA that remained in solution, neither degraded nor recrystallized (Dissolved CLA) (**Fig 5.8**). The second experiment (experimental section 5.13.14.2) was conducted the same way, except that multiple small experiments were run in parallel, and at a given time point the entire contents of that vessel were dissolved in acetonitrile (to dissolve any solids present), then analyzed for CLA by HPLC. This second experiment gave us the total amount of CLA remaining un-degraded at each time point, whether in solution or as a recrystallized solid (Total CLA). The difference between these values provides the amount of CLA that has recrystallized at each time point (using the relationship: Total CLA – Dissolved CLA = Crystallized CLA). The results from these 2 experiments are depicted in **Fig 5.8**. The first experiment shows the decrease in CLA concentration with time by the combined effects of CLA crystallization and degradation (dashed curve), and the second curve shows total CLA (dissolved plus crystalline). Comparing the results from these two experiments, it is quite evident that there is virtually no recrystallized CLA; the two curves are nearly superimposed. This means that at pH 1.2 the loss in CLA solution concentration with time, in the absence of polymer, is due entirely to CLA chemical degradation. We calculated the CLA degradation half-life to be 0.35 h; as shown in **Fig 5.8**, 90% of CLA has been degraded within the first hour of the experiment.

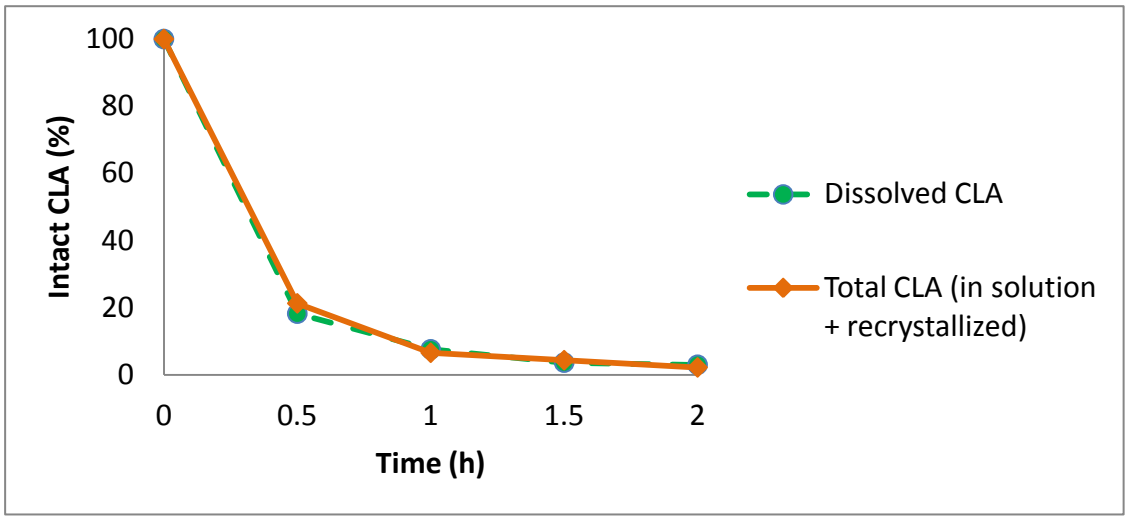

Figure 5.8 Loss of dissolved CLA at pH 1.2. Comparison between amount of dissolved CLA, and amount of dissolved plus recrystallized CLA

5.4.5 Release profile of CLA from ASDs with pH Change

Having confirmed that virtually all loss of CLA from solution at pH 1.2 is due to chemical degradation, we designed the second dissolution experiment (Exp B) to mimic passage of the drug through the gastrointestinal system. In this experiment, ASDs were first dispersed in aqueous HCl (pH 1.2) for 2 h. After 2 h, the pH of the dissolution medium was adjusted to 6.8, which was maintained for 6 h. The dissolution profile for each ASD is presented as the concentration of CLA remaining in solution (HPLC) vs. time (**Fig 5.9a-d**).

a)

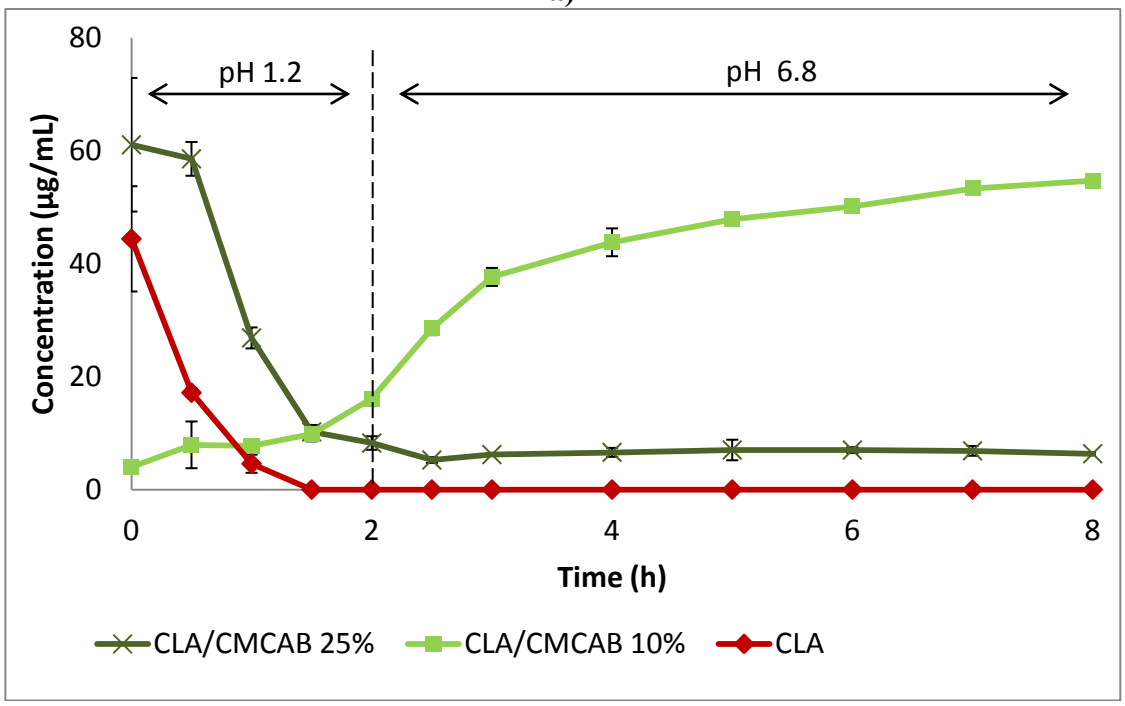
80
60
40
20
0
Concentration (µg/mL)
pH 1.2
pH 6.8
0
2
4
6
8
Time (h)
CLA/CMCAB 25%
CLA/CMCAB 10%
CLA

b)

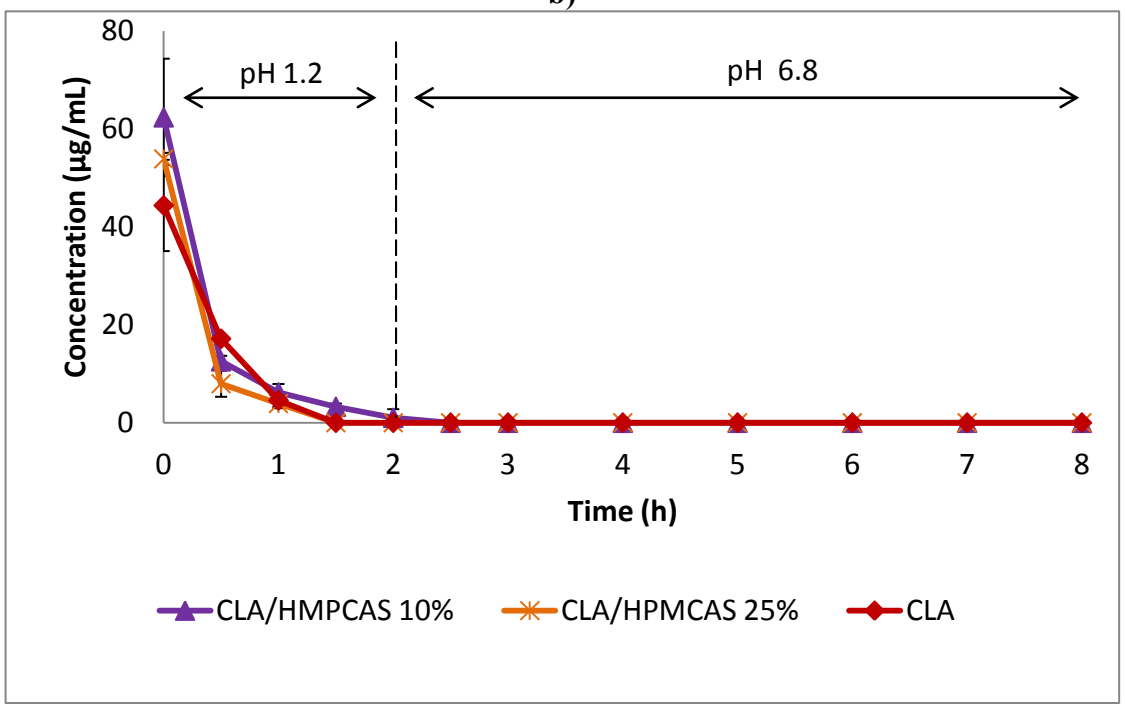
80
60
40
20
0
Concentration (µg/mL)
pH 1.2
pH 6.8
0
1
2
3
4
5
6
7
8
Time (h)
CLA/HMPCAS 10%
CLA/HPMCAS 25%
CLA

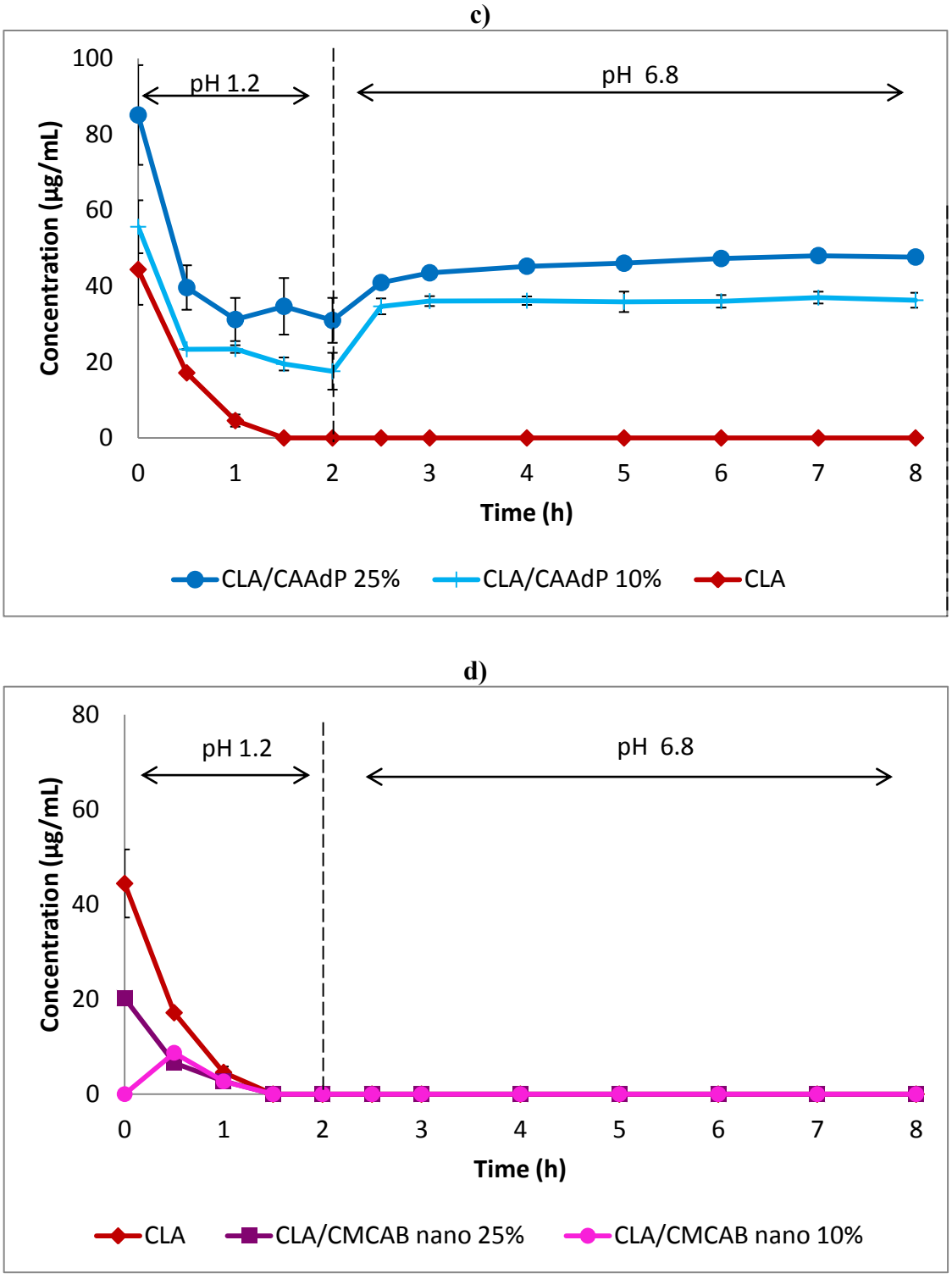

Figure 5.9 Dissolution profiles of CLA and ASDs; pH 1.2 buffer for 2h, then pH 6.8 buffer for 6h (Exp B). Each point is an average of 3 experiments, and error bars indicate one standard deviation, with exception of CLA/CMCAB nano, 10 and 25%, for each of which only one experiment was performed at each time point due to limited sample availability.

A quick inspection of **Fig 5.9** shows a complex dissolution picture with strong dependence on matrix polymer structure. First we can note the behavior of crystalline CLA, the negative control. In each case, an immediate burst of solution concentration is observed at pH 1.2, followed by a rapid decline due to drug degradation. Upon increasing medium pH to 6.8, no enhancement in CLA concentration is observed; indeed virtually no CLA is in solution.

Even more interesting results are observed from the CLA/CMCAB spray-dried dispersions (**Fig 5.9a**). CLA/CMCAB 25% ASD behaves similarly to crystalline CLA; most of the drug released is degraded. A higher initial CLA concentration burst is observed at gastric pH and a slower tailing off vs. time; a small but significant amount of drug (ca. 7 μg/mL) remains dissolved upon switching to neutral pH. In contrast, the CLA/CMCAB 10% ASD particles release CLA to only a minor extent at gastric pH, and then show strong release at small intestine pH, reaching ca. 55 μg/mL CLA concentration; this high level remains steady throughout the rest of the experiment, indicating strong solution stabilization by the polymer. The most obvious explanation for the marked difference in performance between the 10% and 25% ASDs would be the fact that a rather hydrophilic drug is dispersed in a very hydrophobic matrix polymer; at 25% CLA, the release is drug-controlled and rapid at low pH, while at 10% CLA the proportion of hydrophobic CMCAB is much greater, so release is polymer-controlled and negligible. Little CLA chemical degradation occurs at pH 1.2 from the 10% dispersion as indicated by the absence of peaks from degradation products (HPLC), supporting this hypothesis.

The interplay of these factors leads to a fascinating result from the CLA/HPMCAS spray-dried ASDs (**Fig 5.9b**). With the more water-soluble HPMCAS, very rapid CLA dissolution is observed at pH 1.2, nearly matching that observed from crystalline CLA. The only significant difference is a higher peak concentration from the HPMCAS ASDs than that from crystalline CLA (about 60 μg/mL for both CLA/HPMCAS formulations versus 44 μg/mL for free CLA). There is very little difference in dissolution behavior between the 10% and 25% CLA/HPMCAS ASDs. In both cases, CLA solution concentration drops rapidly from the peak while still at pH 1.2, reaching essentially zero CLA in solution before the pH change, and staying at zero after the adjustment to pH 6.8. It seems likely that this behavior is due to the enhanced HPMCAS water solubility vs. CMCAB and CAAdP. The combination of CLA acid solubility and enhanced matrix solubility leads to rapid CLA dissolution at low pH, much faster for example than that

from the CLA/CMCAB 10% ASD, and this dissolved CLA is chemically degraded in the acidic environment.

These pH-switch experiments, attempting to mimic the environments encountered in the GI tract *in vivo*, provide a dramatically different picture of the solution concentration achievable from ASDs of CLA in the very hydrophobic cellulose ester polymer CAAdP (**Fig 5.9c**). For CLA/CAAdP ASDs, both formulations yield high initial drug concentrations (55 and 85 μg/mL for CLA/CAAdP 10% and 25% respectively, against 44 μg/mL for free drug). Drug release from the CAAdP ASDs is influenced strongly by the amount of relatively hydrophilic CLA in the ASD, since CAAdP is even more hydrophobic than CMCAB; thus the 25% drug loaded CLA/CAAdP provides higher drug solution concentration than from the 10% ASD. The concentration of drug then drops by roughly 50% in the first 30 min (from 85 to 40 μg/mL) and remains nearly constant for the next 1.5 h for both formulations. This suggests that some degradation occurs initially (perhaps due to release of drug at the surface of the ASD), but that CAAdP is remarkably effective, at both 10 and 25% drug loadings, at preventing further CLA solution degradation for the rest of the exposure of CLA/CAAdP ASDs to acidic conditions. This is particularly surprising given the low solubility of CAAdP in acidic media; clearly the small amount of dissolved CAAdP is a powerful inhibitor of CLA degradation. The picture of CAAdP effectiveness as an ASD polymer for CLA is changed completely by this experiment vs. the impression gleaned by looking at dissolution at pH 6.8 alone (**Fig 5.7**); these more realistic experiments show that CAAdP ASDs are very effective at generating enhanced CLA solution concentrations.

The results from pH-switch experiments with nanoparticulate CLA/CMCAB ASDs (**Fig 5.9d**) were also revealing. While the synergistic effects of high nanoparticle surface area and stable amorphous dispersion were evident in the pH 6.8 dissolution experiment (**Fig 5.7**), the experiments employing first gastric and then small intestine pH gave very different results. Under these GI tract-mimicking pH conditions, a strong burst of enhanced drug solution concentration from CLA/CMCAB amorphous nanoparticles was observed at pH 1.2, consistent with CLA acid solubility combined with the increased surface area and amorphous effects. However, a subsequent and very rapid drop in solution concentrations was also observed, reaching essentially zero dissolved CLA even before the pH was adjusted to 6.8. After the

increase in pH, the CLA level in solution remained near zero. We interpret these results to mean that the synergistic advantages of the amorphous nanoparticles actually work against the goal of higher CLA bioavailability, because of the enhanced CLA release and solution concentration at low pH, and subsequent chemical degradation of dissolved CLA. This suggests that the CMCAB in the nanoparticle ASDs is not capable of efficiently stabilizing the drug against degradation under these acidic conditions, where CLA solubility is much higher. Since some absorption of the released CLA from the stomach would be expected, slightly better results might be obtained *in vivo* than would be predicted from these *in vitro* low pH release experiments.

Polymer physical properties like pH-dependent solubility and hydrophobicity provide some insight into performance of these CLA ASDs. These carboxyl-containing cellulosic polymers have uniformly poor solubility at pH 1.2, while at pH 6.8 CAAdP and CMCAB have low solubility, but that of HPMCAS is substantially higher (**Table 5.1**). With regard especially to drug release, it is notable that for these polymers swelling is negligible at low pH, but significant swelling is observed at neutral pH, which would lead us to predict that for most drugs at pH 1.2, release from the polymer matrices would be less favorable; clearly, as with amine-containing drugs like CLA, there can be exceptions in some cases. Despite the high CLA solubility at low pH, which might lead us to expect drug-controlled release, some of the ASDs studied were exceptionally good in preventing drug release and degradation at pH 1.2. Still, the impact of the structural differences among the three cellulose derivatives examined is very powerful, as illustrated by the data presented above. The detailed mechanisms behind these observations need to be investigated further, since there are no definitive correlations between the extent of release at pH 1.2 and either polymer solubility or polymer solubility parameter. Given the obvious importance of surface area, as seen by comparing release behavior of spray dried vs. nanoparticulate CMCAB dispersions, this factor should be further investigated in our upcoming studies, in terms of how it impacts release of an acid soluble drug such as CLA.

Having analyzed the ability of each polymer to protect against drug degradation in solution, we wished to examine the relative ability of the ASD polymers to protect the drug against degradation while still within the particles, upon exposure to pH 1.2 buffer. We investigated this question by adding solid ASDs to pH 1.2 buffer and, after time intervals, adding organic solvent to dissolve all organics present (Experimental section 5.13.14.2). In this way we

could assess the amount of un-degraded CLA; the amount inside the particles, plus the amount dissolved in the pH 1.2 buffer, but stabilized against degradation. **Fig 5.10** illustrates then the ultimate performance of each polymer in protecting CLA against degradation at pH 1.2; it is immediately evident that some of the polymers strongly stabilize CLA against degradation, and that the degree of stabilization is highly dependent on polymer chemical functionality. The very hydrophobic CAAdP gives substantial protection of CLA against degradation (60 % remaining after 2h vs. almost zero remaining in the absence of polymer), while CMCAB is not very effective, with HMPCAS being intermediate in this respect. Remember that Exp B (**Fig 5.9a-d**) quantified the amount of CLA intact in solution at pH 1.2; conversion of this amount to percentage (experimental section 5.3.13.2) and subtraction from the corresponding data point from **Fig 5.10** provides an estimate of the amount of CLA that remained intact inside the particles. These combined results quantify the ability of each polymer to protect drug against degradation in solution, and the ability to protect against degradation in the solid phase.

.

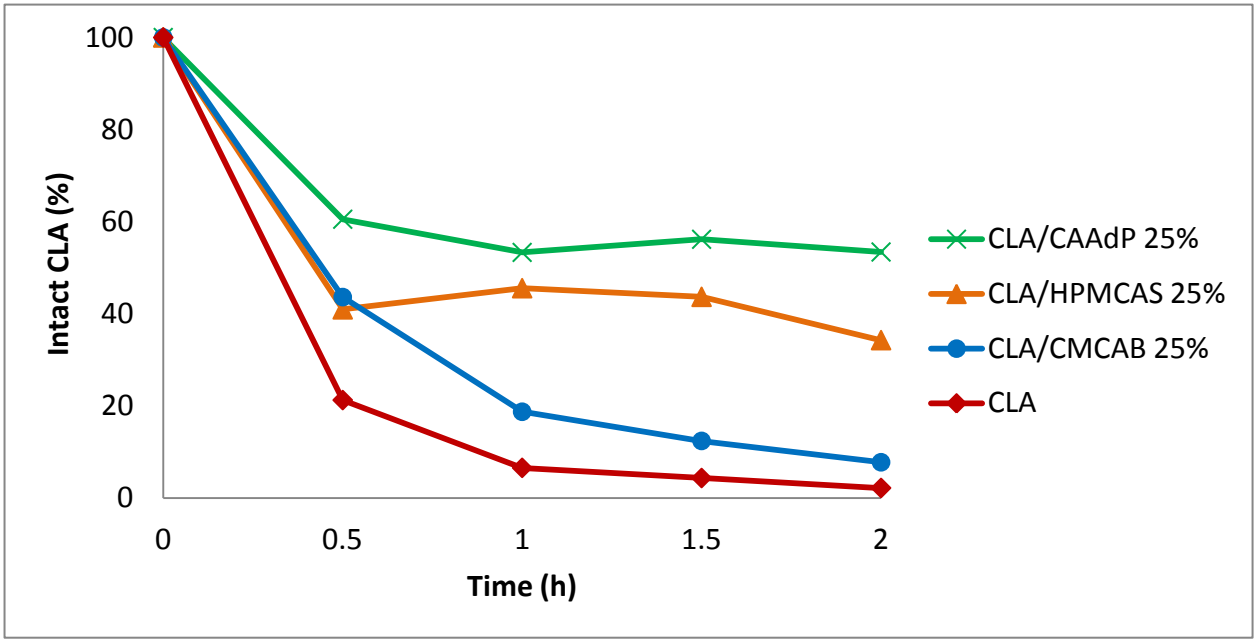

Figure 5.10 Percentage of CLA that remains intact either in solution or inside the ASD particles vs. time at pH 1.2.

After estimating how much intact drug still remained in the particles after 2h, we could also assess the behavior of this encapsulated drug after it was exposed to pH 6.8, for each polymer, by looking at CLA release at pH 6.8 in **Fig 5.9a-d**. We have then attempted, after analysis of the results depicted in **Fig 5.9a-d** and **Fig 5.10**, to explore the dissolution behavior of each CLA/polymer ASD. **Fig 5.11** illustrates the interplay of the different aspects involved in the dissolution of CLA from these ASDs under GI tract-mimicking pH conditions.

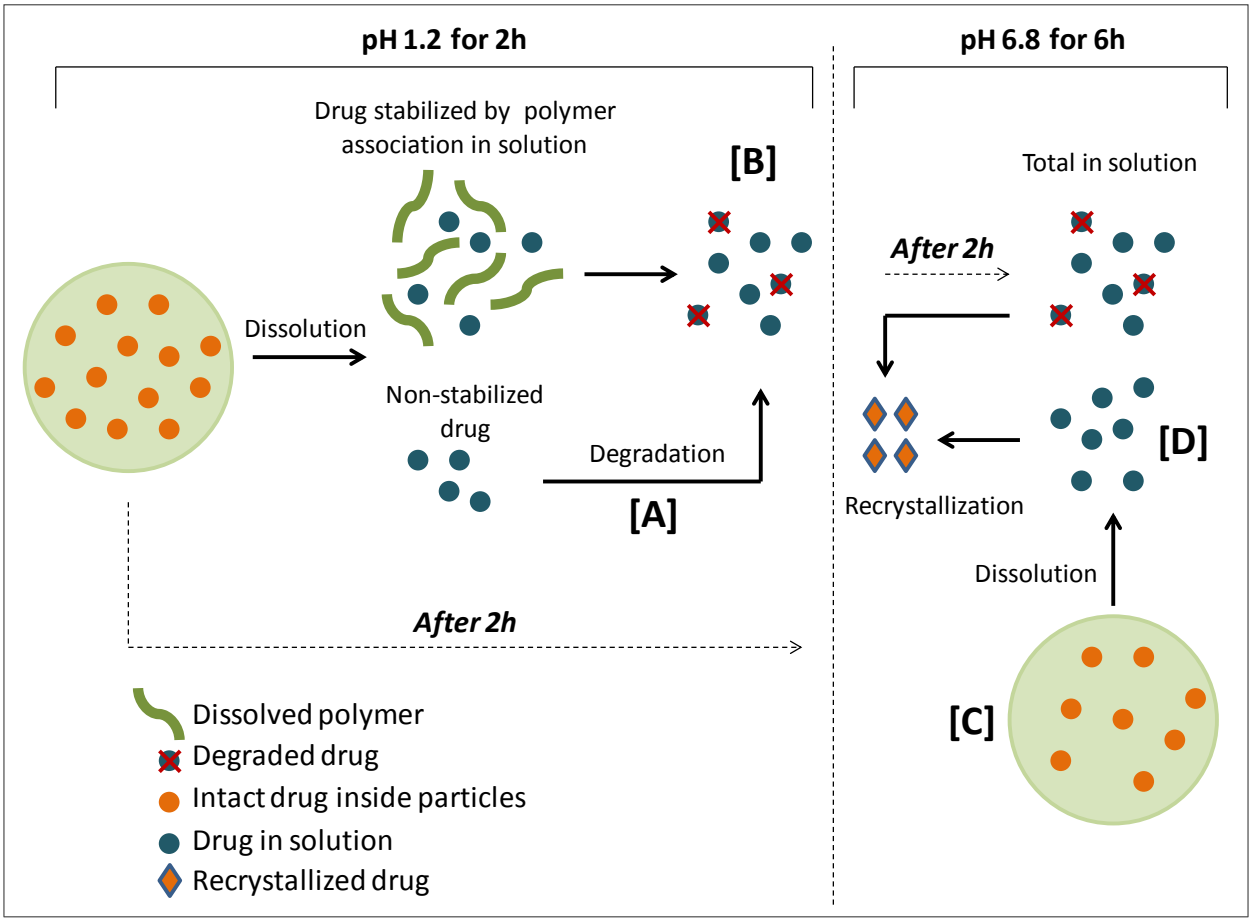

Figure 5.11 Schematic illustration of the different processes occurring during the dissolution of CLA/polymer ASDs under GI-tract mimicking pH conditions.

For CLA/HPMCAS, about 60% of CLA has been released and degraded in 2h (**Fig 5.10**), and 40% remained stable inside the particles (**Fig 5.9b/Fig 5.10**). However, no release is observed at pH 6.8 (**Fig 5.9b**), indicating that, although about 35% of drug still remains intact in the ASD after 2h, HPCMAS will not release any more drug at pH 6.8. This result is surprising but it is consistent with the results of Exp. A (**Fig 5.7**), that presents dissolution from the ASDs

at only pH 6.8, where release of CLA from HPMCAS ASD is very fast (almost 60% is released in the first 30 min), but then the concentration of CLA in solution remains constant. This may simply reflect partitioning of CLA between HPMCAS and the aqueous buffer. CLA/CAAdP 25% shows a much more effective dissolution profile. Only 46% of the drug is degraded within 2h at pH 1.2 (**Fig 5.10**), while 26% remains intact in pH 1.2 solution (**Fig 5.9c**) and 28% remains intact inside the particles (**Fig 5.9c/Fig 5.10**); this 28% is finally released at pH 6.8 leading to a total of 54% drug in solution at the end of the experiment (**Fig 5.9c**). For CLA/CMCAB 25%, release was almost complete at pH 1.2 and nearly all drug that was released was degraded (92%) (**Fig 5.10**), with only about 6% of the drug that was released at pH 1.2 remaining intact and in solution until the end of the experiment (**Fig 5.9a**). No drug was released upon exposure of CLA/CMCAB 25% ASD to pH 6.8 (**Fig 5.9a**), since there was practically no intact drug left inside the particles.

Table 5.2 was compiled by comparing the results from **Fig 5.9a-d** and **Fig 5.10** and summarizes the results previously discussed. It shows a mass balance for CLA after the ASDs were exposed to pH 1.2 for 2h and then to pH 6.8 for 6h. **Fig 5.11** illustrates the processes quantified in **Table 5.2**. **Fig 5.9a-d** provides information on the amount of CLA that was released from the ASD particles at pH 1.2 and remained stable in solution and also the release behavior of the particles once exposed to pH 6.8. **Fig 5.10** provides information on CLA that remained unchanged inside the ASD particles. Therefore, **Table 5.2** shows the percentages of CLA that: have degraded once CLA was dissolved at pH 1.2 (**[A]**), were released at pH 1.2 and remained stable in solution (**[B]**), remained stable inside the particles at pH 1.2 (**[C]**), and finally, CLA that was released when the ASDs were exposed to pH 6.8 (**[D]**) and the total percentage of CLA in solution at the end of the experiment (**[B+D]**), which accounts for drug released at pHs 1.2 and 6.8.

Table 5.2 Quantification of polymer influence on CLA stability and solubility at pH 1.2 and 6.8

	pH 1.2 for 2h			pH 6.8 for 6h		
ASD	**Degraded[1] (%) [A]**	**Stable in solution[2] (%) [B]**	**Intact inside particles[3] (%) [C]**	**Released[2] (%) [D]**	**Total in solution (%) [B+D]**	**Total protected against degradation [B+C]**
CLA/CMCAB 25%	92	6	2	0	6	8%
CLA/HPMCAS 25%	60	0	40	0	0	40%
CLA/CAAdP 25%	46	26	28	28	54	54%

[1]Calculated from Fig 5.10, [2]Calculated from Fig 5.9a-c, [3][C] = 100 – [A] – [B].

This compilation (**Table 5.2 and Fig 5.11**) summarizes the complex interplay of release behavior, protection against acid degradation, and solubility enhancement of CLA, all of which depend strongly on polymer chemistry and properties.

5.5 Conclusions

Stabilization and release of CLA is exceptionally complex due to its acid solubility, acid instability, and low solubility at the neutral pH of the intestines. The interplay of these drug properties with those of the three structurally diverse polymers studied, and with those of experimental systems seeking to mimic the properties of the stomach and those of the small intestine, is even more complicated. The experiments described herein have provided substantial insight into what is going on in these systems, how we can design polymers for successful bioavailability enhancement of CLA, and perhaps the behavior of CLA in current dosage forms *in vivo*[65]. One conclusion we can draw is that there is indeed the potential for synergy between the solubility advantages arising from the high surface area and curvature of nanoparticles, and the high energy of amorphous solid dispersions. Unfortunately we can also conclude that, at least for these polymers and this drug, these combined advantages would be unlikely to translate into enhanced CLA bioavailability. Due to premature dissolution and degradation of CLA at gastric pH, amorphous nanoparticles may not be a useful way to enhance CLA bioavailability.

We also have more insight about what polymer properties are needed to design successful macroparticulate CLA ASDs. The polymer can't be too hydrophilic; HPMCAS for example appears to be too hydrophilic, thereby releasing too much CLA at gastric pH and ultimately delivering considerably less dissolved CLA by the time intestinal pH is reached. The strength of the polymer-CLA interactions is also critical. It appears that these interactions are insufficiently strong in the case of CMCAB, thereby resulting in too little protection of the CLA against low pH degradation, and very little CLA being available for release in the small intestine.

The very hydrophobic polymer CAAdP shows significant promise for enhancing CLA solution concentration and bioavailability. CLA/CAAdP ASDs (both 10 and 25% CLA) are exceptionally efficient in preventing CLA degradation at pH 1.2, and release the remaining intact CLA when exposed to pH 6.8. Interestingly, more intact CLA is released from CLA/CAAdP 25% ASD in the more biorelevant pH switch experiment (48 μg/mL) than in the experiment where the ASD particles were only exposed to pH 6.8 (27 μg/mL); we do not fully understand this phenomenon but it may be that preliminary exposure to low pH permits greater hydration and swelling of CLA/CAAdP dispersion upon exposure to small intestine pH. Whatever the mechanism, this result provides more confidence of successful translation into *in vivo* performance. It will be of great interest to determine whether macroparticulate ASDs based on CAAdP and related cellulose □-carboxyalkanoates[66] are effective at enhancing clarithromycin bioavailability *in vivo*.

These observations may also provide insight into how CLA and its ASDs could behave *in vivo*. By only looking at dissolution at pH 6.8, it is possible to get preliminary indication of the solubility enhancement that each polymer can provide in comparison to the free drug, but it is also important to evaluate the dissolution behavior of the ASDs at gastric pH, especially for drugs like CLA that are prone to acid-catalyzed degradation and for polymers that can provide pH controlled drug release. By looking at the release behavior of these ASDs at pH 1.2 followed by pH 6.8, we obtained critical information about their performance under more realistic conditions. We believe that this experimental protocol should be more frequently a part of initial *in vitro* drug delivery studies, and especially for those involving ASDs (since even for more chemically stable drugs, premature separation of the drug from the ASD by dissolution and subsequent recrystallization could destroy the ASD advantage). Clearly such studies are even

more critical when a particularly acid soluble and/or acid labile drug like CLA is the topic of consideration.

The results from these experiments will serve as a guide on how to best apply these ASDs and will also dictate the modifications that need to be performed to improve their performance for specific applications. The possibility of mixing different polymers with distinct properties with the aim to attain intermediate properties is also another interesting area of research where the results from these experiments will be fundamental.[67] The synergistic effects observed in these studies with the amorphous nanoparticles are also promising for drug-polymer systems in which release in the stomach would be less problematic.

5.6 References

1. Pace, S. N.; Pace, G. W.; Parikh, I.; Mishra, A. K., Novel injectable formulations of insoluble drug. *Pharmaceutical Technology* **1999,** (23), 116-34.

2. Martinez, M. N.; Amidon, G. L., A mechanistic approach to understanding the factors affecting drug absorption: A review of fundamentals. *Journal of Clinical Pharmacology* **2002,** *42* (6), 620-643.

3. Lobenberg, R.; Amidon, G. L., Modern bioavailability, bioequivalence and biopharmaceutics classification system. New scientific approaches to international regulatory standards. *Eur. J. Pharm. Biopharm.* **2000,** *50* (1), 3-12.

4. Li, A. P., Screening for human ADME/Tox drug properties in drug discovery. *Drug Discovery Today* **2001,** *6* (7), 357-366.

5. Wang, Y.-J.; Pan, M.-H.; Cheng, A.-L.; Lin, L.-I.; Ho, Y.-S.; Hsieh, C.-Y.; Lin, J.-K., Stability of curcumin in buffer solutions and characterization of its degradation products. *J. Pharm. Biomed. Anal.* **1997,** *15* (12), 1867-1876.

6. Cermola, F.; DellaGreca, M.; Iesce, M. R.; Montanaro, S.; Previtera, L.; Temussi, F., Photochemical behavior of the drug atorvastatin in water. *Tetrahedron* **2006,** *62* (31), 7390-7395.

7. Prankerd, R. J.; Walters, J. M.; Parnes, J. H., Kinetics for degradation of rifampicin, an azomethine-containing drug which exhibits reversible hydrolysis in acidic solutions. *Int. J. Pharm.* **1992,** *78* (1–3), 59-67.

8. Peterson, W. L.; Graham, D. Y.; Marshall, B.; Blaser, M. J.; Genta, R. M.; Klein, P. D.; Stratton, C. W.; Drnec, J.; Prokocimer, P.; Siepman, N., Clarithromycin as monotherapy for eradication of Helicobacter pylori: a randomized, double-blind trial. *The American journal of gastroenterology* **1993,** *88* (11), 1860-4.

9. Inoue, Y.; Yoshimura, S.; Tozuka, Y.; Moribe, K.; Kumamoto, T.; Ishikawa, T.; Yamamoto, K., Application of ascorbic acid 2-glucoside as a solubilizing agent for clarithromycin: Solubilization and nanoparticle formation. *Int J Pharm* **2007,** *331* (1), 38-45.

10. Salem, I. I.; Duzgunes, N., Efficacies of cyclodextrin-complexed and liposome-encapsulated clarithromycin against Mycobacterium avium complex infection in human macrophages. *International Journal of Pharmaceutics* **2003,** *250* (2), 403-414.

11. Chu, S. Y.; Deaton, R.; Cavanaugh, J., Absolute bioavailability of clarithromycin after oral administration in humans. *Antimicrobial Agents and Chemotherapy* **1992,** *36* (5), 1147-1150.

12. Venkateswaramurthy, N.; Sambathkumar, R.; Perumal, P., Controlled release mucoadhesive microspheres of clarithromycin for the treatment of Helicobacter Pylori infection. *Der Pharmacia Lettre* **2012,** *4* (3), 993-1004.

13. Nakagawa, Y.; Itai, S.; Yoshida, T.; Nagai, T., Physicochemical Properties and Stability in the Acidic Solution of a New Macrolide Antibiotic, Clarithromycin, in Comparison with Erythromycin. *Chemical & Pharmaceutical Bulletin* **1992,** *40* (3), 725-728.

14. Erah, P. O.; Goddard, A. F.; Barrett, D. A.; Shaw, P. N.; Spiller, R. C., The stability of amoxycillin, clarithromycin and metronidazole in gastric juice: Relevance to the treatment of Helicobacter pylori infection. *Journal of Antimicrobial Chemotherapy* **1997,** *39* (1), 5-12.

15. Preidis, G. A.; Versalovic, J., Targeting the Human Microbiome With Antibiotics, Probiotics, and Prebiotics: Gastroenterology Enters the Metagenomics Era. *Gastroenterology* **2009,** *136* (6), 2015-2031.

16. Chu, S.; Park, Y.; Locke, C.; Wilson, D. S.; Cavanaugh, J. C., Drug-food interaction potential of clarithromycin, a new macrolide antimicrobial. *Journal of Clinical Pharmacology* **1992,** *32* (1), 32-36.

17. Barone, J. A.; Moskovitz, B. L.; Guarnieri, J.; Hassell, A. E.; Colaizzi, J. L.; Bierman, R. H.; Jessen, L., Enhanced bioavailability of itraconazole in hydroxypropyl-beta-cyclodextrin solution versus capsules in healthy volunteers. *Antimicrob. Agents Chemother.* **1998,** *42* (7), 1862-1865.

18. Taupitz, T.; Dressman, J. B.; Buchanan, C. M.; Klein, S., Cyclodextrin-water soluble polymer ternary complexes enhance the solubility and dissolution behaviour of poorly soluble drugs. Case example: Itraconazole. *Eur. J. Pharm. Biopharm.* **2013,** *83* (3), 378-387.

19. Constantinides, P. P.; Han, J. H.; Davis, S. S., Advances in the use of tocols as drug delivery vehicles. *Pharm Res* **2006,** *23* (2), 243-255.

20. Lai, F.; Sinico, C.; Ennas, G.; Marongiu, F.; Marongiu, G.; Fadda, A. M., Diclofenac nanosuspensions: Influence of preparation procedure and crystal form on drug dissolution behaviour. *Int. J. Pharm.* **2009,** *373* (1–2), 124-132.

21. Merisko-Liversidge, E.; Liversidge, G. G.; Cooper, E. R., Nanosizing: a formulation approach for poorly-water-soluble compounds. *Eur J Pharm Sci* **2003,** *18* (2), 113-20.

22. Murdande, S. B.; Pikal, M. J.; Shanker, R. M.; Bogner, R. H., Solubility Advantage of Amorphous Pharmaceuticals: I. A Thermodynamic Analysis. *J Pharm Sci-Us* **2010,** *99* (3), 1254-1264.

23. Singhal, D.; Curatolo, W., Drug polymorphism and dosage form design: a practical perspective. *Advanced Drug Delivery Reviews* **2004,** *56* (3), 335-347.

24. Leuner, C.; Dressman, J., Improving drug solubility for oral delivery using solid dispersions. *Eur. J. Pharm. Biopharm.* **2000,** *50* (1), 47-60.

25. Kwong, A. D.; Kauffman, R. S.; Hurter, P.; Mueller, P., Discovery and development of telaprevir: an NS3-4A protease inhibitor for treating genotype 1 chronic hepatitis C virus. *Nature Biotechnology* **2011,** *29* (11), 993-1003.

26. Miller, J. M.; Beig, A.; Carr, R. A.; Spence, J. K.; Dahan, A., A Win–Win Solution in Oral Delivery of Lipophilic Drugs: Supersaturation via Amorphous Solid Dispersions Increases Apparent Solubility without Sacrifice of Intestinal Membrane Permeability. *Molecular Pharmaceutics* **2012,** *9* (7), 2009-2016.

27. Edgar, K. J., Cellulose esters in drug delivery. *Cellulose* **2007,** *14* (1), 49-64.

28. Posey-Dowty, J. D.; Watterson, T. L.; Wilson, A. K.; Edgar, K. J.; Shelton, M. C.; Lingerfelt, L. R., Zero-order release formulations using a novel cellulose ester. *Cellulose* **2007,** *14* (1), 73-83.

29. Shah, N.; Iyer, R. M.; Mair, H. J.; Choi, D. S.; Tian, H.; Diodone, R.; Fahnrich, K.; Pabst-Ravot, A.; Tang, K.; Scheubel, E.; Grippo, J. F.; Moreira, S. A.; Go, Z.; Mouskountakis, J.; Louie, T.; Ibrahim, P. N.; Sandhu, H.; Rubia, L.; Chokshi, H.; Singhal, D.; Malick, W., Improved human bioavailability of vemurafenib, a practically insoluble drug, using an amorphous polymer-stabilized solid dispersion prepared by a solvent-controlled coprecipitation process. *Journal of Pharmaceutical Sciences* **2013,** *102* (3), 967-981.

30. Konno, H.; Handa, T.; Alonzo, D. E.; Taylor, L. S., Effect of polymer type on the dissolution profile of amorphous solid dispersions containing felodipine. *Eur. J. Pharm. Biopharm.* **2008,** *70* (2), 493-499.

31. Ilevbare, G. A.; Liu, H.; Edgar, K. J.; Taylor, L. S., Impact of Polymers on Crystal Growth Rate of Structurally Diverse Compounds from Aqueous Solution. *Molecular Pharmaceutics* **2013,** *10* (6), 2381-2393.

32. Li, B.; Harich, K.; Wegiel, L.; Taylor, L. S.; Edgar, K. J., Stability and solubility enhancement of ellagic acid in cellulose ester solid dispersions. *Carbohydrate Polymers* **2013,** *92* (2), 1443-1450.

33. Li, B.; Konecke, S.; Wegiel, L. A.; Taylor, L. S.; Edgar, K. J., Both Solubility and Chemical Stability of Curcumin are Enhanced by Solid Dispersion in Cellulose Derivative Matrices. *Carbohydr. Polym.* (0).

34. Ilevbare, G. A.; Liu, H.; Edgar, K. J.; Taylor, L. S., Understanding polymer properties important for crystal growth inhibition-impact of chemically diverse polymers on solution crystal growth of ritonavir. *Crystal Growth & Design* **2012,** *12* (6), 3133-3143.

35. Ilevbare, G. A.; Liu, H.; Edgar, K. J.; Taylor, L. S., Maintaining supersaturation in aqueous drug solutions: Impact of different polymers on induction times. *Crystal Growth & Design* **2013,** *13* (2), 740-751.

36. Posey-Dowty, J. D.; Seo, K. S.; Walker, K. R.; Wilson, A. K., Carboxymethylcellulose acetate butyrate in water-based automotive paints. *Surface Coatings International Part B-Coatings Transactions* **2002,** *85* (3), 203-208.

37. Li, B.; Konecke, S.; Harich, K.; Wegiel, L.; Taylor, L. S.; Edgar, K. J., Solid dispersion of quercetin in cellulose derivative matrices influences both solubility and stability. *Carbohydrate Polymers* **2013,** *92* (2), 2033-2040.

38. Kojima, M.; Nakagami, H., Development of controlled release matrix pellets by annealing with micronized water-insoluble or enteric polymers. *Journal of Controlled Release* **2002,** *82* (2-3), 335-343.

39. J., C. W.; Nightingale, J. A. S.; Shanker, R. M.; Sutton, S. C. Basic drug compositions with enhanced bioavailability. 6,548,555, 2003.

40. E., A. L.; Curatolo, W. J.; Herbig, S. M.; Nightingale, J. A. S.; Thombre, A. G. Controlled release by extrusion of solid amorphous dispersions of drugs 6: 706, 283, 2004.

41. Friesen, D. T.; Shanker, R.; Crew, M.; Smithey, D. T.; Curatolo, W. J.; Nightingale, J. A. S., Hydroxypropyl methylcellulose acetate succinate-based spray-dried dispersions: An overview. *Molecular Pharmaceutics* **2008,** *5* (6), 1003-1019.

42. Kar, N.; Liu, H.; Edgar, K. J., Synthesis of cellulose adipate derivatives. *Biomacromolecules* **2011,** *12* (4), 1106-1115.

43. Liu, H.; Kar, N.; Edgar, K. J., Direct synthesis of cellulose adipate derivatives using adipic anhydride. *Cellulose* **2012,** *19* (4), 1279-1293.

44. Ilevbare, G. A.; Liu, H.; Edgar, K. J.; Taylor, L. S., Inhibition of solution crystal growth of ritonavir by cellulose polymers - factors influencing polymer effectiveness. *Crystengcomm* **2012,** *14* (20), 6503-6514.

45. Li, B.; Konecke, S.; Wegiel, L. A.; Taylor, L. S.; Edgar, K. J., Both solubility and chemical stability of curcumin are enhanced by solid dispersion in cellulose derivative matrices. *Carbohydrate Polymers* **2013,** *98* (1), 1108-1116.

46. Merisko-Liversidge, E.; Liversidge, G. G., Nanosizing for oral and parenteral drug delivery: A perspective on formulating poorly-water soluble compounds using wet media milling technology. *Advanced Drug Delivery Reviews* **2011,** *63* (6), 427-440.

47. Johnson, B. K.; Prud'homme, R. K., Chemical processing and micromixing in confined impinging jets. *AIChE Journal* **2003,** *49* (9), 2264-2282.

48. Johnson, B. K.; Prud'homme, R. K., Mechanism for rapid self-assembly of block copolymer nanoparticles. *Physical Review Letters* **2003,** *91*, 118302-1-118302-4.

49. Johnson, B. K.; Prud'homme, R. K., Flash NanoPrecipitation of Organic Actives and Block Copolymers using a Confined Impinging Jets Mixer. *Australian Journal of Chemistry* **2003,** *56* (10), 1021-1024.

50. Liu, Y.; Kathan, K.; Saad, W.; Prud'homme, R. K., Ostwald ripening of β-carotene nanoparticles. *Physical Review Letters* **2007,** *98* (3), 036102-1-036102-4.

51. Gindy, M. E.; Panagiotopoulos, A. Z.; Prud'homme, R. K., Composite Block Copolymer Stabilized Nanoparticles: Simultaneous Encapsulation of Organic Actives and Inorganic Nanostructures. *Langmuir* **2007,** *24* (1), 83-90.

52. Gindy, M. E.; Ji, S.; Hoye, T. R.; Panagiotopoulos, A. Z.; Prud'homme, R. K., Preparation of Poly(ethylene glycol) Protected Nanoparticles with Variable Bioconjugate Ligand Density. *Biomacromolecules* **2008,** *9* (10), 2705-2711.

53. Liu, Y.; Tong, Z.; Prud'homme, R. K., Stabilized polymeric nanoparticles for controlled and efficient release of bifenthrin. *Pest Management Science* **2008,** *64* (8), 808-812.

54. Merisko-Liversidge, E.; Liversidge, G. G.; Cooper, E. R., Nanosizing: a formulation approach for poorly-water-soluble compounds. *European Journal of Pharmaceutical Sciences* **2003,** *18* (2), 113-120.

55. Liu, Y.; Cheng, C.; Liu, Y.; Prud'homme, R. K.; Fox, R. O., Mixing in a multi-inlet vortex mixer (MIVM) for flash nano-precipitation. *Chem. Eng. Sci.* **2008,** *63* (11), 2829-2842.

56. Lu, Y.; Wang, Y.; Tang, X., Formulation and thermal sterile stability of a less painful intravenous clarithromycin emulsion containing vitamin E. *International Journal of Pharmaceutics* **2008,** *346* (1-2), 47-56.

57. Tuteja, A.; Mackay, M. E.; Narayanan, S.; Asokan, S.; Wong, M. S., Breakdown of the Continuum Stokes−Einstein Relation for Nanoparticle Diffusion. *Nano Lett.* **2007,** *7* (5), 1276-1281.

58. Hughey, J. R.; DiNunzio, J. C.; Bennett, R. C.; Brough, C.; Miller, D. A.; Ma, H.; Williams, R. O.; McGinity, J. W., Dissolution enhancement of a drug exhibiting thermal and acidic decomposition characteristics by fusion processing: A comparative study of hot melt extrusion and kinetiSolA (R) dispersing. *Aaps Pharmscitech* **2010,** *11* (2), 760-774.

59. Vehring, R., Pharmaceutical particle engineering via spray drying. *Pharmaceutical Research* **2008,** *25* (5), 999-1022.

60. Sheu, T. Y.; Rosenberg, M., Microstructure of microcapsules consisting of whey proteins and carbohydrates. *Journal of Food Science* **1998,** *63* (3), 491-494.

61. Peres, I.; Rocha, S.; Gomes, J.; Morais, S.; Pereira, M. C.; Coelho, M., Preservation of catechin antioxidant properties loaded in carbohydrate nanoparticles. *Carbohydrate Polymers* **2011,** *86* (1), 147-153.

62. Jafari, S. M.; Assadpoor, E.; He, Y. H.; Bhandari, B., Encapsulation efficiency of food flavours and oils during spray drying. *Dry Technol* **2008,** *26* (7), 816-835.

63. Simonelli, A. P.; Mehta, S. C.; Higuchi, W. I., Dissolution rates of high energy sulfathiazole-povidone coprecipitates II: Characterization of form of drug controlling its dissolution rate via solubility studies. *J. Pharm. Sci.* **1976,** *65* (3), 355-361.

64. Qiu, Y.; Chen, Y.; Zhang, G. G. Z.; Liu, L.; Porter, W., *Developing solid oral dosage forms: Pharmaceutical theory & practice*. First ed.; Academic Press: United States of America, 2009.

65. Chu, S.-Y.; Park, Y.; Locke, C.; Wilson, D. S.; Cavanaugh, J. C., Drug-food interaction potential of clarithromycin, a new macrolide antimicrobial. *Journal of Clinical Pharmacology* **1992,** *32*, 32-36.

66. Liu, H.; Ilevbare, G. A.; Cherniawski, B. P.; Ritchie, E. T.; Taylor, L. S.; Edgar, K. J., Synthesis and structure–property evaluation of cellulose ω-carboxyesters for amorphous solid dispersions. In *Carbohydr. Polym.*, In press. Available online 26 November 2012.

67. Ilevbare, G. A.; Liu, H.; Edgar, K. J.; Taylor, L. S., Effect of Binary Additive Combinations on Solution Crystal Growth of the Poorly Water-Soluble Drug, Ritonavir. *Crystal Growth & Design* **2012,** *12* (12), 6050-6060.

Chapter 6 **Preliminary Studies on Amorphous Solid Dispersions of Anti-HIV Drugs: Ritonavir, Efavirenz and Etravirine**

6.1 Abstract

Ritonavir (RTV), efavirenz (EFV) and etravirine (ETR) are anti-HIV drugs that have poor bioavailability. If the bioavailability of these drugs can be improved by enhancing their solution concentration, HIV treatment, which comprises the concomitant administration of multiple drugs, can become less inconvenient for patients and more affordable for use in third-world countries. Herein, amorphous solid dispersions (ASDs), macro and nanoparticles, of the 3 aforementioned drugs in the cellulosic polymer carboxymethyl cellulose acetate butyrate (CMCAB) were prepared. The RTV and EFV/CMCAB ASDs were efficient in stabilizing the drug in its amorphous form in the solid phase, as confirmed by XRD and DSC, but ETR in the CMCAB solid dispersion could not be made entirely amorphous. Other solvents that might optimize the miscibility between ETR and CMCAB were evaluated and THF was found to be a good candidate. Preliminary studies on the miscibility of these drugs with another promising cellulosic polymer, cellulose acetate adipate propionate (CAAdP) showed that clear films are formed from RTV and EFV/CAAdP THF solutions. Furthermore, RTV/CMCAB ASDs provide significant enhancement of RTV solution concentration. Solution concentration enhancement was lower for EFV/CMCAB ASDs, and ETR/CMCAB solid dispersion provided some ETR solution concentration enhancement, despite not being entirely amorphous.

6.2 Introduction

Human immunodeficiency virus (HIV) related acquired immune deficiency syndrome (AIDS) has claimed over 30 million lives since its discovery in 1981. According to 2012 figures from the United Nations Program on HIV/AIDS (UNAIDS) and the World Health Organization (WHO), about 34 million people are living with HIV in the world,[1] more than two thirds of whom live in sub-Saharan Africa. At least 2 million infected adults live in each of five countries: Ethiopia, India, Kenya, Nigeria and South Africa. In five African countries,

Botswana, Lesotho, Swaziland, Zambia and Zimbabwe, at least one in five adults has HIV or AIDS.

Based on the profound knowledge gained about the HIV replication cycle, several drug targets have been identified over the years and effective treatment options are currently available.[2] Each type of drug acts on a different stage of the HIV life-cycle, and for a more effective therapy, usually a combination of 3 or more drugs is taken. When several such drugs, typically three or four, are taken in combination, the approach is known as Highly Active Antiretroviral Therapy, or HAART.[3]

Since the majority of antiretrovirals are administered orally, their adequate systemic absorption from the gastrointestinal (GI) tract is a prerequisite for successful therapy. More than 20 drugs are currently used in combination for treatment of HIV infection, and many of them have either solubility or permeability related issues.[4] Many HIV drugs are also substrates both for metabolic enzymes (CYP3A4) and transport proteins (P-gp).[5] Consequently, oral absorption and, in turn, bioavailability is very low for many antiretroviral drugs,[6] which leads to patients having to take large pills, several pills at once, and/or at multiple times a day. The larger dose of drug required to overcome the drug's low bioavailability may also cause serious side effects to patients. Considering that HAART is a life-long treatment, HIV patients could have much better quality of life if anti-HIV drugs had higher bioavailability.

In this work, we have selected 3 anti-HIV drugs that have very low water solubility and consequently poor bioavailability: ritonavir (RTV), etravirine (ETR), and efavirenz (EFV) (**Fig 1**), which are drugs that have around 1 μg/mL to less than 10 μg/mL solubility. ETV, (brand name Intelence, formerly known as TMC125) and EFV (some brand names: Sustiva, Stocrin, and Efavir) are non-nucleoside reverse transcriptase inhibitors (NNRTIs). Both nucleoside and non-nucleoside RTIs inhibit the same target, the reverse transcriptase enzyme, an essential viral enzyme which transcribes viral RNA into DNA. RTV, with trade name Norvir (Abbott Laboratories), was first developed as a protease inhibitor, but now is rarely used for its own antiviral activity. It's used mostly as a booster of other protease inhibitors because it is effective in inhibiting a particular liver enzyme, cytochrome P450-3A4 (CYP3A4) that normally metabolizes other protease inhibitors. This inhibition leads to higher plasma concentration of

these protease inhibitor drugs, allowing for lower dose and frequency and improving clinical efficacy.

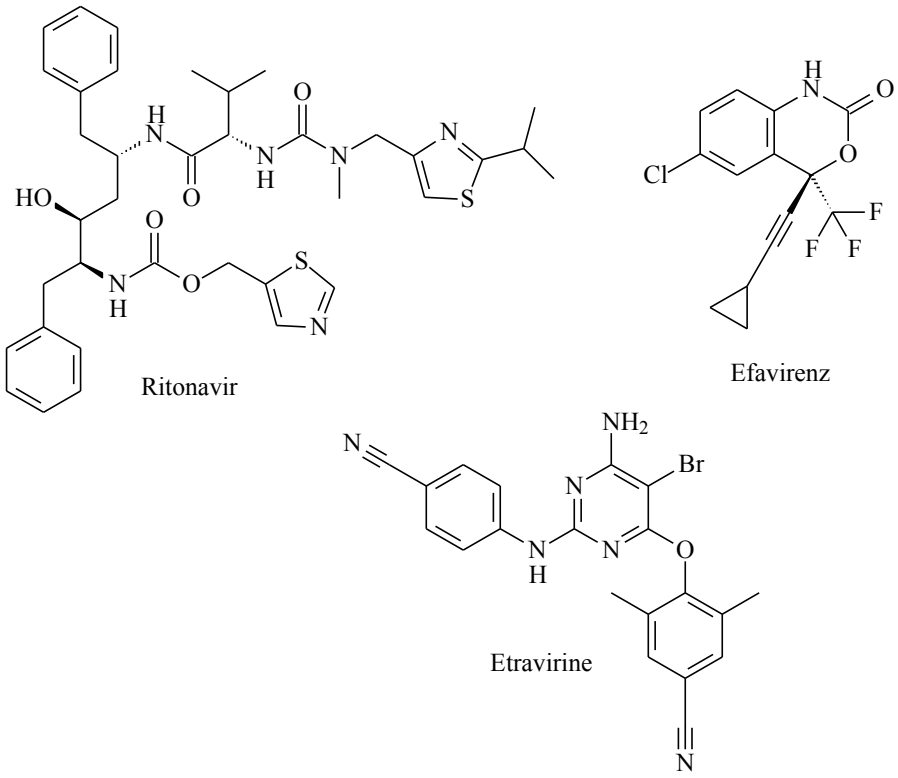

Figure 6.1 Chemical structures of ritonavir, efavirenz and etravirine

Low drug solubility and inadequate oral bioavailability have been addressed using a number of strategies; complexation with cyclodextrins,[7 8] formulation with lipid excipients,[9] conversion into a higher energy polymorph, particle size reduction,[10] or by formulation as an amorphous solid.[11] Incorporation into a solid polymer matrix can enhance solubility by trapping the drug in a metastable amorphous state, eliminating the need to disrupt the crystal lattice in order for the drug to dissolve.[12] Generation of supersaturated drug solutions from amorphous solid dispersions (ASDs) in polymer matrices represents an increasingly important approach for enhancing drug solubility and bioavailability.[13 14 15]

In this work, we prepared ASDs of the 3 aforementioned HIV drugs with carboxymethylcellulose acetate butyrate (CMCAB) (**Fig 2**), which is a cellulose ether ester that

has shown interesting properties for ASDs.[16] [16b] A preliminary study on drug miscibility with another cellulose derivative, cellulose acetate adipate propionate (CAAdP)[17] (**Fig 2**) was also performed. We hypothesized that these ASDs could strongly improve the oral bioavailability of HIV drugs by enhancing their solution concentrations. This improved bioavailability could be used to reduce dose and thus active pharmaceutical expense for key HIV drugs, enabling treatment of more third-world patients per quantity of drug manufactured.

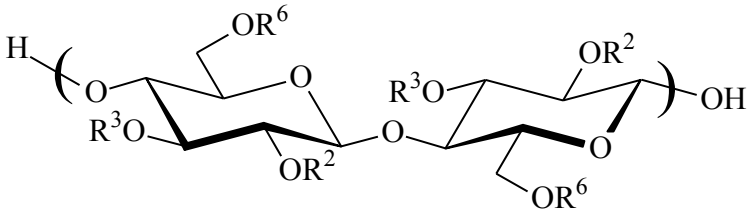

CMCAB: R^2, R^3, R^6 = H, CH_2CO_2H, $COCH_3$ or $COCH_2CH_2CH_3$

CAAdP: R = H, $COCH_3$, $CO(CH_2)_4CO_2H$, $COCH_2CH_3$

Figure 6.2 Chemical structures of CMCAB and CAAdP

6.3 Experimental

6.3.1 Materials

The drugs, efavirenz (EFV) lot # 100613, ritonavir (RTV) lot # 100601, and etravirine (ETR) lot # 110325, were purchased from Attix Pharmaceuticals in Toronto, Ontario, Canada and were used as received. Carboxymethyl cellulose acetate butyrate (CMCAB CAS 641-0.2, approximate MW 22,000, degrees of substitution (DS) (butyrate) = 1.64, DS (acetate) = 0.44, and DS (carboxymethyl) = 0.33) was obtained from Eastman Chemical Company (Kingsport, Tennessee). Cellulose acetate propionate adipate 0.85 (CAAdP, approximate MW 12,000) was synthesized from cellulose acetate propionate (CAP-504-0.2, Eastman Chemical) as previously reported[17]; and had DS (acetate) = 0.04, DS (propionate) = 2.09, and DS (adipate) = 0.33.

Acetone, tetrahydrofuran (THF), methanol and dichloromethane were HPLC-grade. Ethanol, ethyl acetate and dimethylformamide (DMF) were reagent-grade. All solvents were purchased from Fisher Scientific and used as received. Water was purified by reverse osmosis and ion exchange using the Barnstead RO pure ST (Barnstead/Thermolyne, Dubuque, IA, U.S.A.) purification system.

6.3.2 Preparation of ASDs by co-precipitation

CMCAB (450 mg) in 30 mL acetone was stirred at room temperature until the polymer was completely dissolved (approximately 1h). RTV, EFV or ETV (150 mg) was added to this solution and stirred for 10 min. The ASD particles were precipitated from the solution by co-precipitation. The acetone solution containing the dissolved polymer and drug was added drop by drop to 90 mL of water. Acetone was removed from the resulting suspension using a rotary evaporator with water bath temp at 40 °C. The aqueous solution was then freeze-dried to yield ASDs of RTV, EFV and ETR in CMCAB.

6.3.3 Preparation of nanoparticles ASDs using a multi-inlet vortex mixer

Flash nanoprecipitation[18 19 20 21] is a recently developed process for producing well-defined nanoparticles that involves rapid mixing of two or more streams to create high supersaturation of the precipitating species in the presence of an amphiphilic polymer. The high supersaturation leads to rapid nucleation and growth that is ultimately limited by a repulsive barrier that forms on the particle surface. This barrier can be steric, electrostatic, or a combination of both. This process is scalable and has been used to produce stable nanoparticles that incorporated a variety of species including drugs, imaging agents, peptides, and pesticides with controlled particle size distributions.[22 23] Importantly for our purposes, drug particles in the range of tens to the low hundreds of nanometers in diameter have been shown to be advantageous for enhancing dissolution by kinetic means,[24] providing greater relative surface area than larger particles, and larger curvature.

Herein, nanoparticles were formed using a four-jet multi-inlet vortex mixer (MIVM) that was constructed based on a previously reported design[25] in which the diameter and height of the circular mixing chamber were 5.9 mm and 1.45 mm, respectively. CMCAB (100 mg) in 20 mL THF was stirred at room temperature until the polymer was completely dissolved (approximately 30 min). RTV or EFV (33 mg) was added to this mixture and stirred for 10 min. This solution comprised the organic stream that was injected into the MIVM along with the three water streams at 25 ^{o}C. The flow rates were controlled with syringe pumps so that the total volumetric ratio of the four injected streams was 90/10 (V/V) water/THF and the Reynolds number in the mixer was 15,000.[41] The suspensions containing the nanoparticles were recovered from the MIVM and dialyzed to remove THF, free drug, and dissolved polymer molecules. The dialysis was done with 40 mL of the particles in dialysis tubing placed in a 4 L of DI water. The water was changed 4 times over a period of 24 hours. The RTV/CMCAB and EFV/CMCAB ASDs nanoparticles were then isolated by freeze-drying the resulting aqueous mixture.

6.3.4 Powder X-ray diffraction (XRD)

X-ray diffraction patterns were obtained using a Shimadzu XRD 6000 diffractometer (Shimadzu Scientific Instruments. Columbia, Maryland). The geometry of the X-ray diffractometer was the Bragg Brentano parafocusing. The instrument was calibrated using a silicon standard which has a characteristic peak at 28.44^{o} 2θ. The X-ray tube consisted of a target material made of copper (Cu), which emits K_{α} radiation with a power rating of 2,200 Watts and accelerating potential of 60 kV. Experiments were performed using a 40 kV accelerating potential and current of 40 mA. Divergence and scattering slits were set at 1.0 mm and the receiving slit at 10 iris. The experiments were conducted with a scan range from 10 to 50^{o} 2θ. Scanning speed was 1º/min.

6.3.5 Differential scanning calorimetry (DSC)

Differential scanning calorimetry analysis was performed using a TA Instruments Q2000 (TA Instruments, New Castle, DE) attached to a refrigerated cooling accessory. Powders (3-8 mg) were loaded in aluminum T-zero pans. Dry N_2 was used as the purge gas at 50 mL/min. All analyses were performed using a heat/cool/heat procedure. Samples were heated to 100 °C at 20 °C/min, cooled to 25 °C at 100°C/min and heated again to 200 °C at 20 °C/min. Glass transition temperatures (T_g) were determined from second heat scans. The data was analyzed using the Universal Analysis 2000 software for Windows 2000/XP provided with the instrument.

6.3.6 Quantification of HIV drugs by high-performance liquid chromatography with diode-array detection (HPLC-DAD)

The HPLC system was an Agilent 1200 Series consisting of a quaternary pump, online degasser, autosampler, and Agilent chemstation LC 3D software. Chromatography was conducted in reversed phase mode using an Eclipse XDB-C18 column (4.6 x 150 mm ID, particle size 5 μm). Detection was by a DAD detector at 240 nm. The mobile phase consisted of acetonitrile and phosphate buffer (0.05M, pH 5.65). A concentration gradient was programmed; the proportion of acetonitrile stayed at 40% for 1 min, was raised to 60% in 14 min, was reduced back to 40% in 1 min and stayed at 40% for 4 min. Total analysis time was 20 min. The mobile phase was delivered at a flow rate of 1.5 mL/min and the column temperature was maintained at 30 ^{o}C. Sample injection volume was 5 μL.

6.3.7 Calculation of drug loaded in the ASDs particles

Drug loading is expressed as weight percent drug in the polymer matrix. To calculate drug loading, a 10 mg particle sample was dissolved in 10 mL acetonitrile and the concentration of drug was measured by HPLC as described in section 2.6.

6.3.8 *In-vitro* drug release of anti-HIV drugs from ASDs

Dissolution profiles of drugs from ASD particles were compared with those of free drugs. The apparatus used in the dissolution experiments consisted of 250-mL jacketed flasks with circulating ethylene glycol/water (1:1) to control the temperature at 37 °C. Dissolution experiments with the ASDs were performed with initial amount of drug of approximately 25 mg.

Dissolution medium (80 mL 0.05 M potassium phosphate buffer, pH 6.8) was continuously magnetically stirred (37 °C, 200 rpm). Aliquots (0.5 mL) were withdrawn from the suspension every 0.5 h (during the first 2 h), then every hour for 8 h. Phosphate buffer (0.5 mL) was added to maintain constant volume after each aliquot was withdrawn. Each aliquot supernatant was separated from excess solid in solution by ultracentrifugation at 13,000 rpm for 10 minutes. The supernatant was recovered, and drug concentration was determined by HPLC as previously described (section 2.6). ASD dissolution profiles were presented as concentration of drug in solution vs. time.

6.3.9 Preparation of ETR/CMCAB films from different solvents

CMCAB (15 mg) was dissolved in the respective organic solvent (approximately 0.5 mL) in a glass vial, ETR (5 mg) was added to this solution and the mixture was subjected to vortex mixing for 3 min. Films of each solution were cast onto Teflon coated glass plates and allowed to dry at room temperature in a desiccator.

6.3.10 Preparation of CAAdP/drug films

CAAdP (15 mg) was dissolved in acetone or THF (approximately 0.5 mL) in a glass vial; RTV, EFV or ETR (5 mg) was added to this solution and the mixture was subjected to vortex mixing for 3 min. Films of each acetone or THF solution were cast onto Teflon coated glass plates and allowed to dry at room temperature in a desiccator.

6.4 Results and Discussion

6.4.1 Characterization of amorphous solid dispersions

ASDs of EFV, RTV and ETR with CMCAB at 25% drug loading were prepared by spray-drying. Furthermore, we chose to test the hypothesis about the potentially synergistic effects of creating ASDs of drug in polymer to reduce crystallinity, and creating those dispersion particles at nanometer-scale diameters, by comparing spray-dried macroparticles of EFV and RTV in CMCAB with nanoparticles prepared using the MIVM. We then evaluated the ability of those polymers to stabilize these drugs against crystallization in the solid phase by looking at the solid state properties of each drug in the ASD particles by XRD and DSC.

Crystallinity of each drug/polymer ASD was investigated by XRD. An overlay of the XRD diffraction patterns of crystalline RTV, EFV, ETR, and the spray-dried ASDs is shown in **Fig 3a-c** for illustration. As represented in **Fig 3a-b**, crystalline RTV and EFV show characteristic diffraction peaks, while the ASDs showed no diffraction peaks, instead displaying an amorphous halo, which confirms that RTV and EFV can be made amorphous by preparing ASDs in CMCAB at 25% drug loading. The nanoparticle samples of RTV/CMCAB and EFV/CMCAB ASDs, prepared using the MIVM, showed similar results as the spray-dried samples (results not shown).[26] For ETR/CMCAB ASD, the XRD spectrum **(Fig 3c)** shows characteristic crystalline ETR diffraction peaks, which indicates that some ETR is still present as crystals within the ASD.

Overall, these data clearly show that it is possible to make both micron and nanometer-sized particles of RTV and EFV ASD with CMCAB in which the drug is amorphous, confirming strong polymer-drug interaction in the solid phase. However, the current experimental conditions used in the preparation of ETR/CMCAB ASD didn't provide solid dispersions with entirely amorphous ETR.

a)

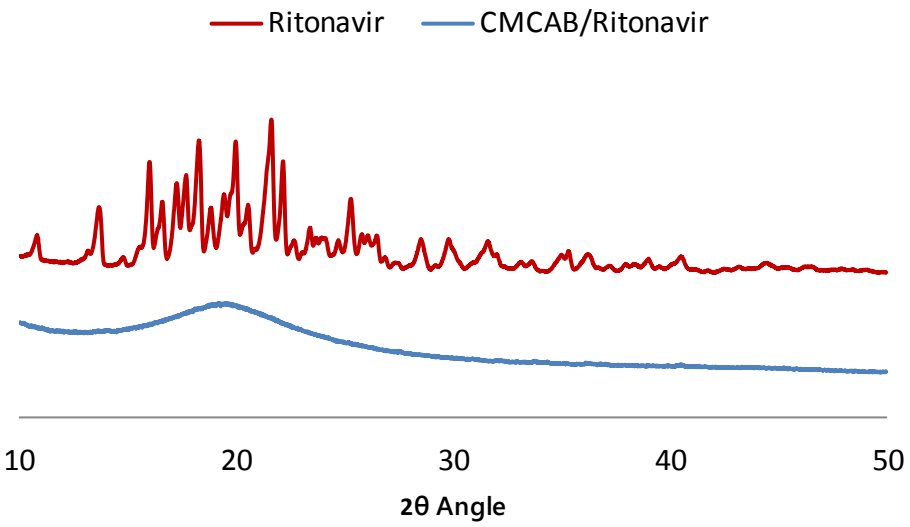
Ritonavir
CMCAB/Ritonavir
10
20
30
40
50
2θ Angle

b)

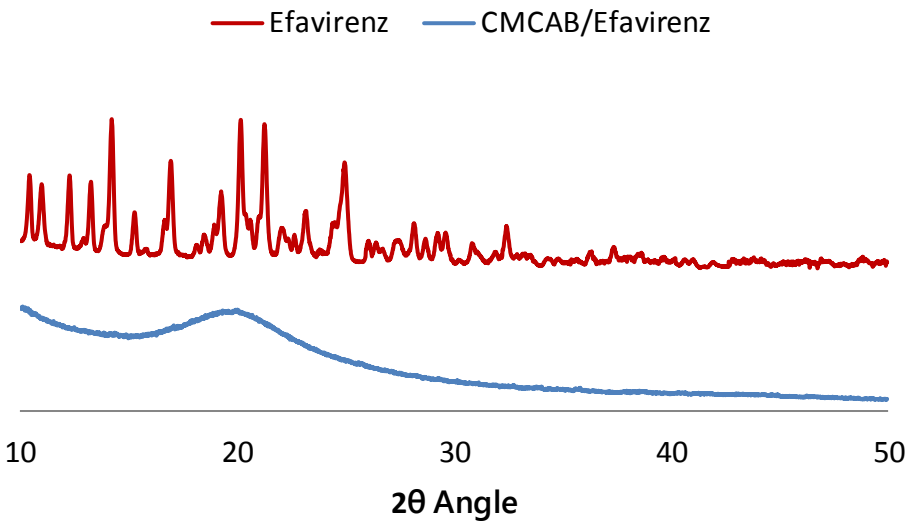
Efavirenz
CMCAB/Efavirenz
10
20
30
40
50
2θ Angle

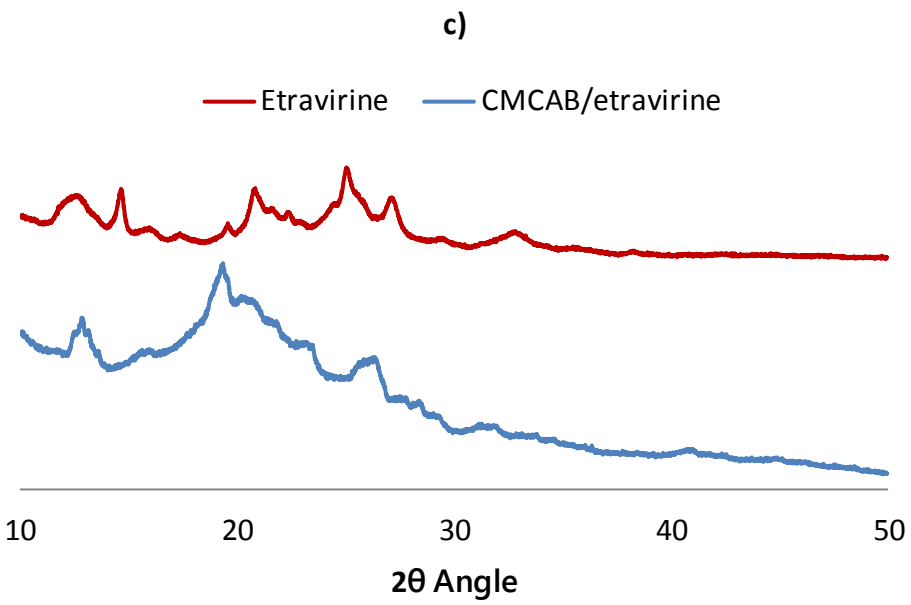

Figure 6.3 X-ray diffraction spectra of spray-dried ASDs: (a) RTV/CMCAB, (b) EFV/CMCAB and (c) ETR/CMCAB, in comparison with crystalline RTV, EFV and ETR respectively

DSC Analysis was performed in all ASDs to confirm the presence of amorphous drug and also polymer/drug miscibility in the ASDs.

One important factor to consider when producing and choosing polymers for amorphous solid dispersions is miscibility, which is the ability to produce a homogeneous single phase where the components are intimately mixed at a molecular level.[27] A miscible amorphous solid dispersion typically has a single T_g, which is lower compared to that of the polymer due to the plasticizing effect of the small molecule drug. Entrapment of the drug in the polymer matrix results in lower drug molecular mobility and may prevent crystallization.

We include the DSC thermograms for crystalline RTV, EFV and ETR, CMCAB and spray-dried samples for illustration (**Fig 4a-c**). DSC thermograms for RTV/CMCAB and CMCAB EFV nanoparticles are not shown here (see this Ref).[26] **Fig 4a-b** shows the absence of melting peaks near 121 and 137 °C for RTV and EFV, respectively, in the polymer dispersions, which indicates that no crystalline drug is present in these ASDs. Moreover, T_g values intermediate between those of amorphous RTV (50 °C)[28] and EFV (33 °C)[29] and that of CMCAB (142 °C) are observed for the ASDs. This is an explicit indication of homogeneous dispersion of

drug within the polymer matrix. The experimental T_g values of RTV/CMCAB and EFV/CMCAB ASDs, micro and nanoparticles, are in good agreement with those calculated using the Fox equation (predicted T_g) (**Table 1**). The T_g found for ETR/CMCAB ASD (**Fig 4c**) is very similar to the T_g of CMCAB, which suggests poor drug/polymer miscibility and therefore, that ETR is not entirely amorphous within the solid dispersion. The difference between T_g values, experimental and calculated using the Fox equation, was in fact significant (**Table 1**) for ETR/CMCAB solid dispersions. The presence of an endothermic peak near 263 °C, the melting temperature of ETR, would confirm the presence of ETR crystals in the ASD, but DSC analysis could not be performed above 200 °C. DSC analysis of polysaccharides containing both pendant carboxyl and hydroxyl groups such as CMCAB should be conducted at temperatures below 200 °C, since above this temperature, crosslinking esterification reactions start to occur. Moreover, the suggested poor drug/polymer miscibility by DSC is in agreement with the XRD results for ETR/CMCAB, which shows characteristic diffraction peaks for crystalline ETR.

a)

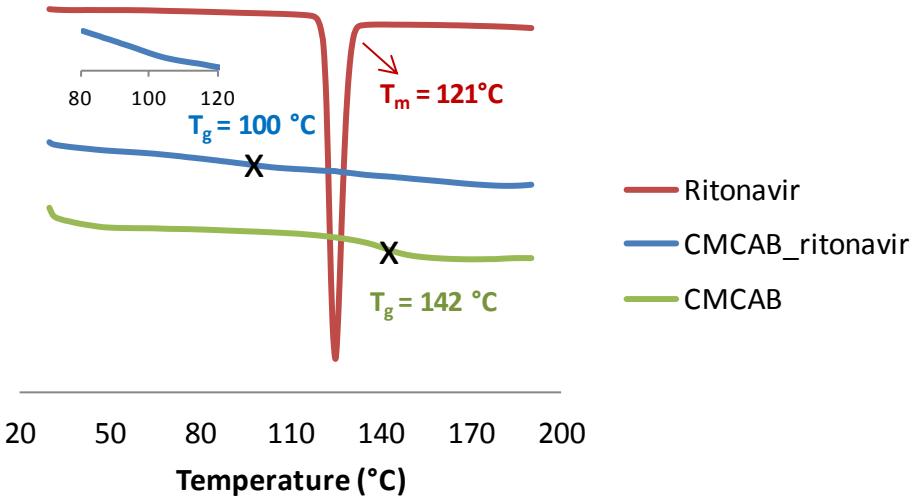
80
100
120
T_m = 121°C
T_g = 100 °C
T_g = 142 °C
Ritonavir
CMCAB_ritonavir
CMCAB
20
50
80
110
140
170
200
Temperature (°C)

b)

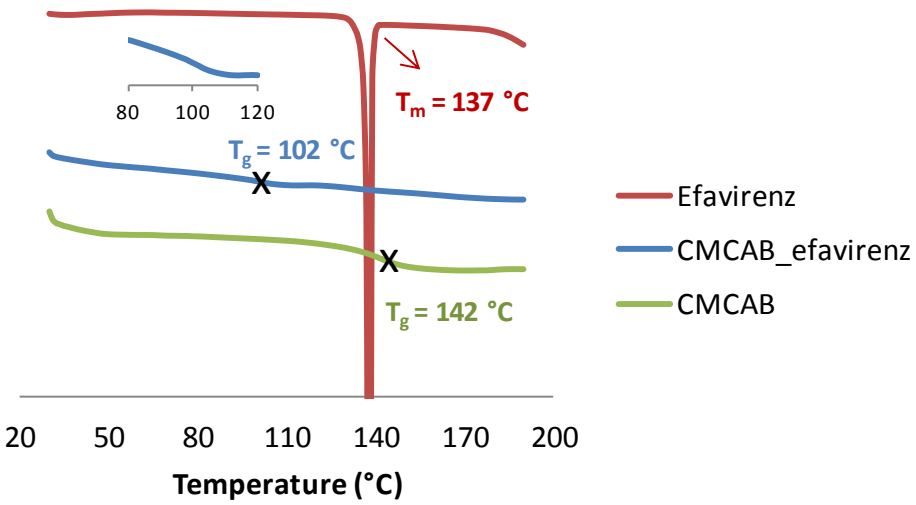
80
100
120
T_m = 137 °C
T_g = 102 °C
T_g = 142 °C
Efavirenz
CMCAB_efavirenz
CMCAB
20
50
80
110
140
170
200
Temperature (°C)

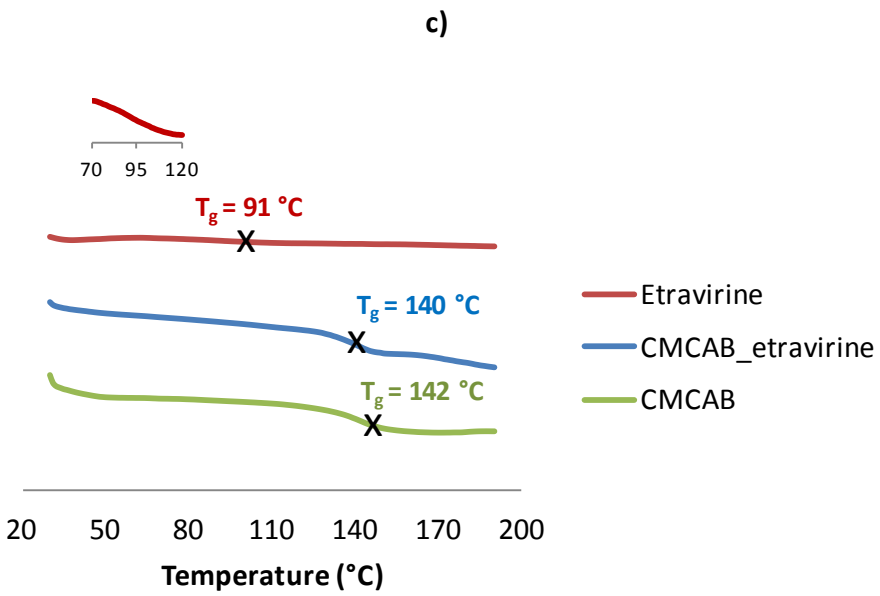

Figure 6.4 DSC thermograms of (a) RTV/CMCAB, (b) EFV/CMCAB and (c) ETR/CMCAB ASDs, in comparison with crystalline RTV, EFV and ETR respectively.

Table 6.1 T_g of ASDs - experimental vs. predicted by Fox equation

	Experimental T_g (°C)	Predicted T_g (°C)
RTV	50	--
EFV	37	--
ETR	91	--
RTV/CMCAB Spray-dried	100	97.3
EFV/CMCAB Spray-dried	94	83
ETR/CMCAB Spray-dried	140	97.6
RTV/CMCAB Nanoparticles	91	105.2
EFV/CMCAB Nanoparticles	99	92.2

Overall, these results show that effective drug-polymer interaction is present in RTV and EFV ASDs leading to miscibility, as indicated by the presence of a single T_g. Furthermore, T_g values of these ASDs exceed likely maximum ambient temperatures (40-50 ºC) by about 50 °C, providing a window that should be more than adequate protection against high ambient humidity and temperature during transport and storage (all ASDs studied showed T_g higher than 90 ºC).

Drug loading of ASD particles was measured by HPLC. High drug incorporation into the polymer matrices was achieved. For the 25% targeted drug loading spray-dried microparticles, RTV/CMCAB, EFV/CMCAB and ETR/CMCAB, actual drug loading ranged from 24.2 to 24.7 %, resulting in a loading efficiency of about 98%. For the 25% targeted drug loading RTV/CMCAB and EFV/CMCAB nanoparticles, the actual value was 19% for the both samples, resulting in a loading efficiency of 75%.

6.4.2 Release profile of anti-HIV drugs from CMCAB ASDs

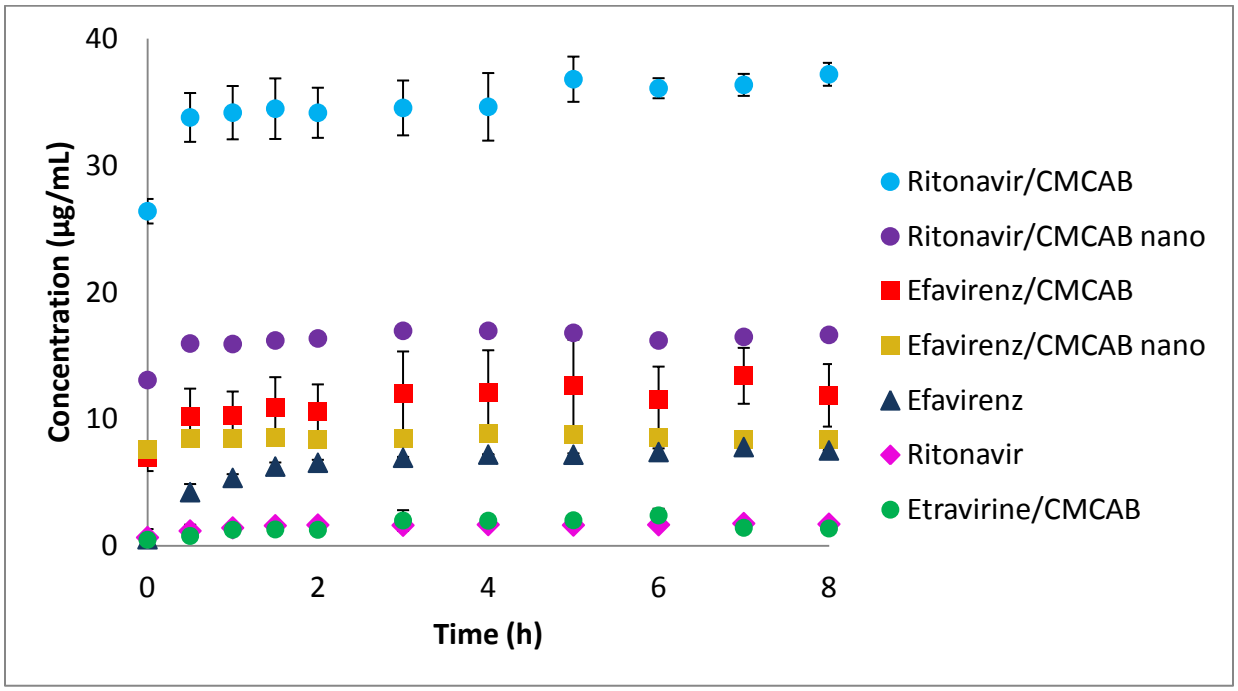

Figure 6.5 Dissolution profiles of anti-HIV drugs ASDs at pH 6.8 buffer. Each point is an average of 3 experiments, and error bars indicate one standard deviation with the exception of nanoparticle ASDs, for which only one experiment was performed due to limited sample availability.

The results from these dissolution experiments showed enhancement of solution concentration from the RTV/CMCAB nanoparticle ASD **(Fig 5)**, generating a substantial, stable level of supersaturation. No significant enhancement of solution concentration was achieved for

EFV/CMCAB nanoparticle ASD. Moreover, spray-dried macroparticles of the ASDs generated higher supersaturation. Interestingly, for the less soluble drug RTV, the macroparticulate RTV/CMCAB ASD affords the highest supersaturation, furnishing more than 20-fold increase in solution concentration, versus 10-fold for RTV/CMCAB nanoparticles. EFV/CMCAB ASD afforded less significant enhancement of solution concentration (1.74-fold increase for microparticles versus 1.28-fold for nanoparticles). Both micro and nanoparticles of RTV/CMCAB and EFV/CMCAB release drugs rapidly in the first 30 min, reaching solution concentrations that remain constant over the remainder of the 8h experiment. **Fig 5** also shows the dissolution profile of ETR/CMCAB solid dispersion particles. The solution concentration of free ETR is not shown for comparison because it is very low and below the detection limit of the HPLC method (1 μg/mL). However, as ETR in solution could be detected from the solid dispersion particles, we can presume that this dispersion provided an enhancement of ETR solution concentration, although its quantification was not possible. Note that although this sample didn't show entirely amorphous ETR within the solid dispersion, it still provided an enhancement in ETR solution concentration.

6.4.3 Evaluation of ETR/CMCAB film from different solvents

Initially, we prepared ETR/CMCAB solid dispersion by dissolving CMCAB and ETR in acetone and precipitating this solution in water. However, the resulting ETR/CMCAB solid dispersion was not entirely amorphous as shown by DSC and XRD (**Fig 3c, Fig 4c**). Different solvents were then tested for their compatibility with ETR and CMCAB. Drug and polymer were dissolved in minimal amount of organic solvent and a film was cast from this solution. The film cast from THF ETR/CMCAB solution was transparent, thus THF is considered a potentially good solvent for dissolving ETR and CMCAB in order to improve ETR and CMCAB miscibility and prepare ASD particles.

Table 6.2 Evaluation of ETR/CMCAB films cast from different solvents

Solvents	Transparent	Translucent	Cloudy
Acetone			X
Methanol			X
Ethanol			X
Dichloromethane/Ethanol (8/2 V/V)			X
THF	X		
Ethyl Acetate		X	
DMF/Methanol (8/2 V/V)		X	

6.4.4 Evaluation of CAAdP/drug films

We have tested a different polymer, CAAdP, for its potential to form ASDs with the three anti-HIV drugs studied. Films were cast for each drug/CAAdP combination dissolved in acetone or THF, and evaluated for their transparency. The resulting RTV, EFV and ETR films cast from acetone solutions were cloudy. The RTV/CAAdP and EFV/CAAdP films cast from THF were transparent, which indicates that THF is a potential solvent to form ASDs in CAAdP with these two drugs. ETR/CAAdP film cast from THF was translucent; therefore THF may not be a good solvent for forming ETR/CAAdP solid dispersions. Other solvents need to be investigated that can provide better miscibility between ETR and CAAdP.

Table 6.3 Evaluation of drug/CAAdP films

Films	Acetone	THF
RTV/CAAdP	Cloudy	Transparent
EFV/CAAdP	Cloudy	Transparent
ETR/CAAdP	Cloudy	Translucent

6.5 Conclusions

We have demonstrated herein that both nanoparticle and microparticle ASDs of the anti-HIV drugs, RTV and EFV with the cellulosic polymer CMCAB are capable of stabilizing the

drug in its amorphous form in the solid phase, as confirmed by XRD and DSC. Furthermore, RTV/CMCAB ASDs provide significant enhancement of RTV solution concentration; a 20-fold increase for spray-dried microparticles versus 10-fold for amorphous nanoparticles. Solution concentration enhancement was lower for EFV/CMCAB ASDs (1.74-fold increase for spray-dried microparticles versus 1.28-fold for nanoparticles). These preliminary results are a great motivation for further studies regarding the development of ASDs of anti-HIV drugs with other cellulose derivatives.[30] [31] As we have also shown in this study, clear films were formed from solutions of RTV and EFV with the cellulose derivative CAAdP,[17] which is a promising polymer for ASD applications.[32] The formation of a clear polymer/drug film usually translates into successful spray-dried ASDs particles.[33] The dissolution profiles of these drugs can be improved depending upon the polymer selected. By extending these structure-property studies to structurally related cellulosic polymers (e.g., cellulose acetate suberate and cellulose acetate sebacate),[30] we can learn how to best apply these ASDs and what are the different polymer properties that are needed to achieve ASDs with optimal performance for specific applications. ETR/CMCAB solid dispersions could not be made entirely amorphous; they showed the continued presence of crystalline ETR by XRD and DSC, but still the solid dispersion provided some ETR solution concentration enhancement. We began the evaluation of other solvents that might optimize the miscibility between ETR and CMCAB, and consequently lead to successful ETR/CMCAB ASDs. A clear film was achieved from ETR/CMCAB THF solution, indicating that ASDs will potentially be formed from spray-drying ETR/CMCAB THF solution. We have also produced films of ETR with CAAdP, which has demonstrated outstanding performance in the formulation of ASDs with a variety of actives,[34] [35] [36] CAAdP is a promising polymer for ASD of ETR.

6.6 References

1. World Health Organization (WHO) http://www.who.int/gho/hiv/en/ (accessed 07/19/13).

2. De Clercq, E., The history of antiretrovirals: key discoveries over the past 25 years. *Reviews in Medical Virology* **2009,** *19* (5), 287-299.

3. Flexner, C., HIV drug development: the next 25 years. *Nature Reviews Drug Discovery* **2007,** *6* (12), 959-966.

4. Amidon, G. L.; Lennernas, H.; Shah, V. P.; Crison, J. R., A theoretical basis for a biopharmaceutic drug classification - The correlation of *in-vitro* drug product dissolution and *in-vivo* bioavailability. *Pharmaceutical Research* **1995,** *12* (3), 413-420.

5. Aungst, B. J., P-glycoprotein, secretory transport, and other barriers to the oral delivery of anti-HIV drugs. *Advanced Drug Delivery Reviews* **1999,** *39* (1-3), 105-116.

6. Williams, G. C.; Sinko, P. J., Oral absorption of the HIV protease inhibitors: A current update. *Advanced Drug Delivery Reviews* **1999,** *39* (1-3), 211-238.

7. Barone, J. A.; Moskovitz, B. L.; Guarnieri, J.; Hassell, A. E.; Colaizzi, J. L.; Bierman, R. H.; Jessen, L., Enhanced bioavailability of itraconazole in hydroxypropyl-beta-cyclodextrin solution versus capsules in healthy volunteers. *Antimicrob. Agents Chemother.* **1998,** *42* (7), 1862-1865.

8. Buchanan, C. M.; Buchanan, N. L.; Edgar, K. J.; Little, J. L.; Malcolm, M. O.; Ruble, K. M.; Wacher, V. J.; Wempe, M. F., Pharmacokinetics of tamoxifen after intravenous and oral dosing of tamoxifen–hydroxybutenyl-β-cyclodextrin formulations. *Journal of Pharmaceutical Sciences* **2007,** *96* (3), 644-660.

9. Constantinides, P. P.; Han, J. H.; Davis, S. S., Advances in the use of tocols as drug delivery vehicles. *Pharmaceutical Research* **2006,** *23* (2), 243-255.

10. Merisko-Liversidge, E.; Liversidge, G. G.; Cooper, E. R., Nanosizing: a formulation approach for poorly-water-soluble compounds. *Eur J Pharm Sci* **2003,** *18* (2), 113-20.

11. Murdande, S. B.; Pikal, M. J.; Shanker, R. M.; Bogner, R. H., Solubility Advantage of Amorphous Pharmaceuticals: I. A Thermodynamic Analysis. *J Pharm Sci-Us* **2010,** *99* (3), 1254-1264.

12. Singhal, D.; Curatolo, W., Drug polymorphism and dosage form design: a practical perspective. *Advanced Drug Delivery Reviews* **2004,** *56* (3), 335-347.

13. Leuner, C.; Dressman, J., Improving drug solubility for oral delivery using solid dispersions. *Eur. J. Pharm. Biopharm.* **2000,** *50* (1), 47-60.

14. Kwong, A. D.; Kauffman, R. S.; Hurter, P.; Mueller, P., Discovery and development of telaprevir: an NS3-4A protease inhibitor for treating genotype 1 chronic hepatitis C virus. *Nature Biotechnology* **2011,** *29* (11), 993-1003.

15. DiNunzio, J. C.; Miller, D. A.; Yang, W.; McGinity, J. W.; Williams, R. O., Amorphous compositions using concentration enhancing polymers for improved bioavailability of itraconazole. *Molecular Pharmaceutics* **2008,** *5* (6), 968-980.

16. (a) Posey-Dowty, J. D.; Seo, K. S.; Walker, K. R.; Wilson, A. K., Carboxymethylcellulose acetate butyrate in water-based automotive paints. *Surface Coatings International Part B-Coatings Transactions* **2002,** *85* (3), 203-208; (b) Posey-Dowty, J. D.; Watterson, T. L.; Wilson, A. K.; Edgar, K. J.; Shelton, M. C.; Lingerfelt, L. R., Zero-order release formulations using a novel cellulose ester. *Cellulose* **2007,** *14* (1), 73-83.

17. Liu, H.; Kar, N.; Edgar, K. J., Direct synthesis of cellulose adipate derivatives using adipic anhydride. *Cellulose* **2012,** *19* (4), 1279-1293.

18. Johnson, B. K.; Prud'homme, R. K., Chemical processing and micromixing in confined impinging jets. *AIChE Journal* **2003,** *49* (9), 2264-2282.

19. Johnson, B. K.; Prud'homme, R. K., Mechanism for rapid self-assembly of block copolymer nanoparticles. *Physical Review Letters* **2003,** *91*, 118302-1-118302-4.

20. Johnson, B. K.; Prud'homme, R. K., Flash NanoPrecipitation of Organic Actives and Block Copolymers using a Confined Impinging Jets Mixer. *Australian Journal of Chemistry* **2003,** *56* (10), 1021-1024.

21. Liu, Y.; Kathan, K.; Saad, W.; Prud'homme, R. K., Ostwald ripening of β-carotene nanoparticles. *Physical Review Letters* **2007,** *98* (3), 036102-1-036102-4.

22. Gindy, M. E.; Ji, S.; Hoye, T. R.; Panagiotopoulos, A. Z.; Prud'homme, R. K., Preparation of Poly(ethylene glycol) Protected Nanoparticles with Variable Bioconjugate Ligand Density. *Biomacromolecules* **2008,** *9* (10), 2705-2711.

23. Gindy, M. E.; Panagiotopoulos, A. Z.; Prud'homme, R. K., Composite Block Copolymer Stabilized Nanoparticles: Simultaneous Encapsulation of Organic Actives and Inorganic Nanostructures. *Langmuir* **2007,** *24* (1), 83-90.

24. Merisko-Liversidge, E.; Liversidge, G. G.; Cooper, E. R., Nanosizing: a formulation approach for poorly-water-soluble compounds. *European Journal of Pharmaceutical Sciences* **2003,** *18* (2), 113-120.

25. Liu, Y.; Cheng, C.; Liu, Y.; Prud'homme, R. K.; Fox, R. O., Mixing in a multi-inlet vortex mixer (MIVM) for flash nano-precipitation. *Chem. Eng. Sci.* **2008,** *63* (11), 2829-2842.

26. Mazumder, S. Synthesis and characterization of drug-containing, polysaccharide-based nanoparticles for applications in oral drug delivery. Virginia Polytechnic and State University 2013.

27. Qiu, Y.; Chen, Y.; Zhang, G. G. Z.; Liu, L.; Porter, W., *Developing solid oral dosage forms: Pharmaceutical theory & practice*. First ed.; Academic Press: United States of America, 2009.

28. Zhou, D. L.; Grant, D. J. W.; Zhang, G. G. Z.; Law, D.; Schmitt, E. A., A calorimetric investigation of thermodynamic and molecular mobility contributions to the physical stability of two pharmaceutical glasses. *Journal of Pharmaceutical Sciences* **2007,** *96* (1), 71-83.

29. Yang, J.; Grey, K.; Doney, J., An improved kinetics approach to describe the physical stability of amorphous solid dispersions. *International Journal of Pharmaceutics* **2010,** *384* (1-2), 24-31.

30. Liu, H.; Ilevbare, G. A.; Cherniawski, B. P.; Ritchie, E. T.; Taylor, L. S.; Edgar, K. J., Synthesis and structure–property evaluation of cellulose ω-carboxyesters for amorphous solid dispersions. In *Carbohydr. Polym.*, In press. Available online 26 November 2012, 2013.

31. Ilevbare, G. A.; Liu, H.; Edgar, K. J.; Taylor, L. S., Understanding polymer properties important for crystal growth inhibition-impact of chemically diverse polymers on solution crystal growth of ritonavir. *Crystal Growth & Design* **2012,** *12* (6), 3133-3143.

32. Ilevbare, G. A.; Liu, H.; Edgar, K. J.; Taylor, L. S., Inhibition of solution crystal growth of ritonavir by cellulose polymers - factors influencing polymer effectiveness. *Crystengcomm* **2012,** *14* (20), 6503-6514.

33. Marks, J.; Wegiel, L.; Taylor, L. S.; Edgar, K. J., Pairwise polymer blends for oral drug delivery Unpublished work, 2013.

34. Li, B.; Harich, K.; Wegiel, L.; Taylor, L. S.; Edgar, K. J., Stability and solubility enhancement of ellagic acid in cellulose ester solid dispersions. *Carbohydrate Polymers* **2013,** *92* (2), 1443-1450.

35. Li, B.; Konecke, S.; Harich, K.; Wegiel, L.; Taylor, L. S.; Edgar, K. J., Solid dispersion of quercetin in cellulose derivative matrices influences both solubility and stability. *Carbohydrate Polymers* **2013,** *92* (2), 2033-2040.

36. Pereira, J. M.; Mejia-Ariza, R.; Edgar, K. J.; Davis, R. M.; Sriranganathan, N.; Taylor, L. S.; Ilevbare, G. A.; McGettigan, H., Interplay of degradation, dissolution and stabilization of clarithromycin and its amorphous solid dispersions. Unpublished work, 2013.

Chapter 7 **Summary and Future Work**

7.1 Synthesis of Amphiphilic 6-Carboxypullulan Ethers

Pullulan is a non-ionic water-soluble polysaccharide.[1] Most pullulan modifications are intended to reduce its water solubility or to introduce charged or reactive groups for functionality.[2] [3] [4] Hydrophobically modified polysaccharides that contain carboxyl groups possess exceptional features for drug delivery and other applications.[5] [6]

In **Chapter 3**, we synthesized amphiphilic 6-carboxypullulan ethers in 2 steps from pullulan (**Fig 7.1**). Carboxyl groups were first regioselectively introduced at C-6 in the pullulan backbone by applying the selective TEMPO oxidation.[7] The oxidized product, 6-carboxypullulan, is even more water-soluble than pullulan. Consequently, further chemical modifications are mainly restricted to reactions that can be performed in water or under heterogeneous conditions. For example, reaction of 6-carboxypullulan with alkyl halides in water is not possible, due to the poor solubility of the alkyl halides in this solvent and to side reactions of the same with water. This problem was circumvented when we discovered that the TBA salt of 6-carboxypullulan is soluble in a range of organic solvents. As a result, the TBA salt of 6-carboxypullulan was reacted homogeneously with various alkyl halides in DMSO and sodium hydroxide at 40 °C to yield 6-carboxypullulan ethers with partial to complete substitution at the 2-, 3-, and 4-OH groups, depending on stoichiometry and reaction conditions.

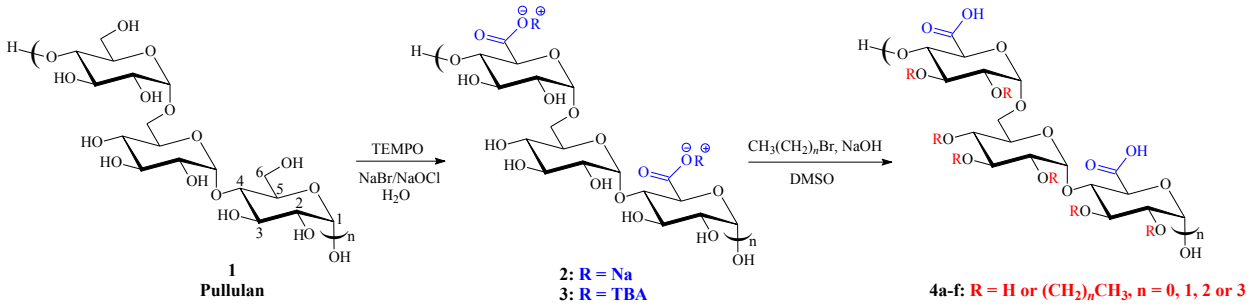

Figure 7.1 Pullulan oxidation and synthesis of 6-carboxypullulan ethers

Thus we have demonstrated that we can append hydrophilic groups on one side of the molecule at C-6 and hydrophobic ether groups on the opposite side at the 2-, 3- and 4-OH positions, creating a potentially amphiphilic molecule. In fact, we found that these carboxypullulan ethers are remarkably potent surfactants. Critical micelle concentration (CMC) for the propyl ether of 6-carboxypullulan, for example, is ca. 7 μg/mL; for comparison, the Pluronics PEO/PPO copolymeric surfactants (non-renewable and non-biodegradable) have CMC values ranging from 4-10,000 μg/mL.[8]

We have not yet successfully measured the molecular weight of the 6-carboxypullulan ethers because of their strong tendency to self-aggregate in all solvents tested. For future work with these 6-carboxypullulan ethers, it will be important to find suitable conditions to measure their molecular weight.

It is also of interest to also study ester derivatives of 6-carboxypullulan. Study of both pullulan ethers and esters is motivated by potential differences in biodegradability. Such esters would be fully biodegradable, degrading by ester hydrolysis reactions.

We have attempted the synthesis of 6-carboxypullulan esters. Esterification of 6-carboxypullulan with acetyl chloride and propionyl chloride furnished 6-carboxypullulan acetate and 6-carboxypullulan propionate respectively, but these products were not soluble in any common organic solvent. The structures of the compounds were then confirmed by solid state ^{13}C NMR. The possibility that esterification with a long alkyl chain or a mixed-ester of the 6-carboxypullulan would provide less regular and consequently more soluble products prompted us to prepare 6-carboxypullulan octanoate and 6-carboxypullulan acetate propionate respectively. But again insolubility was a hurdle in both cases. We believe that the insolubility of 6-carboxypullulan esters is due to formation of crosslinked products. The carboxylic acid groups in the backbone of 6-carboxypullulan can react with the acyl chloride and form mixed anhydrides that can further react with a hydroxyl from another pullulan molecule and form a crosslinked pullulan structure (**Fig7.2**).

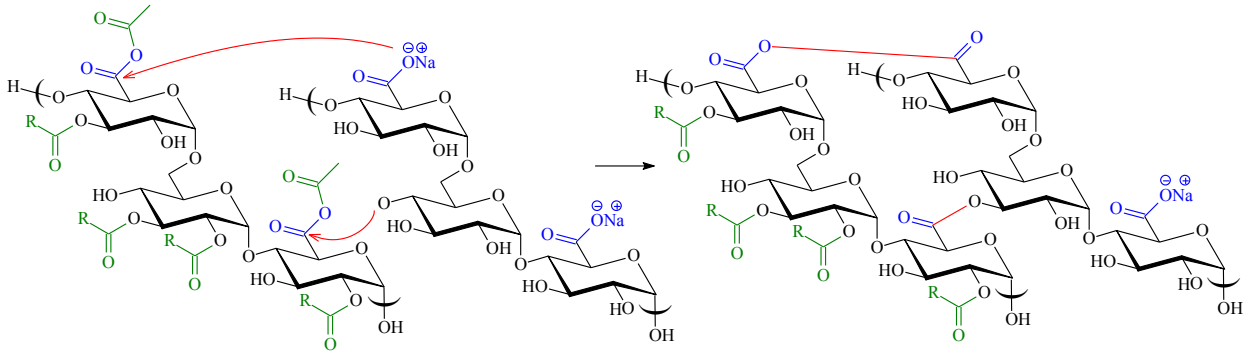

Figure 7.2 Mechanism for crosslinking during esterification of 6-carboxypullulan

It will be important to confirm and eventually circumvent this crosslinking. One approach for the synthesis of 6-carboxypullulane esters would be by first protecting the carboxyl moieties in the starting material with benzyl groups for example, and then follow with the esterification reaction. Finally, deprotection of the benzyl ester can be readily achieved by hydrogenolysis.

The ability to design these benign new surfactants, and make them in a couple of simple steps from renewable polysaccharides, affords exciting new possibilities for use of nanodispersions in bioactive delivery and many other important, demanding applications. Future direction of this work will be to explore the structure-property relationships of these promising surfactants. After developing general synthetic methods for preparation of regioselectively substituted, amphiphilic pullulan esters and ethers, it will be of interest to extend this methodology to obtain a collection of designed amphiphiles based on other polysaccharides, such as cellulose, amylose, pullulan and curdlan to explore the structure-property relationships of these surfactants. These polysaccharides have different extents of flexibility and supramolecular structures; by looking into amphiphiles from rigid rod cellulose, to helical amylose[9] and curdlan[10] (triple helix), to more random coil pullulan[11], it should be possible to obtain deep insights into the influence of solution conformation upon surfactant ability and solubilization potential, while gaining the ability to design even more effective surfactants. Another approach to be pursued will be the regioselective substitution of other hydrophilic/hydrophobic moieties in the anhydroglucose ring, and investigate how substitution will influence key surfactant properties, such as potency, degradability, and ability to solubilize key model drugs,

nutraceuticals, and agrichemicals. These investigations will bring deep insight on how to best develop surfactants with superior performance.

7.2 Regioselectively Modified Pullulan Derivatives Containing Amine and Amide Groups: Potential for Biomedical Applications

New regioselectively modified pullulan derivatives containing amine or amide groups were synthesized. These chemical groups are known to play a fundamental role in the biological activity of important polysaccharides, such as chitin and chitosan. The synthesis began with the bromination of pullulan at C-6 with NBS and Ph_3P to obtain 6-bromo-6-deoxy-pullulan (**Fig 7.3**). This reaction was successfully performed in DMF/LiBr, without the need for any previous dissolution procedure. This is the first time that the bromination of pullulan has been described. In contrast to 6-bromo-6-deoxy-cellulose, brominated pullulan was found to have good organic solubility, which allows for further chemical modification to be performed homogeneously in a range of organic solvents. Hence, esterification of the remaining hydroxyl groups homogeneously in DMF furnished 6-bromo-6-deoxy-pullulan esters (**2**). These compounds were reacted with NaN_3 to yield the corresponding 6-azido-6-deoxy-pullulan esters (**3**). The reaction of an azido compound with PPh_3 yields a versatile iminophosphorane intermediate (see reaction mechanism in Fig 4.6, **Chapter 4**). This reaction is known as Staudinger reaction and is a mild method to reduce an azide to an amine, allowing for the ester groups to remain intact. To date, the only polysaccharide that has been modified using this methodology was cellulose. Pullulan is known for its non-toxicity and biocompatibility, therefore, we have applied this versatile methodology for the synthesis of pullulan derivatives with promising biological properties.

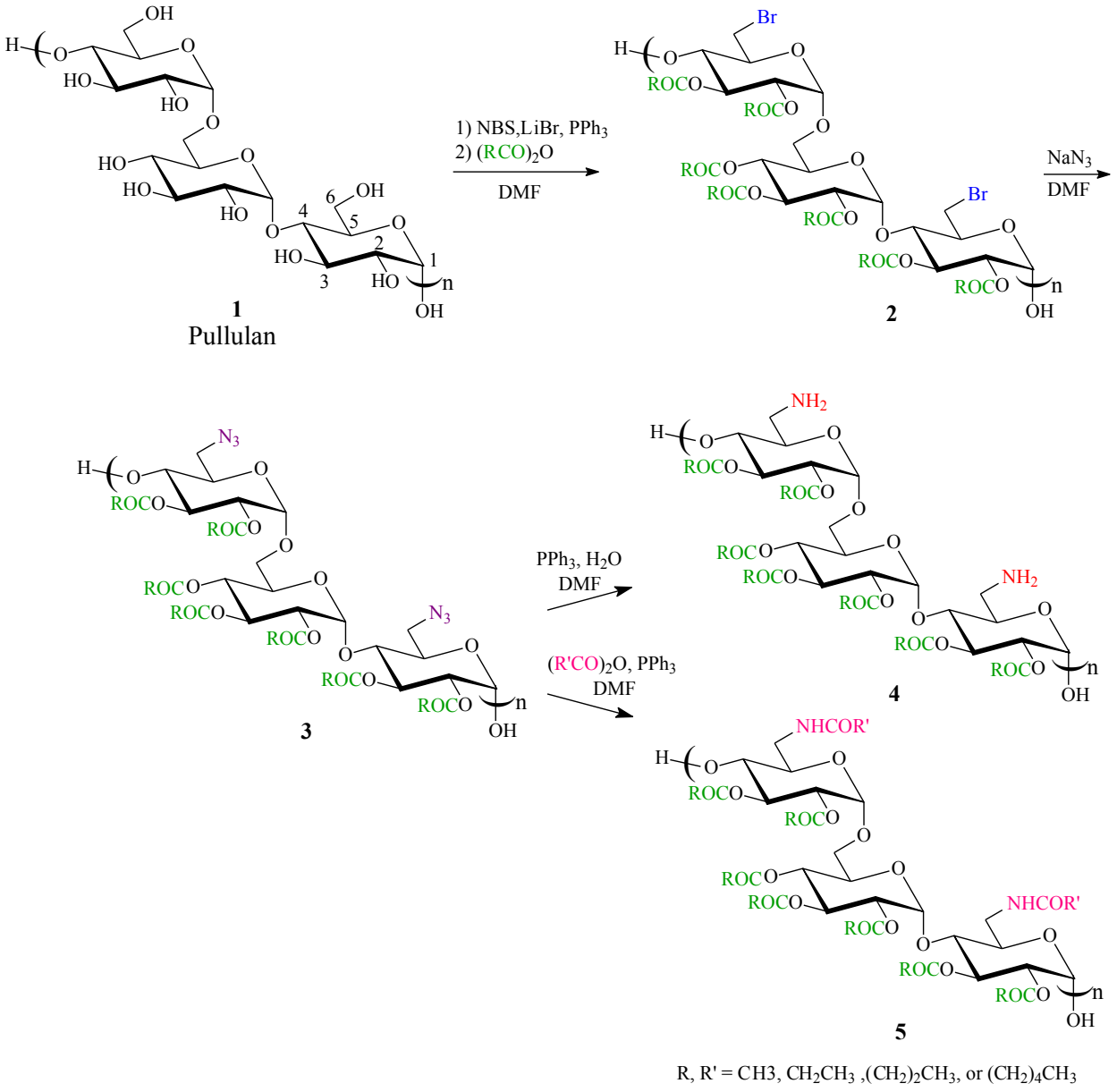

Figure 7.3 Synthesis of 6-amino and 6-amido-6-deoxy-pullulan esters

Herein, the pullulan iminophosphorane intermediates formed during the reaction of 6-azido-6-deoxy-pullulan esters with PPh_3 were hydrolyzed to produce the corresponding 6-amino-6-deoxy-pullulan esters (**4**), or, when the reaction was carried out in the presence of a carboxylic acid anhydride, 6-amido-6-deoxy-pullulan esters (**5**) were obtained in a one step reaction. This methodology permitted the synthesis of products which, when desired, have different N- and O-

acyl groups. All the products were obtained in good yields and with high regioselectivity, as a result of the selective bromination reaction.

As discussed in **Chapter 4**, pullulan derivatives containing amine and amide groups could have potential biomedical applications. The future exploration of these compounds for drug delivery applications will be essential. For example, amorphous solid dispersions could be formed with selected drugs for enhancement of drug solution concentration or drug controlled release.[12] Amine and amide groups in these polymers can form hydrogen bonds that might promote interactions between a drug and the polymer. Interactions of these polymers with specific proteins is also of interest for biomedical applications, for example in opening the tight junctions between enterocytes in the small intestine in order to enhance permeation of therapeutic molecules, like protein drugs, that cannot passively permeate through enterocytes that line the small intestine.[13]

The successful application of the Staudinger reaction to prepare amino and amidopullulan compounds opens new possibilities for the synthesis of other interesting pullulan derivatives. For example, the use of the traceless Staudinger ligation is an attractive approach for the introduction of amides with different acyl groups at the C-6 of pullulan backbone. The traceless Staudinger[14] ligation is a variation on the Staudinger reaction in which a carbonyl group is attached to the phosphine reducing agent through a cleavable linkage. This reaction has been demonstrated with several reagents, but one that is commonly used for this purpose is (diphenylphosphino)methanethiol.[15] The general reaction mechanism for the traceless Staudinger ligation using this reagent is illustrated in **Fig 7.4**.

The functional group R that is eventually to be attached to the azide compound through an amide bond is first bonded to the (diphenylphosphino)methanethiol (**6**) through a thioester bond (**Fig 7.4**). The azide (**7**) and the phosphine (**6**) react to form a phosphazide, which loses nitrogen gas to form an iminophosphorane (**8**) as in the traditional Staudinger reaction. The nitrogen atom of an iminophosphorane such as in **8** has intrinsic nucleophilicity and is then acylated by the thioester. This acylation proceeds via the tetrahedral intermediate **9**, in which the carbon to sulfur bond is cleaved to form amidophosphonium salt **10**. Finally, the amidophosphonium salt (**10**) is next hydrolyzed from the nitrogen, forming the phosphine oxide (**12**) and the free amide (**11**).

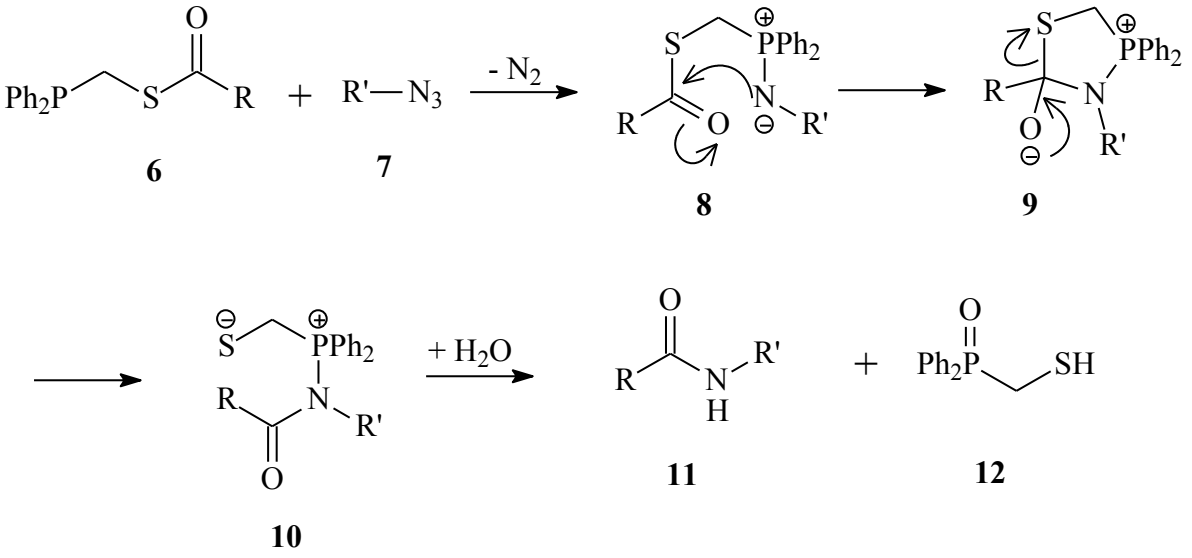

Figure 7.4 Reaction mechanism for the traceless Staudinger ligation mediated by (diphenylphosphino)methanethioester

It will be interesting to apply these reaction conditions for the synthesis of a variety of amidopullulan derivatives (amides with different R groups) starting from 6-azido-6-deoxy-pullulan esters. The reactivity of the iminophosphorane intermediate formed during the Staudinger reaction towards the acyl groups of anhydrides was demonstrated in **Chapter 4**, thus the same reactivity towards thioester is expected. Furthermore, the thiol group in the phosphine oxide (**12**) should render an easier to remove triphenylphosphine oxide byproduct. Structurally different phosphines, more soluble, which are used in reactions with small molecules, are also promising for performing this reaction such that the by-product phosphine oxide is easier to remove. Hanessian explored the one-pot synthesis of methyl 6-azido-6-deoxy-α-D-hexopyranosides from methyl α-D-glucopyranoside with *p*-(dimethylamino)phenyldiphenylphosphine instead of triphenylphosphine.[16] They report that the bromination reaction proceeded as usual in the presence of this reagent, and the isolation of the bromo derivative was facilitated by simply extracting the basic phosphine oxide derivative with aqueous acid.

It will also be exciting to explore the Staudinger reaction methodology for the synthesis of regioselective pullulan macroinitiators, which can be used as starting materials in atom transfer radical polymerization (ATRP). Many methods of surface modification for providing a material with desirable properties for practical applications have been developed.[17] ATRP[18] is a useful method to synthesize graft copolymers with well-defined structures utilizing a variety of monomers such as acrylates, acrylonitrile, methacrylates, and styrene. The application of ATRP to polysaccharides is a potentially attractive technique to prepare novel polysaccharide derivatives with well defined side-chain structures.[19] [20] Using the ATRP method, the "grafting from" approach involves two steps: the introduction of ATRP initiating groups on the polysaccharide backbone (macroinitiator synthesis) and the subsequent graft polymerization. As an example, the synthesis of a bottlebrush structure from a polysaccharide macroinitiator is illustrated in **Fig 7.5**.

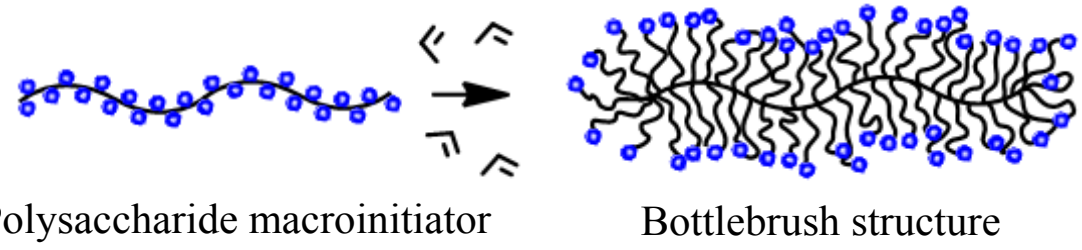

Figure 7.5 Illustration of a bottlebrush structure formed after grafting of a polysaccharide macroinitiator

Surface modification of a biopolymer such as pullulan using the ATRP technique has not been widely studied. The grafting of unmodified pullulan with poly(methylmethacrylate)[21] and methacrylate and acrylamide monomers[22] by ATRP have been reported. The authors demonstrated the preparation of spherical nanoparticles and comblike derivatives respectively. The comblike compounds have shown amphiphilic and thermoresponsive properties. In both cases, pullulan macroinitiator was obtained by partial esterification of the hydroxyl groups of the polysaccharide with 2-bromoisobutyryl bromide in the presence of a base.

By applying the Staudinger reaction methodology described herein, different pullulan macroinitiators can be prepared from modified pullulan (**Fig 7.6**), where the initiator group will be regioselectively introduced at C-6 to the pullulan backbone, in this case, through an amide linkage (**14**). Macroinitiator of modified pullulan can be obtained by acylation of the nitrogen in the pullulan iminophosphorane intermediate (**13**) with 2-bromoisobutyryl bromide in the presence of a base during the Staudinger reaction. These resulting pullulan macroinitiators can in turn, after graft polymerization, afford pullulan derivatives with a wide range of properties.

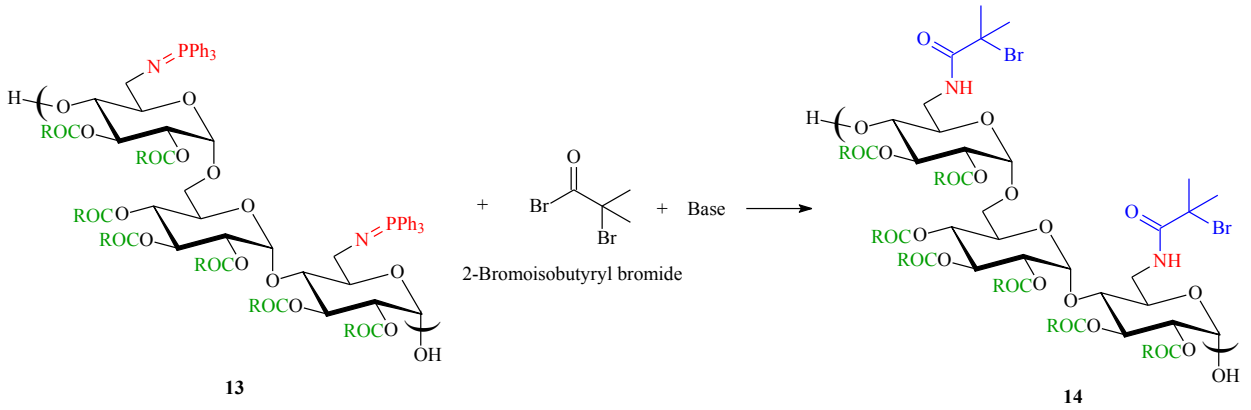

Figure 7.6 Reaction of pullulan iminophosphorane intermediate with 2-bromoisobutyryl bromide to form a pullulan macroinitiator

7.3 Interplay of Degradation, Dissolution and Stabilization of Clarithromycin and its Amorphous Solid Dispersions

Stabilization and release of clarithromycin (CLA) is exceptionally complex due to its high solubility at acidic conditions, acid instability,[23] and low solubility at neutral pH.[24] In **Chapter 5**, amorphous solid dispersions (ASDs) of CLA with three structurally diverse cellulosic polymers, carboxymethyl cellulose acetate butyrate (CMCAB),[25] hydroxypropylmethyl cellulose acetate succinate (HPMCAS)[26] and cellulose acetate adipate propionate (CAAdP),[27] [28] at 10 and 25 wt% drug loading, were prepared by spray-drying. Nanoparticles of CLA in CMCAB were also prepared by flash nano-precipitation[29] in order to

evaluate the effect of size reduction in comparison to spray-dried CLA in CMCAB ASDs. Drug crystallinity and solid state properties of each ASD were studied by X-ray diffraction, differential scanning calorimetry and scanning electron microscopy. CLA was shown to be amorphous and good drug-polymer miscibility was achieved in all ASDs prepared. The drug release profiles of these ASDs were studied at 2 different experimental conditions, one seeking to mimic the properties of the small intestine (pH 6.8), and the other, the passage of the drug through the gastrointestinal tract (pH 1.2 followed by pH 6.8). These experiments showed intriguing results, which have provided us with insight into how CLA and its ASDs could behave *in vivo* and also what polymer properties are needed to design successful macroparticulate CLA ASDs. The solubility increase from nanosizing actually was deleterious to the concentration of intact CLA obtained upon reaching small intestine conditions, since it resulted in release at gastric pH and subsequent degradation of CLA. CLA release was very dependent on polymer chemistry. The more hydrophilic polymer HPMCAS will release too much CLA at gastric pH and will ultimately deliver considerably less dissolved CLA by the time intestinal pH is reached. CMCAB is able to protect CLA from acid degradation in the stomach depending on the drug loading; the 25% formulation is not effective in preventing CLA acidic degradation, while the 10% formulation shows efficient CLA protection. The very hydrophobic polymer CAAdP shows significant promise for enhancing CLA solution concentration and bioavailability. CLA/CAAdP ASDs (both 10 and 25% CLA) are exceptionally efficient in preventing CLA degradation at pH 1.2, and release the remaining intact CLA when exposed to pH 6.8 (**Fig 7.7**).

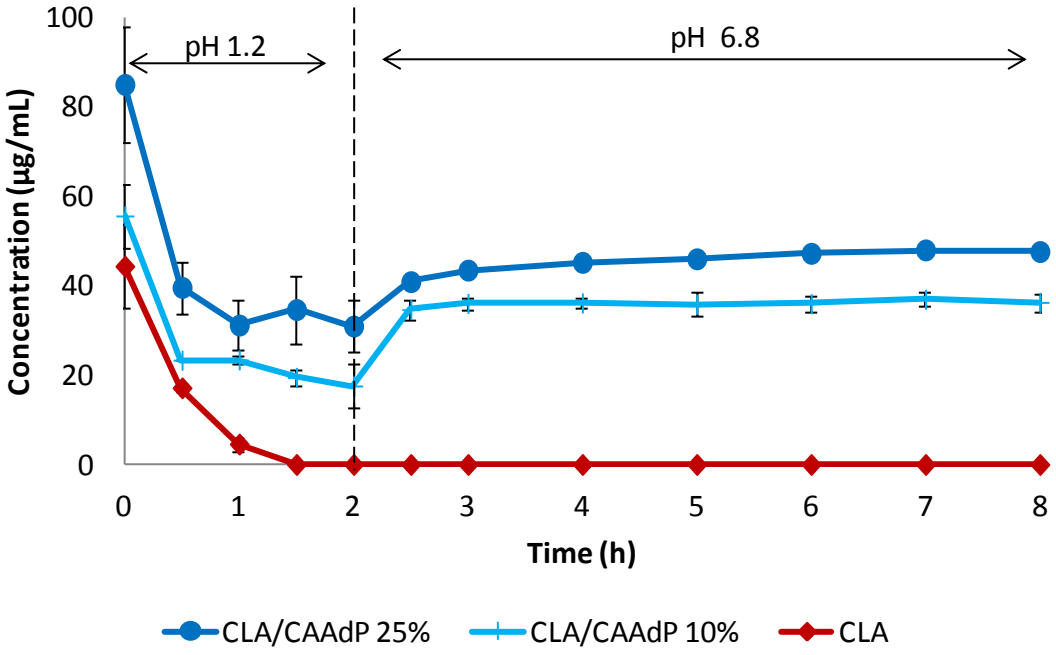

Figure 7.7 Dissolution profile of CLA/CAAdP ASDs (10 and 25 wt% drug loading); pH 1.2 buffer for 2h, then pH 6.8 buffer for 6h (see chapter 5 for dissolution profile of CLA ASDs with other polymers).

The results from these experiments will serve as a guide on how to best apply these ASDs and will also dictate the modifications that need to be performed to improve their performance for specific applications.

It will be enlightening to study other cellulose derivatives for their ability to enhance CLA solubility and to provide protection against acidic degradation. One polymer family of interest is the newly synthesized cellulose ω-carboxyalkanoates,[30] which were designed specifically for application in ASDs (**Fig 7.8**). It will be of great interest to determine whether macroparticulate ASDs based on CAAdP and cellulose ω-carboxyalkanoates are effective at enhancing CLA bioavailability *in vivo*.

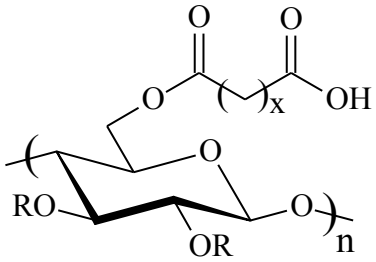

R = H, $COCH_3$, $COCH_2CH_3$ or $COCH_2CH_2CH_3$
R groups are randomly distributed at O-2,3,6 positions
x = 6 or 8

Figure 7.8 Chemical structure of cellulose ω-carboxyalkanoates

By looking at ASDs of CLA with a selection of diverse cellulosic polymers, we will be able to bolster our understanding of the mechanisms by which polymers inhibit drug crystallization and nucleation, which leads to higher drug solution concentrations, and the mechanisms by which they are capable of protecting CLA from acid degradation. Understanding of these mechanisms will provide more confidence to the design of successful ASDs with promising *in vivo* performance. It also will advance our ability to design new polymers for this purpose.

The results of these experiments are also a great motivation because they expand our ability to impact the delivery of other complex drugs such as CLA. We can now apply the knowledge gained from these results on improving the bioavailability of other drugs that suffer not only from poor solubility but that also possess other degradation related issues.

The possibility of mixing different polymers with distinct properties with the aim to attain intermediate properties is also another interesting area of research where the results from these experiments will be fundamental.[31]

The synergistic effects observed in these studies with the amorphous nanoparticles are also promising for drug-polymer systems in which release in the stomach would be less problematic.

7.4 Preliminary Studies on Amorphous Solid Dispersions of Anti-HIV Drugs: Ritonavir, Efavirenz and Etravirine

Ritonavir (RTV), efavirenz (EFV) and etravirine (ETR) are anti-HIV drugs that have poor bioavailability. If the bioavailability of these drugs can be improved by enhancing their solution concentration, HIV treatment, which comprises the concomitant administration of multiple drugs, can become less convenient for patients and more affordable for use in third-world countries. In **Chapter 6** we have demonstrated that both nano- and macroparticle ASDs of the anti-HIV drugs RTV and EFV with the cellulosic polymer carboxymethyl cellulose acetate butyrate (CMCAB) are capable of stabilizing the drug in its amorphous form in the solid phase, as confirmed by XRD and DSC. Furthermore, RTV/CMCAB ASDs provide significant enhancement of RTV solution concentration (**Fig 7.9**); a 20-fold increase for spray-dried macroparticles versus 10-fold for amorphous nanoparticles. Solution concentration enhancement was lower for EFV/CMCAB ASDs (1.7-fold increase for spray-dried microparticles versus 1.3-fold for nanoparticles).

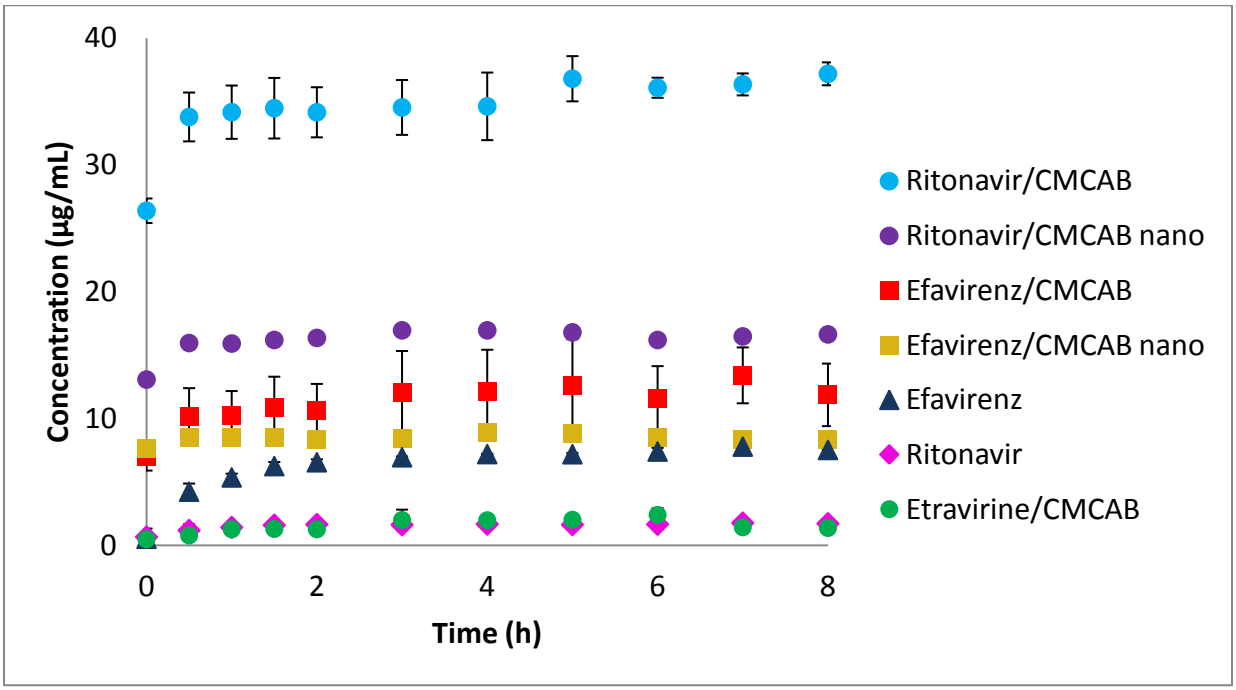

Figure 7.9 Dissolution profiles of anti-HIV drugs ASDs in pH 6.8 buffer

These preliminary results are a great motivation for further studies regarding the development of ASDs of anti-HIV drugs with other cellulose derivatives.[30 32] As we have also shown in this study, clear films were formed from solutions of RTV and EFV with the cellulose derivative CAAdP,[33] which is a promising polymer for ASD applications.[34] The formation of a clear polymer/drug film usually translates into successful spray-dried ASD particles.[31] The dissolution profiles of these drugs can be improved depending upon the polymer selected. ETR/CMCAB solid dispersions could not be made entirely amorphous; they showed the presence of crystalline ETR by XRD and DSC, but still the solid dispersions provided some ETR solution concentration enhancement. We began the evaluation of other solvents that might optimize the miscibility between ETR and CMCAB, and consequently lead to successful ETR/CMCAB ASDs. A clear film was achieved from ETR/CMCAB THF solution, indicating that ASDs can potentially be formed from spray-drying ETR/CMCAB THF solution. We have also produced films of ETR/CAAdP, since CAAdP has demonstrated outstanding performance in the formation of ASDs with a variety of actives,[27 28 35] and therefore is a promising polymer for ASD of ETR.

Therefore, the next step in this work will be the preparation of successful ASDs of ETR in CMCAB and CAAdP based on the results achieved from the film casting experiments and their evaluation on the release and solution concentration enhancement of ETR. It is also of interest to test the cellulose ω-carboxyalkanoates,[30](**Fig 7.8**) for their ability to form ASDs with the anti-HIV drugs. It will be important to determine whether nano and macroparticle ASDs based on such polymers are effective at enhancing the bioavailability of these drugs *in vivo*.

We suggested in **Chapter 5** that other drugs might be evaluated with the polymers studied in that work, and anti-HIV drugs fall into play. These drugs have even lower solubility than clarithromycin. As shown in **Chapter 5**, the dissolution studies performed for clarithromycin ASDs at more biorelevant conditions provided important insight into the potential behavior of ASDs *in vivo*. Therefore, this protocol will be utilized for the evaluation of the dissolution profile of the anti-HIV drugs.

Another important aspect of this project is the preparation of ASDs containing more than one anti-HIV drug. As mentioned earlier, HIV treatment requires the administration of multiple drugs concomitantly and this can create a complex dosing regimen that is not compatible with

patient compliance. If we can incorporate more than 1 drug into these cellulosic polymer ASDs and achieve solution concentration enhancement of each drug, we will be looking at a system that could be a breakthrough in HIV drugs bioavailability enhancement.

The study of ASDs with other polysaccharides that could be used beyond oral drug delivery is also of great interest. The pullulan derivatives synthesized in this dissertation, described in **Chapters 3** and **4**, are potential polymers for ASD applications. They are of special interest because, as described in **Chapter 2**, pullulan possess attractive characteristics. It biodegrades in the body and does not evoke an immune response. It has also been shown to be non-toxic when administered intravenously. Pullulan has a relatively simple structure and can be chemically modified according to the desired application. Moreover many pullulan derivatives that have been prepared for a variety of applications have shown to be as safe as pullulan.[36 37] The pullulan compounds synthesized in this dissertation possess appealing properties for use in drug delivery systems. These derivatives may be used in oral and intravenous drug formulations, and their physical properties are expected to help improve drug performance, such as provide sustained release of the drug and improve the drug's solubility and stability. The incorporation of carboxylic acid groups in the pullulan backbone (**Chapter 3**) will provide anionic compounds that will interact more effectively with drugs containing cationic groups, and the ionic characteristics of these polymers will allow for pH controlled release of the drug within the GI tract. Similarly, cationic pullulan derivatives containing amine/amide groups (**Chapter 4**) can be better candidates in the delivery of anionic drugs. Amine and amide groups in these polymers can form hydrogen bonds that might promote interactions between a drug and the polymer. Interactions of these polymers with specific proteins is also of interest for biomedical applications, for example in opening the tight junctions between enterocytes in the small intestine in order to enhance permeation of therapeutic molecules, like protein drugs, that cannot passively permeate through enterocytes that line the small intestine.[13]

Alongside of the research discussed here for example, such polymers could be used for the delivery of other challenging anti-HIV drugs. One example is Enfuvirtide,[38] which is an HIV fusion inhibitor, the first of a novel class of antiretroviral drugs used in combination therapy for the treatment of HIV-1 infection. It is marketed under the trade name Fuzeon (Roche). Enfuvirtide works by disrupting the HIV-1 molecular machinery at the final stage of fusion with

the target cell, preventing uninfected cells from becoming infected. As with many other classes of drugs, enfuvirtide must be administered in potent combinations with at least two other active drugs otherwise resistance develops rapidly. Enfuvirtide is a complex molecule, and by virtue of its peptide nature, it is degraded in the stomach and therefore requires twice-daily parenteral (subcutaneous injection) administration. Due to the chronic nature of this kind of therapy, this dosage form may be a major problem for the patient's adherence to this drug regimen. Therefore, formulations with pullulan derivatives (oral or yet intravenous, if they are efficient in opening the tight junctions) are a promising approach for delivery of this drug and others that possess such degradability and/or bioavailability related issues.

Finally, but of ultimate importance, will be the *in vivo* study of these ASDs. It's fundamental to understand the distribution of these particles in the body, especially for the nanoparticles, which may reach circulation.

7.5 References

1. Bernier, B., The production of polysaccharides by fungi active in the decomposition of wood and forest litter. *Can. J. Microbiol.* **1958,** *4*, 195-204.

2. Akiyoshi, K.; Yamaguchi, S.; Sunamoto, J., Self-Aggregates of hydrophobic polysaccharide derivatives. *Chemistry Letters* **1991,** (7), 1263-1266.

3. Hirakura, T.; Nomura, Y.; Aoyama, Y.; Akiyoshi, K., Photoresponsive nanogels formed by the self-assembly of spiropyrane-bearing pullulan that act as artificial molecular chaperones. *Biomacromolecules* **2004,** *5* (5), 1804-1809.

4. Jung, S. W.; Jeong, Y. I.; Kim, S. H., Characterization of hydrophobized pullulan with various hydrophobicities. *International Journal of Pharmaceutics* **2003,** *254* (2), 109-121.

5. Dulong, V.; Le Cerf, D.; Picton, L.; Muller, G., Carboxymethylpullulan hydrogels with a ionic and/or amphiphilic behavior: Swelling properties and entrapment of cationic and/or hydrophobic molecules. *Colloids and Surfaces a-Physicochemical and Engineering Aspects* **2006,** *274* (1-3), 163-169.

6. George, M.; Abraham, T. E., Polyionic hydrocolloids for the intestinal delivery of protein drugs: Alginate and chitosan - a review. *Journal of Controlled Release* **2006,** *114* (1), 1-14.

7. de Nooy, A. E. J.; Besemer, A. C.; van Bekkum, H.; van Dijk, J. A. P. P.; Smit, J. A. M., TEMPO-Mediated Oxidation of Pullulan and Influence of Ionic Strength and Linear Charge Density on the Dimensions of the Obtained Polyelectrolyte Chains. *Macromolecules* **1996,** *29* (20), 6541-6547.

8. Kabanov, A. V.; Batrakova, E. V.; Alakhov, V. Y., Pluronic® block copolymers as novel polymer therapeutics for drug and gene delivery. *J. Controlled Release* **2002,** *82* (2–3), 189-212.

9. Tian, Y.; Zhu, Y.; Bashari, M.; Hu, X.; Xu, X.; Jin, Z., Identification and releasing characteristics of high-amylose corn starch–cinnamaldehyde inclusion complex prepared using ultrasound treatment. *Carbohydr. Polym.* **2013,** *91* (2), 586-589.

10. Ochiai, T.; Terao, K.; Nakamura, Y.; Yoshikawa, C.; Sato, T., Rigid helical conformation of curdlan tris(phenylcarbamate) in solution. *Polymer* **2012,** *53* (18), 3946-3950.

11. Shingel, K. I., Current knowledge on biosynthesis, biological activity, and chemical modification of the exopolysaccharide, pullulan. *Carbohydr. Res.* **2004,** *339* (3), 447-460.

12. Kawakami, K., Current status of amorphous formulation and other special dosage forms as formulations for early clinical phases. *Journal of Pharmaceutical Sciences* **2009,** *98* (9), 2875-2885.

13. Rosenthal, R.; Günzel, D.; Finger, C.; Krug, S. M.; Richter, J. F.; Schulzke, J.-D.; Fromm, M.; Amasheh, S., The effect of chitosan on transcellular and paracellular mechanisms in the intestinal epithelial barrier. *Biomaterials* **2012,** *33* (9), 2791-2800.

14. Saxon, E.; Armstrong, J. I.; Bertozzi, C. R., A "traceless" Staudinger ligation for the chemoselective synthesis of amide bonds. *Organic Letters* **2000,** *2* (14), 2141-2143.

15. Soellner, M. B.; Nilsson, B. L.; Raines, R. T., Reaction mechanism and kinetics of the traceless Staudinger ligation. *Journal of the American Chemical Society* **2006,** *128* (27), 8820-8828.

16. Hanessian, S.; Ducharme, D.; Massé, R.; Capmau, M. L., A one-flask preparation of methyl 6-azido-6-deoxy-α-D-hexopyranosides. *Carbohydrate Research* **1978,** *63*, 265-269.

17. Kobayashi, Y.; Saeki, S.; Yoshida, M.; Nagao, D.; Konno, M., Synthesis of spherical submicron-sized magnetite/silica nanocomposite particles. *Journal of Sol-Gel Science and Technology* **2008,** *45* (1), 35-41.

18. Matyjaszewski, K., Atom Transfer Radical Polymerization (ATRP): Current Status and Future Perspectives. *Macromolecules* **2012,** *45* (10), 4015-4039.

19. Ifuku, S.; Kadla, J. F., Preparation of a Thermosensitive Highly Regioselective Cellulose/N-Isopropylacrylamide Copolymer through Atom Transfer Radical Polymerization. *Biomacromolecules* **2008,** *9* (11), 3308-3313.

20. El Tahlawy, K.; Hudson, S. M., Synthesis of a well-defined chitosan graft poly(methoxy polyethyleneglycol methacrylate) by atom transfer radical polymerization. *Journal of Applied Polymer Science* **2003,** *89* (4), 901-912.

21. De Leonardis, P.; Mannina, L.; Diociaiuti, M.; Masci, G., Atom transfer radical polymerization synthesis and association properties of amphiphilic pullulan copolymers grafted with poly(methyl methacrylate). *Polymer International* **2010,** *59* (6), 759-765.

22. Bontempo, D.; Masci, G.; De Leonardis, P.; Mannina, L.; Capitani, D.; Crescenzi, V., Versatile grafting of polysaccharides in homogeneous mild conditions by using atom transfer radical polymerization. *Biomacromolecules* **2006,** *7* (7), 2154-2161.

23. Venkateswaramurthy, N.; Sambathkumar, R.; Perumal, P., Controlled release mucoadhesive microspheres of clarithromycin for the treatment of Helicobacter Pylori infection. *Der Pharmacia Lettre* **2012,** *4* (3), 993-1004.

24. Chu, S. Y.; Deaton, R.; Cavanaugh, J., Absolute bioavailability of clarithromycin after oral administration in humans. *Antimicrob. Agents Chemother.* **1992,** *36* (5), 1147-1150.

25. Posey-Dowty, J. D.; Watterson, T. L.; Wilson, A. K.; Edgar, K. J.; Shelton, M. C.; Lingerfelt, L. R., Zero-order release formulations using a novel cellulose ester. *Cellulose* **2007,** *14* (1), 73-83.

26. Friesen, D. T.; Shanker, R.; Crew, M.; Smithey, D. T.; Curatolo, W. J.; Nightingale, J. A. S., Hydroxypropyl methylcellulose acetate succinate-based spray-dried dispersions: An overview. *Molecular Pharmaceutics* **2008,** *5* (6), 1003-1019.

27. Li, B.; Harich, K.; Wegiel, L.; Taylor, L. S.; Edgar, K. J., Stability and solubility enhancement of ellagic acid in cellulose ester solid dispersions. *Carbohydrate Polymers* **2013,** *92* (2), 1443-1450.

28. Li, B.; Konecke, S.; Harich, K.; Wegiel, L.; Taylor, L. S.; Edgar, K. J., Solid dispersion of quercetin in cellulose derivative matrices influences both solubility and stability. *Carbohydrate Polymers* **2013,** *92* (2), 2033-2040.

29. (a) Johnson, B. K.; Prud'homme, R. K., Chemical processing and micromixing in confined impinging jets. *AlChE J.* **2003,** *49* (9), 2264-2282; (b) Johnson, B. K.; Prud'homme, R. K., Mechanism for rapid self-assembly of block copolymer nanoparticles. *Phys. Rev. Lett.* **2003,** *91*, 118302-1-118302-4.

30. Liu, H.; Ilevbare, G. A.; Cherniawski, B. P.; Ritchie, E. T.; Taylor, L. S.; Edgar, K. J., Synthesis and structure–property evaluation of cellulose ω-carboxyesters for amorphous solid dispersions. In *Carbohydr. Polym.*, In press. Available online 26 November 2012, 2013.

31. Marks, J.; Wegiel, L.; Taylor, L. S.; Edgar, K. J., Pairwise polymer blends for oral drug delivery Unpublished work, 2013.

32. Ilevbare, G. A.; Liu, H.; Edgar, K. J.; Taylor, L. S., Understanding polymer properties important for crystal growth inhibition-impact of chemically diverse polymers on solution crystal growth of ritonavir. *Crystal Growth & Design* **2012,** *12* (6), 3133-3143.

33. Liu, H.; Kar, N.; Edgar, K. J., Direct synthesis of cellulose adipate derivatives using adipic anhydride. *Cellulose* **2012,** *19* (4), 1279-1293.

34. Ilevbare, G. A.; Liu, H.; Edgar, K. J.; Taylor, L. S., Inhibition of solution crystal growth of ritonavir by cellulose polymers - factors influencing polymer effectiveness. *Crystengcomm* **2012,** *14* (20), 6503-6514.

35. Pereira, J. M.; Mejia-Ariza, R.; Edgar, K. J.; Davis, R. M.; Sriranganathan, N.; Taylor, L. S.; Ilevbare, G. A.; McGettigan, H., Interplay of degradation, dissolution and stabilization of clarithromycin and its amorphous solid dispersions. Unpublished work, 2013.

36. Kang, J. H.; Tachibana, Y.; Kamata, W.; Mahara, A.; Harada-Shiba, M.; Yamaoka, T., Liver-targeted siRNA delivery by polyethylenimine (PEI)-pullulan carrier. *Bioorganic & Medicinal Chemistry* **2010,** *18* (11), 3946-3950.

37. Kitano, S.; Kageyama, S.; Nagata, Y.; Miyahara, Y.; Hiasa, A.; Naota, H.; Okumura, S.; Imai, H.; Shiraishi, T.; Masuya, M.; Nishikawa, M.; Sunamoto, J.; Akiyoshi, K.; Kanematsu, T.; Scott, A. M.; Murphy, R.; Hoffman, E. W.; Old, L. J.; Shiku, H., HER2-specific T-cell immune responses in patients vaccinated with truncated HER2 protein complexed with nanogels of cholesteryl pullulan. *Clinical Cancer Research* **2006,** *12* (24), 7397-7405.

38. Lalezari, J. P.; Eron, J. J.; Carlson, M.; Cohen, C.; DeJesus, E.; Arduino, R. C.; Gallant, J. E.; Volberding, P.; Murphy, R. L.; Valentine, F.; Nelson, E. L.; Sista, P. R.; Dusek, A.; Kilby, J. M., A phase II clinical study of the long-term safety and antiviral activity of enfuvirtide-based antiretroviral therapy. *Aids* **2003,** *17* (5), 691-698.

Appendix

Chapter 3 Synthesis of Amphiphilic 6-Carboxypullulan Ethers

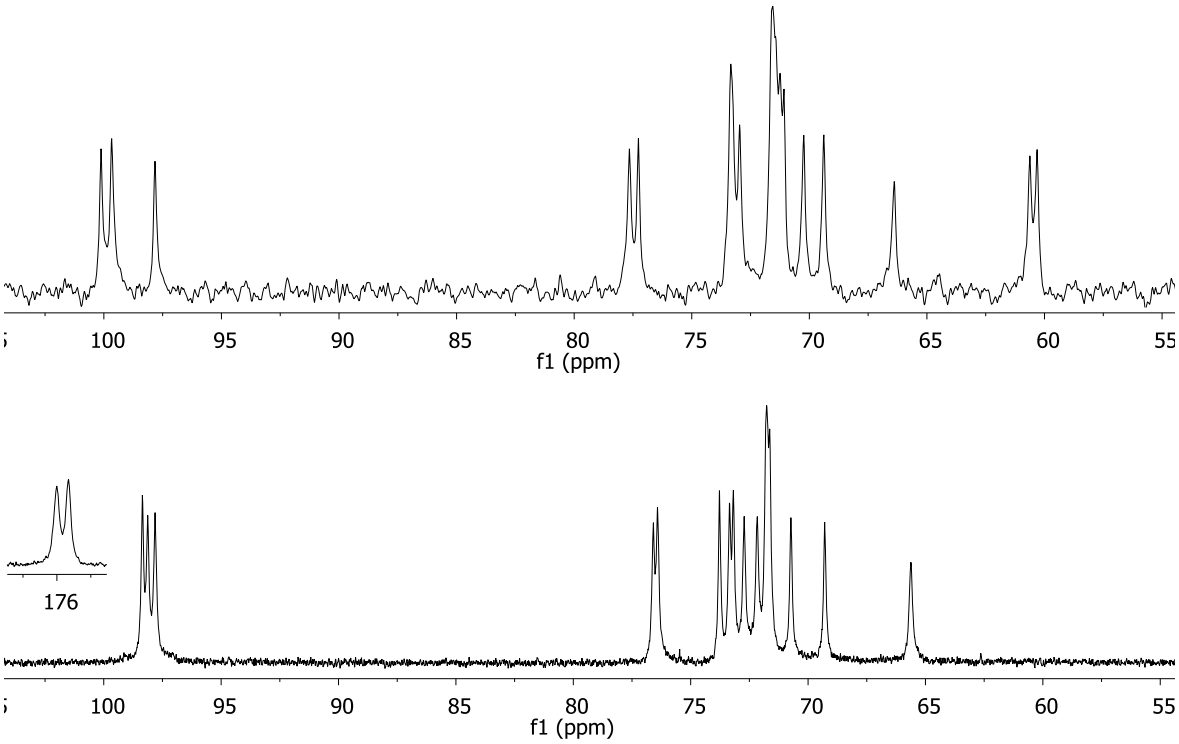

Figure A3.1 ^{13}C NMR spectra of pullulan (above) and 6-carboxypullulan (below) in D_2O

(a)

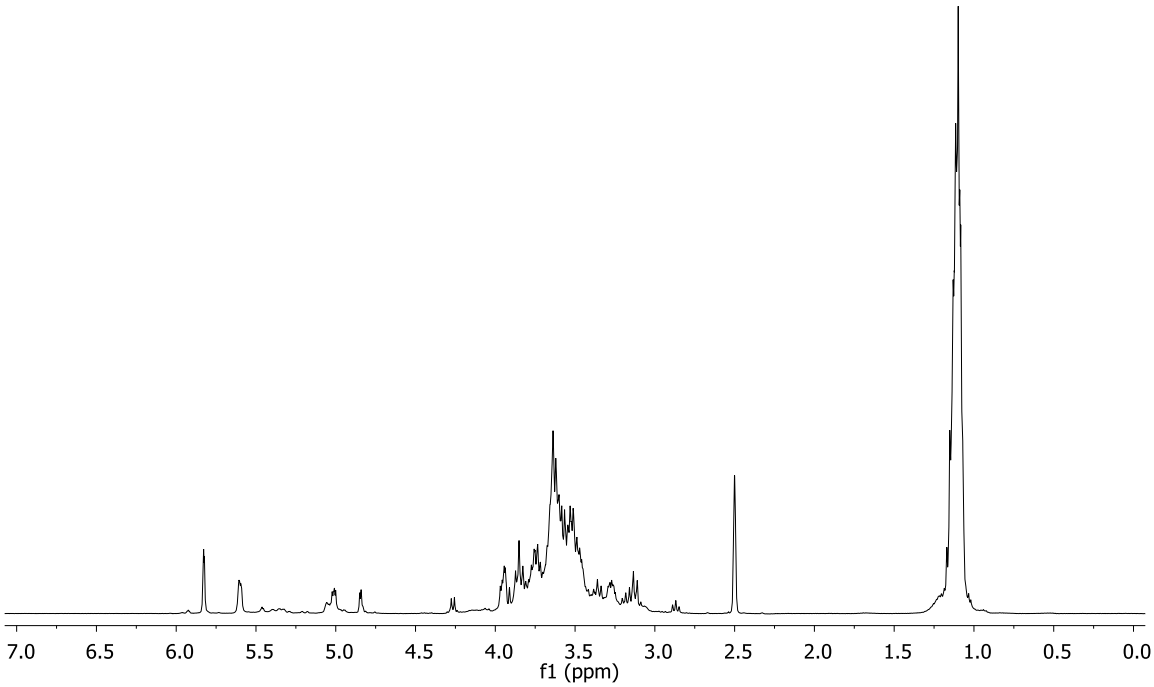

(b)

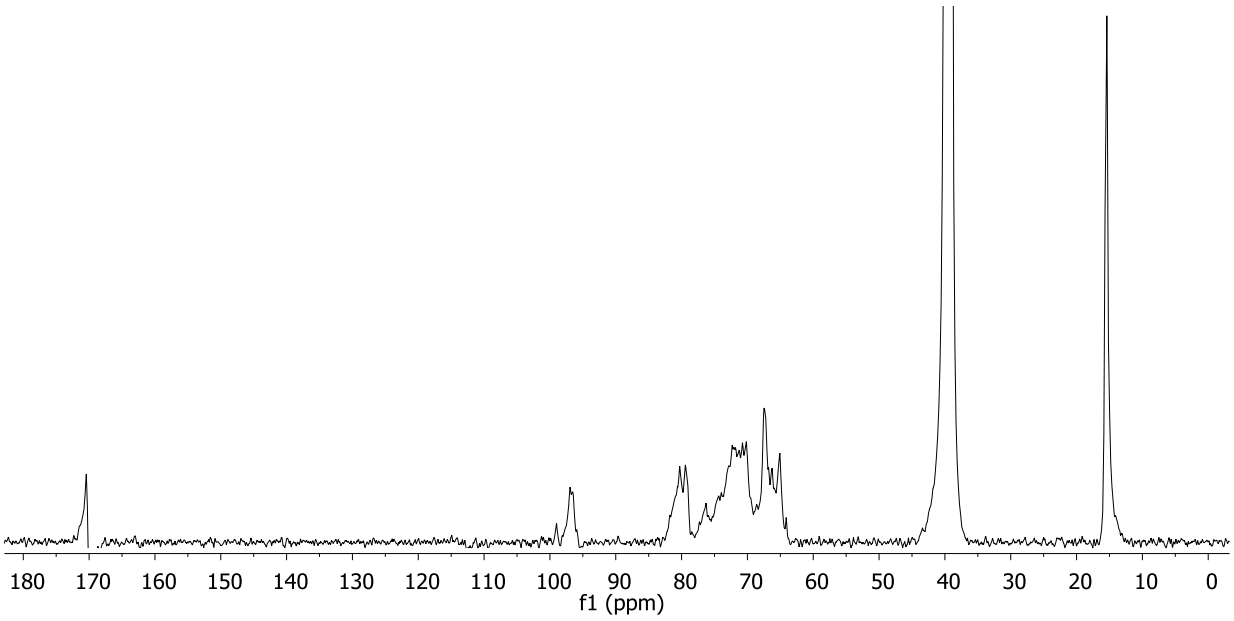

Figure A3.2 ^{1}H **(a)** and ^{13}C **(b)** NMR spectra of ethyl pullulan-6-carboxylate in d_6-DMSO

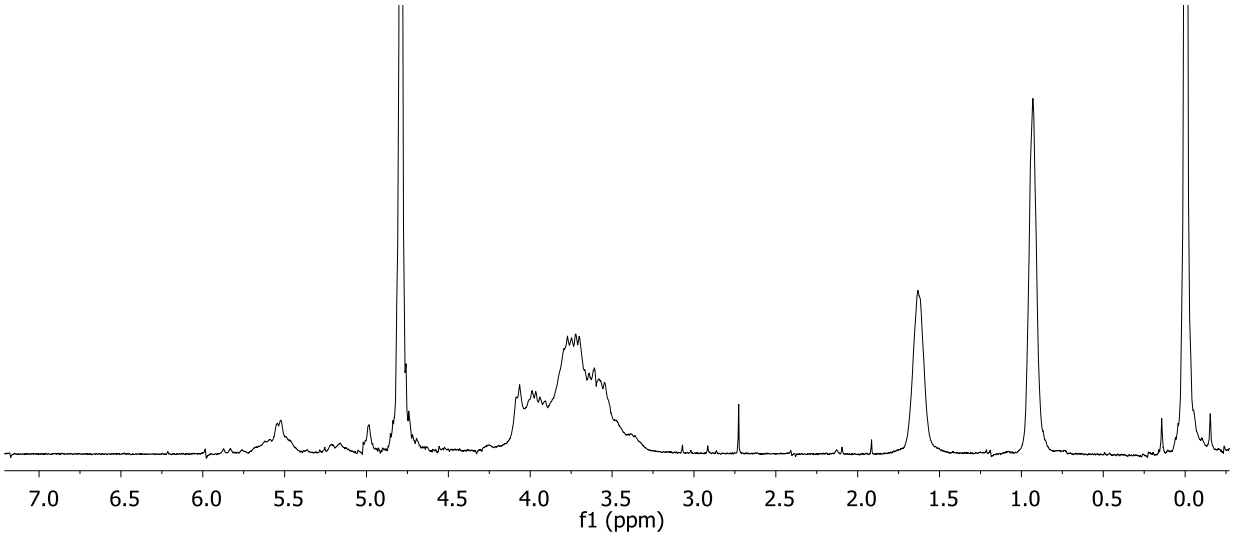

Figure A3.3 ^{1}H NMR spectra of propyl pullulan-6-carboxylate in D_2O

(a)

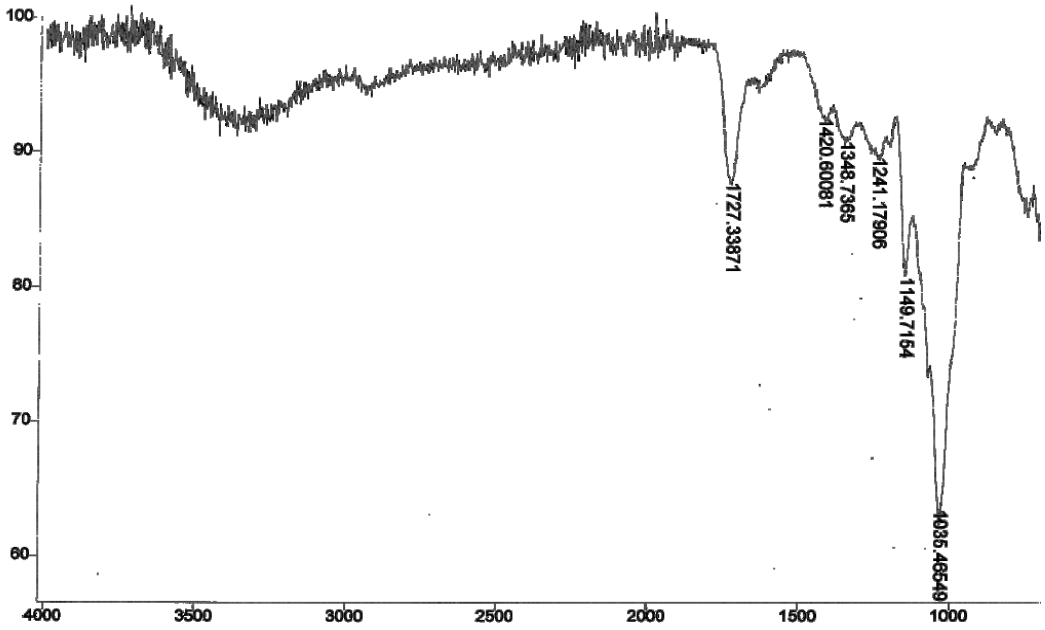

(b)

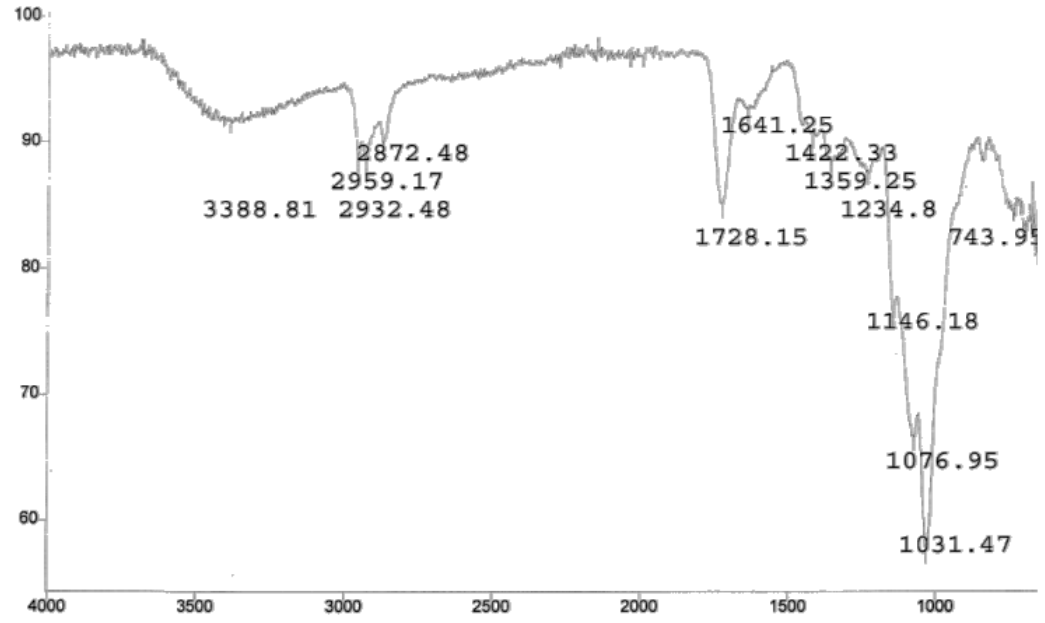

Figure A3.4 IR spectra of **(a)** 6-carboxypullulan and **(b)** butyl pullulan-6-carboxylate

Table A3.1 DS of ester groups in the 6-carboxypullulan ethers

Sample	**Total DS before hydrolysis**	**Total DS after hydrolysis**	**DS of ester[a]**
Butyl-6-CO_2HPull (4c)	3.6	3.27	0.33
Ethyl-6-CO_2Hpull (4a)	5.12	4.85	0.27
Ethyl-6-CO_2Hpull (4e)	7.36	7.02	0.34

The DS was calculated by ^{1}H NMR (see experimental section). [a] Calculated by subtracting the DS after the hydrolysis from the initial DS.

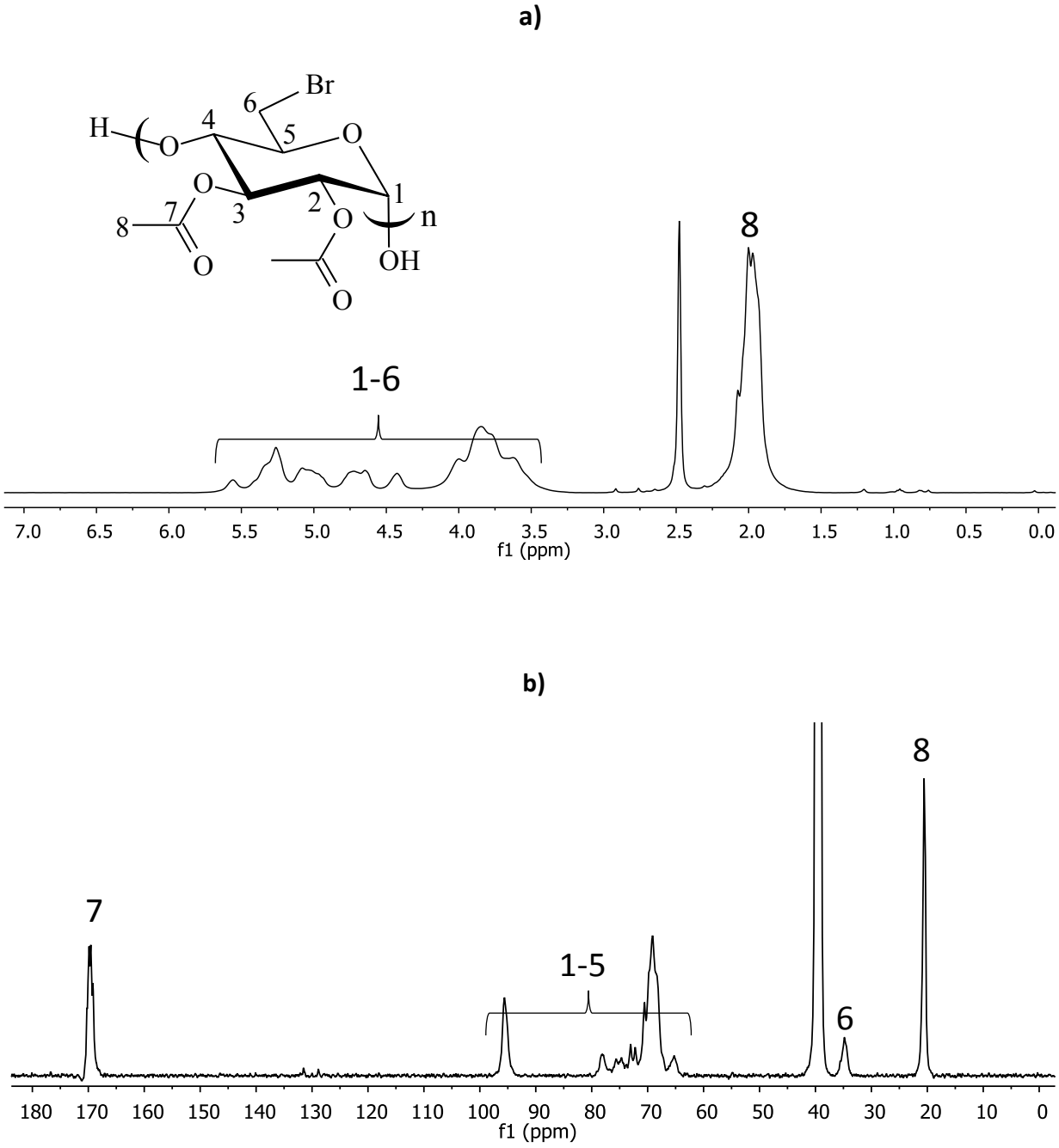

Figure A4.1 (a) ^{1}H and **(b)** ^{13}C NMR of 6-bromo-6-deoxy-2,3,4-O-acetyl-pullulan

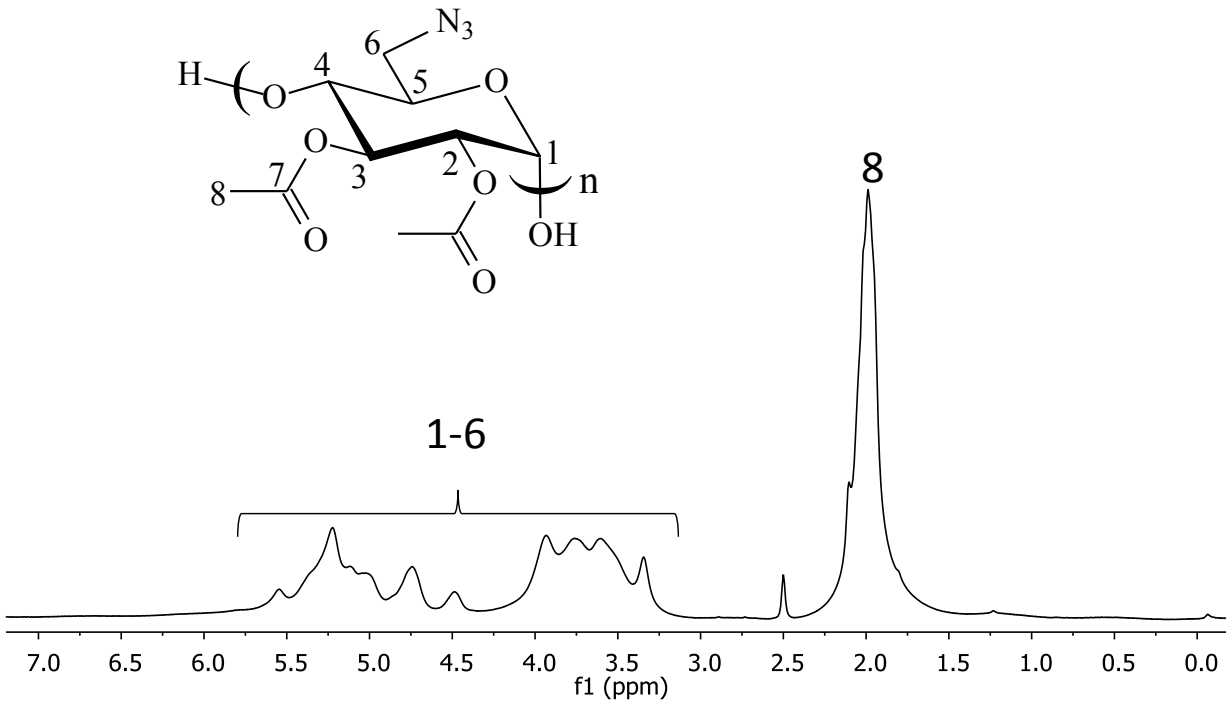

Figure A4.2 ^{1}H NMR of 6-azido-6-deoxy-2,3,4-O-acetyl-pullulan

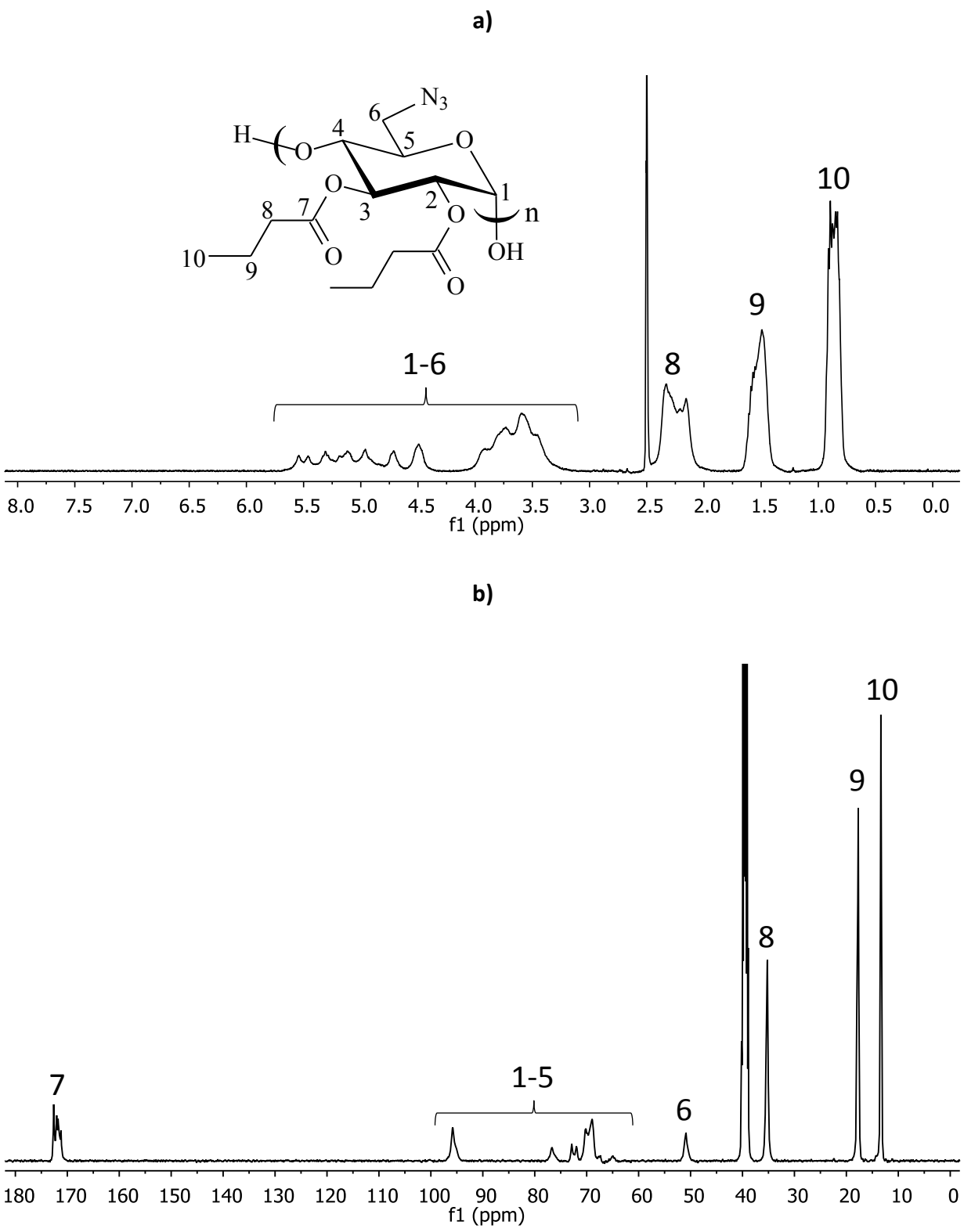

Figure A4.3 (a) ^{1}H and **(b)** ^{13}C NMR of 6-azido-6-deoxy-2,3,4-O-butyryl-pullulan

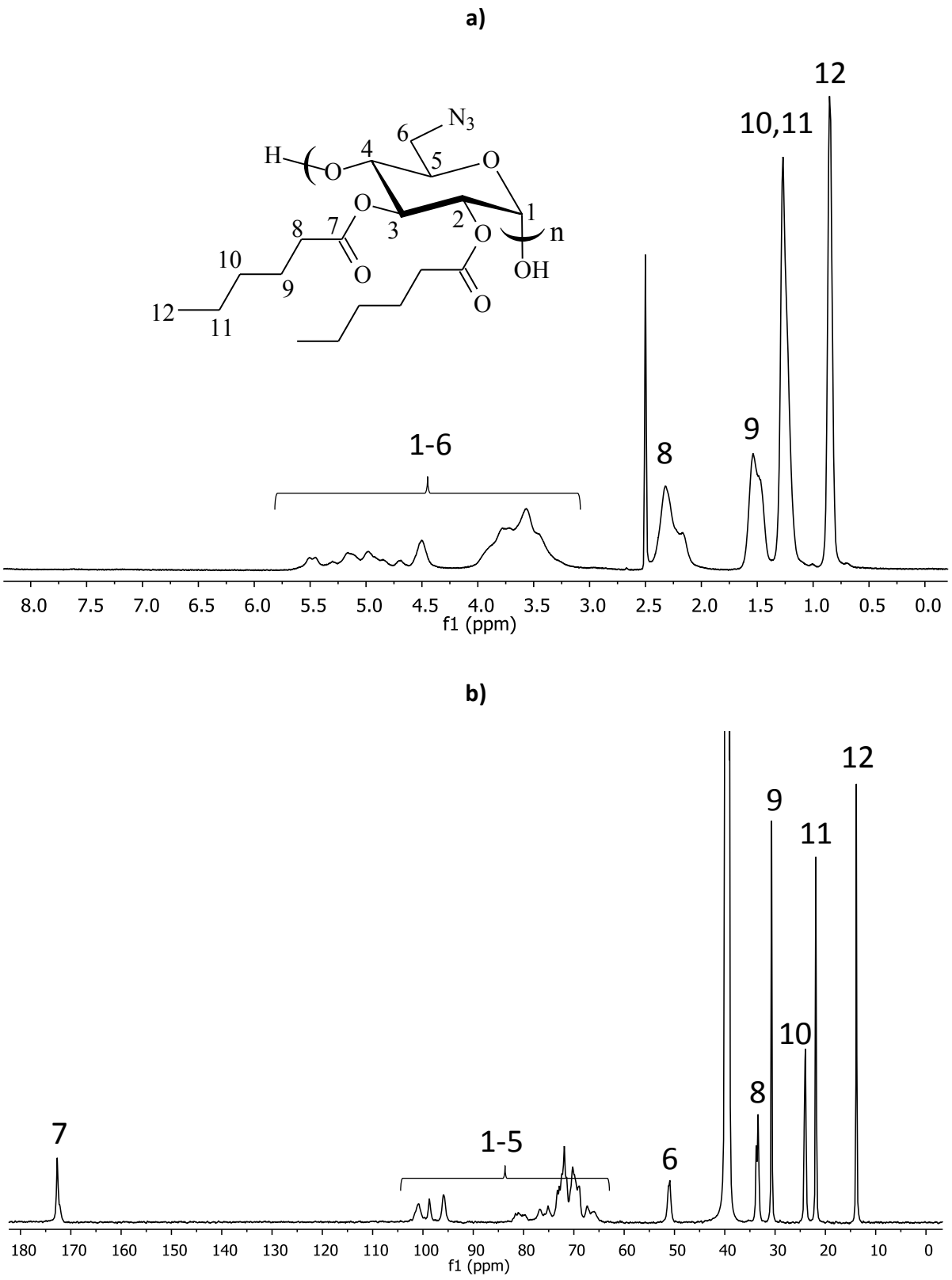

Figure A4.4 (a) ^{1}H and **(b)** ^{13}C NMR of 6-azido-6-deoxy-2,3,4-O-hexanoyl-pullulan

a)

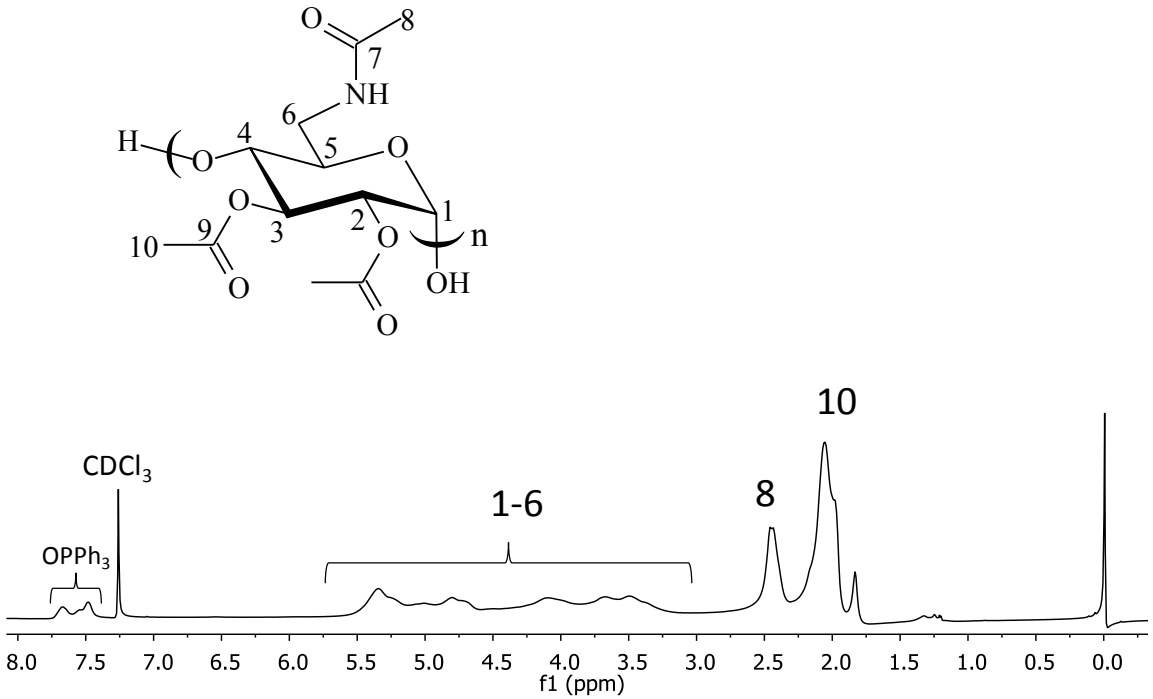

b)

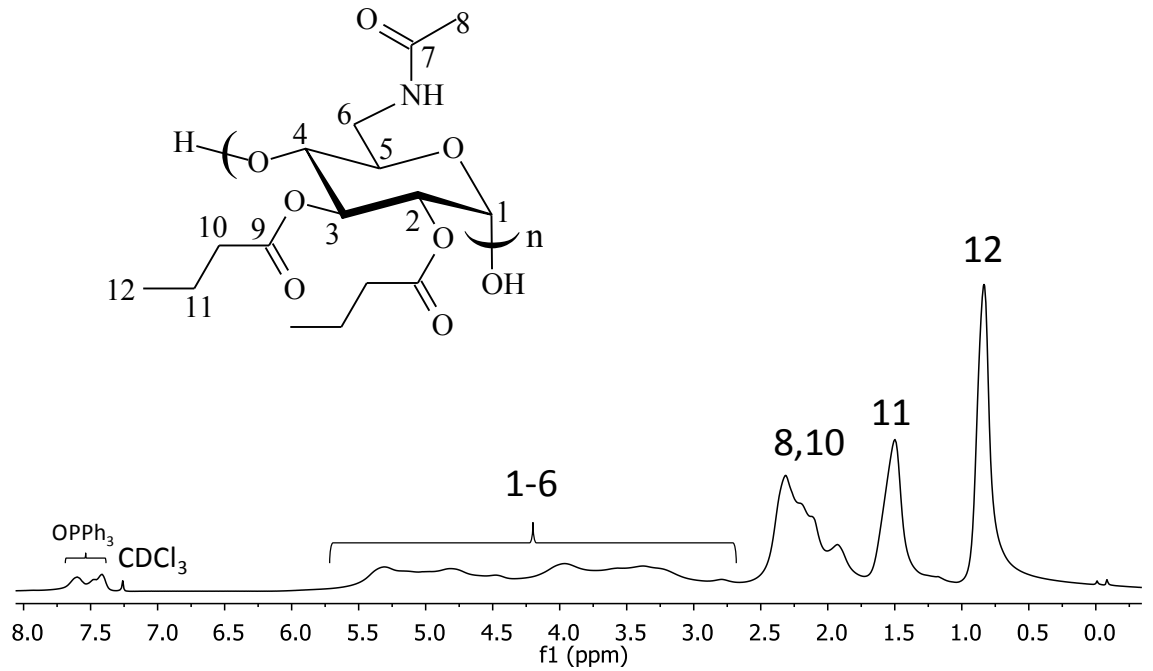

Figure A4.5 ^{1}H NMR of **(a)** 6-acetamido-6-deoxy-2,3,4-O-acetyl-pullulan and **(b)** 6-acetamido-6-deoxy-2,3,4-O-butyryl-pullulan

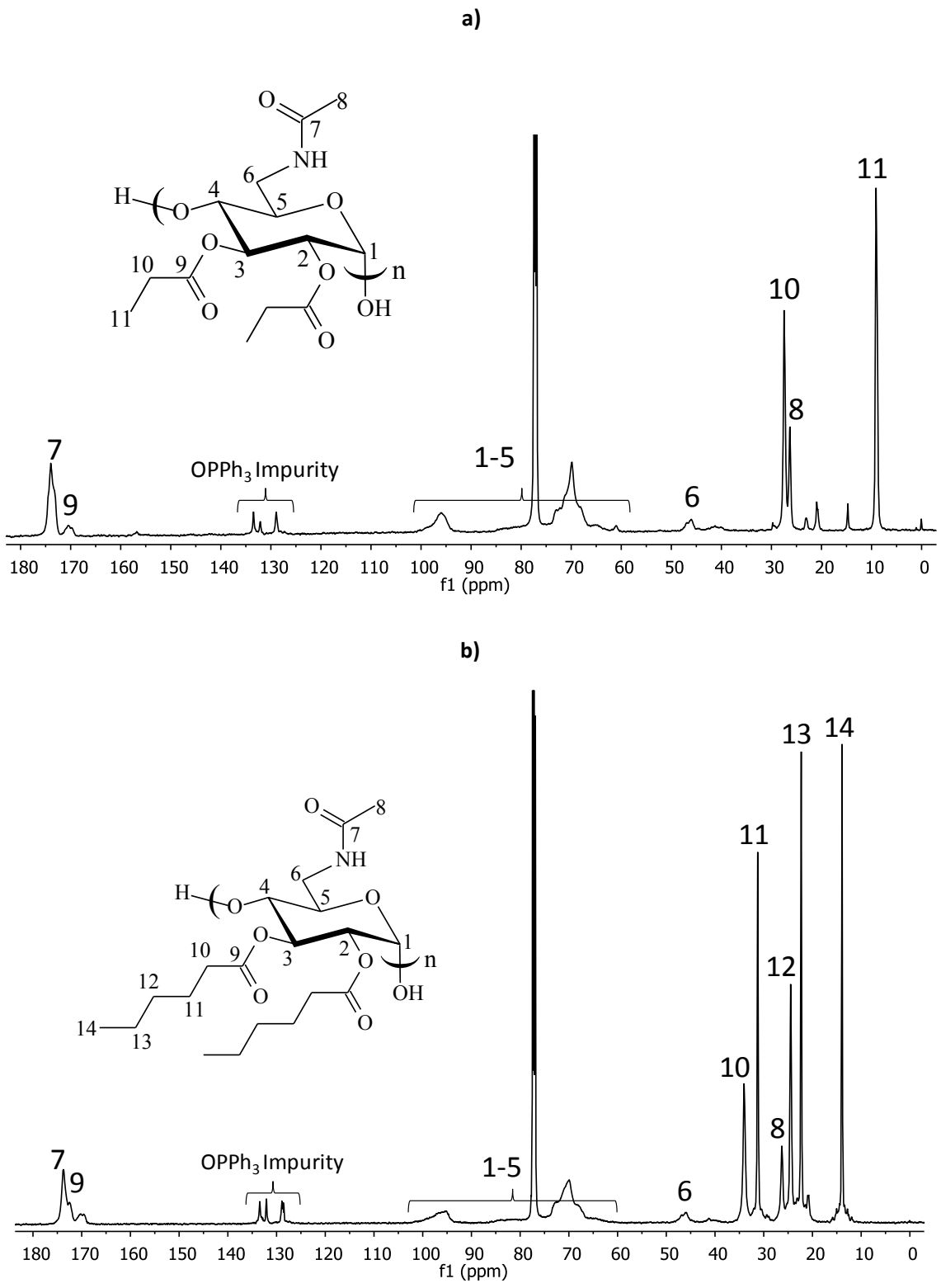

Figure A4.6 ^{13}C NMR of **(a)** 6-acetamido-6-deoxy-2,3,4-O-propionyl and **(b)** 6-acetamido-6-deoxy-2,3,4-O-hexanoyl-pullulan

Chapter 5 Interplay of Degradation, Dissolution and Stabilization of Clarithromycin and its Amorphous Solid Dispersions

DSC Analysis was performed to confirm the presence of amorphous drug and also polymer/drug miscibility in the ASDs. One important factor to consider when producing and choosing polymers for amorphous solid dispersions is miscibility, which is the ability to produce a homogeneous single phase where the components are intimately mixed at a molecular level.[1] Physically separated mixtures of an amorphous active pharmaceutical ingredient (API) and polymer are commonly observed resulting in immiscible systems. Miscible amorphous solid dispersions typically have a single T_g, which is higher compared to the amorphous API due to the antiplasticizing effect of the polymer, resulting in lower molecular mobility and decreased crystallization.

DSC analysis of crystalline CLA, free polymer and ASDs prepared (**Fig A5.1 a, b**) illustrates the absence of a melting peak at 228 °C in the polymer dispersions, which indicates that no crystalline CLA is present in any of the ASDs prepared. Moreover, T_g values intermediate between that of amorphous CLA (109 °C)[2] and that of the respective polymer are observed for all ASDs. This is an explicit indication of homogeneous dispersion of drug within the polymer matrix. For the most part the experimental T_g values of CLA/CMCAB and CLA/HPMCAS ASDs are in good agreement with those calculated using the Fox equation (predicted T_g) (**Table A5.1**). For CLA/CMCAB 25% (spray-dried and nanoparticles) and CLA/HPMCAS 10%, calculated and experimental T_gs are nearly identical. For CLA/CMCAB 10% (spray-dried and nanoparticles) there was a small increase in the T_g from that predicted and for CLA/HPMCAS 25%, the T_g slightly decreased from that predicted. For CLA/CAAdP ASDs, the difference between T_gs, experimental and calculated using Fox equation, was more significant and T_g was lower than that predicted for both formulations. Overall, these results show that effective drug-polymer interaction is present in all ASDs leading to miscibility, as indicated by the presence of a single T_g. Furthermore, T_g values of these ASDs exceed likely maximum ambient temperatures (40-50 ºC) by more than 50 °C, providing a window that should

be more than adequate protection against high ambient humidity and temperature during transport and storage (all ASDs studied showed T_g higher than 100 ºC).

Table A5.1 T_g of ASDs - experimental vs. predicted by Fox equation

	Experimental T_g (ºC)	**Predicted T_g (ºC)**
CLA/CMCAB 10%	140.7	137.3
CLA/CMCAB 25%	130.8	131.6
CLA/CMCAB 10% nano	140.3	137.3
CLA/CMCAB 25% nano	132.4	131.6
CLA/HPMCAS 10%	120.5	120.2
CLA/HPMCAS 25%	113.6	118.2
CLA/CAAdP 10%	115.2	124.1
CLA/CAAdP 25%	109.4	121.3

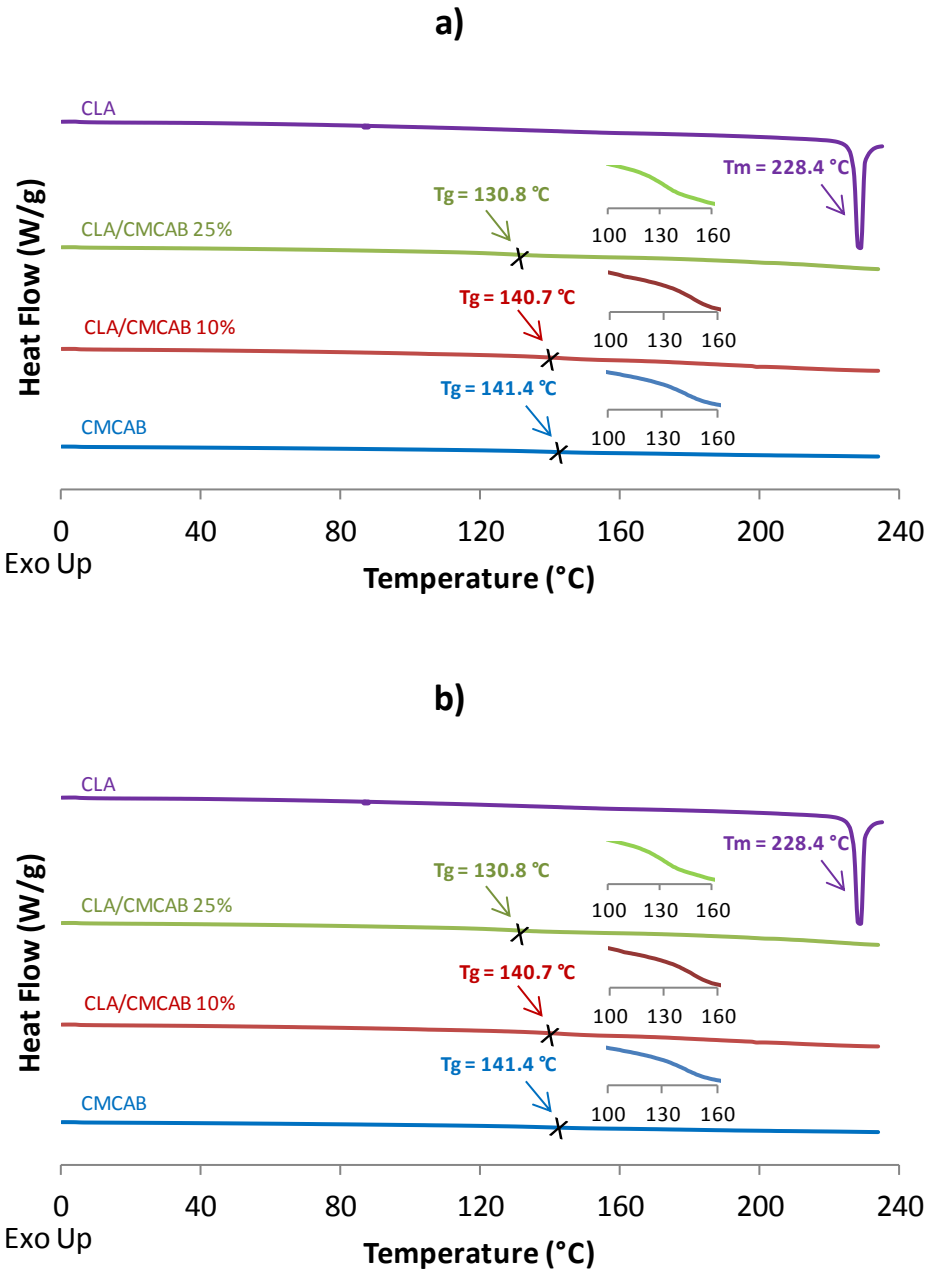

Figure A5.1 DSC thermograms of **a)** CLA/CMCAB ASDs (results from nanoparticles ASDs are shown in Table 1, Chapter 5), and **b)** CLA/HPMCAS ASDs, all in comparison with crystalline CLA

References

1. Yihong Qiu, Y. C., Geoff G.Z. Zhang, Lirong Liu, William Porter, *Developing Solid Oral Dosage Forms: Pharmaceutical Theory & Practice* First ed.; Academic Press: United States of America, 2009.

2. Adrjanowicz, K.; Zakowiecki, D.; Kaminski, K.; Hawelek, L.; Grzybowska, K.; Tarnacka, M.; Paluch, M.; Cal, K., Molecular dynamics in supercooled liquid and glassy states of antibiotics: Azithromycin, clarithromycin and roxithromycin studied by dielectric spectroscopy. Advantages given by the amorphous state. *Molecular Pharmaceutics* **2012,** *9* (6), 1748-1763.